



**COLLEGE OF MEDICINE, BIOLOGICAL SCIENCES AND PSYCHOLOGY**

**SCHOOL OF MEDICINE**

**DEPARTMENT OF**

**INFECTION, IMMUNITY & INFLAMMATION**

**Microparticles as biomarkers of early changes leading to  
Cardiovascular disease in chronic kidney disease**

**© Nima Abbasian**

**This thesis submitted for the degree of Doctor of Philosophy  
at the University of Leicester- 2015**

## **Abstract**

### ***Microparticles as biomarkers of early changes leading to cardiovascular disease in chronic kidney disease***

***Nima Abbasian***

Hyperphosphataemia in patients with advanced chronic kidney disease (CKD) is thought to be an important contributor to cardiovascular risk, in part because of endothelial cell (EC) dysfunction induced by inorganic phosphate (Pi). Such patients also have an elevated circulating concentration of pro-coagulant endothelial microparticles (MPs), leading to a pro-thrombotic state, which may contribute to acute occlusive events. It is hypothesised that hyperphosphataemia leads to MP formation from ECs via an elevation of intracellular Pi, which directly inhibits phosphoprotein phosphatases, triggering a global increase in phosphorylation and cytoskeletal changes. Using cultured human endothelial cells (EAhy926), incubation with elevated extracellular Pi (2.5mM) led to a rise in intracellular Pi concentration within 90min. This was mediated by PiT-1/slc20a1 Pi transporters; and led to global accumulation of Tyr- and Ser-Thr phosphorylated proteins, a marked increase in cellular Tropomyosin-3, plasma membrane blebbing and release of 0.1 – 1 micron diameter MPs. The effect of Pi was independent of oxidative stress or apoptosis. Similarly, global inhibition of phosphoprotein phosphatases with orthovanadate or fluoride also yielded a global protein phosphorylation response and rapid release of MPs. The Pi-induced MPs expressed VE-cadherin and superficial phosphatidylserine, and in a thrombin generation assay were significantly more pro-coagulant than particles derived from cells incubated in medium with a physiological level of Pi (1mM). These data demonstrate a mechanism of Pi-induced cellular stress and signalling which may be widely applicable in mammalian cells; and in ECs provides a novel pathological link between hyperphosphataemia, generation of MPs and thrombotic risk.

**Keywords:** hyperphosphataemia, chronic kidney disease, cardiovascular disease, endothelial cells, Cell Signaling, Microparticle

## **Important note on the layout of this thesis**

The main scientific findings and the methods that were used to obtain them are presented in Chapters 2 to 5 inclusive of this thesis. Most of this material was submitted as a paper to Journal of the American Society of Nephrology and has been published (please see the Publications List below). Supplementary data, and additional detail on the methods are presented in the Appendix to the thesis.

## **Publications, Presentations, Posters, & Academic Awards**

### **Publications**

**Abbasian N**, Burton JO, Herbert KE, Tregunna BE, Brown JR, Ghaderi-Najafabadi M, Brunskill NJ, Goodall AH, Bevington A. Hyperphosphataemia, phosphoprotein phosphatases and microparticle release in vascular endothelial cells. (Paper from this PhD project; *J Am Soc Nephrol*, 2015. doi: 10.1681/ASN.2014070642).

Batool S, **Abbasian N**, Burton JO and Stover CM. Microparticles and their Roles in Inflammation: A Review. *The Open Immunology Journal*, 2013, 6, 1-14

Burton JO, Hamali HA, Singh R, **Abbasian N**, Parsons R, Patel AK, Goodall AH and Brunskill NJ. (2013) Elevated Levels of Procoagulant Plasma Microvesicles in Dialysis Patients. *PLoS ONE* 8(8): e72663.doi:10.1371/journal.pone.0072663

**Abbasian N**, Herbert KE, Bevington A, Brunskill NJ, and Burton JO. Hyperphosphataemia and microvesicle formation: a novel mechanism for cardiovascular risk in chronic kidney disease. *Nephrology Dialysis Transplantation*, vol. 27, suppl no. 2, pp. ii241, 2012 (**Abstract**)

Singh R, **Abbasian N**, Stover CM, Brunskill NJ and Burton JO. Pro-Inflammatory and Pro-Coagulant Characteristics of Platelet Derived Microvesicles in Haemodialysis Patients. *Nephrology Dialysis Transplantation*, vol. 27, suppl no.2, pp. ii241, 2012 (**Abstract**)

### **Oral presentations**

**Abbasian N**, Burton J, Herbert K, Goodall AH, Brunskill NJ, Bevington A. Endothelial inorganic phosphate signalling to Tropomyosin: A molecular basis for generation of acutely pro-coagulant endothelial microparticles in uraemic cardiovascular disease. (*Renal research seminar- Department of Infection, Immunity & Inflammation, University of Leicester, UK, March 2015*)

**Abbasian N**, Burton J, Herbert K, Brunskill NJ, Goodall AH, Bevington A. Hyperphosphataemia signalling and pro-coagulant microparticle release in human vascular endothelial cells. (*M.V. Lomonosov Moscow State University, Moscow, Russia, March 2015*)

**Abbasian N**, Burton J, Herbert K, Brunskill NJ, Goodall AH, Bevington A. Hyperphosphataemia signalling and pro-coagulant microparticle release in human vascular endothelial cells. (*University of Leicester Microvesicles Group Meeting, Department of Cardiovascular Sciences, Glenfield Hospital, University of Leicester, UK, September 2014*)

**Abbasian N**, Burton J, Herbert K, Goodall AH, Brunskill NJ, Bevington A. Endothelial inorganic phosphate signalling to Tropomyosin: A molecular bases for generation of acutely pro-coagulant endothelial microparticles in uraemic cardiovascular disease. (*University of Leicester Microvesicles Group Meeting, Department of Cardiovascular Sciences, Glenfield Hospital, University of Leicester, UK, September 2014*)

**Abbasian N**, Burton JO, Herbert KE, Alison Goodall, Bevington A. Inorganic phosphate toxicity and cardiovascular death in chronic kidney disease: More than just rubble in the arteries. (*Sixth Annual Postgraduate Student Conference, University of Leicester, UK, April 2013*)

**Abbasian N**, Burton JO, Herbert KE, Brunskill NJ, Bevington A. Hyperphosphataemia and microvesicle formation: a novel mechanism for cardiovascular risk in chronic kidney disease. (*Department of Cardiovascular Sciences, University of Leicester, UK, February 2014*)

**Abbasian N**, Burton JO, Herbert KE, Brunskill NJ, Bevington A. Hyperphosphataemia and microvesicle formation: a novel mechanism for cardiovascular risk in chronic kidney disease. (*Renal research seminar- Department of Infection, Immunity & Inflammation, University of Leicester, UK, January 2014*)

**Abbasian N**, Burton JO, Herbert KE, Brunskill NJ, Bevington A. Hyperphosphataemia and microvesicle formation: a novel mechanism for cardiovascular risk in chronic kidney disease. (*Fifth Annual Postgraduate Student Conference, University of Leicester, UK, April 2013*)

**Abbasian N**, Burton JO, Herbert KE, Brunskill NJ, Bevington A. Hyperphosphataemia and microvesicle formation: a novel mechanism for cardiovascular risk in chronic kidney disease. (*East Midlands Renal Research Showcase, Loughborough, UK, April 2012*)

**Abbasian N**, Burton J, Herbert K, Bevington A. Microparticles as biomarkers of early changes leading to cardiovascular disease in chronic kidney disease (CKD). (*Department of Infection, Immunity, & Inflammation, University of Leicester, UK, February 2012*)

**Abbasian N**, Burton J, Herbert K, Bevington A. Microparticles as biomarkers of early changes leading to cardiovascular disease in chronic kidney disease (CKD). (*University of Leicester Microparticles Group Meeting, Department of Cardiovascular Sciences, Glenfield Hospital, University of Leicester, UK, February 2012*)

**Abbasian N**, Burton J, Herbert K, Bevington A. Microparticles as biomarkers of early changes leading to cardiovascular disease in chronic kidney disease (CKD). (*Renal research seminar- Department of Infection, Immunity & Inflammation, University of Leicester, UK, April 2011*)

**Abbasian N**, Burton J, Herbert K, Bevington A. Microparticles as biomarkers of early changes leading to cardiovascular disease in chronic kidney disease (CKD). 15<sup>th</sup> April, 2011; (*University of Leicester Microparticles Group Meeting, Department of Cardiovascular Sciences, Glenfield Hospital, University of Leicester, UK, April 2011*)

### **Posters**

**Abbasian N**, Burton JO, Herbert KE, Brunskill NJ, Bevington A. Microvesicle formation and hyperphosphataemia: a novel mechanism for cardiovascular risk in chronic kidney disease. (*The Renal Association Conference, Newcastle, UK, June 2012*)

Singh R, **Abbasian N**, Stover CM, Brunskill NJ and Burton JO. Pro-Inflammatory and Pro-Coagulant Microvesicles: A Novel Mechanism for Cardiovascular Disease in Haemodialysis Patients. (*Renal Association Conference, Newcastle, UK, June 2012*)

**Abbasian N**, Herbert KE, Bevington A, Brunskill NJ, and Burton JO. Hyperphosphataemia and microvesicle formation: a novel mechanism for cardiovascular risk in chronic kidney disease. (*49<sup>th</sup> ERA-EDTA congress, Paris, France, May 2012*)

Singh R, **Abbasian N**, Stover CM, Brunskill NJ and Burton JO. Pro-Inflammatory and Pro-Coagulant Characteristics of Platelet Derived Microvesicles in Haemodialysis Patients. (*49th ERA-EDTA Congress, Paris, France, May 2012*)

Singh R, **Abbasian N**, Stover CM, Brunskill NJ and Burton JO. Pro-inflammatory and Pro-coagulant Microvesicles: A Novel Mechanism for Cardiovascular Risk in Chronic Kidney Disease. (*East Midlands Renal Research Showcase, Loughborough, UK, April 2012*)

### **Research highlight(s)**

Carney, Ellen F. "Chronic kidney disease: Procoagulant microparticles provide a novel pathogenic link between hyperphosphataemia and cardiovascular risk." *Nature Reviews Nephrology*. doi:10.1038/nrneph.2015.34, Published online 24 March 2015  
**(Research highlights)**

**Press Release:** <http://www2.le.ac.uk/offices/press/press-releases/2015/march/university-of-leicester-study-reveals-how-dietary-phosphate-can-increase-heart-disease-risk>

### **Academic Awards and certificates/diploma**

**Scholarship;** British Council Researcher Links Workshop Participant - Extracellular Vesicles: Mechanisms of Biogenesis and Roles in Disease Pathogenesis, Lomonosov Moscow State University, Moscow, Russia, 1-5 March 2015

**Research grant** from Kidney Research UK (RP30/July 2014) to support further research arising from the work described in this thesis

**Commendation certificate;** for the best oral presentation “Microparticle formation and hyperphosphataemia: A novel mechanism for cardiovascular risk in chronic kidney disease” presented at the Fifth Annual Postgraduate Student Conference- April 2013- University of Leicester- UK.

**Travel Grant/Certificate** for the best abstract submitted to 49<sup>th</sup> ERA-EDTA congress May 24-27, 2012 Paris, France

**Open PhD Scholarship award** Jan 2011 – Dec 2013- University of Leicester- UK

**Silver sponsorship award** 2012-2013; PrimerDesign Ltd- UK

## Acknowledgement

Firstly, I would like to thank my three supervisors Drs Alan Bevington, James Burton, and Karl Herbert. Alan, for his all invaluable supervision, guidance, support and encouragement, without which this project would not have been possible, and James and Karl for their constructive discussion and encouragement. Thank you Karl for HUVECs! Thank you very much, it has been a great pleasure to work on this project with all of you.

I would also like to show my appreciation for my project progress review panel Prof. Nigel Brunskill and Dr Peter Topham for their constructive suggestions and discussions in furthering my project.

I would like to thank Dr Lucia Pinon for assistance with flow cytometry; Mr Stefan Hyman and Miss Natalie Allcock for assistance with TEM and SEM; and Prof. Alison Goodall and Mr Mohammed Ali Alsahli for assistance with CAT assays. The waiting list to do the TGA lasted 2 years but the result from this was worth the waiting! I also thank Prof. Alison Goodall for kindly providing EAhy926 endothelial cell line for this project.

I am grateful to Drs Martha Clokie, Primrose Freestone, and Cordula Stover: to Dr Martha Clokie and Dr Primrose Freestone respectively for allowing me to access the NanoSight equipment and the IEF system in their labs, and to Dr Cordula Stover for being always open for helping and giving advice if I needed.

I thank Jez and Barbara for help with  $^{32}\text{P}$  Uptake experiments (Chapter 4-Figure 4.7 A and B). Also thank you Jez for all the happy time you made for me over my PhD- Every time I have a haircut I will be remembering you saying “Nice haircut! Have you done it yourself?”

A big thank you to everyone in the Renal Lab- Jez, Iza, Maryam, Emma, Chee Kay, Safia, Sumia, Jo, Ravie, Tricia and everyone else who I have worked with; for your friendship and support and joys and fun - “Tea and cake times” you have supplied me with over my time in the Renal Lab.

I would like to thank my Mum and Dad for all their support, encouragements and endless unconditional love without which I would not have this opportunity to be here today and finish this job. I am indebted to you for everything of my life.

Finally, and most importantly, my sincerest thanks to my wife “Maryam” for believing I could do this. Thank you for all the late nights and weekends staying with me in the lab; for all unending love, support and encouragements; for being such a massive “true friend” and bearing with all my bad moods when I have had a difficulty in my work and during my writing up year specially November and December 2014! Also, thank you for listening to all my practices over my presentations at home! Probably you deserve this PhD as much as I do!

## Table of contents

Abstract	I
Important note on the layout of this thesis	II
Publications, presentations, posters, & academic awards	II
Acknowledgement	VI
Table of contents	VII
Table of abbreviations	XII
<b>Chapter 1. General introduction</b>	<b>1</b>
1.1 The clinical problem	1
1.2 Basic kidney anatomy and physiology	1
1.3 Structure and function of the kidney	3
1.3.1 Nephrons	4
1.3.2 Solute transport within the nephron	6
1.4 Chronic kidney disease (CKD) and risk factors	6
1.4.1 Introduction	6
1.4.2 Epidemiology and the scale of the problem	7
1.4.3 Classification of chronic kidney disease (CKD)	9
1.4.4 Chronic kidney disease (CKD) and mineral disturbances	9
1.5 Definition of hyperphosphataemia	10
1.6 Regulation of pi homeostasis in mammals	11
1.6.1 Pi pools in the human body	11
1.6.2 Renal, intestinal, and bone regulation of Pi	14
1.6.3 Hormonal regulation of Pi	17
1.6.3.1 Parathyroid hormone (PTH)	17
1.6.3.2 Calcitriol	17
1.6.3.3 FGF23	18
1.6.3.4 Klotho	20
1.6.4 Regulation by dietary Pi intake	20
1.7 Regulation of cell metabolism and signalling by intracellular Pi (Pi-sensitive enzymes/proteins)	21
1.7.1 Effects of Pi on enzymes regulating protein phosphorylation signals	22
1.8 Probing for intracellular effects of Pi	23
1.8.1 Drugs which should inhibit the transporters	23
1.8.1.1 Ouabain	23
1.8.1.2 Phosphonoformate (PFA)	24
1.8.2 Depletion of intracellular Pi by fructose	25
1.9 Extracellular effects of Pi (ionised Ca effects and nanocrystals)	26
1.10 Factors influencing the Pi concentration in mammalian cells	27
1.10.1 Pi anions and the effect of the membrane potential	27
1.10.2 Active Pi transporters (SLC17/20/34)	27
1.10.2.1 SLC17: Type I Na <sup>+</sup> -dependent Pi co-transporters	27
1.10.2.2 SLC34: Type II Na <sup>+</sup> -dependent Pi co-transporters	29
1.10.2.3 SLC20: type III Na <sup>+</sup> -dependent Pi co-transporters	31
1.10.2.3.1 Introduction	31
1.10.2.3.2 Tissue distribution of SLC20 family of Pi transporters	33
1.10.2.3.3 Structure, topology and homologues of SLC20 (PiT) proteins	33
1.10.2.3.4 Functions of SLC20 (PiT) proteins	34
1.10.2.3.4.1 Functions of SLC20 (PiT) proteins as a viral receptor	34
1.10.2.3.4.2 Functions of SLC20 (PiT) proteins as Pi transporters	35
1.10.2.3.4.3 Other possible functions of PiT proteins	36
1.10.2.3.5 Kinetics of SLC20 (PiT) proteins	36

1.10.2.3.6 Regulation of SLC20 transporters through phosphorylation and/or de-phosphorylation	37
1.11 The cardiovascular system and the endothelium	38
1.11.1 Introduction	38
1.11.2 Structure of blood vessels	40
1.11.3 The endothelium	40
1.12 CVD risk factors in CKD	44
1.12.1 Traditional risk factors	44
1.12.2 Novel and non-traditional (uraemic) risk factors	44
1.13 CVD in CKD and the role of Pi	45
1.14 The mechanism of cardiovascular damage in hyperphosphataemia	46
1.14.1 The “classical” explanation: Pi and soft tissue calcification of atheromatous plaques	46
1.14.2 Newer views	48
1.14.2.1 A new variant of the “classical” explanation. CaPi nanocrystals as biological stimulus acting on cells	48
1.14.2.2 Pi as the “new cholesterol”- may exert clinically important effects even within the normal range of plasma Pi concentration	50
1.14.2.3 Pi may be toxic in its own right, possibly through intracellular effects	51
1.15 Management of hyperphosphataemia	53
1.16 Cell membrane derived microparticles (MPs)	53
1.16.1 Introduction	53
1.16.2 Clinical importance of MPs	54
1.16.3 <i>in vivo</i> and <i>in vitro</i> MP stimuli	55
1.16.4 MP structure, composition and surface markers	56
1.16.5 MP formation	58
1.16.5.1 An insight into different types of extracellular vesicles	58
1.16.5.2 Cell activation	61
1.16.5.3 Cell apoptosis	62
1.16.6 Microparticle involvement in health and disease	63
1.16.6.1 Microparticles in CKD	64
1.16.6.2 Microparticles in CVD	65
1.16.7 MPs’ biological function	66
1.16.8 MP clearance	68
1.16.9 Methods for MP measurement	69
1.17 Summary	69
1.18 Thesis hypothesis	70
1.19 Thesis aims and structure	72
<b>Chapter 2. Methods and materials</b>	<b>73</b>
2.1 General materials	73
2.2 Choice of experimental model	73
2.3 Gelatin coating plates for HUVECs	75
2.4 HUVEC culture medium and passaging	75
2.5 EAhy926 culture medium and passaging	76
2.6 Experimental incubations and choice of Pi supplemented medium	76
2.7 Mycoplasma screening	76
2.8 Microparticle isolation	77
2.9 Isolation and measurement of detached cells following chronic (24h) incubation	78
2.10 Nanoparticle tracking analysis (NTA)	78
2.11 Flow cytometry analysis of microparticles	79
2.12 Transmission electron microscopy (TEM)	81
2.13 Scanning electron microscopy (SEM)	81
2.14 Dynamic light scattering (DLS)	81

2.15 Determination of apoptosis and cell death	83
2.15.1 MTT assay	83
2.15.2 DNA fragmentation (DAN laddering)	83
2.15.3 TUNEL-coupled hoechst staining	84
2.15.4 Trypan blue exclusion test (TBET)	84
2.15.5 Flow cytometry (annexin V/PI staining)	84
2.16 Determination of ROS generation	87
2.16.1 DCFDA and flow cytometry	87
2.16.2 DCFDA-coupled hoechst staining	88
2.16.3 DHE	88
2.16.4 NBT	89
2.17 Assay of nitric oxide synthase (NOS) activity	89
2.18 Protein measurement/detection techniques	90
2.18.1 Lowry protein assay	90
2.18.2 Bio-rad RC DC protein assay	90
2.18.3 Protein sample preparation	91
2.18.3.1 Preparing global cell lysate for separation on SDS-PAGE gels	91
2.18.3.2 Histone extraction for separation on SDS-PAGE gels	91
2.19 Immunoblotting and gel staining	92
2.20 2-D electrophoresis (2-DE)	93
2.21 Mass spectrometry	93
2.22 Measurement of cell layer Pi	93
2.23 <sup>32</sup> Pi transport assays	94
2.24 Determination of inhibitory effect of Pi on tyrosine and serine/threonine phosphatase (PTPase and PSPase) activity	94
2.25 Thrombin generation assay (TGA) using calibrated automated thrombography (CAT)	94
2.26 ATP measurement	95
2.27 Glycolytic rate (lactate production measurement)	95
2.28 Determination of DNA content of protein particles from the medium	96
2.29 RNA techniques	97
2.29.1 Transfection with siRNA	97
2.29.2 Primer design and DNA sequencing	97
2.29.3 Total RNA extraction from cell monolayer	97
2.29.4 Total RNA extraction from Pi-derived MPs	98
2.29.5 Reverse transcription (RT) reaction (cDNA synthesis)	99
2.29.6 PCR (polymerase chain reaction)	100
2.29.7 Agarose gel electrophoresis	101
2.29.8 RT-qPCR	101
2.30 <sup>45</sup> Ca deposition on cell monolayer	102
2.31 Statistical analysis	103

### **Chapter 3. Effect of pi on microparticle (MP) release from EAhy926 endothelial cells**

3.1.1 High [Pi] acutely induces microparticle (MP) release from EAhy926 cells	104
3.1.2 Pi-derived MPs are strongly pro-coagulant	106
3.2 Results	107
3.2.1 Acute (90min) hyperphosphataemia enhances EAhy926 cells' membrane blebbing	107
3.2.2 Acute (90min) hyperphosphataemia increases microparticle release from EAhy926 cells	108
3.2.3 Acute (90min) Pi-induced MP release from EAhy926 cells depends upon pi influx into the cells	111
3.2.4 Chronic (24h) hyperphosphataemia increases detachment of EAhy926 cells	112

3.2.5 Chronic (24h) microparticle output is not attributable to the action of calcium phosphate nanocrystals from the high Pi medium	116
3.2.6 Pi-derived MPs are strongly pro-coagulant	118
3.3 Discussion	120
3.3.1 Hyperphosphataemia enhances CD144/PS positive MP release from EAhy926 endothelial cells	120
3.3.2 Particle output from high Pi medium does not arise from Ca/Pi deposition on the cells or nanocrystal formation in high Pi medium	120
3.3.3 High intracellular Pi drives particle release from EAhy926 cells	121
3.3.4 Pi enhances particle sedimentation and/or aggregation	121
3.3.5 High [Pi]-derived MPs are strongly pro-coagulant	122

## **Chapter 4. High [Pi] raises intracellular Pi concentration by transport through active Na<sup>+</sup>-linked PiT-1 (SLC20a1) Pi transporters**

4.1 Introduction	124
4.2 Results	127
4.2.1 Pi transporter characteristics of EAhy926 endothelial cells	127
4.2.2 Hyperphosphataemia increases cell layer Pi in EAhy926 cells	129
4.2.3 Hyperphosphataemia raises intracellular Pi concentration by transport through active Na <sup>+</sup> -linked PiT-1 (SLC20a1) Pi transporters	132
4.3 Discussion	134
4.3.1 Hyperphosphataemia acutely enhances cell layer Pi in EAhy926 endothelial cells	134
4.3.2 Transport of Pi depends on extracellular sodium concentration in EAhy926 cells and is mediated predominantly by PiT-1	134

## **Chapter 5. Mechanism of Pi-induced microparticle release**

5.1.1 Pi induces global changes in protein phosphorylation	136
5.1.2 Proteomic analysis demonstrates Pi-induced changes in tropomyosin expression and histone distribution	136
5.2 Results	138
5.2.1 Pi has little effect on oxidative stress and cell death	138
5.2.2 Effect of Z-VAD-FMK Caspase-3 inhibitor on Pi-induced EMP output	147
5.2.3 Effect of Rho kinase inhibitors on Pi-induced EMP output	148
5.2.4 Inhibitory effect of Pi on phosphoprotein phosphatases	149
5.2.5 Hyperphosphataemia alters global protein phosphorylation and/or dephosphorylation	151
5.2.6 Acute and chronic effect of fructose on protein phosphorylation and/or dephosphorylation	155
5.2.7 Effect of intracellular Pi on cytoskeletal regulatory protein (TM-3)	157
5.2.8 High Pi-derived MPs are enriched in histones	161
5.3 Discussion	163
5.3.1 Elevated Pi has no significant effect on ROS and cell apoptosis in EAhy926 cells	163
5.3.2 High Pi modulates protein phosphorylation	163
5.3.3 High [Pi] alters in tropomyosin expression and histone distribution	165

## **Chapter 6. General discussion and future work**

6.1 General discussion	167
6.1.1 Rapid Pi-stimulation of MP output implies a direct "pi signal" within endothelial cells	167
6.1.2 Pi induced particle release is independent of apoptosis	168

6.1.3 Pi induces a distinct and sustained form of cell stress through global changes in protein phosphorylation	169
6.1.4 Phosphate stress is associated with rapid changes in the cytoskeletal regulator tropomyosin	171
6.1.5 Clinical implications of these effects of Pi	172
6.1.6 Hyperphosphataemic states, independent of kidney disease, are also associated with thrombotic and/or embolic events	174
6.1.7 Broader implications of these findings	174
6.2 Summary of the present position and future work	174
<b>Appendix</b>	177
Appendix A (Culture & Test medium composition)	177
Appendix B (Reagents & Buffers)	180
Appendix C (Supporting data)	189
Supporting data to Chapter 3	189
Supporting data to Chapter 4	194
Supporting data to Chapter 5	195
<b>References</b>	210

## Table of Abbreviations

ATP	Adenosine triphosphate
ADP	Adenosine diphosphate
ADHR	Autosomal-dominant hypophosphatemic rickets
ADMA	Asymmetric dimethylarginine
BMP-2	Bone morphogenetic protein-2
CKD	Chronic Kidney Disease
CVD	Cardiovascular Disease
cIMT	Carotid intima-media thickness
DAPK-1	Death-associated protein kinase-1
DLS	Dynamic Light Scattering
EPO	Erythropoietin
ESRD	End Stage Renal Disease
eGFR	Estimated glomerular filtration rate
ECs	Endothelial cells
EMPs	Endothelial Microparticles
EDHF	Endothelium-derived hyperpolarizing factor
FGF23	Fibroblast growth factor 23
FGF23R	Fibroblast growth factor 23 receptor
F-1-P	Fructose-1-phosphate
FACS	Fluorescence-activated cell sorting
Glv-1	Gibbon ape leukaemia virus
GP	Glycoproteins
GI	Gastro-intestinal
GIT	Gastro-intestinal tract
GFR	Glomerular Filtration Rate
GBM	Glomerular Basement Membrane
HUVEC(s)	Human Umbilical Vein Vascular Endothelial Cell(s)
HAEC	Human aortic endothelial cells
IMT	Intima-media thickness
LGA	Low-grade albuminuria
LMW-PTP	Low Molecular Weight Protein Tyrosin Phosphatase
MVs	Microvesicles
MP(s)	Microparticle(s)
MASMCs	Mouse aortic smooth muscle cells
MTT	3-(4, 5-dimethylthiazolyl-2)-2, 5-diphenyltetrazolium bromide
NOS	Nitric oxide synthesis
NO	Nitric oxide
NTA	Nanoparticle Tracking Analysis
NAC	N-Acetyl-L-cysteine
NBT	Nitrobluetetrazolium
OPN	Osteopontin
PTCs	Proximal Tubular Cells
PPP	Phosphoprotein phosphatases
PSer	Phosphatidylserine
PE	Phosphatidylethanolamine
Pi	Inorganic Phosphate (Orthophosphate)
PPi	Pyrophosphate
PTH	Parathyroid hormone
PFA	Phosphonoformate
PMPs	Platelet Microparticles
PSPase	Phosphoserine/threonine protein phosphatases
PTPase	Phosphotyrosine protein phosphatases
RBC	Red Blood Cell

ROS	Reactive Oxygen Species
Ram-1	Rat amphotropic retrovirus
RMPs	Red Blood Cell Microparticles
SLC17	Solute Carrier 17
SLC34	Solute Carrier 34
SLC20	Solute Carrier 20
SMCs	Smooth muscle cells
SEM	Scanning Electron Microscopy
TM	Tropomyosin
TM-3	Tropomyosin-3
TF	Tissue Factor
TSP-1	Trombospondin-1
TEM	Transmission Electron Microscopy
TUNEL	Terminal deoxynucleotidyl transferase dUTP nick end labeling
VEC(s)	Vascular Endothelial Cell(s)
VSMC(s)	Vascular Smooth Muscle Cell(s)

# Chapter 1. General Introduction

---

## 1.1 The clinical problem

Strong evidence exists implying a direct relationship between Cardio Vascular Disease (CVD) and Chronic Kidney Disease (CKD) (Foley *et al.*, 1998<sub>a</sub>). There are several biochemical abnormalities in CKD patients which may increase the risk of Cardio Vascular (CV) complications (Ellam & Chico, 2012; Razzaque, 2011). One of these is the circulating concentration of inorganic phosphate (Pi) (Ellam & Chico, 2012; Razzaque, 2011) which rises to a high level in the blood of patients with impaired kidney function (i.e. CKD patients). Increase in plasma Pi concentrations is collectively known as hyperphosphataemia. Traditional cardiovascular risk factors fail to show up in early CKD disease development (see Figure 1.18), therefore identifying novel early stage risk factors and biomarker(s) for CKD cardiovascular disease is an emerging area of interest.

Previously studies of the role of higher plasma Pi levels in promoting cardiovascular risk in patients with CKD centred on the role of Pi in vascular calcification as manifested by changes in smooth muscle cells underlying vascular endothelial cells (Giachelli *et al.*, 2001; Shanahan *et al.*, 2011). However more recent studies have been shedding light on newer views on the role of high Pi in athero-occlusive events in CKD which may depend on cellular effects of Pi itself on vascular endothelial cells (VECs) rather than on extracellular calcium phosphate precipitation (Di Marco *et al.*, 2012; Di Marco *et al.*, 2008; Shuto *et al.*, 2009). The research described in this thesis is a study of these newer mechanisms, investigating the involvement of Pi in cell (patho)-physiology and dysfunctions in VEC which may ultimately lead to new interventions to control the problem of Pi-induced cardiovascular problems in CKD.

## 1.2 Basic Kidney anatomy and physiology

The macro-anatomy of kidneys, ureters, bladder, and urethra is depicted in Figure 1.1.

The kidneys are two ellipsoid bean-shaped organs which are situated retroperitoneally in the abdomen, approximately between the eleventh thoracic and third lumbar vertebrae (Edmund Lamb, 2011). Each is 12 cm long and weighs approximately 150-200g in humans.

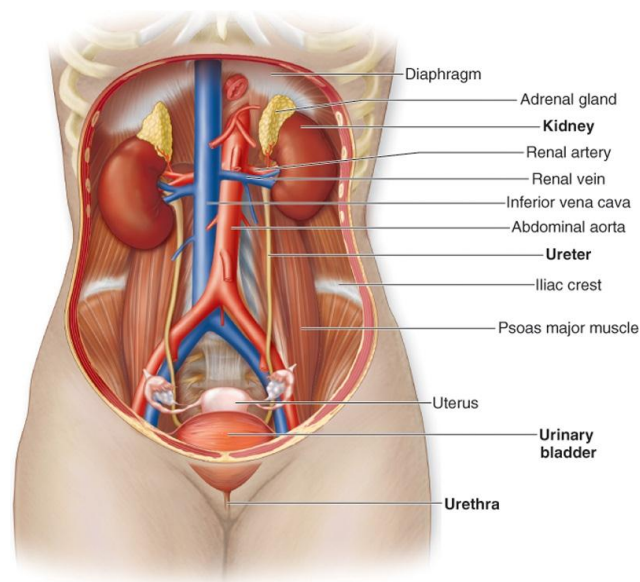


Figure 1.1. Schematic showing the renal system: *Note that* the right kidney is located lower than the left one and each is supplied with blood via the renal artery (afferent artery) which drains into the renal vein (efferent vein). Urine produced by the kidneys is excreted from the bladder, where it has been drained from the kidneys through the ureters and finally passed out of the body through the urethra (Edmund Lamb, 2011).

URL: [http://academic.kellogg.edu/herbrandsonc/bio201\\_mckinley/Urinary%20System.htm](http://academic.kellogg.edu/herbrandsonc/bio201_mckinley/Urinary%20System.htm) Last access date: 05/04/2011 (Permission acquired from McGraw-Hill)

The kidney, in mammalian species, comprises a cortex and medulla (i.e. outer and inner segments). The organ is made up of functional units (nephrons) and a specialised microvasculature (Feehally *et al.*, 2008) (Figure 1.2). Damage to the nephrons (Section 1.3.1) can have irreversible consequences after birth since the number of nephrons is determined during prenatal development (Feehally *et al.*, 2008). Therefore screening of the population for renal defects is an important objective for nephrologists with the ultimate aim of taking early diagnostic/therapeutic action to slow down the progression of impaired renal function.

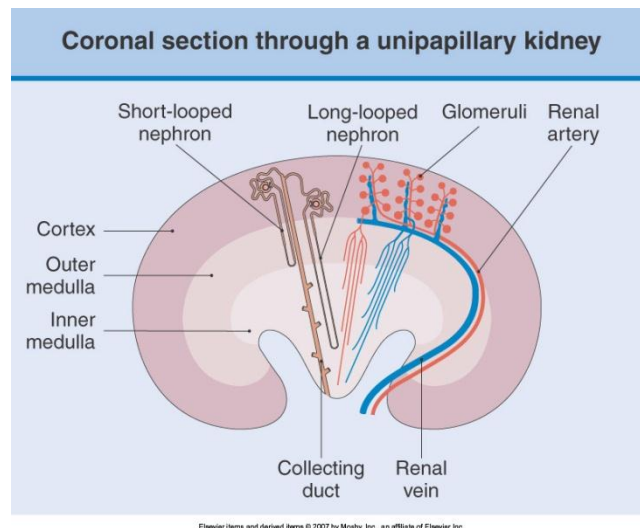


Figure 1.2. A frontal section through the kidney. The outer medulla is divided into outer stripe and inner stripe (not shown). Picture adapted from (Feehally *et al.*, 2008).

### 1.3 Structure and function of the Kidney

Each kidney is composed of an outer non distensible fibrous capsule which surrounds and protects the cortex and medulla, (i.e. inner parts), against invading microorganisms and trauma. The cortex, itself, encloses the medulla, as seen in Figure 1.2.

In humans, each kidney consists of a quite variable number of functioning units called the **nephrons**, ranging between 0.4 to 1.2 million, of which short-looped nephrons are more frequent than the long-looped ones (Edmund Lamb, 2011). Under normal physiological conditions, in humans, each kidney receives approximately 12.5% of the cardiac output (Berne *et al.*, 2000).

The kidneys play a fundamental role in regulating body homeostasis, biosynthesis, catabolism, and blood pressure; besides their predominant role in eliminating body wastes such as urea, ammonium, and creatinine (through excretion in the urine) and re-absorption of water, Pi, glucose and many other nutrients and metabolites (Lote, 2000; Hladky & Rink, 1986). Maintaining homeostasis of the blood plasma and electrolytes, especially sodium and potassium, is a major physiological function of the kidneys (Edmund Lamb, 2011), as is synthesis of the enzyme **renin** which regulates blood pressure, and crucial hormones such as **erythropoietin** (EPO), which stimulates bone marrow to produce red blood cells (RBC), and **calcitriol**, which is involved in calcium

absorption by the gastrointestinal tract (GIT). Furthermore metabolism of **insulin** (both degradation and reabsorption) has been demonstrated to be a prominent physiological function of the kidneys (Feehally *et al.*, 2008; Edmund Lamb, 2011).

### 1.3.1 Nephrons

Nephrons are the fundamental functional units of the renal system situated within the cortex and medulla of each kidney. Morphologically, nephrons have been classified into superficial, midcortical, and juxtamedullary nephrons in accordance with their position (Figure 1.3) within the cortex in the kidney. They are also sub-divided into short-looped and long-looped nephrons, which differ in the length of the loop of Henle, and have differential roles in the urine concentrating mechanism of the kidney (Jamison, 1987).

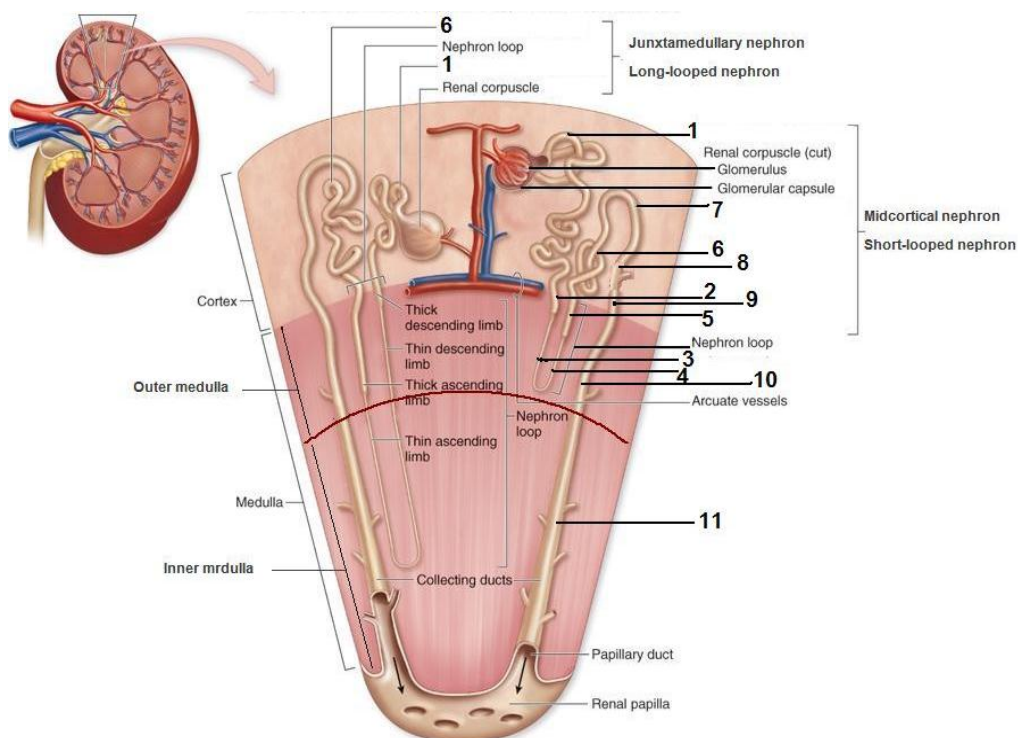


Figure 1.3. A schematic showing the nephron and its specialised compartments; A cross sectional view of specialised segments of renal tubule; (1) proximal convoluted (pars convolute) tubule (PCT), (2) proximal straight (pars recta) tubule (PST), (3) thin descending limb of the loop of Henle (tDLH), (4) thin ascending limb of the loop of Henle (tALH), (5) thick ascending limb of the loop of Henle (TAL), macula densa (Not shown), (6) distal convoluted tubule (DCT), (7) connecting tubule (CNT), (8) Initial collecting tubule (ICT), (9) cortical collecting duct (CCD), (10) outer medullary collecting duct (OMCD), and (11) inner medullary collecting duct (IMCD).

Picture modified from URL:

[http://academic.kellogg.edu/herbrandsonc/bio201\\_mckinley/Urinary%20System.htm](http://academic.kellogg.edu/herbrandsonc/bio201_mckinley/Urinary%20System.htm) Last access date: 05/04/2011 (Permission acquired from McGraw-Hill)

Considering a nephron as a closed-ended tube-like apparatus, with a glomerulus and a tubule as its main structural segments, this can be further divided into several distinctive regions with different resorptive and secretory functions and properties. The “U” shaped cortical closed-ended section is called Bowman’s capsule. The glomerulus - a tuft of specialised arteriole-derived capillaries is embedded between the walls of this “U” region and together Bowman’s capsule and the glomerulus form the so-called renal corpuscle. The glomerulus comprises quite different segments and their relevant cell types are depicted in Figure 1.4. These include Mesangium (M), Podocyte (PO), Foot process (F), Parietal Epithelium (PE), Glomerular Basement Membrane (GBM), Urinary Space (US), and Endothelium (E) (Feehally *et al.*, 2008). Bowman’s capsule is where the filtrate passes from the vascular system into the tubule system which has an epithelial structure. The filtrate in the urinary space within the renal corpuscle drains into the remaining tubular subdivisions of the nephron and finally enters the bladder, before being excreted through the urethra (Giebisch and Windhager, 2005; Feehally *et al.*, 2008).

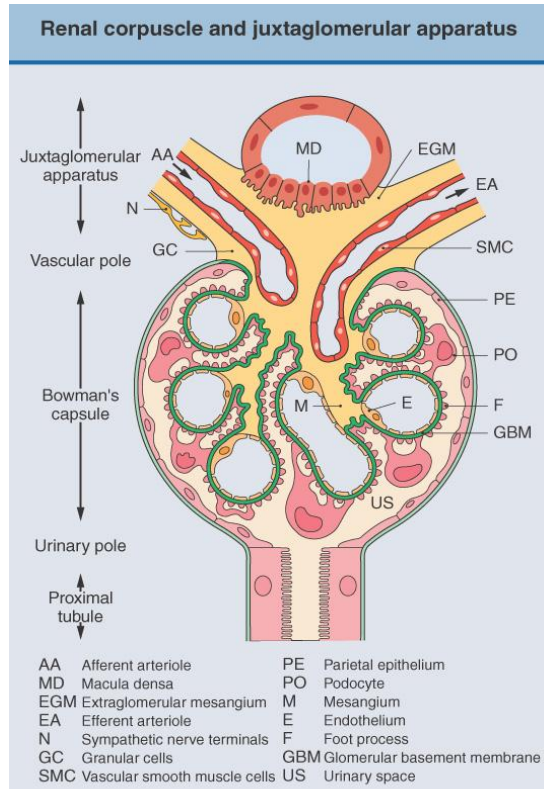


Figure 1.4. Structure of the renal corpuscle and juxtaglomerular apparatus; Renal corpuscle comprised of Bowman’s capsule and glomerulus. Blood enters the capsule via afferent arteriole and leaves there via efferent arteriole. After entering into the renal corpuscle, blood passes through the GBM into the urinary space, where the filtrate undergoes further processing through the remaining tubular segments of the nephron (Not shown). Picture reproduced from (Feehally *et al.*, 2008).

(Adapted with permission from Kriz W, Kaisling B: Structural organization of the mammalian kidney. In Seldin D, Giebisch G (eds): The Kidney, Philadelphia, Lippincott Williams & Wilkins, 2000, pp.587-654.)

### **1.3.2 Solute transport within the nephron**

Blood flows into the glomerular capillaries of the renal corpuscle, where the endothelial cells of the capillaries' tufts are enclosed within specialised parts of the renal corpuscle, i.e. the GBM, & Podocyte foot processes. This is the site where the filtration of water and small solutes occurs via approximately 70nm pores, i.e. fenestrations, of the endothelial cells and is subjected to an approximately 17 mm Hg net filtration pressure. Little net filtration occurs at the site of direct contact of endothelial cells with mesangial cells, i.e. in the centre of glomerulus (Giebisch and Windhager, 2005). Instead subsequent filtration occurs through the GBM and between the podocytes. The GBM is an anionic charged membrane (a sheet of extracellular matrix), limiting the permeability of the filtration barrier to molecules and solutes smaller than 70 kDa. The basement membrane owes its anionic charge to the sialic and carboxylic acid residues of its proteoglycans (Giebisch and Windhager, 2005). Another negatively charged part of the filtration barriers is the podocytes which, with the basement membrane, together promote the filtration of solutes which are positively charged (Giebisch and Windhager, 2005).

The ultrafiltrate of the blood plasma, after passing through the filtration barriers within the glomerulus into the urinary space, is processed by two major mechanisms to form the urine:

- 1) Selective reabsorption of solutes through the tubules.
  
- 2) Further concentration by reabsorption of water, and active secretion of solutes/toxins into the residual tubular fluid from the capillaries surrounding the tubule (Giebisch and Windhager, 2005).

## **1.4 Chronic Kidney Disease (CKD) and risk factors**

### **1.4.1 Introduction**

Chronic kidney disease (CKD) refers to a heterogeneous group of disorders that irreversibly affects the functions and structure of one or both kidneys and can further progress to end-stage renal disease (ESRD) with high mortality. CKD is a growing public health problem worldwide among all populations (Harambat *et*

*al.*, 2012) with more prevalence in women than men (Stevens *et al.*, 2007) and an increased incidence by age (Zhang & Rothenbacher, 2008). CKD has been implicated to have an interrelationship with other diseases for example cardiovascular diseases (CVD), hypertension, glomerulonephritis, diabetes mellitus, and other unknown causes (Susztak *et al.*, 2005; Jha *et al.*, 2013). Moreover, a number of systemic disorders and risk factors can increase the speed of CKD development for instance hyperphosphataemia, proteinuria, and hyperlipidemia (Vaziri, 2006).

#### **1.4.2 Epidemiology and the scale of the problem**

CKD has become a worldwide public health issue with a prevalence estimated to be 8-16% across the globe (Jha *et al.*, 2013). A systemic review of literature published between January 1980 to December 2007 demonstrated a 16% and 13% CKD prevalence in Europe and the US respectively (Covic *et al.*, 2009). CKD has a worldwide prevalence (Figure 1.5) and involves time-dependent progressive loss of renal function or development of abnormal kidney structure or both. Due to the lack of universal agreement on the stages of CKD development, definition, and classification and even more importantly because CKD starts developing asymptotically at early stages, management and treatment of this global problem remained controversial (Levey *et al.*, 2003). On the other hand, failure to diagnose early and treat CKD can allow it to progress to ESRD, kidney failure and eventually death if renal replacement therapy is not available. Therefore, early diagnosis and treatment are important, for example by monitoring proteinuria in susceptible individuals such as diabetics, or defining new biomarkers (Edelstein, 2010).

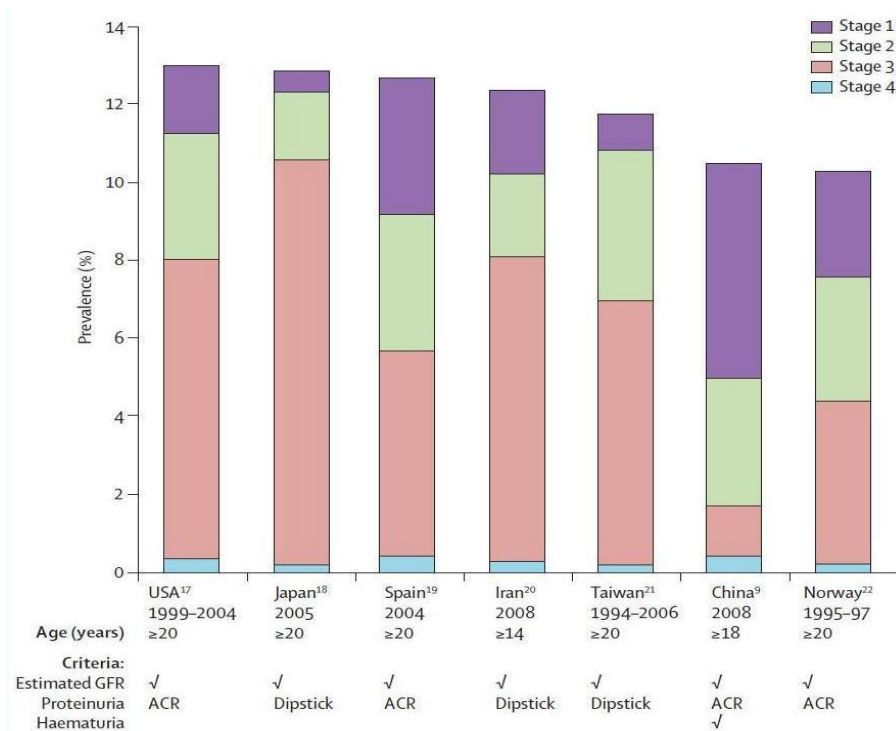


Figure 1.5. Diagram demonstrates the occurrence of chronic kidney disease (Stage1 to 4) in populations, in seven different countries. ACR=albumin-to-creatinine ratio. GFR=glomerular filtration rate (James *et al.*, 2010)

The rate of progression of CKD has been shown to correlate strongly with the rate of damage to the tubules and the interstitial cells between them (so-called tubulo-interstitial injury) (Arici *et al.*, 2004; Brunskill, 2004). It is thought that this occurs because proteinuria damages the tubules but the exact mechanism by which proteins leaking into the tubule do this is poorly understood. In proteinuria PTCs interact with a wide range of urinary proteins: albumin may be important, but a growing body of evidence implicates activation of urinary complement proteins *in vivo* by PTCs as a contributor to this progressive tubulo-interstitial injury (Peake *et al.*, 2002). Although glomerular damage may result in complement proteins and their products leaking into the tubular lumen, it has also been demonstrated that complement deposits in the luminal space may also be generated locally by the PTCs themselves (Peake *et al.*, 2002; Sheerin *et al.*, 2008).

### 1.4.3 Classification of Chronic Kidney Disease (CKD)

Depending on the glomerular filtration rate (GFR) in patients with progressive CKD, five stages of disease development have been identified namely; CKD1-5 (Marieb & Hoehn, 2007) which are listed in Table 1.1.

Stage	Description	Range of GFR (ml/min/1.73m <sup>2</sup> )
CKD1*	Kidney damage with normal or slightly increased GFR	≥ 90
CKD2	Kidney damage with mild decrease in GFR	60-89
CKD3	Moderately reduced GFR	30-59
CKD4	Severely decreased GFR	15-29
CKD5	End-Stage of the disease i.e. kidney failure	< 15

Table 1.1. Classification of CKD. Adopted from (Marieb & Hoehn, 2007).

\*CKD1 generally coincident with the presence of protein in the urine

Allowing for the donor's age, sex, and ethnic origin, the GFR is estimated from serum creatinine level (James *et al.*, 2010; Koeppen & Stanton, 2007). CKD may start progressing regardless of the decline in the GFR but be accompanied by proteinuria, therefore regardless of GFR, changes in proteinuria (especially albuminuria) can be a reliable diagnostic marker of CKD (Greenberg & Cheung, 2005).

### 1.4.4 Chronic Kidney Disease (CKD) and mineral disturbances

CKD patients are at high risk of cardiovascular (CV) morbidity and mortality. There is an increasing body of evidence from epidemiology indicating that CKD patients, if not dying from their kidney disease, may do so from an increased CV risk they have developed, arising from a complicated interrelationship between the onset of progressive kidney disease and CV complications (Gansevoort *et al.*, 2013; O'Rourke & Safar, 1999). This is partly due to biochemical abnormalities which may start developing while the kidneys' normal function fails. These mineral-related disturbances include (but are not restricted to) Pi, calcium, PTH, and vitamin D (Covic *et al.*, 2009). Biochemical abnormalities in Pi metabolism and homeostasis, may contribute to a greater mortality risk in individuals with or without kidney disease (Covic *et al.*, 2009; Bevington *et al.*, 1990). As discussed in Section 1.3.; the kidneys play a fundamental role in maintaining body Pi homeostasis (Bevington *et al.*, 1990; Bansal, 1990). This homeostatic effect of the kidneys on Pi arises from the fact that healthy kidneys

reabsorb filtered Pi and excrete excess dietary Pi out the body in the urine. Therefore, as CKD progresses, which is manifested by a decline in the number of functional units of the kidneys (nephrons) and a fall in glomerular filtration (GFR), this results in Pi retention leading to hyperphosphataemia. A systematic review in 2008 (Covic *et al.*, 2009) demonstrated that disturbances in Pi may lead to an even greater mortality risk among CKD patients than calcium and PTH.

### **1.5 Definition of hyperphosphataemia**

Hyperphosphataemia is one of the commonest serum biochemical abnormalities in CKD patients. Pi, inorganic phosphate or orthophosphate, the variably charged anion of phosphoric acid, can be found chemically in circulation as, dihydrogen phosphate  $\text{H}_2\text{PO}_4^-$  and mono-hydrogen phosphate  $\text{HPO}_4^{2-}$ . ( $\text{HPO}_4^{2-}$  and  $\text{H}_2\text{PO}_4^-$  are the two naturally occurring ionic forms of Pi which co-exist in equilibrium at a normal physiological pH and are present in plasma of a healthy individual bound to proteins, in complexes with metal cations such as calcium and magnesium, or in the form of free Pi which is the predominant form). Dietary Pi is absorbed in the intestine and is filtered and reabsorbed in the kidneys. The absorption and reabsorption involve both passive diffusion between cells through paracellular pathways (Bansal, 1990) and active transport which is mediated via transmembrane sodium-dependent Pi co-transporters (Murer & Biber, 1996; Werner *et al.*, 1998). The serum Pi concentration can be influenced by age, sex, dietary Pi intake, gastro intestinal health and/or disorders, and renal handling (Ahmed & Behzad, 2011; Bevington *et al.*, 1990; Levi & Popovtzer, 1999). Organic phosphate (probably phospholipid) also occurs in circulation and (for reasons that are not understood) shows an inverse relationship with the Pi concentration (Muhlbauer & Fleisch, 1990).

Besides defects in kidney function as predominant cause, hyperphosphataemia may also occur following a number of transient or even long-lasting defects, for example large scale tissue destruction (leading to release of Pi from dead or dying cells, or endocrine disorders, for example abnormal circulating concentrations of parathyroid hormone (PTH) and calcitriol (Ahmed & Behzad,

2011). In addition, artefactual hyperphosphataemia may also be observed when there is a time lag between blood taking and separation of the serum from it (Ahmed & Behzad, 2011) as a result of Pi release from the blood cells.

## **1.6 Regulation of Pi homeostasis in mammals**

To achieve a normal Pi concentration in a healthy adult, there are tightly controlled hormonal and non-hormonal mechanisms that exert regulatory effects on the kidneys, intestine, and bone Pi homeostasis. The regulation of Pi is complex in order to maintain the extra- and intra-cellular Pi levels in a steady state and this may also be affected by pH (Kemp *et al.*, 1988<sub>b</sub>).

### **1.6.1 Pi pools in the human body**

Pi is an important inorganic anion involved in biosynthesis of functionally important biochemical molecules such as DNA, RNA, phosphoproteins, cell membrane phospholipids (Caplan, 2005), adenosine di- and triphosphates (ADP and ATP) which are substantial energy transfer molecules in all living organisms (Werner *et al.*, 1998) as well as regulation of processes such as oxidative phosphorylation (Bose *et al.*, 2003; Phillips *et al.*, 2009), glucose metabolism, and triacylglycerol synthesis (Razzaque, 2011) and by playing a part in regulation of 2,3-diphosphoglycerate (2,3-DPG) which has been shown to be involved in influencing oxygen-carrying capacity of haemoglobin (Bansal, 1990). Pi may also be involved in intracellular cell signalling (Section 1.7). The total body content of Pi in a healthy adult has been estimated to be about 20,000 mmols of which 17,000 and 3,000 mmols exist in the skeleton (in conjunction with calcium in the form of hydroxyapatite) and soft tissues respectively (Ahmed & Behzad, 2011). Only a small part of this is present in the plasma in which the normal concentration range is about 0.8-1.5 mmol/L.

An adult takes in approximately 40 mmols of Pi in their diet daily (e.g. by consuming meat, eggs, nuts, vegetables, fish, and canned food) (González-Parra *et al.*, 2012<sub>a</sub>) and to maintain steady state the same amount needs to be excreted from the body either in faeces (approx. 14 mmol/day) or in the urine (approx. 26 mmol/day) (Ahmed & Behzad, 2011). This indicates the substantial role of the kidneys in maintaining total body Pi level, meaning that defects in

normal renal function culminate in Pi disorders. This means that a reduction in the number of functioning units of the kidney, i.e. nephrons, may lead to mild to severe Pi retention which further results in the increase in the plasma level of Pi which is known as hyperphosphataemia. This abnormality in Pi metabolism has been implicated in increased risk of cardiovascular disease in ESRD (Li *et al.*, 2006) (Sections 1.12, 1.13, and 1.14).

Figure 1.6 depicts organ metabolism of Pi in a healthy adult and Figure 1.7 summarises important organ/membrane transporters involved in controlling Pi homeostasis.

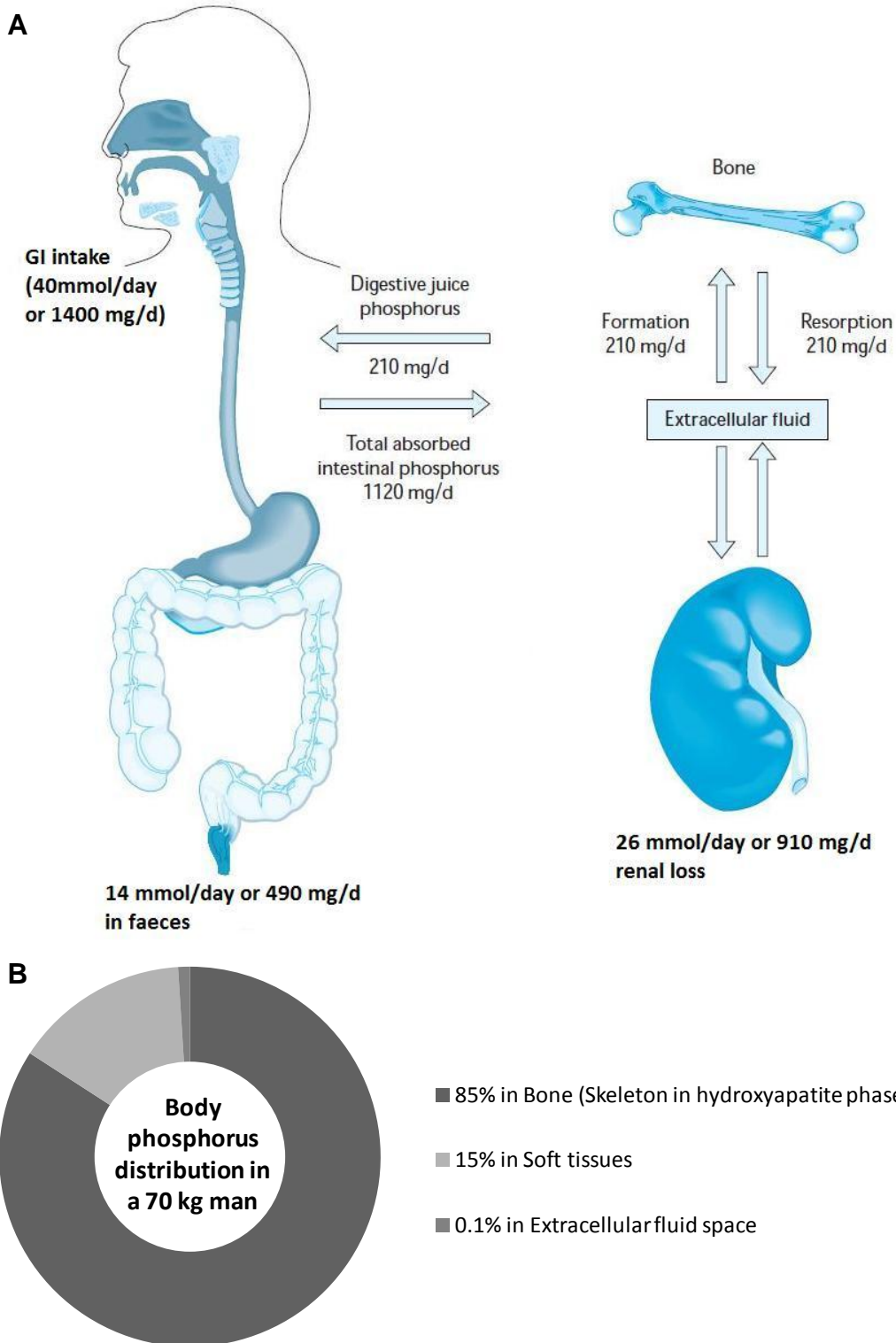


Figure 1.6. Phosphate metabolism/homeostasis and body distribution in a healthy adult. (A) Three major mechanisms of Pi homeostasis have been depicted namely dietary intake, gastrointestinal absorption and renal reabsorption. Picture and data in the figure represent a combination of data and figure obtained from (Ahmed & Behzad, 2011; Levi & Popovtzer, 1999). Masses quoted in mg refer to elemental phosphorus not Pi. (B) Depicts widespread body Pi distribution. Diagram drawn from information given in (Bansal, 1990).

Beside kidneys, which are predominant regulators of Pi homeostasis in the body via reabsorption of Pi from the glomerular filtrate by the tubular epithelial cells (Murer & Biber, 1996); absorption of Pi within the gastrointestinal tract (GIT) following gastrointestinal intake (GI) of Pi plays a substantial role in Pi homeostasis. Defects in any part of these regulatory systems may result in either hypo- or hyperphosphataemia (Levi & Popovtzer, 1999; Bevington *et al.*, 1990; Ahmed & Behzad, 2011).

### **1.6.2 Renal, intestinal, and bone regulation of Pi**

In a healthy individual, the level of intra- and extracellular Pi is precisely regulated in accordance with maintaining the level of it within a normal range (i.e. 0.8-1.5 mM). As described in Figure 1.6 and 1.7., the extracellular Pi concentration is modulated via intestinal absorption of Pi from the diet, bone formation and/or resorption, and excretion in the urine and faeces (Bergwitz & Jüppner, 2011; Ahmed & Behzad, 2011).

The kidneys are the main organs which function to maintain the extracellular Pi concentration. Much of the dietary Pi intake is excreted from body in order to keep the body Pi level normal and herein the Kidneys play a substantial role. The renal proximal tubular epithelial cells express two specialised epithelial sodium dependent Pi co-transporters (i.e. NaPi-IIa and IIc) (Section 1.10.2.2) and also the sodium-dependent PiT-2 transporter (Section 1.10.2.3). NaPi-IIa and IIc together perform active Pi reabsorption from the tubular lumen back into the extracellular fluid. Excess Pi is not reabsorbed from the tubular fluid and is hence excreted in the urine. Regulation of the balance between Pi reabsorption versus excretion requires regulation of the activity of the epithelial sodium-dependent Pi transporters. This involves processes such as the translocation of pre-synthesised Type-IIa sodium-dependent Pi transporter from intracellular compartments to the renal brush border membrane in response to a restricted Pi diet (Lotscher *et al.*, 1997).

Renal Pi handling as well as intestinal absorption and bone resorption imply the existence of a mechanism of Pi sensing by cells of these tissues/organs which are also responding to potent hormonal stimuli such as parathyroid hormone

(PTH), fibroblast growth factor 23 (FGF23), 1,25-dihydroxy-vitamin D (1,25-(OH)<sub>2</sub>-D) (Bergwitz & Jüppner, 2011) and also small molecules (e.g. dopamine) (Kumar, 2009) and metabolic factors (Forster *et al.*, 2013). These involve Pi sensing by a number of different tissues and organ specific Na<sup>+</sup>-dependent Pi co-transporter proteins namely NaPi-I (Type-I), NaPi-II (Type-II), and NaPi-III (Type-III) from the SLC17, SLC34, and SLC20 gene families respectively (Werner *et al.*, 1998; Forster *et al.*, 2013) These transport phosphate in the form of Pi across the plasma membranes in a sodium dependent, secondary-active co-transport manner. These transporters are described in more detail in Section 1.10.2. Besides plasma membrane sodium-dependent Pi transporters, there are other (non-sodium-dependent) Pi transporters in cell compartments for instance in mitochondria (coupled to H<sup>+</sup> and dicarboxylate) and endoplasmic reticulum (coupled to Ca<sup>2+</sup>-ATP<sub>ase</sub>) (Bevington *et al.*, 1992).

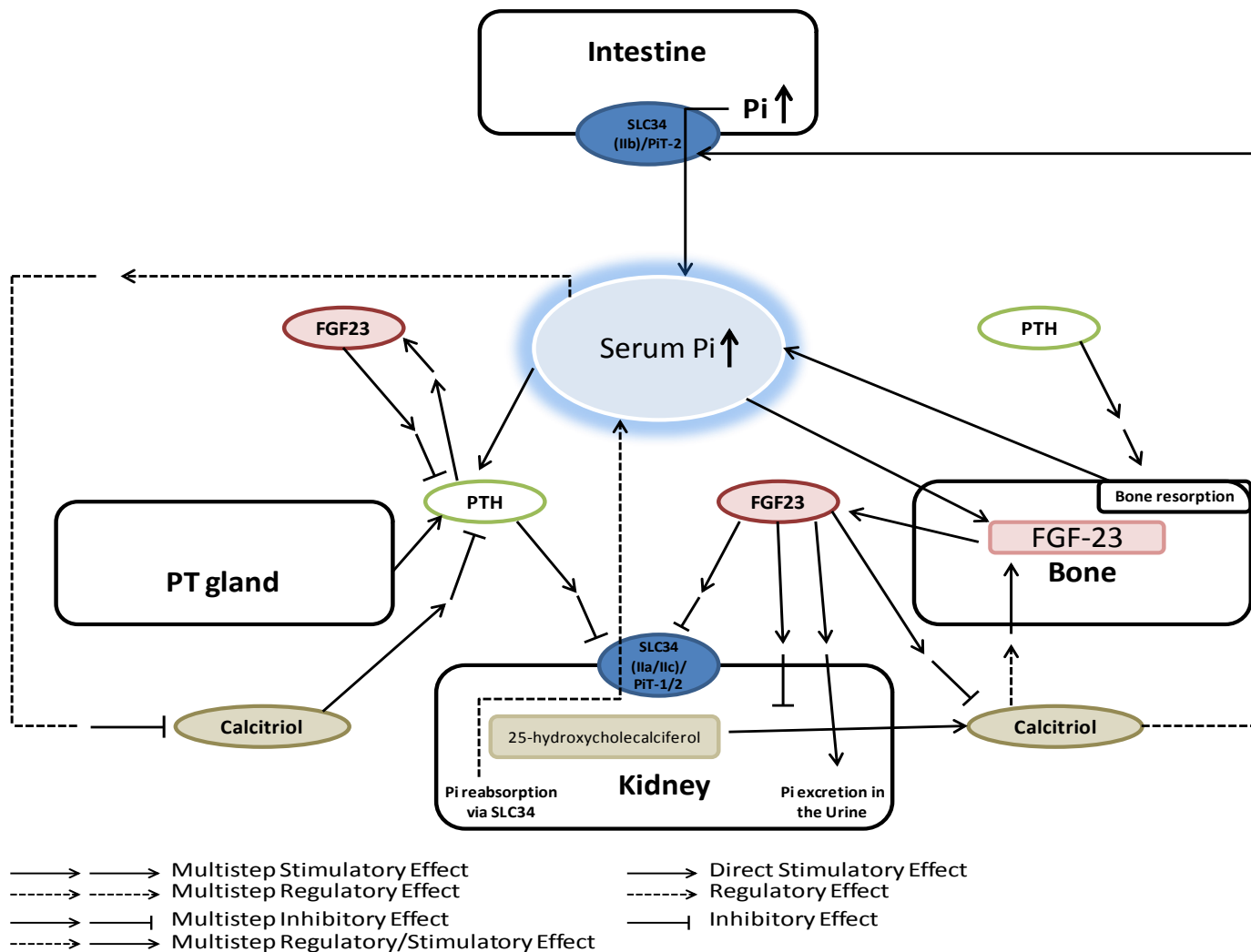


Figure 1.7. Schematic diagram depicting serum Pi homeostasis and possible regulators. Body Pi homeostasis is governed by three main regulatory processes. Intake of Pi through diet, hormonal regulation (e.g. PTH, Calcitriol, and FGF23), and renal excretion. There are also substantial regulatory effects on transport between compartments, for example through NaPi transporters, which contribute to this regulation. See Section 1.6.3 for details. Diagram drawn from information given in references cited in Section 1.6.3.

### **1.6.3 Hormonal regulation of Pi**

As mentioned in Section 1.6., there are a number of hormones and metabolic mechanisms involve in Pi sensing and intracellular Pi homeostasis notably PTH, FGF23, Klotho, and 1,25-(OH)<sub>2</sub>-D<sub>3</sub> which regulate Pi balance within normal physiological range (0.8-1.5mM).

#### **1.6.3.1 Parathyroid Hormone (PTH)**

PTH secretion is regulated by several factors. Important inhibitors of PTH secretion are dietary Pi deprivation and 1, 25-(OH)<sub>2</sub>-vitamin D<sub>3</sub> (Ellam & Chico, 2012). The Pi transporter PiT-1 (of the slc20 gene family) is expressed in parathyroid gland and its expression can be modulated by Pi deprivation and 1, 25-(OH)<sub>2</sub>-vitamin D<sub>3</sub> (Miyamoto *et al.*, 2000). The renal brush border expression/activation of the renal proximal tubular epithelial cells' (PTCs') Pi transporters (i.e. NaPi-IIa) is influenced by PTH level (Tenenhouse, 2005). PTH increases the renal Pi excretion by inhibiting PTC NaPi-dependent Pi reabsorption (Tenenhouse, 2005). The level of PTH may be reduced by an increased level of FGF23 (Isakova *et al.*, 2011). Furthermore, hyperphosphataemia (which can result in a decrease in the free circulating calcium ion concentration - through Pi binding to calcium ions), can signal through PTH secretion, decreased renal Pi reabsorption and resulting increased renal calcitriol output (Figure 1.7) to increase the absorption of calcium from intestine. PTH has been shown to be a CV risk factor and associated with CV mortality and morbidity (Ellam & Chico, 2012).

#### **1.6.3.2 Calcitriol**

Calcitriol also known as 1,25-(OH)<sub>2</sub>-D<sub>3</sub> is the active form of vitamin D in circulation secreted by the kidney and produced from renal 25-hydroxycholecalciferol by the enzyme 1-alpha hydroxylase. Calcitriol is predominately produced by the kidneys but other cells also locally produce this (Ellam & Chico, 2012). The enzyme (i.e. 1-alpha hydroxylase) is expressed in a wide range of cell types like endothelial cells, kidney cells, and vascular smooth muscle cells and therefore provides the local synthesis of calcitriol in organs or tissues other than the kidneys but because these cells lack klotho (Section 1.6.3.4) this local calcitriol synthesis is not responsive to FGF23 (Ellam & Chico,

2012). Low dietary Pi intake resulting in hypophosphataemia has been shown to stimulate renal secretion of calcitriol by increasing the renal expression of 1-alpha-hydroxylase (1 $\alpha$ (OH)ase) which in turn stimulates intestinal NaPi-IIb expression to increase the absorption of Pi (Razzaque, 2011). In addition, 1, 25-(OH)<sub>2</sub>-vitamin D<sub>3</sub> production reduces when kidneys are damaged resulting in hyperphosphataemia and an increased PTH secretion resulting in hyperparathyroidism and increased risk of cardiovascular events (Gansevoort *et al.*, 2013). In addition, the synthesis of calcitriol can be decreased by excessive FGF23 (Isakova *et al.*, 2011).

The largely inactive hydroxylated form of vitamin D (i.e. 25-hydroxyvitamin D) is converted to the active form (1,25-dihydroxyvitamin D) by 1-alpha hydroxylase. A counter-regulatory enzyme (i.e. 24-hydroxylase) also exists, and the balance between these hydroxylases is affected by excess FGF23 resulting in production of 24,25-dihydroxyvitamin D (Ellam & Chico, 2012) (see Section 1.6.3.3 below).

### **1.6.3.3 FGF23**

Fibroblast growth factor 23 (FGF23), the circulating phosphaturic factor produced by bones, inhibits the renal NaPi (i.e. NaPi-IIa and IIc) transport activity (Gattineni *et al.*, 2009) resulting in renal Pi excretion (Yamazaki *et al.*, 2010). Damage to the normal function of the kidneys (as in CKD) results not only in hyperphosphataemia (Section 1.5) but also in an increase in serum concentration of FGF23 (Scialla & Wolf, 2014) and Figure 1.7. FGF23 receptor (FGF23R) is expressed in the kidneys but not in other cells such as endothelial cells (Ellam & Chico, 2012). FGF23 influences metabolism of vitamin D (Quarles, 2008). FGF23 suppresses the renal expression of 1 $\alpha$ -hydroxylase and induces 24-hydroxylase, resulting in decreased 1,25 (OH)<sub>2</sub>D (Yamazaki *et al.*, 2010). Higher levels of FGF23, like higher levels of serum Pi, are associated with the progression of CKD (Isakova *et al.*, 2011). These higher levels of FGF23 may act on renal NaPi transporters (see above) and therefore result in an increase in renal Pi wasting in CKD patients whose serum Pi levels also are elevated. In other words, this increase in FGF23 tends to retain serum Pi levels within physiological range.

The FGF23 gene promoter comprises two vitamin D response elements (VDREs) (Orfanidou *et al.*, 2012) which may contribute to the regulation of FGF23 by calcitriol shown in Figure 1.7. In human embryonic kidney cell line HEK293 cells, FGF23 and extracellular Pi result in enhanced FRS2 $\alpha$ /Erk1/2/Erg1 phosphorylation upon binding of FGF23 to its receptor (FGFR) and its co-receptor Klotho (Yamazaki *et al.*, 2010) (see Section 1.6.3.4 below). Active mutation in the FGF23 gene results in autosomal-dominant hypophosphatemic rickets (ADHR) and inactive mutation of the gene promotes hyperphosphatemic familial tumoral calcinosis (Yamazaki *et al.*, 2010; Bergwitz *et al.*, 2006). An increase in FGF23 levels has been associated with cardiovascular mortality (Scialla & Wolf, 2014) in both CKD patients (Fliser *et al.*, 2007) and in the general population with normal kidney function (Obi & Hamano, 2012; Scialla & Wolf, 2014; Ellam & Chico, 2012) which is thought to work through involvement of higher serum FGF23 levels in left ventricular hypertrophy (Scialla & Wolf, 2014).

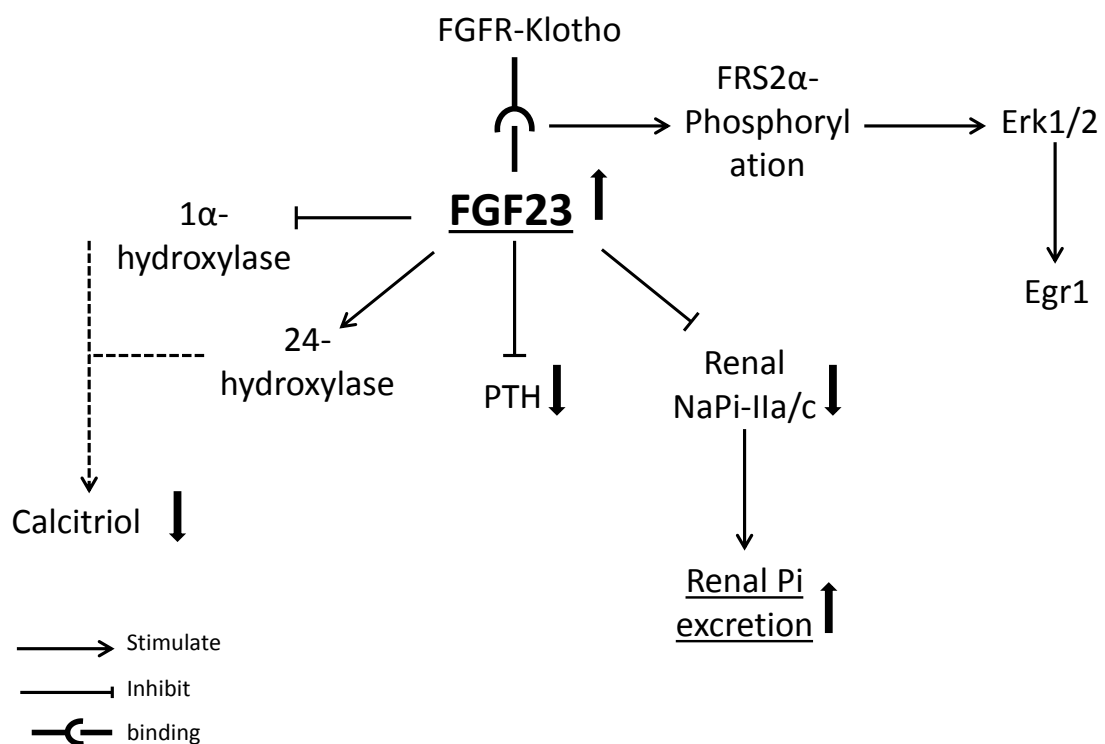


Figure 1.8. Depicts the FGF23 axis. Drawn from information and references provided in Section 1.6.3.3. Early growth response-1 (Egr1) and FGF23 receptor substrate 2 $\alpha$  (FRS2 $\alpha$ ).

#### **1.6.3.4 Klotho**

Klotho is an anti-aging protein which has been implicated in Pi homeostasis through interplay with FGF23 or other hormones involved in Pi homeostasis like 1,25-[OH]<sub>2</sub> vitamin D and PTH (Bian *et al.*, 2014). It can be found in two forms with distinct functions: 1) membrane Klotho and 2) secreted Klotho (Kuro-o, 2010). Membrane Klotho works as a co-receptor for the FGF23 receptors (Ellam & Chico, 2012; Scialla & Wolf, 2014) and co-stimulation of the FGF23-Klotho receptor complex by FGF23 decreases the activity of renal NaPi (NaPi-IIa and IIc) transporters (Gattineni *et al.*, 2009). In this regard Klotho requires FGF23 to exert its function, although the other form of Klotho (i.e. secreted form) may function independent of FGF23 signalling for example by regulating the activity of glycoproteins on the cell surface and growth factor receptors (Kuro-o, 2010) or by attenuating apoptosis and senescence in vascular endothelial cells (Ikushima *et al.*, 2006). In the kidneys, Klotho is expressed in distal tubules of the kidneys where FGFR1 is predominately expressed and therefore the distal tubule is more likely to be the site of FGF23 action (Yamazaki *et al.*, 2010). Polymorphisms in the Klotho gene have been associated with coronary atherosclerosis (Arking *et al.*, 2003).

#### **1.6.4 Regulation by dietary Pi intake**

Dietary Pi contains both organic and inorganic phosphate (Pi) and affects serum Pi levels via gastro-intestinal (GI) absorption of Pi which is mediated by NaPi-IIb transporters (Tenenhouse, 2005; Giral *et al.*, 2009). Organic phosphate in the gut is hydrolysed enzymatically to Pi before being absorbed by the intestine (Gonzalez-Parra *et al.*, 2012<sub>a</sub>). A five-year cohort study looking at the correlation between dietary Pi intake (and/or Pi to protein ratio) and mortality in haemodialysis patients demonstrated that both high Pi and high Pi to protein ratio diets increased death hazard ratios (HR) (Noori *et al.*, 2010). In a culture of rat fibroblasts, Pi deprivation increases the expression of SLC20 Pi transporters (Kavanaugh & Kabat, 1996) however this may not be a general phenomenon in all cell types. Furthermore, dietary Pi affects renal Pi reabsorption. At least part of this effect may be hormonal rather than a direct effect of Pi on renal tubular cells. In healthy individuals, low Pi intake in the diet reduces the level of circulating FGF23 (Isakova *et al.*, 2011) and conversely a diet high in Pi

stimulates FGF23 secretion (Isakova *et al.*, 2011). However, administering lanthanum carbonate as a Pi-binding agent and dietary Pi restriction in pre-dialysis (PD) patients with CKD to reduce and maintain serum Pi level seems not to have any regulatory impact on the level of FGF23 within 24 hours (Isakova *et al.*, 2011).

As will be noted in Section 1.9, part of the effect of dietary Pi may occur through the direct effect of the extracellular Pi concentration on the circulating ionised calcium concentration. High Pi intake, resulting in hyperphosphataemia, decreases the serum calcium concentration which in turn stimulates PTH secretion and contributes to secondary hyperparathyroidism (Ellam & Chico, 2012).

### **1.7 Regulation of cell metabolism and signalling by intracellular Pi (Pi-sensitive enzymes/proteins)**

Pi has ubiquitous roles in cell signalling (possibly though inhibitory effects on phosphotyrosine protein phosphatases (PTPases) and phosphoserine/threonine protein phosphatases (PSPases)), and regulation of cell structure and intracellular energy metabolism (Buzalaf *et al.*, 1998; Szajerka & Kwiatkowska, 1984; Zhang & VanEtten, 1991; Bevington *et al.*, 1992; Khandelwal & Kamani, 1980). If such Pi signalling exists, this needs “Pi sensors” in cells to detect the Pi concentration. Pi serves as an important modulator of the activity of some enzymes and other regulatory proteins (Ahmed & Behzad, 2011; Razzaque, 2011; Brand & Söling, 1975; Beg *et al.*, 1978), which directly turns an enzyme activity either on or off (Bevington *et al.*, 1992) for example rat liver phosphofructokinase (Brand & Söling, 1975) and 3-hydroxy-3-methylglutaryl-(HMG)-CoA-reductase (Beg *et al.*, 1978).

As reviewed previously (Bevington *et al.*, 1992) the concentration threshold at which different enzymes respond to [Pi] is varied. These Pi-responsive enzymes regulate important biological processes namely; anaerobic glycolysis, modulation of oxygen transport, ion transport, phospho-protein turnover, muscle contraction, gluconeogenesis, and mitochondrial, glycogen, glutamine, purine nucleotide, and nucleic acid metabolism (Bevington *et al.*, 1992).

### 1.7.1 Effects of Pi on enzymes regulating protein phosphorylation signals

In principle particularly important Pi-sensitive enzymes are those which regulate cell function by controlling intracellular protein phosphorylation signals. In mammals, there is no evidence of Pi sensitive protein kinases (neither activating nor inhibitory), however Pi can regulate protein-tyrosine phosphatases and serine/threonine phosphatases by inhibiting them (Cole *et al.*, 2004; Zhang & VanEtten, 1991; Buzalaf *et al.*, 1998; Szajerka & Kwiatkowska, 1984; Rath *et al.*, 1995) (Figure 1.9).

The activity of two phosphoprotein phosphatases (PPP) (i.e. PPP-I and PPP-II, EC 3.1.3.16) from rabbit liver have been shown to be inhibited by Pi and pyrophosphate (PPi) while using casein as a substrate. However the effect of Pi on these enzymes was found to depend on the protein substrate: using histone as a substrate, Pi was found to activate these enzymes (Khandelwal & Kamani, 1980). Furthermore, four separate rat liver phosphatases (HMG-CoA-reductase phosphatases) also have been shown to be inhibited in a concentration dependent manner in the presence of Pi (GIL *et al.*, 1982).

Purified PPPs from bovine thyroid (PPP-I, IIA, IIB, and III, EC 3.1.2.16) have been shown to be strongly inhibited by Pi and also by PPi, NaF, and ATP. The inhibitory effect of Pi was reversed by adding  $Mn^{2+}$  but not  $Mg^{2+}$ ,  $Ba^{2+}$ ,  $Cu^{2+}$ ,  $Cd^{2+}$ ,  $Ca^{2+}$ ,  $Zn^{2+}$ , and  $Fe^{2+}$  suggested that Pi may exert metal ion binding effects in modulating these enzymes (Kasai & Field, 1983) possibly via entering the active site to bind to the divalent cation (i.e.  $Mn^{2+}$ ) which is essential for the catalytic function of these enzymes.

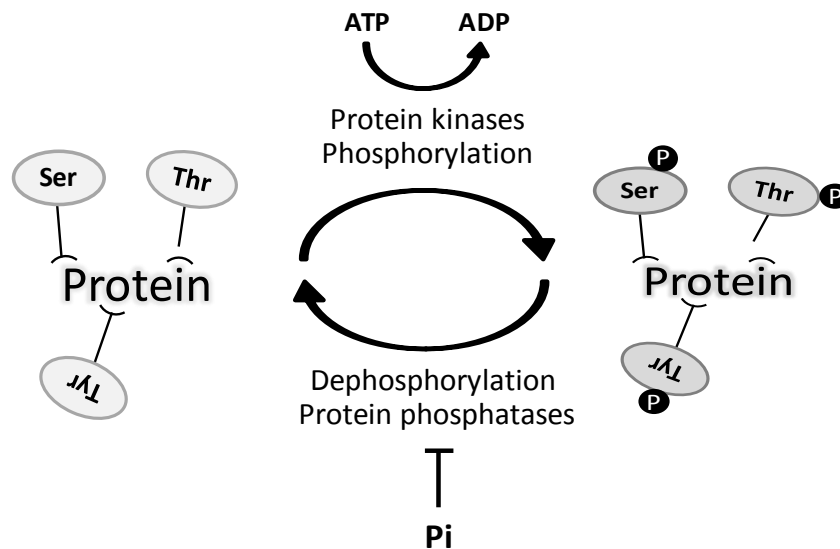


Figure 1.9. Schematic picture of protein phosphorylation/de-phosphorylation. Ser: Serine, Thr: Threonine, Tyr: Tyrosine, P: Phosphate, Pi: inorganic phosphate, ATP: Adenosine triphosphate, and ADP: Adenosine diphosphate.

## 1.8 Probing for intracellular effects of Pi

### 1.8.1 Drugs which should inhibit the transporters

#### 1.8.1.1 Ouabain

Ouabain is a cardiac glycoside (Capella *et al.*, 2001) (see Figure 1.10 for structure) which inhibits the  $\text{Na}^+/\text{K}^+$ -ATPase which is responsible for maintaining the trans-membrane sodium gradient across the plasma membrane (Ogawa *et al.*, 2009) and therefore administering Ouabain collapses the sodium gradient across the plasma membrane. Upon insertion into the transmembrane domain of the sodium-potassium pump, Ouabain antagonises the bound  $\text{K}^+$  therefore resulting in an increased intracellular sodium concentration (Ogawa *et al.*, 2009). The transport of Pi across the plasma membrane into the cytosol depends on the transmembrane sodium gradient (as the transport of Pi through NaPi transporters is driven by this gradient (Section 1.10.2)). Thus, collapsing the plasma membrane sodium gradient using Ouabain should reduce the driving force pumping Pi into the cells, and this is expected to decrease the intracellular Pi concentration and to blunt the increase in intracellular Pi concentration in cells in Pi-loaded medium or in hyperphosphataemia.

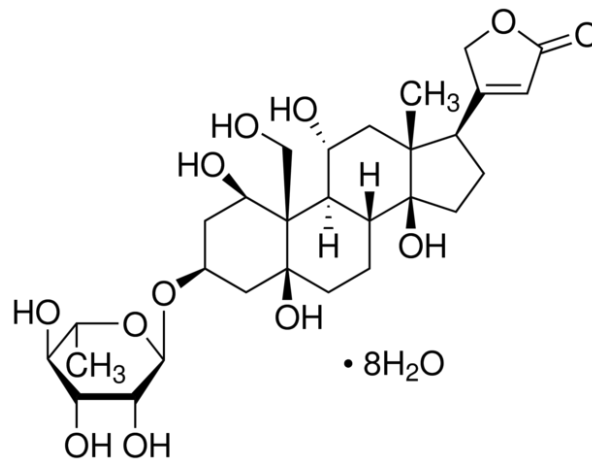


Figure 1.10. A diagram of ouabain structure.

### 1.8.1.2 Phosphonoformate (PFA)

PFA is a structural analogue of Pi in which one hydroxyl group is replaced with a carboxyl group (Villa-Bellosta & Sorribas, 2009) (see Figure 1.11 for structure). PFA is a specific competitive inhibitor of renal NaPi transporters of the SLC34 gene family (Szczepanska-Konkel *et al.*, 1990; Szczepanska-Konkel *et al.*, 1986). However, this inhibitor has been reported to be a less potent inhibitor for PiT (SLC20 family) transporters which serve as Pi transporters in vascular cells (Ravera *et al.*, 2007; Villa-Bellosta *et al.*, 2007). Oocytes expressing PiT proteins treated with 0.3 mM unlabelled Pi in the presence or absence of 1mM PFA showed no statistically significant change in  $^{32}\text{P}$ i uptake which indicates that (at least in this model) this analogue is not a good inhibitor of PiT transporters (Ravera *et al.*, 2007). However, other laboratories have reported apparently successful inhibition of PiT transporters in vascular endothelial cells (Di Marco *et al.*, 2008) and vascular smooth muscle cells (Giachelli, 2003) in which the predominant Pi transporters are members of the SLC20 family. PFA may also however have other biological effects. For example it is also a pyrophosphate (PPi) analogue and like PPi it may have inhibitory effects on calcium phosphate crystal formation (Sage *et al.*, 2011).

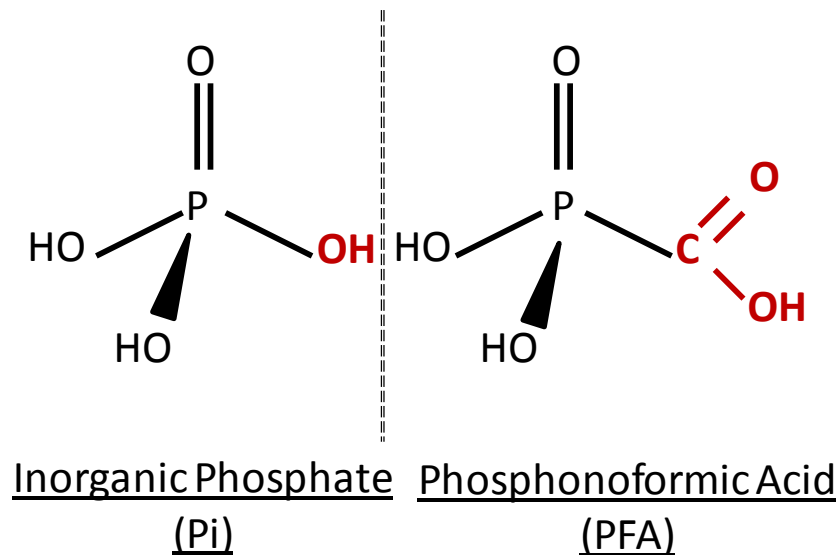


Figure 1.11. A diagram of Pi and PFA structures.

### 1.8.2 Depletion of intracellular Pi by Fructose

It has been shown in liver cells that fructose loading results in an acute intracellular depletion of ATP and Pi depletion (Woods *et al.*, 1970) transiently within as little as 10 minutes. This intracellular Pi sequestration arises from accumulation on fructose-1-phosphate (F-1-P) within cells which is formed by the enzyme fructokinase (Figure 1.12). F-1-P then is converted to a triose sugar by F-1-P aldolase (Aldolase B) and can be further metabolised to pyruvate and lactate (Cox, 2002). Furthermore, AMP deaminase degrades AMP to IMP and increases the uric acid production (Woods *et al.*, 1970). This adenine nucleotide degrading enzyme is inhibited by Pi (and hence activated by Pi depletion) and IMP is a well-known inhibitor of aldolase B in the liver cells. Consequently, sequestration of Pi results in an increase in IMP which inhibits the removal of F-1-P in these cells by inhibiting aldolase B and therefore F-1-P transiently accumulates in the liver cells (Figure 1.12).

This depletion of Pi through F-1-P acting as a Pi sink described within liver cells may also occur in human aortic endothelial cells (HAEC) and fructose has been shown in these cells to induce the inflammatory molecule ICAM-1 which in turn enhances endothelial cell dysfunction and inflammation (Glushakova *et al.*, 2008).

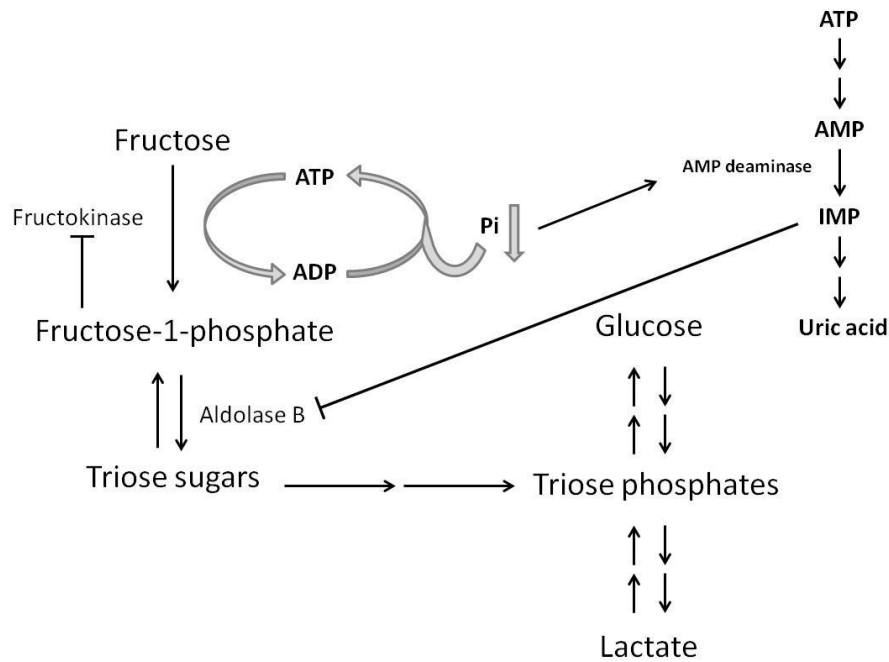


Figure 1.12. Hepatic metabolism of fructose. Fructose is phosphorylated to F-1-P in hepatocytes. Accumulation of F-1-P induces the sequestration of Pi and a drop in intracellular ATP levels. (Diagram drawn from information provided in (Mayes, 1993; Cox, 2002; Woods *et al.*, 1970)).

### 1.9 Extracellular effects of Pi (ionised Ca effects and nanocrystals)

Pi can result in a drop in ionized calcium levels in solution and as a result exerts biological effects on cells via calcium depletion. Consequently high extracellular Pi levels *in vivo* may result in secondary hyperparathyroidism and renal osteodystrophy by lowering the ionised calcium concentration which stimulates PTH secretion. This reciprocal effect of Pi on ionised calcium concentration is known as the “Trade-off hypothesis” (Adler *et al.*, 1985). This complexation of Pi with calcium can also result in Ca-Pi nanocrystal (complex) formation. *In vivo* experiments looking at the effect of Pi on calcium ion concentration showed that the rise in Pi concentration needs to be as great as 1.2mM to result in a significant drop in calcium ion concentration (i.e. 0.025mM) which is enough to induce PTH secretion (Adler *et al.*, 1985) resulting in secondary hyperparathyroidism. However, this drop in Pi concentration *in vivo/ in situ* results in significant changes in serum pH and  $[\text{HCO}_3^-]$  which partly compensates for the drop in ionised calcium concentrations  $[\text{Ca}^{2+}]$  to adjust this back to its normal levels (Adler *et al.*, 1985).

*In vitro* studies using serum-free and protein-free medium, however, indicate that the drop in calcium concentration is not statistically significant over changes in [Pi] from 1 to 2.5mM (having raised Pi from 1 to 2.5mM). This suggests that the effects of such Pi concentration changes studied in this thesis do not arise from changes in the ionised calcium concentration (Adler *et al.*, 1985).

## **1.10 Factors influencing the Pi concentration in mammalian cells**

### **1.10.1 Pi anions and the effect of the membrane potential**

Pi is a major intracellular anion in mammals. Inside-negative membrane potential tends to exclude and repel this negatively charged anion from the cytosol. To overcome this tendency, mammalian cells express active Pi transporters (Section 1.10.2.) which accumulate Pi anions in the cytosol against the electrical gradient of the membrane potential (Bevington *et al.*, 1990; Kemp & Bevington, 1993<sub>a</sub>; Kemp *et al.*, 1988<sub>b</sub>). The SLC (Solute Carrier) transporters consist of 52 gene families that in human comprise about 395 transporter related genes (Hediger *et al.*, 2013). Among all these mammalian SLC transporters, three different families namely SLC17, 20, and 34 have been shown to be responsible for the transport of Pi across the plasma membrane, and are further discussed in the following sections (1.10.2.1 to 3).

### **1.10.2 Active Pi transporters (SLC17/20/34)**

#### **1.10.2.1 SLC17: Type I Na<sup>+</sup>-dependent Pi co-transporters**

This group of transporters comprises nine different but structurally related proteins (Table 1.2. adapted from (SLC TABLES, 2014) and (Reimer, 2013)). The first gene, i.e. the SLC17A1 gene encodes the NPT1 protein which is expressed in kidney, liver, and brain, and is responsible for organic anion, Pi, and chloride transport (Reimer & Edwards, 2004; Reimer, 2013). This transporter was initially identified in an expression cloning study in *Xenopus laevis* oocytes as a Pi transporter (Virkki *et al.*, 2007) but later shown to be more related to organic anion transporters and therefore classified in the vesicular glutamate transporter family (Bellocchio *et al.*, 2000; SLC TABLES, 2014) i.e. not a strict Na<sup>+</sup>-dependent Pi transporter (Reimer & Edwards, 2004; Biber *et al.*, 1993). Therefore this transporter and the other members of this gene family are not further discussed in this thesis.

Gene	Protein	Aliases	Transport type	Substrates	Tissue and cellular expression
<b>SLC17A1</b>	NPT1	NaPi1	electrogenic, Cl-dependent; C/Na <sup>+</sup> ; channel	organic anions, phosphate, chloride	kidney, liver
<b>SLC17A2</b>	NPT3		unknown	unknown	heart, muscle, brain, placenta, lung, liver, kidney, pancreas
<b>SLC17A3</b>	NPT4		electrogenic	organic anions	liver, kidney, small intestine, testis
<b>SLC17A4</b>	Na <sup>+</sup> /PO <sub>4</sub> -cotransporter homologue		unknown	unknown	small intestine, colon, liver, pancreas
<b>SLC17A5</b>	sialin	AST, VEAT	C / H <sup>+</sup>	sialic acid, other acidic sugars	ubiquitous
<b>SLC17A6</b>	VGLUT2	DNPI	electrogenic, Cl-dependent	glutamate	brain (neurons only), endocrine
<b>SLC17A7</b>	VGLUT1	BNPI	electrogenic, Cl-dependent	glutamate	brain (neurons only), endocrine
<b>SLC17A8</b>	VGLUT3		electrogenic, Cl-dependent	glutamate	brain (neurons, glia), liver, kidney
<b>SLC17A9</b>	VNUT		electrogenic, Cl-dependent	purine nucleotides	brain (neurons), adrenal, thyroid

Table 1.2. SLC17 transporters function and tissue distribution adopted from (SLC TABLES, 2014; Reimer, 2013) (URL: <http://slc.bioparadigms.org/> access date 01/04/2015).

### 1.10.2.2 SLC34: Type II Na<sup>+</sup>-dependent Pi co-transporters

Members of the SLC34 gene family (i.e. SLC34A1, SLC34A2, & SLC34A3) encode membrane proteins namely NaPi-IIa, NaPi-IIb, and NaPi-IIc responsible for Na<sup>+</sup>-dependent Pi co-transport in the brush border of proximal tubular cells (SLC TABLES, 2014; Custer *et al.*, 1994; Werner *et al.*, 1998) (Table 1.3). Apart from their Na<sup>+</sup>-dependent Pi transport activity, these 80-90 kDa membrane proteins (with eight membrane-spanning domains) are thought to be N-glycosylated at N<sub>298</sub> and N<sub>328</sub> extracellularly (Murer & Biber, 1996). In 1995, Hayes and colleagues demonstrated that NaPi-II transporter contains several sites of phosphorylation by protein kinase C but not A (Hayes *et al.*, 1995). Using phorbol ester (i.e. 12, 13-didecanoate) as a protein kinase C activator resulted in a time-dependent inhibition of NaPi-II function and transport activity which was prevented by protein kinase C inhibitor staurosporine (Hayes *et al.*, 1995). Type-II NaPi transporter (i.e. NaPi-IIa) undergoes post-translational modification in response to PTH and increased dietary Pi, meaning that PTH and dietary Pi result in internalisation and subsequent lysosomal degradation of NaPi-IIa in brush borders of renal proximal tubular cells which results in a decrease in renal proximal tubular Pi reabsorption (Murer *et al.*, 1999).

Gene	Protein	Aliases	Transport type	Main Substrates	Transport dependency	Tissue and cellular expression	Human gene locus	Reference sequence accession ID
<b>SLC34A1</b>	NaPi-IIa	Napi-3, NPT2, npt2	C / Na, HPO <sub>4</sub> <sup>2-</sup>	Pi (divalent)	Na <sup>+</sup> / Li <sup>+</sup>	kidney (proximal tubule), osteoclasts, neurons	5q35	NM_003052.4
<b>SLC34A2</b>	NaPi-IIb		C / Na, HPO <sub>4</sub> <sup>2-</sup>	Pi (divalent)	Na <sup>+</sup> / Li <sup>+</sup>	small intestine, lung, testis, liver, secreting mammary gland	4p15	NM_006424.2
<b>SLC34A3</b>	NaPi-IIc		C / Na, HPO <sub>4</sub> <sup>2-</sup>	Pi (divalent)	Na <sup>+</sup> / Li <sup>+</sup>	kidney (proximal tubule)	9q34	NM_080877.2

Gene	pH dependency	MW (kDa)	Identification	Substrate affinity at pH 7.4	Functionally	Stoichiometry (Na <sup>+</sup> :Pi)	Post-transcriptional modification
<b>SLC34A1</b>	High	80-90	Functional expression cloning using <i>X.laevis</i> oocytes	100 μM for divalent Pi/ 40 mM for Na <sup>+</sup>	Electrogenic	3:1	N-glycosylation
<b>SLC34A2</b>	High	-	Mouse embryo EST clone	100 μM for divalent Pi/ 40 mM for Na <sup>+</sup>	Electrogenic	3:1	N-glycosylation
<b>SLC34A3</b>	High	75	Human embryo EST clone	100 μM for divalent Pi/ 40 mM for Na <sup>+</sup>	Electroneutral	2:1	N-glycosylation

Table 1.3. SLC34 transporters function and tissue distribution from information provided in (SLC TABLES, 2014; Segawa *et al.*, 2002; Forster *et al.*, 1999; Bacconi *et al.*, 2005). (URL: <http://slc.bioparadigms.org/> access date 01/04/2015)

### **1.10.2.3 SLC20: Type III Na<sup>+</sup>-dependent Pi co-transporters**

#### **1.10.2.3.1 Introduction**

Pi is an important structural and metabolic anion whose regulation and homeostasis is narrowly regulated by absorption of dietary Pi by the gut and reabsorption by the kidneys. In the proximal tubular cells (PTC) of the kidneys the reabsorption of Pi is through mainly type-II sodium-dependent Pi co-transporters (i.e. NaPi-IIa and -II-c) while absorption in the gut and intestine is mediated via NaPi-IIb type-II transporters (see the previous section). These type II transporters mediate trans-epithelial Pi transport, but a different family of transporters is mainly responsible for secondary-active transport of Pi across the plasma membrane of other cell types in mammals against a chemical and electrical gradient. This further family of sodium-dependent Pi co-transporters is the type-III sodium-dependent Pi transporters belonging to class twenty of the solute carrier transporters (i.e. SLC20). This group consists of SLC20A1 and SLC20A2 genes which encode PiT-1 and PiT-2 proteins respectively (SLC TABLES, 2014). PiT-2 alongside with NaPi-IIa and NaPi-IIc are the most abundant Pi symporters in the kidney while PiT-1 is documented to have a broad spectrum expression in nearly all tissues/organs and cell types.

Gene	Protein	Aliases	Transport type	Substrates	Tissue and cellular expression	Human gene locus
<b>SLC20A1</b>	PiT-1	gibbon ape leukemia virus receptor 1, GLVR1, Glvr1, FLJ41426, DKFZp686J2397	C / Na <sup>+</sup> , H <sub>2</sub> PO <sub>4</sub> <sup>-</sup>	Pi (monovalent)	widely expressed	2q13
<b>SLC20A2</b>	PiT-2	amphotropic murine leukemia virus receptor 2, GLVR2, Glvr-2, MLVAR	C / Na <sup>+</sup> , H <sub>2</sub> PO <sub>4</sub> <sup>-</sup>	Pi (monovalent)	widely expressed, kidney (proximal tubule)	8p111

Gene	Reference sequence accession ID	pH dependency	MW (kDa)	Identification	Substrate affinity at pH 7.4	Functionally	Stoichiometry (Na <sup>+</sup> :Pi)
<b>SLC20A1</b>	NM_005415	Nothing significant	74	Functional expression cloning using X.laevis oocytes	≤100 μM for monovalent Pi/ 50 mM for Na <sup>+</sup>	Electrogenic	2:1
<b>SLC20A2</b>	NM_006749	Nothing significant	70-75	Functional expression cloning using X.laevis oocytes	≤100 μM for monovalent Pi/ 50 mM for Na <sup>+</sup>	Electrogenic	1:1

Table 1.4. SLC20 transporters function and tissue distribution adopted from (SLC TABLES, 2014) and information provided in Section 1.10.2.3. (URL: <http://slc.bioparadigms.org/> access date 01/04/2015)

#### **1.10.2.3.2 Tissue distribution of SLC20 family of Pi transporters**

Apart from spleen (Werner *et al.*, 1998), SLC20 transporters have a wide tissue expression and hence this suggests that they may play a 'Housekeeping' role in Pi homeostasis, maintaining intracellular Pi concentration (Nishimura & Naito, 2008; Ravera *et al.*, 2007). As mentioned earlier (Sections 1.6.2, 1.6.4 and Figure 1.7), PiT-2 is expressed in the PTCs of the kidney and plays an important role in Pi reabsorption besides NaPi-IIa and NaPi-IIc. Both transporters are also involved in intestinal absorption of Pi which is mediated mainly by NaPi-IIb. In addition, PiT proteins are responsible for Pi homeostasis in bone, soft tissue, brain, vascular smooth muscle cells (VSMCs), and vascular endothelial cells (VECs) (Nishimura & Naito, 2008; Di Marco *et al.*, 2008; Li *et al.*, 2006).

As this kind of transporter is expressed in diverse tissues/organs, and may be important in controlling the distribution of Pi across the plasma membrane, any defects in the regulation of these co-transporter proteins or the expression of mutated proteins may in principle cause mild to severe pathophysiological conditions, resembling the tissue effects of hypo- or hyperphosphataemia (i.e. disorders of Pi homeostasis) (Bevington *et al.*, 1990).

#### **1.10.2.3.3 Structure, topology and homologues of SLC20 (PiT) proteins**

Protein glycosylation studies, epitope tagging of N- and C- termini, and computer based analysis of PiT proteins/amino acid sequences over the past two decades suggest that the two members of SLC20 sodium-coupled Pi transporters, i.e. PiT-1 and PiT-2, have multiple membrane spanning regions (Kavanaugh & Kabat, 1996). They have been predicted to have two hydrophobic domains which span the membrane 10-12 times and are linked with an extracellular hydrophilic loop (Werner *et al.*, 1998) (Figure 1.13). They share about 25% sequence homology with a putative Pi permease of *Neurospora crassa* (Pho-4<sup>+</sup>) (Kavanaugh & Kabat, 1996; Johann *et al.*, 1992) and were first described as cell-surface receptors for viruses Glvr-1 and Rmp-1 (Section 1.10.2.3.4). The predicted 679- and 656-amino acid proteins for PiT-1 and PiT-2 respectively (Miller *et al.*, 1994; O'Hara *et al.*, 1990) are thought to have a mass of 70 kDa while glycosylated (Farrell *et al.*, 2002) with a reduced

molecular weight after treatment with N-glycosidase F (Farrell *et al.*, 2002). On Western blots, PiT proteins appear as a 70 kDa protein (Dai *et al.*, 2013; santa cruz biotechnology, 2014). NH<sub>2</sub> and COOH termini have been proposed to be extracellular and there is a large intracellular loop (Forster *et al.*, 2013) (Figure 1.13).

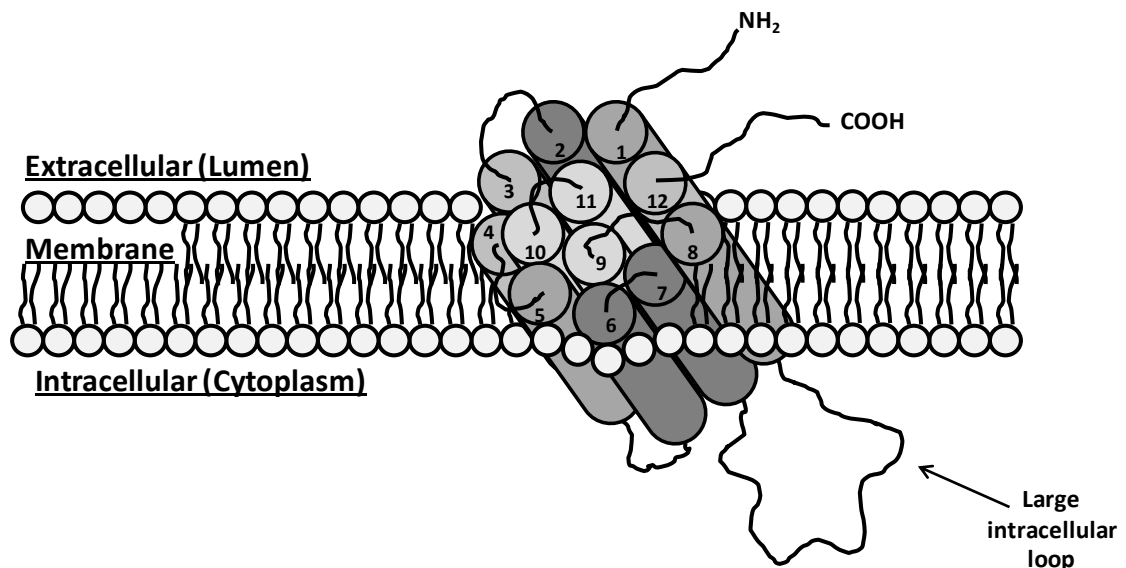


Figure 1.13. Cartoon demonstrating schematic topology/structure of Type-III Sodium-dependent Pi transporters. Picture redrawn from information provided in Section 1.10.2.3.3 and (Forster *et al.*, 2013).

#### 1.10.2.3.4 Functions of SLC20 (PiT) proteins

In mammals, there are dual functions for PiT proteins which were initially characterised from their role as gamma-retrovirus receptors (Section 1.10.2.3.4.1) and later on a Pi transport activity was also attributed to these proteins (Section 1.10.2.3.4.2). Recent studies indicating new emerging functional roles and properties for PiT transporters are described below (Section 1.10.2.3.4.3) (Miller & Miller, 1992).

##### 1.10.2.3.4.1 Functions of SLC20 (PiT) proteins as a viral receptor

SLC20 transporters were initially identified as membrane retroviral receptors for gamma-retroviruses like gibbon ape leukaemia virus (Glv-1) (O'Hara *et al.*, 1990) and rat amphotropic retrovirus (Ram-1) (Miller *et al.*, 1994). Infection with these viruses depends upon an initial interaction between the host cells and the viruses, which is believed to be mediated through cellular receptors which have been shown to be SLC20 or PiT transporters (Farrell *et al.*, 2009). Homology

studies revealed sequence similarities between Ram-1 and Glvr-1 with Pho-4<sup>+</sup> (a gene implicated in phosphate uptake in *Neurospora crassa*) which suggested that these virus receptors may serve as ion transporters as well (Johann *et al.*, 1992; Miller *et al.*, 1994). Two important stretches of amino acid residues, i.e. 550 to 558 and 232 to 260, collectively referred to as region A and B respectively, have been shown to serve virus entry at a post-binding step for the former (i.e. region A) and virus binding and entry for the latter (i.e. region B) (Farrell *et al.*, 2002). With the CHO cell line as an exception; all mammalian cells so far studied are susceptible to murine leukaemia virus infection (Salaun *et al.*, 2001). The apparent resistance of CHO hamster cells to Ram-1 infection may occur through secretion of a soluble-factor by these cells which impairs virus envelope-cell receptor interaction necessary for virus binding and entrance (Miller & Miller, 1992; Miller & Miller, 1993).

#### **1.10.2.3.4.2 Functions of SLC20 (PiT) proteins as Pi transporters**

Back in 1994 Olah and colleagues demonstrated that gibbon ape leukemia virus receptor (Glvr-1) functions as a human Pi transporter (Olah *et al.*, 1994). Furthermore, by expression cloning using oocytes of *Xenopus laevis*, two classes of retroviral receptors Glvr-1 and also Ram-1 were identified to express high affinity Na<sup>+</sup>-dependent Pi symport activity (Kavanaugh *et al.*, 1994). Glvr-1 and Ram-1 were later on classified as type-III sodium-dependent Pi co-transporters.

The Type-III family of Pi transporters includes SLC20A1 and SLC20A2 which encode PiT-1 and PiT-2 membrane-spanning proteins respectively (SLC TABLES, 2014; Forster *et al.*, 2013). These two membrane proteins share about 60% sequence homology (Collins *et al.*, 2004) and enable Pi entry into the cells (Forster *et al.*, 2013). Amino acid sequence analysis revealed two conserved residues within human PiT-1 and PiT-2 transporters which are critical for Pi transport function, namely glutamate (E<sub>70</sub>) and histidine (H<sub>502</sub>) for PiT-1 and PiT-2 respectively (Bottger & Pedersen, 2011).

#### **1.10.2.3.4.3 Other possible functions of PiT proteins**

Creation of mouse conditional and null alleles of PiT-1 demonstrated a non-redundant role of PiT-1 in embryonic development (Festing *et al.*, 2009). Furthermore, RNA interference studies targeting PiT-1 silencing in HeLa and HepG2 cells have shown that PiT-1 plays an important role in cell proliferation and signalling regardless of its transport activity and independent of PiT-2 transporter (Beck *et al.*, 2009). Furthermore PiT-1 depletion delays the cell cycle, tumour growth, mitosis, and cytokinesis (Beck *et al.*, 2009).

PiT transporter proteins are also thought to play substantial roles in extracellular matrix and cartilage calcification (Cecil *et al.*, 2005; Kobayashi *et al.*, 2014). In addition, high Pi-induced VSMC calcification is inhibited by PFA, suggesting PiT-mediated VSMC calcification (Villa-Bellosta & Sorribas, 2009).

#### **1.10.2.3.5 Kinetics of SLC20 (PiT) proteins**

Functional expression cloning using *Xenopus laevis* oocytes revealed that at pH 7.5, SLC20 transporters (PiT-1 and PiT-2) display apparent substrate affinities of approximately  $\leq 200\mu\text{M}$  and  $50\text{mM}$  for monovalent Pi and  $\text{Na}^+$  as substrates respectively (Ravera *et al.*, 2007). The transport activity of these transmembrane proteins depends on a trans-membrane sodium gradient, although  $\text{Li}^+$  may also substitute for  $\text{Na}^+$  but with reduced transport rate (Ravera *et al.*, 2007). PiT transporters stoichiometrically transport monovalent Pi with a 2:1  $\text{Na}^+:\text{Pi}$  ratio (Figure 1.14 and Table 1.4) and are not significantly sensitive to pH, although the apparent Pi affinity is reported to be reduced in the pH range 6.2-6.8 to about  $50\mu\text{M}$  (Ravera *et al.*, 2007). Some studies also indicate that alkaline pH and phosphonoformic acid (PFA) (see also Section 1.8.1.2) inhibit these transporters (Collins *et al.*, 2004; Denison *et al.*, 2009).

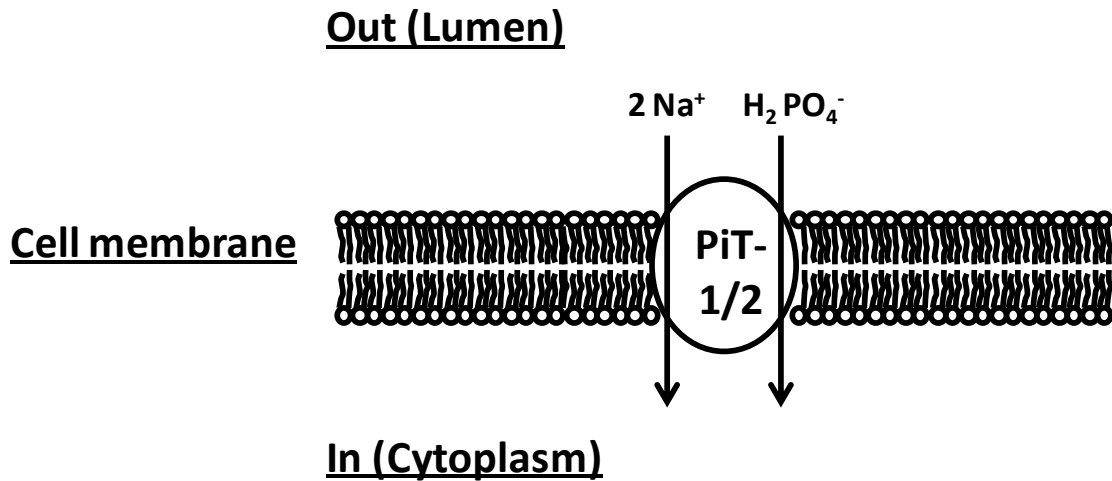


Figure 1.14. Type-III of Na<sup>+</sup>-dependent Pi symporters. Two members of the SLC20 Pi transporters, i.e. PiT1 and PiT-2, transport Pi actively in a pH insensitive and electrogenic manner with 2:1 Na<sup>+</sup>:monovalent Pi stichiometry.

#### **1.10.2.3.6 Regulation of SLC20 transporters though phosphorylation and/or de-phosphorylation**

PiT-1 and PiT-2 amino acid sequences include several susceptible phosphorylation sites for protein kinases between residues 250 and 450 of these transporters' cytoplasmic domains (Jobbagy *et al.*, 1999). Activating protein kinase C $\epsilon$  (PKC $\epsilon$ ) by phorbol 12-myristate 13-acetate (PMA) in NIH 3T3 cells has been shown to enhance Pi uptake through PiT-2 but not PiT-1 (Jobbagy *et al.*, 1999). Furthermore, it has been shown that p38 mitogen-activated protein kinase (MAPK) undergoes phosphorylation following PiT-1 depletion (Beck *et al.*, 2009). This depletion in PiT-1 has been shown not to have any impact of Erk1/2 (Beck *et al.*, 2009). In HEK293 cells (which have a low expression level of klotho) a higher extracellular [Pi] has been shown to increase the phosphorylation of FGF23 receptor subunit 2 $\alpha$  (FRS2 $\alpha$ ) and PiT-1 via Raf/MEK/ERK signalling pathway and increased expression of early growth response-1 (EGR1) (Yamazaki *et al.*, 2010).

## **1.11 The Cardiovascular system and the endothelium**

### **1.11.1 Introduction**

The cardiovascular system (composed of the heart, the blood vessels; including arteries, capillaries, and veins, and the blood, plays an integral role in transporting essential material including nutrient substances and oxygen to body organs and tissues and eliminating metabolic byproducts from them (Figure 1.15). The transport and exchange of substances between the vascular vessels and tissues and underlying cells happens through the blood which fills the blood vessels (Koeppen & Stanton, 2009). There are two major types of circulation which propel blood through the lungs and to all other tissues and organs of the body namely the pulmonary and systemic circulation.

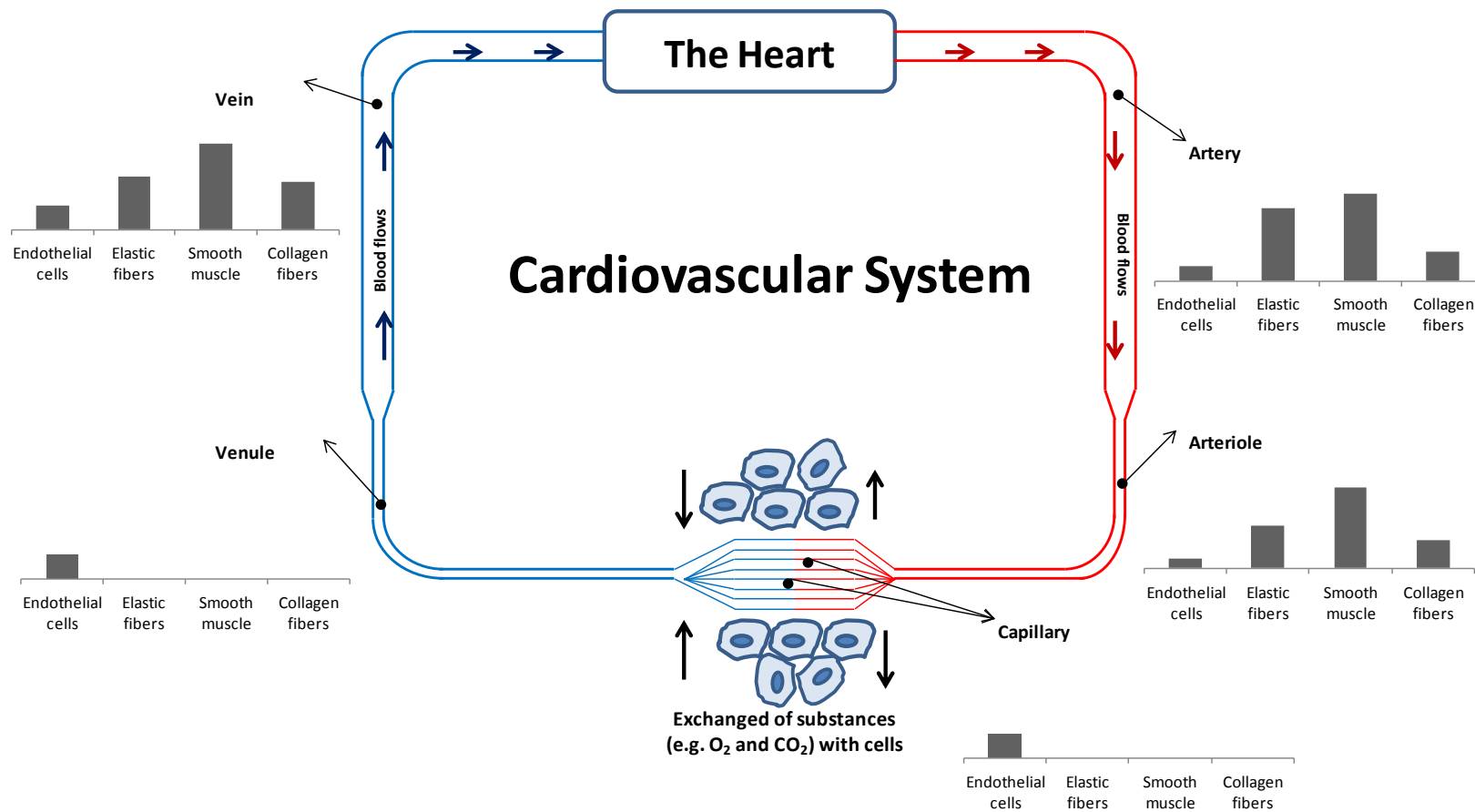


Figure 1.15. Schematic structure of the cardiovascular system. The artery, arteriole, venule, and vein can have a wide range of diameter and thickness from as small as 8 $\mu$ m diameter and 0.5 $\mu$ m thickness in a capillary to 30mm diameter and 1.5mm thickness in vena cava. A vein is 5mm diameter and 0.5mm thickness (**y-axes of each histogram depict the relative amounts of the constituents of each blood vessel shown on the x-axes** (redrawn from (Koeppen & Stanton, 2009))).

### 1.11.2 Structure of blood vessels

Blood vessel walls are constructed of three main layers namely; the tunica intima, media, and adventitia (Figure 1.16). Blood vessels are lined by the endothelium comprising a layer of endothelial cells.

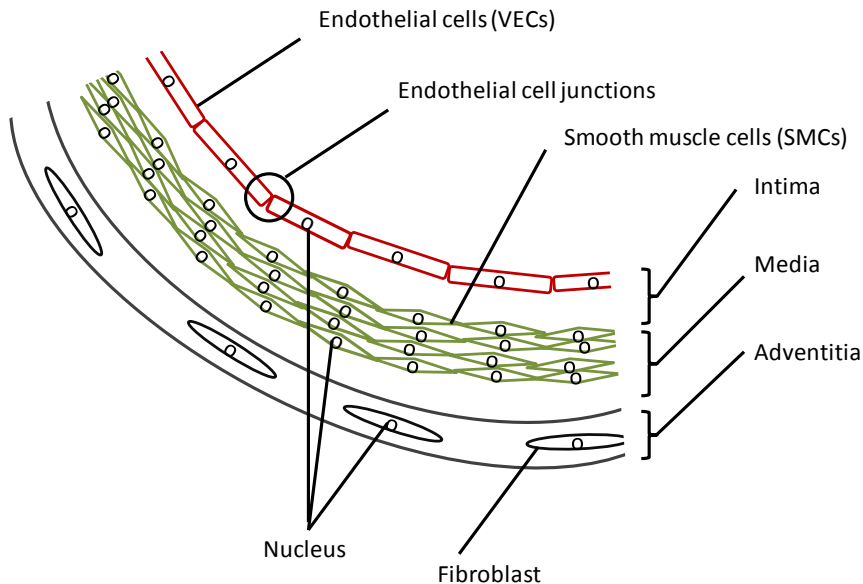


Figure 1.16. Schematic structure of the blood vessel wall. The blood vessel walls are constructed of 1) tunica intima; comprising endothelial cells and internal elastic membrane. Endothelial cell junctions consist of e.g. VE-CD144 (cadherin) (Dejana *et al.*, 2008) and VE-CD146 (Bardin *et al.*, 2001), 2) tunica media: consisting of smooth muscle cells, and 3) tunica adventitia; fibroblasts, elastic/collagen fibers, and external elastic membrane.

### 1.11.3 The endothelium

Endothelial cells are positioned at the interface between blood and tissues and comprise a layer of cells which is actively involved in blood haemostasis, immune function, and inflammatory reactions and responses (Galley & Webster, 2004). In humans this layer consists of about  $10^{13}$  cells and weighs approximately one kilogram (Galley & Webster, 2004). The cells arise from embryonic haematopoietic cells (Choi *et al.*, 1998) and produce nitric oxide (NO),  $\text{PGI}_2$ , and endothelium-derived hyperpolarizing factor (EDHF) which regulates the vascular tone (Figure 1.16) (Galley & Webster, 2004; Stankevičius *et al.*, 2003). They also express and produce a number of adhesion molecules and cytokines (Table 1.5) and are therefore involved in an array of pro- and anti-inflammatory responses (Galley & Webster, 2004). The normal function of endothelial cells is dependent on a number of factors, for example the

bioavailability of NO which is an important endothelium-derived vasoactive factor with vasodilatory and antiatherosclerotic properties (Fliser *et al.*, 2003) and also prevents platelet activation (van Hinsbergh, 2012). The synthesis of this endothelium-derived factor is regulated by asymmetric dimethylarginine (ADMA) which is an endogenous inhibitor of NO synthase (NOS) (Boger, 2004), the enzyme which is involved in conversion of L-arginine to NO and L-citrulline (Figure 1.17) (Palmer *et al.*, 1988). Endothelial cells can be activated in response to an array of inflammatory cytokines, metabolic stress, hypoxia, ischaemia, and vasoactive agents (Semenza, 2010; Matsubara & Ziff, 1986; Schulz *et al.*, 2008) but depending on whether the cells have an arterial or venous location (van Hinsbergh, 2012). However DNA microarray analysis of fifty-three cultured EC cell lines (arteries, veins, and microvascular ECs) showed that different endothelial cells express different gene expression profile (Chi *et al.*, 2003) which suggest this fact that depending on the type, different endothelium lines may respond to a particular metabolic stress or intervention differently. Endothelium, principally, controls the haemostasis by the control of blood coagulation, platelet adhesion and activation, fibrinolysis, platelet disintegration, and vasoregulation (van Hinsbergh, 2012). The Extrinsic coagulation pathway requires the availability of an initiator which is the transmembrane glycoprotein tissue factor (TF) expressed by some endothelial cells and other tissues which initiate coagulation by constructing a complex with coagulation factors (i.e. FVII/VIIa, FIXa, and FX) which eventually results in the formation of fibrin clot and coagulation (Eilertsen & Østerud, 2004; McVey, 1999).

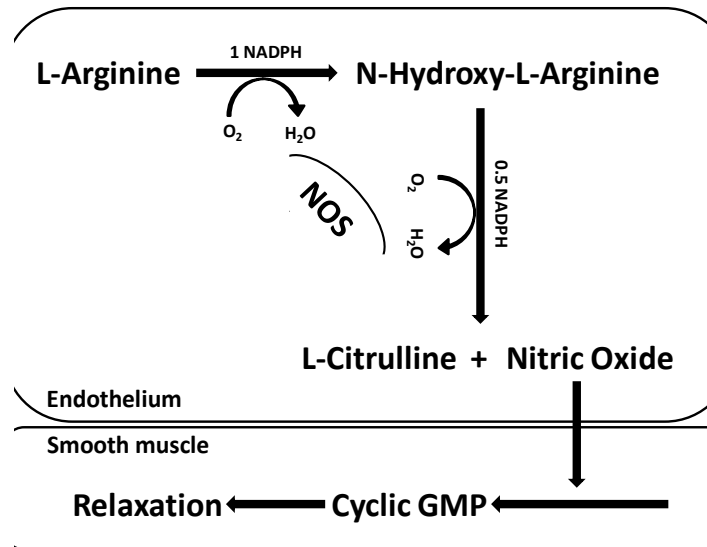


Figure 1.17. Schematic presentation of the conversion of L-arginine to NO and endothelium-dependent smooth muscle cell relaxation. Endothelial cells together with the underlying smooth muscle cells modulate the blood vessel tension by vasoregulation. In endothelial cells, the conversion of L-arginine to NO mediated by NOS activates soluble guanylyl cyclase and the removal of calcium ions by cyclic GMP (cGMP) and prevention of contractile apparatus and relaxation of smooth muscle cells (Lincoln *et al.*, 1994; Moncada *et al.*, 1991)

<b>Mediator/antigenic markers</b>	
<b>Procoagulant factors</b>	von Willebrand factor Thromboxane A2 Thromboplastin Factor V Platelet activating factor Plasminogen activator inhibitor
<b>Growth factors</b>	Insulin like growth factor Transforming growth factor Colony stimulating factor
<b>Vasoconstricting factors</b>	Angiotensin converting enzyme Thromboxane A2 Leukotrienes Free radicals Endothelin
<b>Vasodilators</b>	Nitric oxide Prostacyclin
<b>Inflammatory mediators</b>	Interleukins 1, 6, 8 Leukotrienes MHC II
<b>Lipid metabolism</b>	LDL-receptor Lipoprotein lipase
<b>Matrix products</b>	Fibronectin Laminin Collagen Proteoglycans Proteases
<b>Antithrombotic factors</b>	Prostacyclin Thrombomodulin Antithrombin Plasminogen activator Heparin
<b>Specific/selective antigens</b>	CD31 CD54 CD62e CD105 CD106 CD141 CD144 CD146

Table 1.5. Some important mediators and antigenic markers secreted/expressed by the endothelial cells. Endothelial cells secrete an array of mediators and express a variety of specific and selective antigenic markers which determine their cellular function and recognition in the human body. Table constructed from data in (Thambyrajah *et al.*, 2000; Landray *et al.*, 2004; Peters *et al.*, 2003; Galley & Webster, 2004).

## **1.12 CVD risk factors in CKD**

### **1.12.1 Traditional risk factors**

Aging, diabetes, hypertension, dyslipidemia, and smoking are considered as traditional factors increasing the CV mortality and morbidity (Stenvinkel *et al.*, 2008; Yamamoto & Kon, 2009) (Figure 1.18). In CKD patients, impaired HDL cholesterol function and extended LDL cholesterol oxidation result in abnormal and atherogenic lipid profiles (Gansevoort *et al.*, 2013). The association of decreased kidney function/filtration and Pi retention are, however, independent of diabetes, hypertension, and smoking even though these traditional CV risk factors receive considerable attention in control and management of CVD in CKD.

### **1.12.2 Novel and Non-traditional (Uraemic) risk factors**

Novel and Non-traditional (uraemic) risk factors (accelerating the progression of CV complications) are emerging and are increasingly regarded as important in CKD progression. These include abnormalities in calcium and Pi homeostasis, proteinuria, albuminuria and anaemia, oxidative stress, hyperhomocysteinaemia, uraemic toxins, chronic inflammation, and abnormal lipoprotein levels (Covic *et al.*, 2009; Stenvinkel *et al.*, 2008) (Figure 1.18). The circulating level of ADMA is also affected by CKD as this inhibitor of endothelial NO synthase is primarily regulated by the kidneys and if kidney function fails, the level of this factor increases in circulation (Leone *et al.*, 1992).

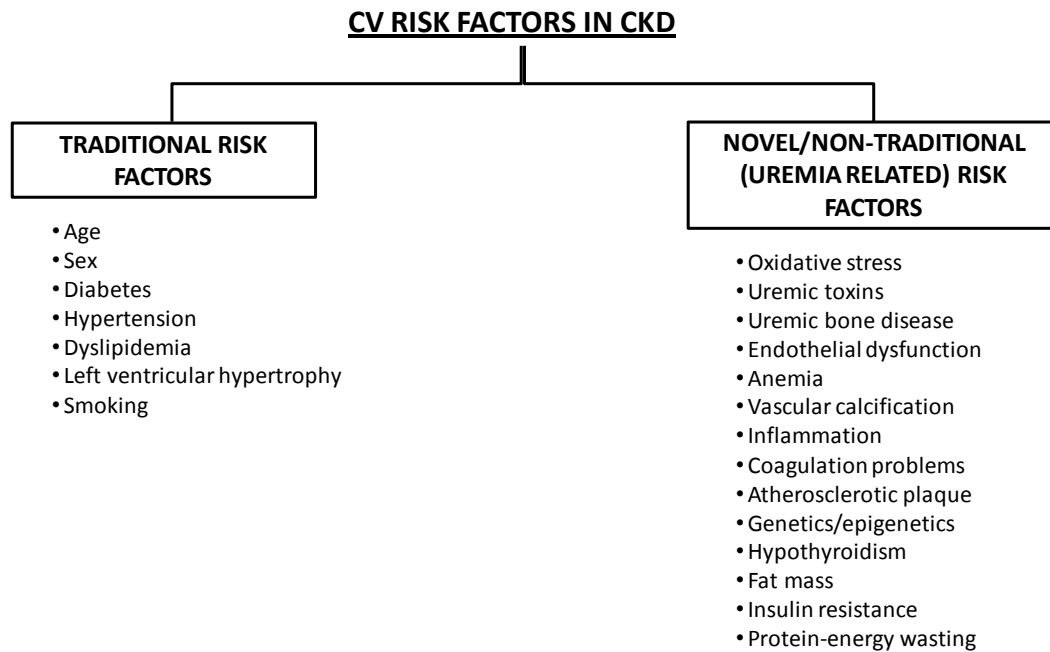


Figure 1.18. Traditional, novel and uraemia related CV risk factors in CKD. Major cardiovascular traditional risk factors and novel and uraemia-driven risk factors are depicted. (Drawn from the information in (Stenvinkel *et al.*, 2008); Figure1).

### 1.13 CVD in CKD and the role of Pi

First reported in 1836 (Bright, 1837; Gansevoort *et al.*, 2013) it is now widely accepted that CKD patients are at high risk of CV mortality including stroke, peripheral vascular disease, coronary artery disease, arterial stiffness, vascular calcification, and sudden death. Reports indicate that about half of patients with CKD die from CV complications even though they do not die from their kidney failure *per se* (Covic *et al.*, 2009). The CV risk in CKD patients is multifactorial (Gansevoort *et al.*, 2013). One possible reason behind increased incidence of heart disease amongst CKD patients is persistent exposure to traditional (Section 1.12.1) and non-traditional (Section 1.12.2) CV risk factors (Covic *et al.*, 2009) besides decreased eGFR and increased albuminuria (Gansevoort *et al.*, 2013). Since decreased eGFR is associated with mineral disturbances and abnormalities including retention of Pi, which starts occurring after filtration falls (i.e. CKD3; eGFR 30-60 mL/min per 1.73m<sup>2</sup>) (Gansevoort *et al.*, 2013), and is thought to play a significant part in developing heart diseases and an increased CV mortality and events. When eGFR falls as far as 30 ml/min per 1.73m<sup>2</sup> (i.e. CKD4/5), approximately half of the CKD patients start developing left-ventricular hypertrophy and a decreased expression of endothelial NO synthase which is

driven partly because of hypertension in these patients (Gansevoort *et al.*, 2013). At least *in vitro* it is known that Pi inhibits NO synthase in endothelial cells (Shuto *et al.*, 2009) and hyperphosphataemia occurs as eGFR falls below 30-60 ml/min per 1.73m<sup>2</sup>. Taken together it can be concluded that hyperphosphataemia plays a substantial role in left-ventricular hypertrophy and coronary endothelial dysfunction even in early stages of CKD. Thus, even slight increase in serum Pi levels may require clinical attention.

In CKD patients another important factor is the fact that endothelial survival factor (i.e. angiopoietin-1) and the pro-inflammatory angiopoietin-2 undergo modulations. The former decreases while the latter rises to a high level (Shroff *et al.*, 2013; David *et al.*, 2010). This results in an inducible negative effect on normal endothelial and vascular function.

In advanced stages of kidney disease serum Pi level rises to as high as 2.5mM referred to as hyperphosphataemia (Section 1.5). Several reports have shown a prominent contributing role for an elevated serum Pi level in vascular smooth muscle cells (VSMCs) calcification *in vivo* and *in vitro* (Giachelli, 2003). Hyperphosphataemia is associated with severe arterial calcification in patients with chronic kidney disease (CKD) which arises because of osteochondroblastic transformation and calcification in vascular smooth muscle cells (VSMCs) (Giachelli, 2003).

## **1.14 The mechanism of cardiovascular damage in hyperphosphataemia**

### **1.14.1 The “Classical” explanation: Pi and soft tissue calcification of atheromatous plaques**

In CKD patients, as well as the general population with normal kidney function, vascular calcification is a strong predictor of cardiovascular mortality and events. It is now recognised that hyperphosphataemia plays a contributing and substantial role in the molecular mechanisms underlying this life-threatening pathologic condition (Marulanda *et al.*, 2014; Giachelli *et al.*, 2005). The severity of vascular calcification, in CKD patients has been shown to be higher than in the general population. In a study (Oh *et al.*, 2002) of 39 CKD patients with a

childhood-onset of CKD, ranging in age between 19-39, and duration with CKD between 7-34 years, it was shown that comparing to matched controls these patients have developed more incidence of coronary artery calcification and increased carotid arteries intima-media thickness (IMT). The onset of calcification and carotid IMT in these patients has been shown to be associated with non-traditional and uraemia-related CV risk factors for instance serum calcium-phosphate products and dialysis. However the carotid IMT also correlated with traditional CV risk factors (Section 1.12.1). Among this study population, however, the severity of CV mortality depended on the CKD stage of each individual, with more severe outcome in those undergoing dialysis than those received kidney transplantation. The serum Pi in these patients was  $1.72 \pm 0.31$  mM in dialysis patients,  $1.55 \pm 0.36$  mM in post-transplantation patients, and  $1.08 \pm 0.27$  mM in healthy controls which was shown to be significantly higher in the CKD population compared to controls. This indicates that high serum Pi might play a substantial part in developing coronary artery calcification and carotid IMT besides other contributing risk factors (e.g. serum calcium, PTH, albumin, and creatinine).

In another study (Schwarz *et al.*, 2000), with 54 older participants (around  $69 \pm 14$  years old) were studied of which 27 had kidney diseases and the rest were control patients with coronary artery disease but with no kidney problem recorded. Coronary intima-media thickness was shown to be higher in kidney patients comparing to controls, however the increase in media thickness was more profound compared to intima thickness of coronary arteries. Furthermore, the composition of plaques in these two study groups (i.e. CKD and non-CKD patients with coronary artery disease) were different, meaning that the former developed calcified plaques whereas the latter's plaques were mostly fibroatheromatous. Interestingly, it has been shown that the mineral in the calcified plaques of CKD patients with hyperphosphataemia was mostly composed of calcium-phosphate and hydroxyapatite but the presence of calcium-oxalate crystals was not observed, suggesting elevated serum Pi but not oxalate in CKD patients is deposited with calcium in coronary arteries possibly contributing to an increased risk of CV mortality.

Taken together (Schwarz *et al.*, 2000; Oh *et al.*, 2002) these studies indicate that CKD patients with hyperphosphataemia are at more risk of excessive vascular calcification and atherogenic complications comparing to patients with no apparent kidney function problems. The exact mechanisms, however, are still elusive, though prolonged exposure to CV risk factors (as discussed in Section 1.12) may be a crucial contributor.

### **1.14.2 Newer views**

#### **1.14.2.1 A new variant of the “classical” explanation. CaPi nanocrystals as biological stimulus acting on cells**

In CKD patients with hyperphosphataemia, SMCs undergo osteogenic gene expression alterations, resulting in VSMC osteogenic differentiation and calcification which is manifested by morphological changes from SMCs to osteochondrocyte like cells (Giachelli, 2003). The possibility of calcium-phosphate (CaPi) nanocrystals (about 160nm in diameter) acting on vascular cells was first considered by (Sage *et al.*, 2011) who examined the stimulatory effect of CaPi nanocrystals, (derived from hyperphosphataemic milieu from cultured mouse aortic smooth muscle cells (MASMCs) *in vitro*), on bone morphogenetic protein-2 (BMP-2) and osteopontin (OPN) gene expression. These two major genes involved in the process of osteogenic differentiation and calcification show increased expression under hyperphosphataemic conditions *in vitro* (Sage *et al.*, 2011). The over-expression of the former gene in hyperphosphataemic milieu has been demonstrated to be reversed in the presence of Pi analogue pyrophosphate (PPi) which serves as a so-called “crystal poison” inhibiting CaPi nanocrystal formation. This apparent effect of CaPi nanocrystals on osteogenic gene upregulation (i.e. BMP-2, OPN but not osterix “Osx”, core-binding-factor- $\alpha$ 1 “Cbfa1”) ceased after removal of nanocrystals from the medium. Incidentally, synthetic hydroxyapatite nanocrystals at greater than 25 $\mu$ g/mL have also been shown to mimic stimulatory effects of CaPi nanocrystals on BMP-2 and OPN expression in MASMCs. *In vitro* effects of high Pi on calcium deposition on MASMCs were abolished in the presence of pyrophosphate and fetuin-A which both inhibit mineralisation. Furthermore, in their system (Sage *et al.*, 2011) the authors

show that this effect of high Pi on MASMCs calcification is time and dose dependent. Interestingly, the effect of high Pi on calcium deposition has been shown to be independent of the presence of cells (i.e. MASMCs and HEK-293 cells) suggesting that a cell-independent mechanism like direct interaction between calcium and Pi is involved in this process. Taken together, these data suggested that rather than soluble Pi in high Pi medium, it is CaPi nanocrystals that modulate the expression levels of osteogenic genes in these cells and that this mechanism rather than cell involvement *per se* governs this process.

Furthermore, osteoblastic differentiation and calcification of VSMCs have been suggested to be partly mediated by secretion of some inflammatory mediators like TNF $\alpha$  from cells of the monocyte/macrophage lineage which further results in an enhanced calcification of vascular cells (Nadra *et al.*, 2005). *In vitro* internalisation of CaPi microcrystals by human monocyte-derived macrophages has been demonstrated to trigger intracellular signalling through PKC and downstream ERK1/2 activation resulting in secretion of some pro-inflammatory cytokines namely TNF $\alpha$ , IL-1 $\beta$ , and IL-8. These pro-inflammatory cytokines secreted following internalisation of CaPi microcrystals by macrophages activated cultured endothelial cells (i.e. HUVECs) to over-express E-selectin, P-selectin, VCAM-1, and ICAM-1 in a time dependent manner to recruit leukocytes under haemodynamic shear flow (Nadra *et al.*, 2005). The extent and the speed of monocyte/macrophage lineage response to CaPi microcrystals however tended to depend on the size of the particles with more severity in the smallest (<1 $\mu$ m diameter) particles' size range (Nadra *et al.*, 2005; Ewence *et al.*, 2008).

As Pi plays an inevitable part in formation of these co-called CaPi nanocrystals and/or microcrystals and these crystals have been implicated in the pathogenesis of atherosclerotic plaque destabilisation and vascular cell death (Ewence *et al.*, 2008), secretion of pro-inflammatory cytokines and activation of endothelial cells (Ewence *et al.*, 2008; Nadra *et al.*, 2005), and modulation in osteogenic gene expression and calcium deposition even in the absence of

cells (Sage *et al.*, 2011), these suggest a crucial contribution to Pi's mechanism of action to some extent independent of Pi influx into the cells.

#### **1.14.2.2 Pi as the “new cholesterol”- may exert clinically important effects even within the normal range of plasma Pi concentration**

For many years the general assumption with regards to the level of Pi, accounting for increased CV events (especially with regard to vascular calcification), was that modest to severe hyperphosphataemia in CKD patients was required for CV events to occur. However, over the past decade a mounting body of evidence has suggested that higher serum Pi levels even well within the normal range (especially close to the upper-limit of 1.5mM; normal range is 0.8-1.5mM) are also significantly associated with an increased CV risk and poor cardiac outcomes in patients with or without kidney diseases (Ellam & Chico, 2012; Lee *et al.*, 2012) and therefore this is referred to as a “stealthier” killer by some authors (Gonzalez-Parra *et al.*, 2012<sub>b</sub>). In a population-based study consisting of 8953 participants with normal kidney function, high serum Pi levels greater than 1.3mM were shown to be associated with elevated low-grade albuminuria (LGA) (Lee *et al.*, 2012) which *per se* increases the risk of CV events and mortality (Danziger, 2008). In another population-based cohort study consisting of 13,340 subjects, higher serum Pi levels were shown to be associated with increased CV risk (i.e. carotid intima-media thickness (cIMT)) independent of participants' eGFR, hypercholesterolemia, diabetes, age, sex, and hypertension (Onufrak *et al.*, 2008). Additionally, in a study on patients with coronary disease but no record of overt hyperphosphataemia, it has been shown that higher Pi levels well within the normal range are associated with all-cause mortality and cardiovascular outcomes (Tonelli *et al.*, 2005). Foley, *et al.*, 2009, demonstrated that there is a link between higher serum Pi levels and increased coronary atherosclerosis in a large population of young adults with no concomitant kidney disease and overt hyperphosphataemia (Foley *et al.*, 2009).

Taken together, these data imply that high Pi levels within the normal range (e.g.  $\geq 1.3 \leq 1.5$  mM) may accelerate the onset and development of CV mortality in the general population with or without kidney diseases.

These rather novel and newer emerging effects of high serum Pi levels within the normal range on poor cardiac output and CV risks might be attributable to multimechanism effects of high Pi on modulation of hormones which are responding to cellular shifts of Pi (i.e. phosphatonins; Section 1.6.3). These may include (but are not restricted to) inhibition of 1,25-dihydroxyvitamin D synthesis (Portale *et al.*, 1989) and increased PTH (Smogorzewski *et al.*, 1993) both of which are considered as predictors of cardiovascular mortality in populations without kidney disease (Ellam & Chico, 2012). Other Pi-sensitive hormones also implicated to be affected with Pi in the general population with normal kidney function include for example FGF23 (Section 1.6.3.3) where high serum Pi levels have been reported to increase the level of such a phosphatonin enough to increase the risk of CV mortality (Gonzalez-Parra *et al.*, 2012<sub>b</sub>).

In 2012, Ellam and colleagues reviewed Pi as a “new cholesterol” meaning that just like cholesterol (i.e LDL cholesterol), intervention to manage Pi even though the level is not particularly high, but within the normal physiological range, may benefit the general population and prevent development of atherosclerotic vascular mortalities (Ellam & Chico, 2012). The unhealthy lifestyle of modern human such as frequency of having canned products and prepared food which are all rich in Pi and/or Pi-containing preservatives, and on the other hand emerging evidence shedding light on effects of high Pi levels in vascular biology and pathobiology such as athero-occlusive phenomena, suggests that intervention to manage serum Pi levels might have vascular benefits even in the general population (Ellam & Chico, 2012).

#### **1.14.2.3 Pi may be toxic in its own right, possibly through intracellular effects**

Elevated serum Pi levels for prolonged periods may exert toxic and damaging effects on blood cells and underlying endothelial and smooth muscle cells. As

reviewed elsewhere (Razzaque, 2011) these might include (but are not restricted to) an impaired cell signalling, increased cell death, impaired fertility, renal dysfunction, vascular calcification, premature aging (Ohnishi & Razzaque, 2010; Yamada *et al.*, 2014), increased tumorigenesis, and enhanced systemic inflammation and malnutrition (Yamada *et al.*, 2014). However this is still an open debate and direct proof of these proposed effects is still the subject of research. Klotho knockout mice demonstrated features of premature aging and a reduced life span. Klotho and NaPi-IIa knockout mice (i.e. favouring Pi excretion), recovered from these features, however feeding these double-knockout animals with high dietary Pi supplements restored premature aging-like features, indicating that premature aging in these animals is predominantly Pi toxicity dependent (Ohnishi & Razzaque, 2010). In a recent study (Yamada *et al.*, 2014) feeding rats (i.e control and adenine-induced CKD rats) with 0.3% to 1.2% dietary Pi concentrations for two months, serum and tissue levels of TNF- $\alpha$  were increased. In this study the apparent Pi toxicity involved premature aging-like phenotypes, vascular calcification, malnutrition, and mortality without any effect on kidney function. All of the observed Pi-induced changes were blunted after feeding animals (i.e. CKD rats with 1.2% Pi-containing diet) with 6% lanthanum carbonate as a Pi binder.

*In vitro* elevated Pi has been reported to result in a decrease in nitric oxide (NO) production (Shuto *et al.*, 2009), an enhanced reactive oxygen species (ROS) generation (Shuto *et al.*, 2009; Di Marco *et al.*, 2008) and induction of apoptosis (Di Marco *et al.*, 2008; Peng *et al.*, 2011) in endothelial cells. On the other hand, others also have shown that increase in extracellular Pi enhances autophagy in endothelial cells (ECs) (Hsu *et al.*, 2014) and also vascular smooth muscle cells (VSMCs) (Dai *et al.*, 2013). In ECs Pi-induced autophagy has been shown to be mediated through an inhibitory effect of Pi on Akt/mTOR signalling pathway (Hsu *et al.*, 2014). Induction of autophagy in endothelial cells, however, has also been shown to diminish Pi-induced apoptosis (Hsu *et al.*, 2014) which indicates that in the presence of autophagy, apoptosis may be a less significant contributor to Pi toxicity in ECs. Shuto and colleagues 2009 demonstrated that bovine aortic endothelial cells (BAECs) exposed to high Pi generate ROS via

NADPH oxidase in a process dependent on Pi influx into the cells; and in these cells higher extracellular Pi has been shown to have an inhibitory phosphorylation effect on nitric oxide synthase (NOS) by activating PKC resulting in a decreased NO production. The apparent induction of reported apoptosis in endothelial cells (Di Marco *et al.*, 2008) has been reported to be partly ROS mediated.

### **1.15 Management of hyperphosphataemia**

Dietary interventions to control serum Pi levels such as protein diet restriction has been shown to be associated with greater risk of mortality in CKD patients (Shinaberger *et al.*, 2008) however a course of Italian Mediterranean Diet (IMD) received by healthy individuals and CKD patients (stage 2 and 3) showed that in both study groups IMD reduced serum Pi and microalbuminuria levels and decreased the progression of CKD and CVD risk (De Lorenzo *et al.*, 2010).

Most prominent measures that nephrologists have taken to control the hyperphosphataemia in CKD patient are through prescribing Pi binders (e.g. Pi binders including sevelamer (Tonelli *et al.*, 2010)) and dietary Pi restriction (Martin & Gonzalez, 2011). Pi binders are classified into calcium-containing and calcium-free Pi binders (Tonelli *et al.*, 2010) however using Pi binders in CKD patients remains controversial (Navaneethan *et al.*, 2009) suggesting that newer interventions and more detailed trials need to be considered.

### **1.16 Cell Membrane Derived Microparticles (MPs)**

#### **1.16.1 Introduction**

As early as 1967, platelet derived membrane vesicles, less than 0.1µm in diameter, were reported in human plasma and have been called “platelet dust” (Marja J. VanWijk, *et al.*, 2003). This early term, has been largely replaced by the more modern term Microparticles (MPs) and/or Microvesicles (MVs) (Abbasian *et al.*, 2012; Burton *et al.*, 2013). First discovered in 1946 (CHARGAFF & WEST, 1946) MPs are submicron membrane derived vesicles which have been reported to be released from plasma membrane of a number of different cells including (but not restricted to) endothelial cells (Chironi *et al.*,

2009), vascular smooth muscle cells (Essayagh *et al.*, 2005; Flynn *et al.*, 1997), platelets (Horstman & Ahn, 1999; Burnouf *et al.*, 2014), leukocytes (Mesri & Altieri, 1999; Mesri & Altieri, 1998), erythrocytes (van Beers *et al.*, 2009; Camus *et al.*, 2012), and lymphocytes (Mostefai *et al.*, 2008) following cell growth, activation, and apoptosis (i.e. cell compromised particle release) (Chironi *et al.*, 2009; Marja J. VanWijk, *et al.*, 2003). Their putative size range is from 0.1- 1 $\mu$ m (Abbasian *et al.*, 2012; Batool *et al.*, 2013) however in some reports also their size is reported to be from 50nm to 1 $\mu$ m (Burnier *et al.*, 2009). They have been named after their cells of origin, for instance, Endothelial Microparticles (EMPs); MPs derived from the endothelium (Brodsky *et al.*, 2004), Platelet Microparticles (PMPs); MPs derived from the blood platelets (Burnouf *et al.*, 2014), and Red Blood Cell Microparticles (RMPs); MPs derived from the red blood cells (Tissot *et al.*, 2010; Donadee *et al.*, 2011). MPs exist in the blood of healthy individuals (Berckmans *et al.*, 2001) but their number in circulation has been reported to go up under certain disease and/or stress conditions for example; End Stage Renal Disease (ESRD) and Chronic kidney disease (CKD) (Burton *et al.*, 2013; Faure *et al.*, 2006; Boulanger *et al.*, 2007), Pre-eclampsia (González-Quintero *et al.*, 2003), Cardiovascular disease (CVD) (Blann *et al.*, 2009; Morel *et al.*, 2005; VanWijk *et al.*, 2003), Diabetes (Jung *et al.*, 2011; Sabatier *et al.*, 2002; Tramontano *et al.*, 2010), Severe hypertension (Preston *et al.*, 2003), Metabolic Syndrome (MS) (Ueba *et al.*, 2008), Infectious and inflammatory disease (Andriantsitohaina *et al.*, 2012; Ardoin *et al.*, 2007), and Vascular dysfunction and remodelling (Agouni *et al.*, 2008; Burnier *et al.*, 2009; Chironi *et al.*, 2010).

### **1.16.2 Clinical Importance of MPs**

Considerable interest has been shown in MPs in the past decade by many clinicians and related scientists in the fields of Cardiovascular Diseases (CVD) and Renal Medicine in particular due to their possible early diagnostic value in these diseases' progression and development. The importance of MPs is not solely restricted to their role as a biomarker (Burger *et al.*, 2013) of endothelial dysfunction (Nozaki *et al.*, 2009), but also more recently has been extended to their role as potential biological messengers (Hoyer *et al.*, 2010), having a part in pathological angiogenesis (Brill *et al.*, 2005; Kim *et al.*, 2004; Mezentsev *et*

*al.*, 2005; Weber & Mause, 2011), vascular integrity dysfunction (Tual-Chalot *et al.*, 2010; George, 2008), inflammation (Ardoin *et al.*, 2007; McGregor *et al.*, 2006; Puddu *et al.*, 2010; Buesing *et al.*, 2011; Batool *et al.*, 2013) and also as drug-delivery vehicles (Tang *et al.*, 2012; van Dommelen *et al.*, 2012). Improved knowledge of MPs' formation, structural composition, sites of effects, biological effects and monitoring their plasma level in individuals susceptible to diseases such as ESRD (Dursun *et al.*, 2009), CVDs (Dursun *et al.*, 2009), Multiple Sclerosis (MS) (Chironi *et al.*, 2009), Pulmonary Arterial Hypertension (PAH) (Tual-Chalot *et al.*, 2010), and a number of other associated complications may open the door to more effective therapeutic approaches and earlier detection strategies in the above named complications.

### **1.16.3 *In vivo* and *in vitro* MP stimuli**

MPs are shed from the surface of their parent cells (e.g. platelets and endothelial cells) in response to a wide range of physiological and artificial stimuli. Several cytokines, stress stimuli and apoptosis inducers (for examples; TNF- $\alpha$ , IL1 $\beta$ , Menadione, and H<sub>2</sub>O<sub>2</sub>) may induce MP formation from cells *in vitro* and *in vivo* (Table 1.6). Other stimuli capable of inducing MP formation *in vitro* have been proposed, such as endothelial nitric oxide synthesis (NOS) disruption (Chironi *et al.*, 2009) which may exert its impact on MP liberation through disrupting the intact structure of the vascular endothelium. More recently, uraemic toxins also have been shown to be able to induce release of membrane vesicles from the cells of the vascular system (Chironi *et al.*, 2009) which will be discussed in more detail in the following section (Section 1.16.6.1).

	Stimuli	Reference
<b>Vitro</b>	Calcium ionophore (A23187)	(Yin <i>et al.</i> , 2008)
	TNF- $\alpha$	(Banfi <i>et al.</i> , 2005; Faure <i>et al.</i> , 2006)
	Thrombospondin-1 (TSP-1)	(Camus <i>et al.</i> , 2012)
	LPS	(Weisshaar <i>et al.</i> , 2013)
	C5b-9	(Wiedmer <i>et al.</i> , 1990)
	ROS (H <sub>2</sub> O <sub>2</sub> -induced ROS)	(Houle <i>et al.</i> , 2007)
	Uremic toxins (indoxyl sulphate, p-cresol, homocysteine)	(Faure <i>et al.</i> , 2006; Zhu <i>et al.</i> , 2012)
<b>Vivo</b>	Thrombospondin-1 (TSP-1)	(Camus <i>et al.</i> , 2012)
	Shiga toxin-induced haemolytic uraemic syndrome (STEC-HUS)	(Ge <i>et al.</i> , 2012)
	Thrombin (serine protease of the clotting cascade)	(Batool <i>et al.</i> , 2013)
	ADP	(Batool <i>et al.</i> , 2013; Gawaz, 2001)
	LPS	(Weisshaar <i>et al.</i> , 2013)
	C5b-9	(Wiedmer <i>et al.</i> , 1990)

Table 1.6. Some *in vivo* and *in vitro* MP stimuli.

#### 1.16.4 MP structure, composition and surface markers

MPs are cell membrane blebs without a nucleus that have a bilayered phospholipid membrane (Morel *et al.*, 2011). The structure and composition of them depend strongly on their cellular origin and the way that they have been formed (e.g. cell activation or apoptosis (from compromised cells)). MPs have been reported to express aminophospholipids (i.e. phosphatidylserine (PSer) (Lacroix & Dignat-George, 2012) and phosphatidylethanolamine (PE) (Larson *et al.*, 2012)) on their surface.

MPs contain mRNA, miRNA, DNA, protein, lipids and other cytoplasmic/cell surface marker(s) from their parent cells (Table 1.7) and therefore are considered to be potent bioactive messengers influencing the activities of their potential target cells (Puddu *et al.*, 2010; Hoyer *et al.*, 2010).

In this laboratory (Chapter 5-Figure 5.14) and others (Banfi *et al.*, 2005) it has been shown that MPs contain Histones. In 2005, Cristina Banfi and colleagues (Banfi *et al.*, 2005) demonstrated that TNF- $\alpha$  stimulated human endothelial cells (HUVECs) to generate MPs that express an array of cytoskeleton components (e.g. actin, myosin, and vimentin), chaperones (e.g. stress-70 protein and 47, 27, and 10 kDa heat shock protein), nucleosome components (e.g. Histones), enzymes (e.g. GAPDH, pyruvate kinase), vesiculation markers (e.g. annexin A2 and A1), protein folding promoters (e.g. calnexin precursor), signalling

molecules (e.g. Ras-related protein Ral-A), and other proteins (e.g. collagen-binding protein2 precursor) as determined by MALDI and LC-MS/MS. Furthermore, some MPs have been reported to be Tissue Factor (TF) positive (Aharon *et al.*, 2009) while some other MPs may have binding sites for classical pathway complement protein C1q (Peerschke *et al.*, 2008).

Platelet-derived MPs have been shown to comprise platelet membrane constituents for example P-selectin (Zeiger *et al.*, 2000; van der Zee *et al.*, 2006), glycoproteins (GP) Ib, IIb-IIIa (i.e. integrin  $\alpha_{IIb}\beta_3$ ) (Peerschke *et al.*, 2008). In patients with peripheral arterial disease, PMPs have been shown to be significantly P-selectin positive (Zeiger *et al.*, 2000; van der Zee *et al.*, 2006) and therefore may modulate the activation of the alternative pathway of the complement (Peerschke *et al.*, 2008). GP IIb-IIIa has been implicated in platelet adherence to human artery sub-endothelium, and its deficiency has been shown to be associated with loss of platelet adhesion and aggregation in blood (Sakariassen *et al.*, 1986). Furthermore, active conformation (conformational change) of the GP IIb-IIIa (Caen & Rosa, 1995), presented on the surface of platelets, has been demonstrated to be responsible for PMP formation; and it is the main receptor for fibrinogen binding on platelets (i.e. through amino acid sequence arg-gly-asp "RGD" of fibrinogen) (Marja J. VanWijk, *et al.*, 2003). This has been shown by excessive loading of RGD to saturate RGD-fibrinogen binding sites on platelets, and interestingly both binding of fibrinogen to the activated platelets and PMP formation have been shown to be blunted, indicating a crucial role of active form of GP IIb-IIIa on platelets for MP formation and fibrinogen binding (Marja J. VanWijk, *et al.*, 2003).

MPs (and some special cells including platelets and endothelial cells) have been shown to express gC1qR (Yin *et al.*, 2008), a cellular protein that is ubiquitously expressed and can enhance C1q (of the classical complement pathway) binding on expressing cells/particles and activate C1 of the complement pathway (Peerschke *et al.*, 2006). Table 1.7 presents some important detection markers of MPs.

Surface expressing molecule/protein	Definition or Alternative Name	Type of MP	Reference
CD3		T cells	(Takeshita <i>et al.</i> , 2014)
CD31	PECAM:platelet-endothelial cell adhesion molecule		(Takeshita <i>et al.</i> , 2014)
CD36	Cluster of differentiation 36	Platelet and Endothelial cells	(Alkhatatbeh <i>et al.</i> , 2013)
CD41	GPIIb	Platelet	(Yin <i>et al.</i> , 2008)
CD42a		Platelet	(Burton <i>et al.</i> , 2013)
CD45		Leukocyte	(Faure <i>et al.</i> , 2006)
CD54	ICAM-1:intercellular adhesion molecule 1		(Simak <i>et al.</i> , 2006)
CD55		Platelet	(Yin <i>et al.</i> , 2008)
Cd59		Platelet	(Yin <i>et al.</i> , 2008)
CD62E	E-selectin	Endothelial cells	(Lee <i>et al.</i> , 2012)
CD62P	P-selectin		(van der Zee <i>et al.</i> , 2006; Zeiger <i>et al.</i> , 2000)
CD105	Endoglin, a proliferation-associated molecule		(Brogan <i>et al.</i> , 2004)
CD144	VE-cadherin	Endothelial cells	(Burton <i>et al.</i> , 2013; Dursun <i>et al.</i> , 2009)
CD146	S endo 1, an endothelial junctional protein	Endothelial cells	(Dursun <i>et al.</i> , 2009)
gC1qR/p33 (gC1qR)	A multifunctional cellular protein	Platelet	(Yin <i>et al.</i> , 2008)

Table 1.7. Some markers for cell-derived microparticles.

## 1.16.5 MP formation

### 1.16.5.1 An insight into different types of extracellular vesicles

Intact eukaryotic cells (ranging in size from 2µm diameter and typical about 25µm diameter) contain membrane-bound organelles such as the nucleus however blood platelets (thrombocytes) (2-4µm diameter (Gawaz, 2001)) have no nucleus and endothelial cells are typically in the range of 10-70µm diameter (Erdbuegger *et al.*, 2006). In cell biology and physiology, there are different types of secreted vesicles and extracellular organelles derived from cells upon activation and/or apoptosis (compromised cells/stressed). Exosomes, Microparticles, and Apoptotic blebs (bodies) are the three most extensively characterised groups. They differ from one to another in several ways namely; marker protein composition/surface markers, size range, cells of origin, isolation procedures, site of release from their parental cells, and affinity for Annexin V binding (Mause & Weber, 2010). These differences define their functional characteristics and biological functions. Exosomes are smaller than 100nm diameter (El-Andaloussi *et al.*, 2012; Keller *et al.*, 2006) while MPs are between 100-1000nm diameter (Mause & Weber, 2010; Burton *et al.*, 2013; Abbasian *et*

*al.*, 2012), and apoptotic blebs are even bigger (i.e. >500nm and can be up to 5000nm diameter (Crescitelli *et al.*, 2013)). As expected from their size, there would be a need for higher centrifugation speeds to sediment exosomes and then MPs and finally apoptotic blebs for example 100,000xg is required for exosomes (Keller *et al.*, 2011), 18,000xg -20,000xg for microparticles (Burger *et al.*, 2014; Jy *et al.*, 2004) and 2,000xg for apoptotic blebs (Crescitelli *et al.*, 2013) although this is still a subject for discussion and a universal protocol for isolation still has to be agreed in this field. Furthermore, apoptotic blebs are big cellular fragments which can be formed following fully developed apoptosis and which express P<sub>Ser</sub> on their surface and consequently have a very high affinity for annexin V binding. MPs, on the other hand, start blebbing off the surface of plasma membranes upon cellular activation and/or early apoptosis (cell compromised). They are similar to apoptotic blebs but, depending on the course of their formation (i.e. cell activation or apoptosis) they possess differing degrees of affinity for annexin V binding. In contrast, exosomes have a low to null affinity for annexin V binding and are formed following fusion of a multi-vesicular body (MVB) with the cell membrane and contain cytoplasmic material (El-Andaloussi *et al.*, 2012; Théry *et al.*, 2002).

There are also other groups of extracellular vesicles which can be distinguished from MPs and other extracellular vesicles and one as such is autophagic vacuoles. Following autophagy induction in cells and formation of autophagic vacuoles; release of such vacuoles (vesicles) to the extracellular milieu can occur following caspase-dependent cleavage of the plasma membrane (Sirois *et al.*, 2012). They are >100nm diameter and display one or more autophagic markers such as LC3, LAMP2, ATP and annexin V (Pallet *et al.*, 2013). Human endothelial cells have been shown to release LC3/annexin V dual labelled MV in response to serum starvation (Pallet *et al.*, 2013).

Under normal (resting) physiological conditions, membrane phospholipid asymmetry in intact living cells is in favour of distributing aminophospholipids (for instance phosphatidylserine (P<sub>Ser</sub>) and phosphatidylethanolamine (PE)) in the inner leaflet of the cell membrane, and phosphatidylcholine and

sphingomyelin in the outer leaflet. However under certain circumstances, for example cell activation and apoptosis, enzymes (i.e. transmembrane lipid translocation enzymes) namely flippase (aminophospholipid translocase), floppase, and lipid scramblase change this cell membrane asymmetry and hence such aminophospholipids (e.g. Pser and PE) are redistributed and externalised. In this way, apoptotic and/or activated membrane blebs comprise an abundance of Pser and /or PE on their surface resulted from abnormality in aminophospholipid redistribution on the outer leaflet of the lipid bilayer (Chironi *et al.*, 2009; Freyssinet & Toti, 2010; Zwaal *et al.*, 2005).

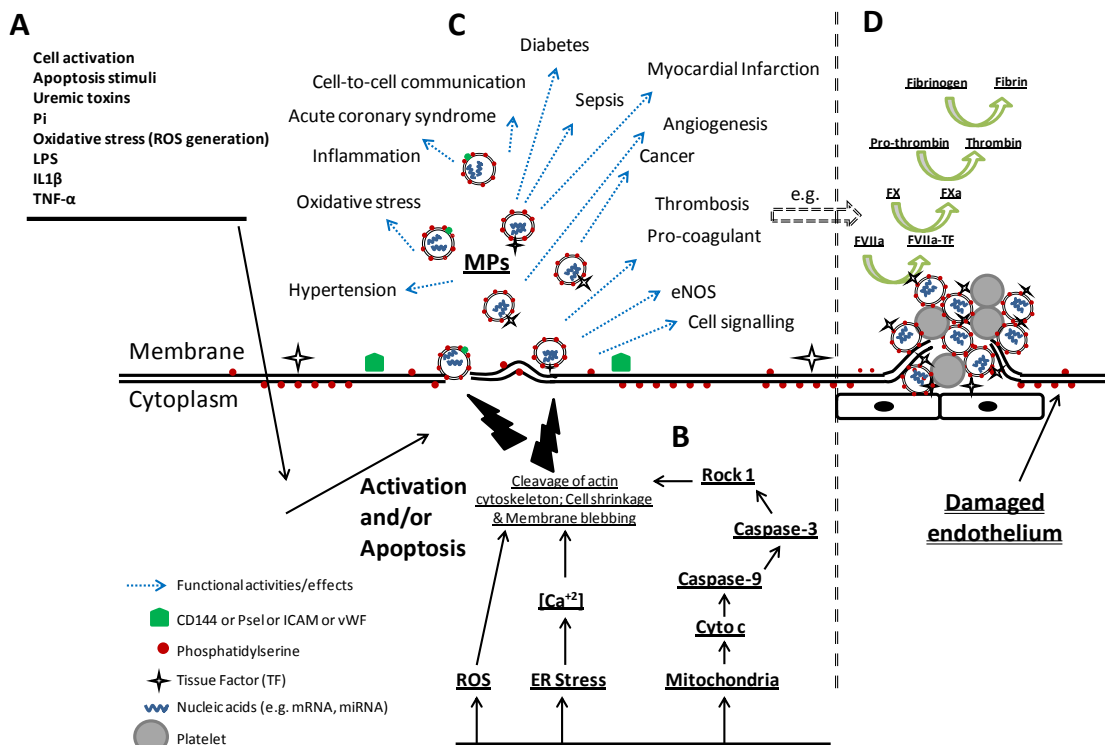


Figure 1.19. Schematic diagram depicting microparticle formation and a possible mechanism of MP action. (A) Cells' (e.g. from endothelial cells, lymphocytes, leukocytes, platelets, and vascular smooth muscle cells) Stimulation via either a receptor dependent or a receptor-independent intracellular pathway results in (B) cell activation and/or apoptosis (C) Released MPs express surface markers from their parent cells and contain cytoplasm, nucleic acids, mRNA and miRNA, which all may play a role in cell-to-cell communication, angiogenesis, thrombosis, inflammation, cell signalling, and more as indicated in figure. (c & D) As an example of MPs functional significance, TF/PS positive MPs are implicated in an accelerated progression of coagulation activation and thrombin generation. Picture drawn from information in Sections 1.16.5, 1.16.7

### 1.16.5.2 Cell activation

Cell activation has been suggested to be one of major contributing mechanisms resulting in cell membrane blebbing and MP formation (Boulanger & Dignat-George, 2011; Burnier *et al.*, 2009; Chironi *et al.*, 2009; Marja J. VanWijk, *et al.*, 2003). Following exposure of cells (e.g. Platelets, ECs, VSMC, & RBC) to an effective agonist, as exemplified in Figure 1.19-A and Table 1.6, there will be shedding of vesicles from the cells into the surrounding extracellular milieu which results from structural changes in the membrane-associated cytoskeleton (including talin, actin, vinculin, and Tropomyosin) (Chironi *et al.*, 2009; Houle *et al.*, 2007). It has been shown that agonists leave their impact on cells principally, through enhancing the cellular concentration of signalling ions such as calcium and Pi which, in turn, can result in activation/inhibition of downstream signalling and compromise intact cell function and membrane integrity. One such important downstream signalling pathway involves dysregulation in cytoskeleton regulatory protein Tropomyosin (TM) which impacts actin stress fibre formation and the cell focal adhesions (Houle *et al.*, 2007; Pellegrin & Mellor, 2007). In human vascular endothelial cells (VECs), under stress conditions such as oxidative stress induced by hydrogen peroxide, an important protective mechanism by which cells maintain their plasma membrane integrity and function is the formation of actin stress fibres (Houle *et al.*, 2007). The formation of actin stress fibres and the cells' focal adhesions depends upon phosphorylation of cytoskeleton regulatory protein TM on Ser-283 which is mediated by a kinase (i.e. DAPK-1) which is regulated by an inhibitory phosphorylation on Ser-308 (Houle *et al.*, 2007; Bovellan *et al.*, 2010; Jin *et al.*, 2006). It has been shown that the non-phosphorylatable TM mutant (Ser-283-Ala) of VECs under stress condition, is associated with an impaired stress fibre formation and consequent MP formation (Houle *et al.*, 2007) emphasising the important pivotal role of TM phosphorylation in maintaining cell integrity and that impairment of this TM can potentially result in the loss of stress fibre formation and MP formation. This suggests an important contribution of TM biology in actin stress fibre formation and MP output in cells (e.g. VECs) under stress and this potential mechanism of MP formation will be considered in more detail in Chapters 5 and 6 of this thesis.

In addition, during PSer externalisation, intracellular calcium concentration plays a contributing role in cytoskeleton reorganisation. An increase in the cytosolic calcium ion ( $\text{Ca}^{2+}$ ) concentration can be a signal triggering several intracellular signalling pathways resulting in externalisation of aminophospholipids including PSer and activation of a calcium-dependent proteolytic enzyme (i.e. Calpain) leading to the splicing of the membrane cytoskeleton (Chironi *et al.*, 2009; Marja J. VanWijk, *et al.*, 2003) and concomitant MP formation.

Cell (s)	Agonist (s)
Platelet	Thrombin, Calcium ionophore A23187, C5b-9 of the complement system, ADP + Collagen
EC/Monocyte/SMC	Bacterial lipopolysaccharide, cytokine (e.g. TNF- $\alpha$ , and IL-1), C5b-9, Hydroperoxide

Table 1.8. Cells and their possible activating agonist(s) (Chironi *et al.*, 2009; Marja J. VanWijk, *et al.*, 2003)

### 1.16.5.3 Cell apoptosis

Cell apoptosis (cell compromised or type-I programmed cell death) has been implicated to be an important derivative mechanism of MP formation (Boulanger & Dignat-George, 2011; Enjeti *et al.*, 2008; George, 2008; Marja J. VanWijk, *et al.*, 2003; Chironi *et al.*, 2009). Release of such microparticles (i.e. apoptotic MPs), in turn, may stimulate adjacent cells to release further microparticles of other origins in situ by induction of apoptosis in corresponding cells. This has been shown in some cell types for instance following incubation of Jurkat T cell-derived apoptotic microparticles with RAW 264.7 cells (macrophages), NIH3T3 cells, and L929 cells *in vitro* (Distler *et al.*, 2005). Jurkat T cell-derived MPs stimulated macrophages to release more MPs derived from the induction of apoptosis in these cells by Jurkat T cell-derived MPs. However this amplification loop of cell death and MP liberation was not seen in either NIH3T3 or L929 cells, indicating cell specificity in the damaging/stimulating effects of a given type of MP on other cells (Distler *et al.*, 2005).

In terms of a mechanism, release of cell apoptosis-associated microparticles is Rho-associated kinase (ROCK-1) dependent. In this concept, an apoptosis inducer activates caspases within the cells which, in turn, cleave the resting Rho to active Rho. Active Rho then activates ROCK-I (Sebbagh *et al.*, 2001).

Active ROCK-I increases force generation through increase in phosphorylation of myosin light-chain, myosin ATPase activity, and coupling of actin-myosin filaments in the plasma membrane and, as a consequence, this would increase cell contraction and subsequent cell membrane blebbing and vesiculation (Chironi *et al.*, 2009; Marja J. VanWijk, *et al.*, 2003; Sebbagh *et al.*, 2001) (Figure 1.19-B). Therefore, MPs formed upon cell apoptosis may contain DNA fragments resulted from redistribution of the fragmented DNA from the nuclear region into the vesicles through coupling to the actin-myosin filaments (Chironi *et al.*, 2009; Marja J. VanWijk, *et al.*, 2003).

As explained in Section 1.16.5.1. above, both apoptotic bodies and MPs derived from apoptotic cells, may be produced by a similar mechanism and, in terms of their characteristics, they can share a number in common such as expressing aminophospholipids on their surface and antigenic/protein markers from their cells of origin. What makes an important difference between these two cell fragments is the difference they have in size. Apoptotic bodies are 500nm to 5000nm however MPs are between 100nm to 1000nm. This suggests an overlap in their size (apoptotic bodies and MPs of 500nm to 1000nm) and makes absolute differentiation between them more challenging. Another potential problem is the possibility that apoptosis-derived MPs are sometimes just fragments of apoptotic bodies generated after apoptotic body release from cells. In other words, an agonist may stimulate cells to release big (e.g. 5000nm diameter) apoptotic bodies and apoptotic bodies can be fragmented in the following steps to MPs. A detailed characterisation of apoptotic bodies and MPs for their content and stability and functional properties requires further research.

#### **1.16.6 Microparticle involvement in health and disease**

In peripheral blood of healthy individuals, readily measurable concentrations of MPs have been reported (Berckmans *et al.*, 2001) which have been shown mainly to be of platelet origin. This homeostatic state is compromised under different pathological states which subsequently results in release of an elevated number of MPs from different cells into circulation which can potentially increase thrombosis and athero-occlusive states (Mallat *et al.*, 2000;

Mallat *et al.*, 1999; Bernal-Mizrachi *et al.*, 2004). Two common disease states in which the number of MPs has been reported to increase will be discussed here; namely chronic kidney disease (CKD) and cardio vascular disease (CVD) whereby endothelial MPs are increasingly recognised as powerful markers for vascular dysfunction (Dursun *et al.*, 2009).

#### **1.16.6.1 Microparticles in CKD**

Mounting evidence indicates that the circulating number of MPs (including endothelial and platelet microparticles) increases in diseases involving abnormalities in the normal function of human kidneys. In hypertensive patients with an impaired renal function (declining eGFR) it has been shown that there is an increase in circulating apoptotic EMPs (i.e. CD31+/Annexin V+) (Hsu *et al.*, 2013; Huang *et al.*, 2010). It has previously been shown in this laboratory that in comparison with matched controls, patients on haemodialysis (HD) or peritoneal dialysis (PD) have elevated levels of pro-coagulant MPs of both platelet and endothelial origins (Burton *et al.*, 2013). In patients with end-stage renal failure (ESRF) and chronic kidney disease (CKD) an increased cardiovascular risk is derived partly due to endothelial dysfunction, arterial stiffness, and atherosclerosis (Amabile *et al.*, 2005; Dursun *et al.*, 2009; Amabile *et al.*, 2012). This endothelial dysfunction in ESRF has been suggested to be caused as a result of damaging effect of endothelial derived microparticles in these patients on the endothelial cells, as *in vitro* there has been seen about 50% decrease in endothelial nitric oxide release following incubation of endothelial cells with a medium containing EMPs derived from patients with ESRF (Amabile *et al.*, 2005). Also, another report indicates that in ESRD, laminar shear stress is a crucial driving force which induces endothelial cell apoptosis and plasma MP formation (Boulanger *et al.*, 2007). Furthermore, CD144/146 positive microparticles (MPs of endothelial origin) have been shown to be higher than in patients with chronic renal failure (CRF) and HD patients (Faure *et al.*, 2006).

Uremic toxins (Vanholder *et al.*, 2003<sub>a</sub>; Vanholder *et al.*, 2003<sub>b</sub>; Duranton *et al.*, 2012) have been implicated in damaging effects on endothelial cells' normal functionality and integrity, by inducing atherosclerosis, arterial stiffness,

vascular calcification, and abnormalities of vascular repair and neointimal hyperplasia (Brunet *et al.*, 2011). Some important uremic toxins involved in endothelial dysfunction and atherosclerosis are guanidine compounds, advanced glycation end products (AGE), p-cresol, indoxyl sulphate, ADMA, Pi, TNF, leptin,  $\beta_2$ -microglobulin, and indole-3 acetic acid (Brunet *et al.*, 2011). Uremic toxin-induced endothelial dysfunction has been manifested by the release of endothelial MPs from cells after *in vitro* incubation with uremic toxins. The mechanism underlying uremic toxin-induced MP release however is elusive. Two uremic toxins (indoxyl sulphate and p-cresol) have been shown to stimulate endothelial cells *in vitro* to release microparticles (Faure *et al.*, 2006). P-cresol, also, has been shown *in vitro* to result in a poor endothelial function in a Rho-dependent manner resulting in decrease in endothelial permeability and reorganisation of the actin cytoskeleton (Cerini *et al.*, 2004). Incidentally, homocysteine (Hcy) has also been shown to result in an elevation in release of procoagulant MPs from endothelial cells *in vitro*. It is possible that the increased superficial P<sup>Ser</sup> expression on Hcy-derived EMPs (rather than tissue factor (TF) positivity of these particles) may be important in their pro-coagulant effect (Zhu *et al.*, 2012). It has been recently reported that Pi can result in an increase in the generation of MPs from endothelial cells *in vitro* (Di Marco *et al.*, 2012). Preliminary experiments from this laboratory have also shown that high levels of extracellular Pi, as found in CKD patients, stimulate endothelial cells *in vitro* to release microparticles (Abbasian *et al.*, 2012), an effect which is accompanied by Pi influx into the cells. However the molecular mechanism underlying this Pi-induced MP formation was unclear and is a major subject of this thesis.

#### **1.16.6.2 Microparticles in CVD**

The involvement and contribution of cell derived plasma microparticles in the pathogenesis of cardiovascular diseases (CVD) (Tushuizen *et al.*, 2011; VanWijk *et al.*, 2003) including atherogenesis and atherothrombosis (Shantsila *et al.*, 2010) has been studied extensively over the past decade. MPs have potent pro-inflammatory properties and can promote coagulation and even work as part of an amplification loop for endothelial cell death and further MP release (Fink *et al.*, 2011; Rautou *et al.*, 2011). Per unit of surface area, PMPs have

been reported to pose 50-100-fold more pro-coagulant capacity than activated platelets *per se* (Shantsila *et al.*, 2010; Sinauridze *et al.*, 2007). In patients with pre-existing coronary artery disease, it has been shown that there is an increase in circulating apoptotic EMPs (i.e. CD31+/Annexin V+) (Werner *et al.*, 2006). In patients with heart failure, EMPs have been reported as a reliable and useful indicator (marker) of endothelial dysfunction (Nozaki *et al.*, 2010).

#### **1.16.7 MPs' biological function**

The most studied of all functional characteristics attributed to MP is their involvement in haemostasis and thrombosis. As described in Section 1.16.4 above, microparticles may express negatively charged phospholipids (i.e. PSer/PE) on their surface and hence offer a suitable site for the binding of factor II, Va, and Xa of the coagulation cascade (Figure 1.19-D). This gives a pro-coagulant property to MPs (Chironi *et al.*, 2009) as PSer acts as an assembly point for prothrombinase complex formation, resulting in coagulation cascade activation (Figure 1.19-D). Moreover, MPs expressing PSer on their surface provide a high affinity site for binding of Annexin V in the presence of a physiological concentration of  $Ca^{2+}$  (Chironi *et al.*, 2009) which tags MPs to be recognised and engulfed by macrophages. Other biological functions of MPs beside pro-coagulability include (but are not restricted to) pro- and anti-inflammatory effects, and cell-to-cell communication, however this is an open ongoing area of research which is still in progress.

There are also Tissue Factor (TF) (Key, 2010<sub>a</sub>) and Histones-containing MPs which may also have potential involvement in modulating coagulation and thrombotic states by promoting activation of the contact pathway (Ammollo *et al.*, 2011) and inhibition of fibrinolysis (Longstaff *et al.*, 2013). Expression of TF glycoprotein (an initiator of coagulation) on MPs depends on both the cells of origin and the trigger for MP formation; meaning that different cells (depending upon cellular activation or apoptosis) may express a different extent of active TF positivity - for instance activated endothelial cells in comparison to apoptotic EMPs are more TF positive (Lechner *et al.*, 2007). TF is the receptor for factor VIIa (FVIIa) of blood coagulation and can initiate the coagulation cascade

(Mackman, 2009) and it is modulated via the intracellular PI3K/Akt signalling pathway (Eisenreich *et al.*, 2009). Collectively these indicate that, depending on the extent of superficial expression of one or more of the following: P-Ser, and/or Histones, and/or TF; MPs would be biologically active to a different extent and may contribute in different ways to thrombosis. This (i.e. expressing two or more of these pro-coagulant accelerating/initiator/stabiliser factors) suggests a potential synergistic role of these factors in MPs' pro- and/or anti-inflammatory/coagulant effects.

As discussed above (Section 1.16.4) MPs may express binding sites for C1q, a component of the classical complement cascade, and hence may modulate an array of cellular responses resulting in inflammation and thrombosis (Peerschke *et al.*, 2008). Furthermore, gC1qR/p33 (gC1qR) expressing PMPs have been shown to enhance the classical complement cascade (Yin *et al.*, 2008) and therefore compromise vascular function and result in atherosclerosis. Furthermore, P-selectin expressing platelets (and possibly PMPs) may enhance activation of the alternative complement cascade (Del Conde *et al.*, 2005).

CD36 is a class B scavenger receptor (an 88kDa glycoprotein) (Kuriki *et al.*, 2002) expressed in many cells including (but not restricted to) platelets (it exists in  $\alpha$  granules (Gawaz, 2001)), monocytes (Alessio *et al.*, 1996), and some endothelial (Dawson *et al.*, 1997) and epithelial cells (Susztak *et al.*, 2005). It has been recently shown that MP liberated from endothelial cells, monocytes (Alkhatatbeh *et al.*, 2013), and possibly platelets are positive for CD36. On the other hand activated cells such as platelets and endothelial cells can also synthesis and secrete trombospondin-1 (TSP-1) (Gawaz, 2001) a ligand for CD36 (Alkhatatbeh *et al.*, 2013; Leung *et al.*, 1992) which has properdin-like repeats (Simantov *et al.*, 2001; Prater *et al.*, 1991). It has therefore been previously suggested that TSP-1 can bind to the surface of MPs, activated platelets and other blood cells including endothelial cells (Kehrel *et al.*, 1996) via CD36 or integrins (e.g.  $\alpha_{IIb}\beta_3$ ; GPIIb-IIIa) and act as an antiangiogenic agent or suppressive of endothelial cells' proliferation and migration (Lawler & Lawler, 2012). It has also previously been shown in this laboratory (Abbasian, 2010)

that complement factor p (cfp or properdin) binding to PTECs may be mediated through CD36 which may result in local complement activation in the tubular lumen adjacent to proximal tubular epithelial cells. In a similar way it is possible that binding of complement properdin to CD36 positive MPs in circulation may modulate local activation of complement and enhance vaso-occlusive phenomenon, tissue inflammation, immune responses, and autoimmune diseases (Kemper *et al.*, 2010; Schwaeble & Reid, 1999).

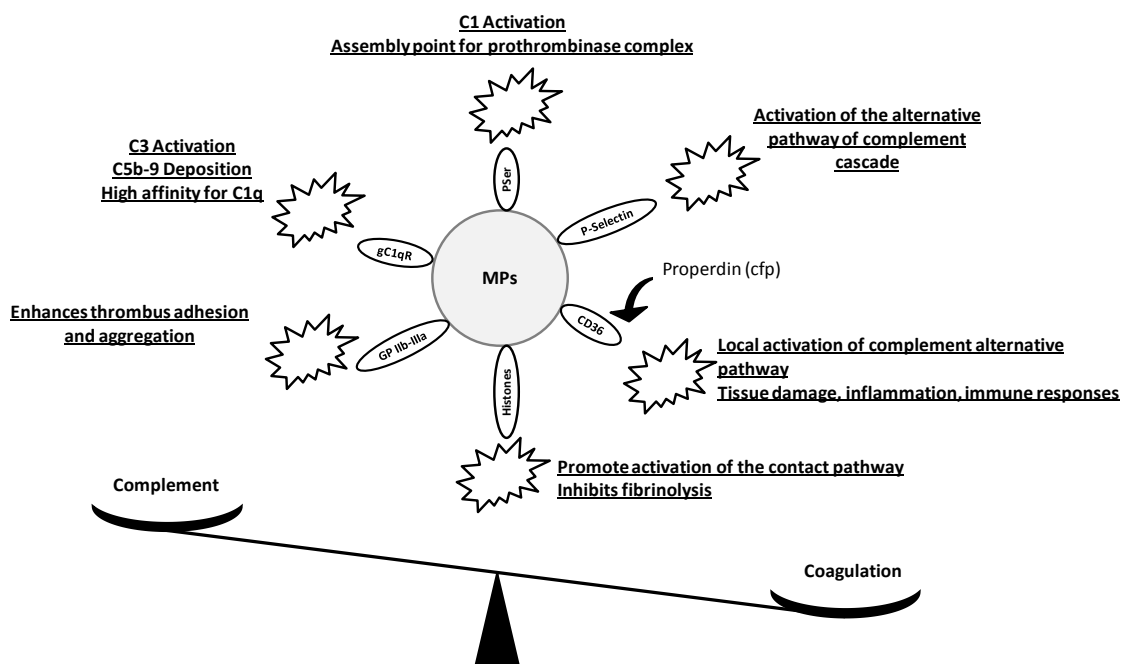


Figure 1.20. Schematic diagram summarising ways in which MPs might mediate complement activation and/or coagulation in the absence of immune complex formation. Picture depicts potential cross-talk between complement and coagulation and possible ways by which MPs could interfere in this paradigm. MPs expressing gC1qR, P-Selectin and aminophospholipids (e.g. PSer) activate C1, C3, C4 and alternative pathway of the complement cascade and enhance C5b-9 deposition. Histones also can both promote activation of the contact pathway (Ammollo *et al.*, 2011) and inhibit fibrinolysis (Longstaff *et al.*, 2013) and hence result in a pro-thrombotic state. Integrins (GP IIb-IIIa) also promote platelet activation, adhesion and aggregation (Gawaz, 2001) Picture drawn from information in Sections 1.16.4., and 1.16.7 and (Peerschke *et al.*, 2008; Gawaz, 2001; Ammollo *et al.*, 2011; Longstaff *et al.*, 2013).

### 1.16.8 MP Clearance

MP clearance can be obtained via engulfment by macrophages. MPs express PSer for which there are receptors on macrophages and therefore PSer-expressing and apoptotic or endothelial cells expressing PSer can be detected by macrophages and been removed from the milieu (Zwaal *et al.*, 2005). Jurkat T cell-derived apoptotic MPs have been shown to be engulfed by macrophages

*in vitro* (Distler *et al.*, 2005). Furthermore, gC1qR expressing MPs (Section 1.16.4) have binding sites for C1q and therefore providing a complex which can be recognised and engulfed by macrophages however the precise mechanism involved in MP clearance is still not fully understood and needs further elucidation.

#### **1.16.9 Methods for MP measurement**

Detection techniques required to enumerate and characterise cell derived microparticles are a challenging and emerging new area in nano-particle detection research. The “golden standard” and widely used technique is flow cytometry or fluorescence-activated cell sorting (FACS) (Robert *et al.*, 2009; Robert *et al.*, 2012; Robert *et al.*, 2011) as this technique provides the possibility to characterise multiple antigenic markers on MPs, making use of multi-coloured labelling and high sensitivity FACS. However, it should be taken into account that the lower limit detection threshold of FACS’ MP detection is about 300nm (Dragovic *et al.*, 2011) while MPs are between 100-1000nm diameter. Ultracentrifugation, ELISA, Dynamic Light Scattering (DLS) (Boyd *et al.*, 2011), atomic force microscopy (Boyd *et al.*, 2011; Leong *et al.*, 2011), Scanning Electron Microscopy (SEM), Transmission Electron Microscopy (TEM) (Burton *et al.*, 2013), and the NanoSight; Nanoparticle Tracking Analysis system (NTA) (Gardiner *et al.*, 2013; Dragovic *et al.*, 2011; Burton *et al.*, 2013) with detection limit of 50nm diameter (Dragovic *et al.*, 2011) also have been recently used or are being developed as techniques to study MPs - each with their own advantages and pitfalls (Mullier *et al.*, 2011; Larson *et al.*, 2013; Dey-Hazra *et al.*, 2010; Ayers *et al.*, 2011; Shah *et al.*, 2008).

#### **1.17 Summary**

Patients with CKD are at high risk of CVD morbidity and mortality (Giachelli, 2003). In patients with CKD as well as healthy individuals with a normal kidney function, higher serum Pi levels, even well within the physiological range, are associated with increased risk of CV complications (Ketteler *et al.*, 2012; Onufrak *et al.*, 2008). In CKD patients this can be worsen because of a drastic reduction in the number of nephrons which are crucial in Pi homeostasis.

Consequently excretion of excess Pi is impaired, leading to hyperphosphataemia (Bevington *et al.*, 1990; Ahmed & Behzad, 2011). More recently, it has been shown that specified trans-membrane proteins, collectively known as sodium-coupled Pi transporters (NaPi) are actively involved in cellular Pi homeostasis (Werner *et al.*, 1998; Li *et al.*, 2006; Mune *et al.*, 2009).

On the other hand, microparticles (MP), also referred to as membrane vesicles (MV), are submicron sized fragments of the plasma membrane which can be derived from a number of cell types, shedding into extracellular fluid following cell activation and apoptosis (Morel *et al.*, 2011; Freyssinet, 2003). Numbers of MPs have been shown to increase in a series of physiological/ patho-physiological conditions, including CKD and CVD (Amabile & Boulanger, 2011; Koga *et al.*, 2005), and are associated with increased cardiovascular risk (Marja J. VanWijk, *et al.*, 2003; Mallat *et al.*, 2000).

There is evidence from earlier reports indicating that an elevated concentration of extracellular Pi leads to endothelial cell apoptosis (Di Marco *et al.*, 2008), and ROS generation (Shuto *et al.*, 2009), which are possible mechanisms of MP formation, but the exact mechanism by which Pi damages the cells and/ or induces apoptosis and ROS generation is not yet fully determined.

Understanding and controlling the mechanisms of MP formation, for example following activation and/or apoptosis in response to hyperphosphataemia, could potentially be a useful aspect of CKD treatment and could open up new insights into both prognostic and therapeutic aspects of CKD.

### **1.18 Thesis hypothesis**

The hypothesis of this project is that hyperphosphataemia leads to MP formation from ECs or induces changes in MPs' (bio)-physical properties via an elevation of intracellular Pi, which directly inhibits phosphoprotein phosphatases, triggering a global increase in phosphorylation and cytoskeletal changes.

Briefly, at least 3 mechanisms can be envisaged through which Pi could do this:

**1) Pi enters cells through SLC20 (i.e. PiT) transporters;**

Triggering cell signalling “activation” and/or apoptosis and/or ROS generation.  
Giving rise to membrane vesiculation and, as a consequence, formation of MP and/or other MV.

**2) Pi directly acts on cell-derived particles;**

Increasing particle sedimentation and/or aggregation.  
Altering the functional effects of released particles, e.g. Thrombin generation capability.

It is known for example that MPs released from certain cell types contain histones (Banfi *et al.*, 2005) which are positively charged at physiological pH and potentially can bind Pi anions (Ord & Stocken, 1966). Histones are known to promote thrombin generation (Ammollo *et al.*, 2011) and impair fibrinolysis (Longstaff *et al.*, 2013).

**3) Pi binds to extracellular Ca;**

Forming Calcium Phosphate (CaPi) complexes and CaPi nanocrystals.  
These are deposited on the cells and activate them by a process like that which has been described in the action of nanocrystals on vascular smooth muscle cells (Sage *et al.*, 2011).

These three mechanisms are summarised in Figure 1.21.

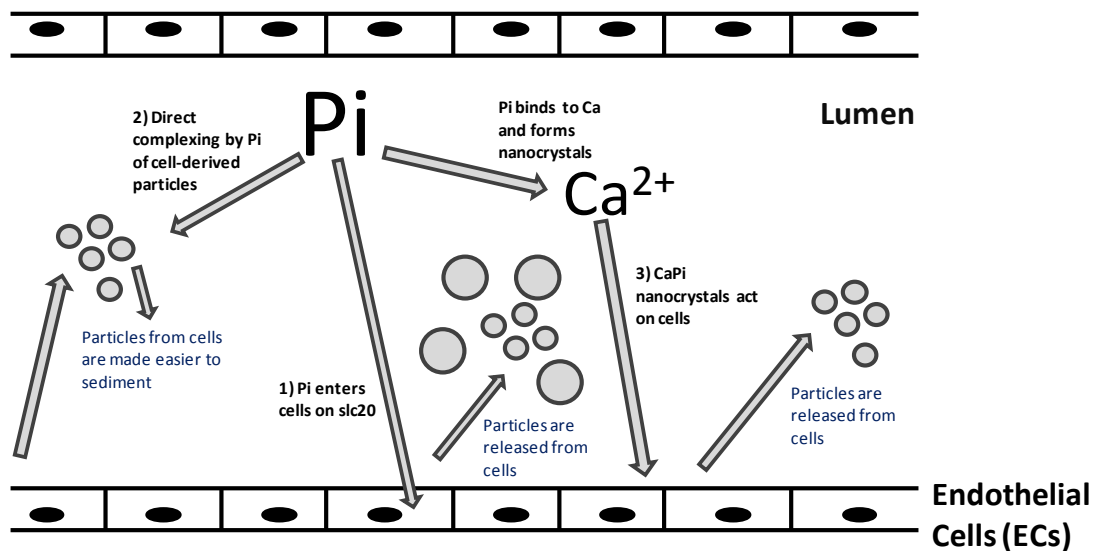


Figure 1.21. Schematic of hypothesis summary indicated three potential mechanisms of Pi action on endothelial cells (ECs) in a hyperphosphataemic milieu.

### 1.19 Thesis Aims and structure

In view of the importance of hyperphosphataemia and microparticles in cardiovascular disease associated with CKD, this project's aims were to investigate this in cultured VECs as follows:

In chapter 3 – examining the effect of extracellular Pi on MP release from cultured VECs and investigating the pro-coagulant properties of MPs derived from endothelial cell cultures treated with a Pi load

In chapter 4 – showing that an extracellular Pi load leads to an increase in intracellular Pi concentration

In chapter 5 – showing the effect of a Pi load on global patterns of protein phosphorylation and investigating the effect of Pi on gross changes in intracellular proteins and MP proteins

## Chapter 2. Methods and Materials

---

### 2.1 General materials

Through this thesis, unless otherwise stated, all reagents and materials, i.e. chemicals and biochemicals, were purchased from Sigma. Sterile tissue culture 75 cm<sup>2</sup> and 25 cm<sup>2</sup> Flasks were purchased from Corning (Nonpyrogenic sterile polystyrene), 35mm<sup>2</sup> 6-well and 22mm<sup>2</sup> 12-well plates were from Nunclon and Corning (Nonpyrogenic sterile polystyrene) respectively. Other plastic consumables were purchased from Sarstedt and BD plastipak.

### 2.2 Choice of experimental model

Cultures of Human Umbilical Vein Endothelial cells (HUVEC) (kindly provided by the Department of Cardiovascular disease-University of Leicester- Dr Karl Herbert), and an immortalised Human Endothelial cell line (EAhy926) (Edgell *et al.*, 1983) (kindly provided by the Department of Cardiovascular disease-University of Leicester- Professor Alison Goodall) were used in this study.

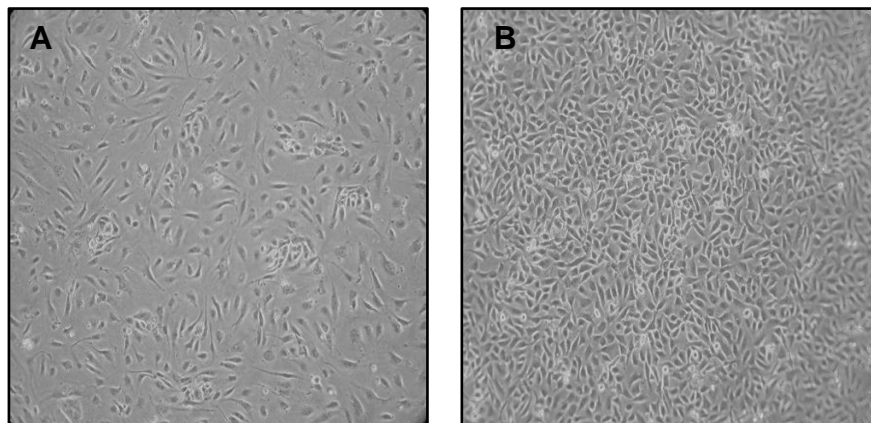


Figure 2.1. Inverted micrographs of EAhy926 and HUVECs. (A) photomicrograph of two days old HUVEC plated on a gelatin-coated plastic culture flask (area; 25 cm<sup>2</sup>), (C) photomicrograph of two days old EAhy926 endothelial cells (i.e 2 days after seeding) plated on a normal plastic culture flask (area; 25 cm<sup>2</sup>). All culture dishes were incubation at 37<sup>0</sup>C/5% CO<sub>2</sub>. Note the cobblestone morphology of HUVECs and EAhy926 cells and that the EAhy cells achieve heavier confluence than HUVECs (*Original Magnification 100X*).

Endothelial cells have a variety of biological functions for instance keeping a tightly regulated balance between coagulation and fibrinolysis, regulating vascular tone by production of endothelium-derived relaxing factors (e.g. NO, PGI<sub>2</sub>, and EDHF) and vasoconstricting factors (e.g. endothelin, and thromboxane) (see Section 1.11.3). They also express a number of cell surface and junctional proteins such as VE-CD144 cadherin and CD146 (see Table 1.5). Furthermore VECs express endothelium specific trans-membrane proteins involved in ion and amino acid transport such as glucose transporters and phosphate transporters (namely SLC20 or PiT transporters but not SLC17 and SLC34 transporters which are mainly expressed in epithelia) (see Section 1.10.2).

HUVECs (Jaffe *et al.*, 1973) and the HUVEC-derived EAhy926 endothelial cell line (Edgell *et al.*, 1983) have been widely used to study the effects of different agonists and stress stimuli (including Pi) on endothelium function and (patho)-physiology (Di Marco *et al.*, 2012; Di Marco *et al.*, 2008; Li *et al.*, 1998; MA *et al.*, 2012; Fang *et al.*, 2009; Pan *et al.*, 2009). The EAhy cell line is a permanent endothelial cell line derived from the fusion of human umbilical vein endothelial cells (HUVECs) with a permanent human lung carcinoma cell line (A549) which is a cancer epithelial cell line; and express human factor VIII-related antigen (Edgell *et al.*, 1983).

EAhy926 cells were used as the main endothelial culture model throughout this project (with the key findings confirmed in HUVECs) as this line of cells is a convenient and reliable *in vitro* model of endothelial cell biology to investigate the effects of high extracellular Pi on MP formation, cell signalling, and phosphorylation pattern. Unlike HUVECs these cells grow reasonably fast and therefore using such an experimental model gave this opportunity to rapidly, accurately, and consistently study the effect of one or multi agonist/metabolic stress stimuli on biology and patho-physiology of endothelial cells.

### **2.3 Gelatin Coating plates for HUVECs**

3.5ml of 2% (w/v) stock Gelatin (Sigma G1393) and 66.5ml of Phosphate Buffered Saline (PBS) (Invitrogen 14190-136) were mixed to make a Gelatin solution of 0.1% (v/v). Appropriate volumes (varying from 500 $\mu$ l to 5ml according to the area of the culture vessel) of this 0.1% solution was added to each 25 cm<sup>2</sup>, 75 cm<sup>2</sup> flask (Nonpyrogenic sterile polystyrene), and 35mm, and 22mm diameter culture wells (Nunclo<sup>TM</sup>Surface) respectively to cover the surface of the vessels completely. After incubation in the culture hood overnight, gelatin solution was rinsed away with Hanks Balanced Salt Solution (HBSS) (Appendix A-3) to remove phosphate-derived from PBS. Flasks and plates were stored at (4°C) until used.

### **2.4 HUVEC Culture Medium and passaging**

Cells were maintained in Medium 200 (Invitrogen M-200-500) with 2% (v/v) LSGS serum substitute (Invitrogen S-003-10), 2mM L-glutamine, penicillin (10<sup>2</sup> IU/ml) and streptomycin (100 $\mu$ g/ml) at 37°C in a humidified 5% CO<sub>2</sub> atmosphere. Cells were routinely sub-cultured on 75cm<sup>2</sup> culture flasks every 4-6 day before reaching ~70-80% confluence. Growth Medium was aspirated and cells were washed three times with 10ml Hanks Balanced Salt Solution (HBSS) to remove serum from the cells. 4ml of Trypsin-EDTA (T/E) (Invitrogen 25300) was added to each 75cm<sup>2</sup> culture flask and then incubated at 37°C for <4min to allow time for the cells to detach from the flask. 11ml of the complete growth medium described above was then added to the flask to inhibit the trypsin. Cells were sedimented at 200xg for 5 minutes and washed with a further 20ml of growth medium. The cell pellet was then re-suspended in 4ml fresh growth medium. Cells were plated at 70x10<sup>4</sup> cells/75cm<sup>2</sup> flask or 30x10<sup>4</sup> cells/35mm diameter 6-well on Gelatine-Coated plastic cell culture vessels. Cells were fed with 15ml/75cm<sup>2</sup> flask and 2ml/35mm six-well of fresh growth medium after an initial two days incubation in a humidified atmosphere at 37°C/5% CO<sub>2</sub>. Cells were then re-fed every other day to obtain approximately 70% confluence before experiments or further sub-culture.

## 2.5 EAhy926 Culture Medium and passaging

Cells were maintained in DMEM (Life Technologies ref 11880) with 10% (v/v) heat-inactivated foetal bovine serum (FBS), 2mM L-glutamine, penicillin ( $10^2$  IU/ml) and streptomycin (100 $\mu$ g/ml) at 37°C in a humidified 5% CO<sub>2</sub> atmosphere. Cells were routinely sub-cultured on 75cm<sup>2</sup> culture flasks every 4-6 day before reaching ~70-80% confluence. Growth Medium was aspirated and cells were washed three times with 10ml Hanks Balanced Salt Solution (HBSS) to remove serum from the cells. 4ml of Trypsin-EDTA (T/E) (Invitrogen 25300) was added to each 75cm<sup>2</sup> culture flask and then incubated at 37°C for <4min to allow time for the cells to detach from the flask. 11ml of the complete growth medium described above was then added to the flask to inhibit the trypsin. Cells were sedimented at 200xg for 5 minutes and washed with a further 20ml of growth medium. The cell pellet was then re-suspended in 4ml fresh growth medium. Cells were plated at 70x10<sup>4</sup> cells/75cm<sup>2</sup> flask or 30x10<sup>4</sup> cells/35mm diameter six-well on normal plastic cell culture vessels. Cells were fed with 15ml/75cm<sup>2</sup> flask and 2ml/35mm six-well plate with fresh growth medium after an initial two days incubation in a humidified atmosphere at 37°C/5% CO<sub>2</sub>. Cells were then re-fed every other day to obtain approximately 70% confluence before experiments or further sub-culture.

## 2.6 Experimental incubations and choice of Pi supplemented medium

Experimental incubations were performed in MEM (Life Technologies Ref 21090) with 2mM L-glutamine, penicillin ( $10^2$  IU/ml) and streptomycin (100 $\mu$ g.ml<sup>-1</sup>), at pH 7.4 with 1.8mM [Ca<sup>2+</sup>] and 1mM [Pi]. To model hyperphosphataemia NaH<sub>2</sub>PO<sub>4</sub> was added to raise the [Pi] to 2.5mM – a concentration which has been used extensively elsewhere to investigate the effect of higher extracellular Pi on endothelial cell (dys)-function (Di Marco *et al.*, 2008; Peng *et al.*, 2011; Di Marco *et al.*, 2012). Medium harvested from experimental incubations was subjected to centrifugation as shown in Table 2.1.

## 2.7 Mycoplasma screening

Mycoplasma contamination is a common contamination happening in cultured cells, therefore cultures were tested against mycoplasma using EZ-PCR

Mycoplasma Test Kit (GENEFLOW; 20-700-10). The assay was done as described in the manufacturer’s instructions. The assay relies on PCR followed by agarose gel electrophoresis to detect amplified DNA fragments of various mycoplasma species as well as acholeplasma and spiroplasma species according to the manufacturer’s stated assay specificities.

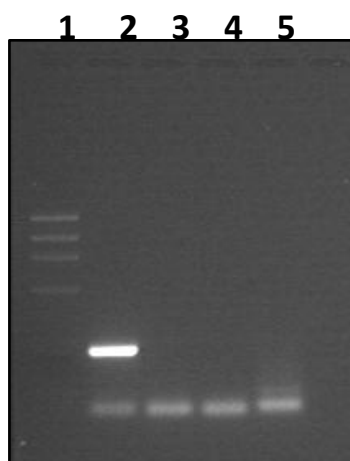


Figure 2.2. PCR gel electrophoresis to screen for mycoplasma contamination in cultures of EAhy926 endothelial cells. (Lane 1) molecular ladder (Lane 2) positive control provided in the kit (Lane 3) sample 1 derived from growing stock EAhy926 culture (Lane 4) sample 2 derived from a randomly selected stored EAhy926 cell suspension from the liquid nitrogen cell bank (Lane 5) negative control (water). (35 PCR amplification cycles were applied).

## 2.8 Microparticle Isolation

Microparticles were isolated from the culture medium as described previously (Burton *et al.*, 2013) with slight modification (Table 2.1).

Step number	Starting material	Centrifugation applied	Fraction analysed
1	Medium from cultures	1500 x g at 20°C for 20 min	Fraction 1. Resuspended pellet
2	Supernatant from Step 1	18000 x g at 20°C for 30 min	-----
3	Resuspended pellet from Step 2	18000 x g at 20°C for 30 min	Fraction 2 (Microparticles). Resuspended pellet from Step 3
4	Medium from cultures	18000 x g at 20°C for 30 min	Fraction 3. Assay total protein in pellet.

Table 2.1. Centrifugation steps applied to conditioned medium from EAhy926 cells

Briefly, medium from cultures was centrifuged (Step 1) at 1,500xg, at 20°C for 20 min to remove detached cells and large particles/apoptotic bodies. The top 90% of the supernatant from Step 1 was centrifuged (Step 2) at 18,000xg, at 20°C for 30 min to pellet microparticles. The top 90% of the supernatant from

this step was aspirated and the pellet resuspended in the following 0.2µm filtered MP-Buffer (145mM NaCl, 2.7mM KCl, 10mM Hepes, pH 7.4) and recentrifuged (Step 3) as before to wash microparticles before resuspending again in MP buffer and storing at -80°C for further analysis.

## 2.9 Isolation and measurement of detached cells following chronic (24h) incubation

Following incubation of cells with medium containing 1mM or 2.5mM [Pi] for 24h, medium was harvested and total particles/detached cells sedimented at 18,000xg, at 20°C, for 30min (Step 4, Fraction 3-Table 2.1) followed by precipitation of protein with 0.3M perchloric acid (PCA) and assay of total protein (Classics Lowry *et al.*, 1951) (Section 2.18.1).

## 2.10 Nanoparticle Tracking Analysis (NTA)

The number and size of the particles in fractions isolated as in Table 2.1 was analysed by Nanoparticle Tracking Analysis (NTA) using a NanoSight LM10 (Figure 2.3 and Table 2.2) with NTA software v2.2 (NanoSight Ltd, Amesbury, UK) and 90 second video capture as previously described (Burton *et al.*, 2013) (Table 2.2).

Camera Control	Value/State
Camera level	12
Reproducibility	High
Polydispersity	Medium
Recording time	90secs
Particle Detection	Value/State
Screen Grain	8
Extract Background	Ticked
Detection Threshold	4 Multi
Blur	Auto
Min Track Length	Auto
Min Expected Particle Size	30 ± 20

Table 2.2. Settings applied to the NanoSight for NTA of MPs.

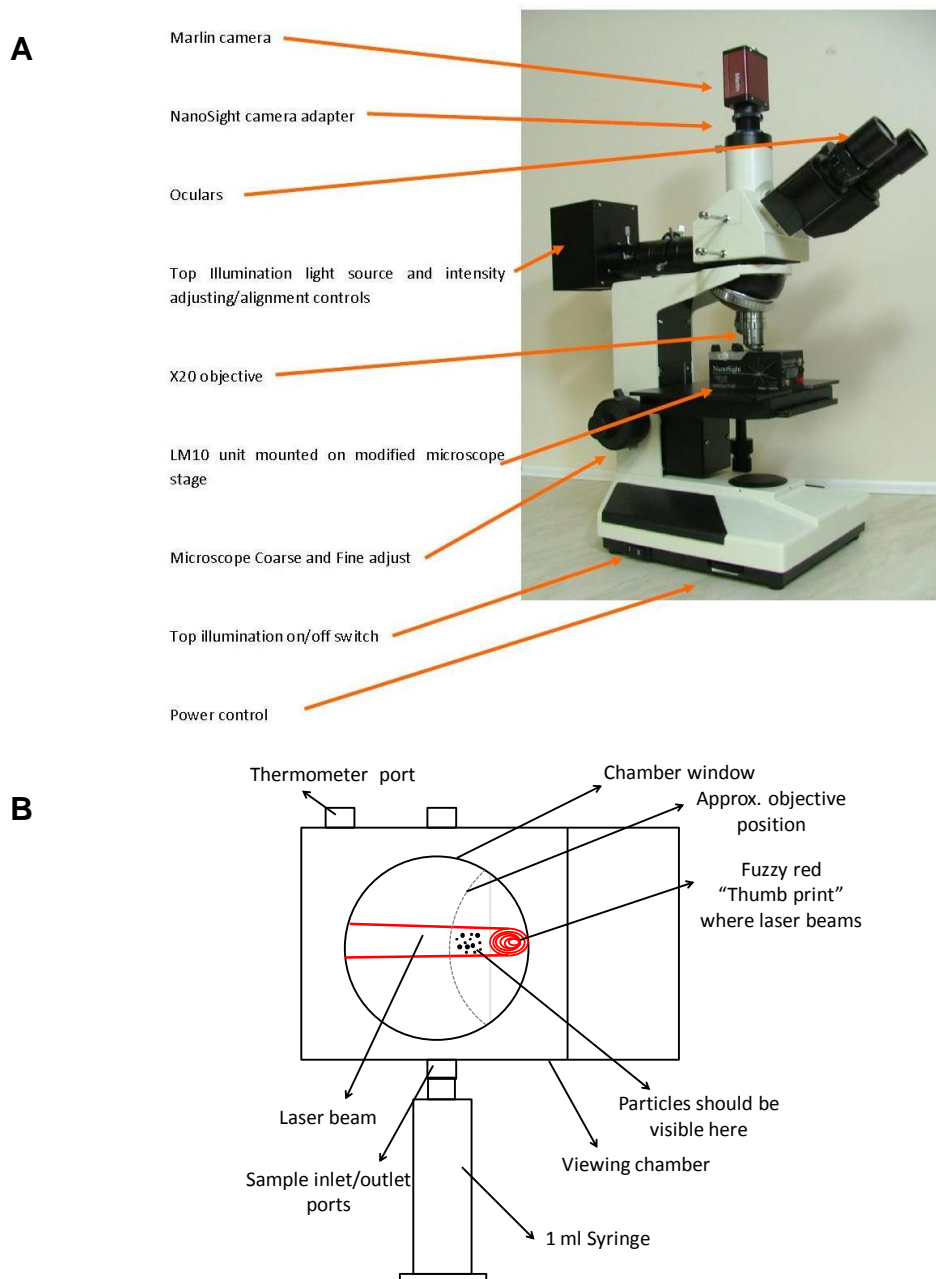


Figure 2.3. Nanoparticle Tracking Analysis (NTA) with a NanoSight LM10. (A) NanoSight LM10 microscope unit (Carr & Malloy) (B) Sample chamber, re-drawn from (Carr & Malloy).

## 2.11 Flow Cytometry Analysis of Microparticles

Samples (38 $\mu$ l, Fraction 2-Table 2.1) were thawed and mixed with 32 $\mu$ l of 1x Annexin V-Binding buffer with calcium (BD Pharmingen Ref 556454). 5 $\mu$ l each of Anti-Human CD144 (VE-Cadherin)-PE (eBioscience), and Annexin V-FITC (BD Pharmingen) was added and samples stored in the dark for 25min followed by dilution to a final volume of 500 $\mu$ l with Annexin V-Binding buffer before analysis on a Flow Cytometer (BD FACSAria<sup>TM</sup> II; Becton Dickinson, BD

Bioscience, San Jose, USA). Samples incubated with Mouse IgG1-PE (BioCytex) were used as isotype control. Samples incubated with Annexin V-FITC in Binding Buffer without calcium were used as a negative control for Annexin V binding. MPs were initially gated according to their size (i.e. FSC vs. SSC) and subsequently analysed according to their CD144 and Annexin V status as previously described (see Figure 2-3 in (Robert *et al.*, 2009)) (Figure 2.4). Gating and compensation adjustments were carried out using Megamix (BioCytex) beads of 0.5, 0.9, and 3 $\mu$ m diameter and single labelling of particles with either CD144-PE or Annexin V-FITC as previously described (Robert *et al.*, 2009). Events were gated according to size in a Forward/Side scatter dot plot.

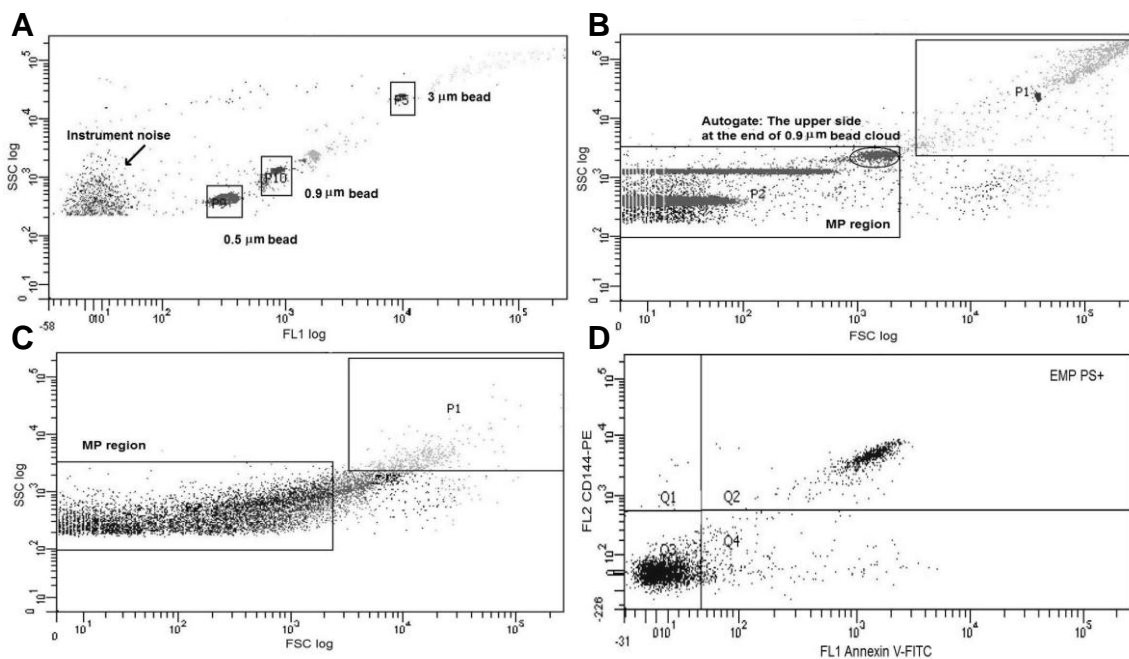


Figure 2.4. Gating and detection of MPs using flow Cytometry. (A) Side scatter log (SSC log) versus FL1 fluorescence properties of beads of 0.5, 0.9, and 3 $\mu$ m diameter (Megamix) to adjust the forward scatter (FSC) parameter. (B) Determination of MP analysis region by setting up an autogate around events between 0.5 $\mu$ m and 0.9 $\mu$ m fluorescent beads. (C) An example of endothelial microparticle (EMP) size distribution (D) dual labelling of MPs using CD144-phycoerytherin (PE) (indicative of CD144 expressing MPs) and Annexin V-FITC (indicative of PS expressing MPs).

## The following settings were applied for MP analysis

Parameter	Type	Voltage	Log
FSC	A,H	248	On
SSC	A,H	229	On
FITC	A	340	On
PE	A	300	On
Threshold parameter		Threshold	
FSC		200	
SSC		200	
Compensation		Voltage	
PE-FITC		-	
FITC-PE		3.8	

Table 2.3. Settings applied to FACS Aria II for MP detection.

### 2.12 Transmission Electron Microscopy (TEM)

Particles from 1mM and 2.5mM Pi-treated cultures (Fraction 2-Table 2.1) were fixed in 25% (v/v) Glutaraldehyde followed by two 1% (w/v) uranyl acetate washes and air-drying, and viewed using a JEOL JEM1400 TEM with an accelerating voltage of 80kV. Images were captured by a Megaview III digital camera with iTEM software.

### 2.13 Scanning Electron Microscopy (SEM)

Sub-confluent cells on 13mm round coverslips were treated with 1 or 2.5mM [Pi] medium for 90min and then fixed in 2.5% glutaraldehyde in 0.1M Sodium Cacodylate with 2mM Calcium chloride pH7.4, followed by analysis on a Hitachi S3000H scanning electron microscope with an accelerating voltage of 5kV.

### 2.14 Dynamic Light Scattering (DLS)

For comparison with NTA, DLS measurements were performed with a Malvern Zetasizer Nano Series equipped with a 633nm laser to look at size distribution in phosphate-induced versus control MPs released from cultures. This technique gives information on particle size from fluctuations in scattered light intensity due to the Brownian motion of particles suspended in a liquid. DLS can detect particles as small as 1nm in diameter and as large as 1µm diameter. The principle behind DLS is similar to NTA but, unlike NTA, DLS does not allow simultaneous visualising and recording of particles' size, motion, and intensity.

However, in contrast to NTA, DLS allows an easier and faster approach for sample preparation and instrument administration.

The DLS is equipped with a sample loading port (Figure 2.5) where a cuvette can be inserted (depending on different applications and the solvent in which samples are prepared, different cuvettes/aperture can be used: e.g. if the main application is size measurement, a disposable polystyrene cuvette can be used or if molecular weight measurements are of interest then a Glass aperture is recommended) (Malvern Ltd, 2012).

500µl of each sample (Unspun Medium from cells-Table 2.1) was measured in disposable polystyrene cuvettes. A measurement position of 4.65mm from the cuvette wall, an attenuator setting of 10, and a controlled temperature of 20°C were applied for all measurements. Each sample was run in duplicate and each run carried out for 140 sec. To obtain the intensity size distribution, the Z-Average (diameter in nm), and the polydispersity index (Pdl) of samples, the instrument was set up on an autocorrelation function (“multiple narrow mode” set for a “polydisperse” sample i.e. a sample in which considerable particle size variation was expected). All the other settings were the instrument default settings (e.g. the default threshold was set between 0.05-0.01).

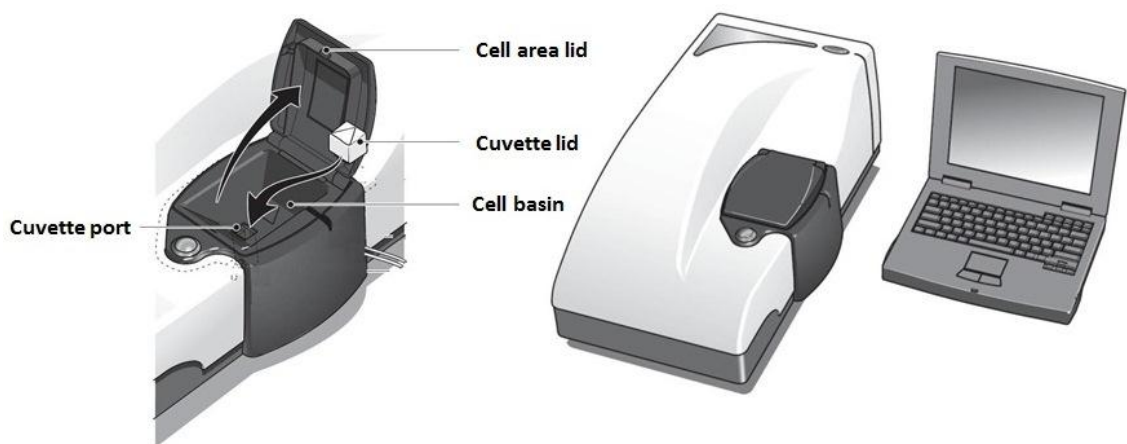


Figure 2.5. A Zetasizer instrument. Picture depicts a typical Zetasizer and a computer with installed zetasizer software. Pictures adopted from (Malvern Ltd, 2012).

## **2.15 Determination of Apoptosis and Cell Death**

### **2.15.1 MTT Assay**

Cultures were incubated in Hanks Balanced Salt Solution (HBSS) without phenol red containing 2mg/ml MTT (Sigma M5655) for 4h at 37°C in a culture incubator. Medium was aspirated and the insoluble formazan product in the cell layer was dissolved in DMSO followed by measurement of absorbance at 595nm.

### **2.15.2 DNA fragmentation (DNA laddering)**

Analysis of DNA fragmentation was performed as described by (Kotamraju *et al.*, 2000). Briefly, cells were treated with 1mM Pi and 2.5mM Pi for 24h. Cells treated with 100-200µM H<sub>2</sub>O<sub>2</sub> were used as positive controls. To suppress DNA fragmentation additional high Pi media supplemented with 100µM Caspase Inhibitor Z-VAD-FMK (R&D Systems) or vehicle control (DMSO) were used. After cell incubation the medium was removed and the adherent monolayer harvested in 250µl of Cell Dissociation Buffer (Sigma) and topped up with their relevant medium followed by centrifugation at 3,000xg, 4°C, 10min. Using a hypotonic lysis buffer (10mM Tris-HCL, pH 8.0, 10mM EDTA, 0.5% Triton X-100) cell pellets were lysed. 0.1 mg/ml RNase A (Sigma-Aldrich) was added to digest the RNA for 30min at 37°C. Proteinase K (1mg/ml) (Sigma) was added and samples further incubated at 37°C for 30min. An equal volume of phenol, chloroform, and isoamyl alcohol (25:24:1) (Sigma) was mixed with the nucleic acid solution to extract DNA followed by DNA precipitation in 1:1 v/v isopropyl alcohol at -20°C for 24h. DNA was collected by centrifugation at 12,000xg, 4°C, 15min and the DNA pellet was washed in 70% ethanol (v/v) and re-pelleted as before. DNA pellets were air-dried and resuspended in 25µl 1x TE. DNA concentrations were determined spectrophotometrically. 5µg DNA was mixed with sample buffer (0.25% bromophenol blue (w/v), 30% glycerol (v/v)) and run on 1.5% (w/v) agarose gel containing 1µg/ml ethidium bromide for 4h and visualised by a UV transilluminator.

### **2.15.3 TUNEL-coupled Hoechst Staining**

TUNEL staining was carried out on cultures on glass coverslips using an In Situ Cell Death Detection Kit, (Fluorescein labelled) (Roche ref 11684795910). Nuclei were stained at the final step with Hoechst 33342 (Sigma) at 1µg/ml for 5min, at room temperature before being analysed by fluorescence microscopy (Nikon Eclipse Ti80 inverted epifluorescence microscope). From each experimental condition four randomly selected fields were examined and fluorescein staining assessed in approximately 50 Hoechst-stained cells per field.

### **2.15.4 Trypan Blue Exclusion Test (TBET)**

Cells were stimulated with test medium containing 1mM Pi, 2.5mM Pi, and 1mM Pi supplemented with 30µM Menadione as a positive control. Cultures were incubated in a humidified incubator at 37°C, 5% CO<sub>2</sub> for 90min, 8h, 24h, and 48h. At the end of each incubation time, test medium was decanted, 250µl of Cell Dissociation Buffer (Sigma) added per well and incubated for 10-20min at 37°C. The dissociated cell monolayer was added back to the relevant test medium and cells collected by centrifugation at 200xg for 5min. The pellet was re-suspended in 1ml of fresh culture medium. 100µl of cell suspension was added to 100µl of a 0.5% solution of Trypan blue. Cells were blind-counted on a haemocytometer and stained cells were scored as dead cells. A minimum of 100 cells were counted for each data point in a total of eight microscopic fields. Data were expressed as percentage of live cells comparing to the control (1mM Pi treated cells).

### **2.15.5 Flow Cytometry (Annexin V/PI Staining)**

Apoptosis was assessed by Annexin V-FITC (BD Pharmingen) and propidium iodide (BD Pharmingen) staining as described in (Di Marco *et al.*, 2008) using a FACSCalibur flow cytometer with Cellquest acquisition software. In the same experiments Forward Angle Light Scattering (FSC) was used as an index of apoptotic cell shrinkage.

Viable cells express phosphatidylserine (PSer) in the internal leaflet of the plasma membrane (PM). This normal PM asymmetry is disrupted when cells undergo stress, leading to PSer externalisation from the inner leaflet of the PM to the external leaflet of the cells. Furthermore, an intact PM is impermeable to viability dyes; for example propidium iodide (PI). When apoptosis is triggered, this leads to plasma membrane PSer externalisation in a time dependent manner, with less externalisation happening at early stages and this becomes exacerbated as time goes by. At the same time the PM is losing its integrity, permitting penetration of PI from the surroundings into the cells. Therefore, the PI can be run in conjugation with Annexin V to measure apoptosis. Annexins are a family of calcium-dependent phospholipid-binding proteins that have a high affinity for PSer in the presence of calcium. So cells at different stages of apoptosis are stained with the conjugates in proportion to the stages of apoptosis that the cells have reached (Figure 2.6 C).

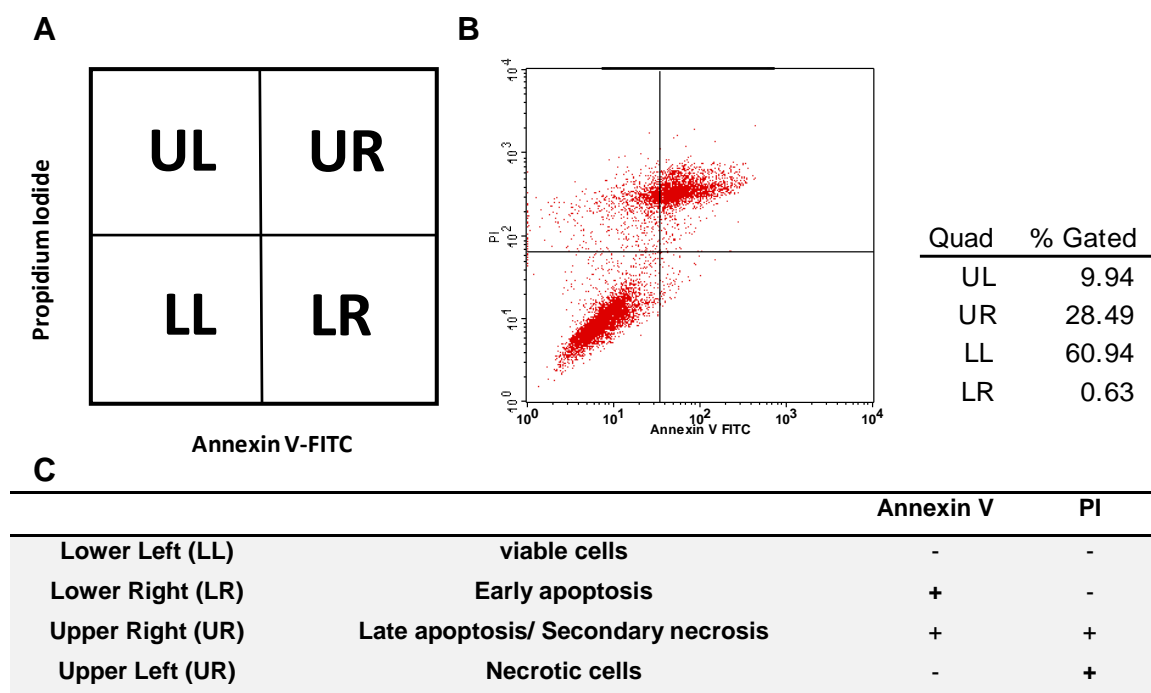


Figure 2.6. Apoptosis detection by dual labelling with Annexin V-FITC/PI using Flow Cytometry. Two filters are used; FL1 for FITC and FL2 for PI. (A) a model representation of Annexin V-FITC (FL1 filter) vs. Propidium Iodide (PI) (FL2 filter) cytogram showing quadrant regions where dual or non-labelled events fall, (B) an example randomly drawn from experimental data showing dual-labelling of cells by annexin V-FITC/PI, (C) a table showing a guideline for interpretation of data; e.g. early apoptosis is defined as events labelled solely with annexin V-FITC (i.e. cells which are expressing PSer but not labelling with PI (an indication that the plasma membrane is not leaky).

Briefly, EAhy926 cells ( $30 \times 10^4$  cells seeded on 6-well 35mm diameter wells) were grown to confluence. At confluence, cells were treated with 1mM vs. 2.5mM [Pi] over a time course. Cells treated with 30 $\mu$ M Menadione were used as positive controls. At the end of the incubation times, test media were collected from cells into 30ml Universal tubes. Cultures were placed on crushed-ice and the cell monolayer harvested by scrapping as rapidly as possible in 500 $\mu$ l of ice-cold PBS without calcium and magnesium. Harvested cells were transferred into tubes containing the corresponding supernatant from the same culture which had been harvested in the total cells (monolayer and floating cells) were collected by centrifugation at 650xg for 5min and 4°C. The supernatant was aspirated and the pellet washed once more in ice-cold PBS followed by collecting the cells as before. At the final step, PBS supernatant was aspirated and the cell pellet suspended in 50 $\mu$ l of staining buffer (i.e. staining mix) for Annexin V-FITC (BD Pharmingen™, 556419)/PI (BD Pharmingen™, 556463) (5 $\mu$ l Annexin V-FITC + 5 $\mu$ l PI + 40 $\mu$ l of Annexin V-binding buffer “Appendix B-19.2” for each sample) and incubated in the dark for 25 min.

To control the specificity of Annexin V-FITC binding, and also to gate the cells and adjust compensations on the Flow Cytometer instrument, the following control staining were made at a the same time:

**Control 1** to gate the cells (viable cells): Pellet of cells suspended in 50 $\mu$ l of Annexin-V binding buffer. This is also referred to as “unstained sample”.

**Control 2** to gate and adjust Annexin positive population of cells: Pellet of cells suspended in 50 $\mu$ l of Annexin V-binding buffer containing 5 $\mu$ l Annexin V-FITC. If any cells fell in the UR region of the cytogram (Fig 2.8A), these were corrected to fall in LR by applying compensations.

**Control 3** to screen Annexin V binding specificity: Pellet of cells suspended in 50 $\mu$ l of Buffer B (Ca-free) (Appendix B-19.3) containing 5 $\mu$ l Annexin V-FITC. It was checked that this did not result in any cells falling in LR and/or UR.

**Control 4** to gate and adjust PI positive population: Pellet of cells suspended in 50µl of Annexin V-binding buffer containing 5µl of PI. If any cells fell in UR (Fig 2.8A), these were corrected to fall in UL by applying compensations.

All controls were incubated in the dark with the other samples for 25min.

At the end of the incubation time, 450µl of either Annexin-V-binding buffer or Buffer B as appropriate was added to the tubes and tubes were centrifuged at 650xg for 5min and 4°C. Supernatant was aspirated and the pellet suspended in 500µl of either Annexin-V-binding buffer or Buffer B as appropriate (This step was run twice). Samples were then run on a FACS Calibur flow cytometer (Becton Dickinson) using settings as indicated in Table 2.4 below within no more than 1hour. Forward- and side-scatter signals were triggered to detect 10,000 events followed by sample analysis using CallQuest software (Becton Dickinson).

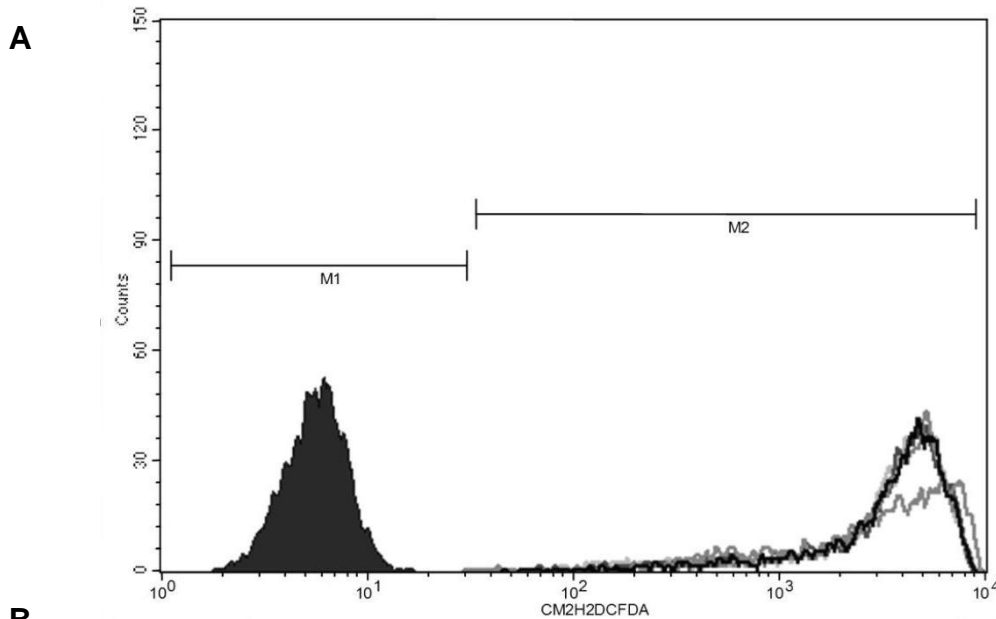
Parameter	Voltage	Amp gain	Log/Lin
FSC	E-1	2.28	Lin
SSC	350	1	Lin
FL1	482	1	Log
FL2	382	1	Log
Threshold parameter		Threshold	
FSC		52	
Compensation		Voltage	
FL1-FL2		2.2%	
FL2-FL1		41.7%	

Table 2.4. Settings applied to FACS Calibur for dual labelling with Annexin V-FITC/PI to detect apoptosis.

## 2.16 Determination of ROS Generation

### 2.16.1 DCFDA and Flow Cytometry

Trypsinised cell monolayers were incubated in IMDM-without phenol red (Invitrogen Ref 21056) containing 10µM CM-H<sub>2</sub>DCFDA (Invitrogen) at 37°C, under 5% CO<sub>2</sub>, in air for 30min and were washed twice in PBS before analysis on a FACSCalibur flow cytometer with Cellquest acquisition software using filter FL1.



**B**

Parameter	Voltage	Amp gain	Log/Lin
FSC	E-1	2.28	Lin
SSC	369	1	Lin
FL1	399	1	Log
Threshold parameter		Threshold	
FSC		52	

Figure 2.7. DCFDA fluorescent probe applied to detect intracellular ROS by Flow Cytometry. (A) Representative histogram showing intact cells stained with no added probe (i.e. M1 gate as a control) and DCFDA positive events falling in M2 (B) Instrument settings on FACSCalibur for ROS measurement using DCFDA.

### 2.16.2 DCFDA-Coupled Hoechst Staining

Adherent cultures on coverslips were stained with CM-H<sub>2</sub>DCFDA as above (Section 2.16.1) followed by staining of the nuclei with Hoechst 33342 at 1µg/ml for 5min, at room temperature, before analysis by fluorescence microscopy as in the TUNEL assay (Section 2.15.3).

### 2.16.3 DHE

Cells were treated with 0.8, 1.8, and 2.8mM [Pi] for 30, 60, and 90min at 37°C, 5% CO<sub>2</sub> in air and humidified atmosphere using HBSS as control medium ([Pi] = 0.8mM). ROS-sensitive dye dihydroethidium (DHE) (10µM) (Sigma) was added to the incubations for the last 30min of the incubations. Cultures were trypsinised, and re-suspended in PBS before being sonicated, followed by determination of fluorescence intensity (Excitation 518nm/Emission 605nm) in a 96-well plate on a Perkin Elmer FluoroCount fluorescent plate scanner.

#### **2.16.4 NBT**

ROS generation was determined colorimetrically in Pi-treated cells using a nitrobluetetrazolium (NBT) assay (Sigma Ref 74032) as previously described (Shuto *et al.*, 2009). Briefly, HBSS containing 0.2% NBT (Sigma) was set up as control medium (Pi concentration 0.8mM). After reaching 60-70% confluence, cells seeded on 22mm 12-well culture plates were treated with medium containing 0.8, 1.8, 2.8mM [Pi] for 30min, 60min, and 90min at 37°C, under a humidified 5% CO<sub>2</sub> atmosphere. Cells treated with 0.8mM [Pi] medium supplemented with 30µM Menadione were used as positive control. N-Acetyl-L-cysteine (NAC) (Sigma) at a final concentration of 10mM was used as a negative control suppressing ROS generation. After cell treatment as above, medium was removed and the cell monolayer was gently rinsed twice with PBS to remove extracellular bound formazan. Methanol (200µl per well) was added to fix the cells and then the cells were air-dried before adding 240µl and 280µl of 2M KOH and DMSO respectively per well to solubilise cell membranes and dissolve formazan respectively. To aid solubilisation, plates were placed on a shaker for 15min at room temperature. The absorbance of samples was determined at 650nm.

#### **2.17 Assay of Nitric Oxide Synthase (NOS) activity**

Nitric Oxide Synthase (NOS) activity in intact cultures was assessed from the rate of generation of L-citrulline (as a by-product of conversion of L-arginine to NO) (Bachetti *et al.*, 2004). L-citrulline was determined by high-performance liquid chromatography as described in (Evans *et al.*, 2007). Briefly, cells on 35mm six-well plates were treated with 1mM and 2.5mM [Pi] for 90min. Test medium was removed and the monolayer rinsed three times in ice-cold 0.9% NaCl. 150µl of 0.3M perchloric acid (PCA) was added/well and cells scraped on ice to precipitate proteins. Samples were centrifuged as 3,000xg, 4°C for 10min to sediment proteins. The protein pellet was used to determine total cell layer protein and an equal volume of Freon-Tri-Octylamine mixture (22% v/v Tri-n-octylamine: 78% v/v 1,1,2-trichlorotrifluoroethane) was added to the supernatant and agitated vigorously to neutralise the PCA. The neutralised

aqueous-top phase was stored at -80°C for determination of L-citrulline by HPLC.

## **2.18 Protein measurement/detection techniques**

### **2.18.1 Lowry Protein Assay**

Lowry protein assay (Lowry *et al.*, 1951) (Folin Assay) was performed to determine total cell protein and protein content of sedimentable 18,000xg protein particle pellets released from cells into the medium (Fraction 3-Table 2.1). Briefly, the pellet of total cell protein and/or sedimentable protein particles from the medium was dissolved in 200µl or 100µl respectively of 0.5M NaOH (Appendix B-2), agitated and then incubated in water-bath at 70°C for 30min to dissolve the proteins.

Protein in 0.5M NaOH was diluted down 1:1, 1:10, or 1:50 in 0.5M NaOH where necessary to bring the concentration within the range of the calibration standards (0, 50, 100, 150, 200, 300, 400, & 500mg/ml) (Appendix B-5). Then 50µl of samples (either diluted or neat) and standards were pipetted onto an Alpha Labs 96-well microtitre plate pre-loaded with 10µl Nano-pure water. In the next step, 600µl Folin Protein Assay Reagent C was added, consisting of 25ml Reagent A (Appendix B-3) mixed with 500µl Reagent B (Appendix B-4), and subsequently 60µl Folin-Ciocalteu's phenol reagent (Sigma F9252) diluted down 1:2 v/v with water was added into each well and gently shaken and incubated at room temperature for 40min. After this time, the absorbance was read on a Titertek Multiscan Spectrophotometer at 650nm.

### **2.18.2 Bio-Rad RC DC protein assay**

Bio-Rad protein determination was performed as described in manufacturer's instruction (Bio-Rad RC DC; 500-0119-0122) for proteins in Lysis Buffer containing β-2M (Appendix B-6). Unlike DC protein assay, RC DC is compatible with the presence of β-Mercaptoethanol and detergent in protein sample(s). Therefore it has been used to measure the protein content in lysates from cells prepared in Lysis Buffers suitable for SDS-PAGE.

Briefly, 25µl of standards (0-2mg/ml BSA in 1% IGEPAL detergent) and cell lysate samples were pipetted into 1.5ml Eppendorf tubes and then 125µl of RC Reagent I added into each tube. The tube was vortexed and incubated at room temperature for 1min. Thereafter, 125µl RC Reagent II was added into each tube, and tubes agitated followed by a 5 min centrifugation at 14,000xg. After this, tubes were inverted to get rid of the supernatant and then 127µl Reagent A' (5µl of DC Reagent S mixed with each 250µl of DC Reagent) was added to each tube. Tubes were agitated and incubated at room temperature for 20 minutes (until the protein precipitate was completely dissolved). The tube was then vortexed and 1ml of DC Reagent B added to each tube. The tubes were vortexed again and incubated for 15 min at room temperature. After this, the absorbance was read at 750nm.

### **2.18.3 Protein sample preparation**

#### **2.18.3.1 Preparing global cell lysate for separation on SDS-PAGE gels**

Cells treated on 35mm diameter 6-well plates were lysed in Complete Lysis Buffer containing protease/phosphatase inhibitors (Appendix B-6) in almost all experiments in this study or in Lysis Buffer without phosphatases inhibitors (Appendix B-6 where phosphatase inhibitors had to be removed from the recipe and replaced with extra water instead). The latter was done in experiments checking the specificity of phosphor-specific-antibodies in which the cell lysates were pre-treated with Alkaline phosphatase (Biolabs) (Appendix C-Figure 5.1). Cell lysates were sonicated for a few seconds before protein measurements as described in Section 2.18.1 or 2.

#### **2.18.3.2 Histone extraction for separation on SDS-PAGE gels**

Histone proteins were extracted from the cell lysates as described before (Ito & Adcock, 2002) with some modifications (Abcam, 2014). Briefly, cells treated with control (1mM Pi) and high Pi (2.5mM Pi) medium were washed twice in ice-cold 0.9% NaCl supplemented with 5mM Sodium Butyrate to retain levels of Histone acetylation and then lysed in Lysis buffer (Appendix B-6 without β-2M) and incubated on ice for 30 minutes to sediment any cell debris, histones and nuclei. Lysates were then centrifuged at 10,000xg for 10min at 4°C. The

supernatant was decanted and stored at  $-80^{\circ}\text{C}$  for further use in Western Blotting and the pellets were washed in half the volume of Lysis Buffer without  $\beta$ -2M and centrifuged as before. Pellets were re-suspended in 0.2N HCl and incubated at  $4^{\circ}\text{C}$  overnight. Samples were centrifuged at  $10,000\times g$  for 10min at  $4^{\circ}\text{C}$  and then the supernatant decanted and the protein content was measured using Bio-Rad DC assay (BIO-RAD). Samples were stored at  $-80^{\circ}\text{C}$  until use.

### **2.19 Immunoblotting and Gel Staining**

Cell lysates were subjected to SDS-PAGE (20 $\mu\text{g}$  protein per lane) followed by either immunoblotting or in- gel staining by Silver Stain Plus (Bio-Rad) (Appendix B-23) or RAPIDstain<sup>TM</sup> Reagent (Calbiochem) as described in the manufacturer's instructions. Immunoblotting was performed onto nitrocellulose membranes (Amersham) followed by probing with primary antibodies against Histone H2B (Cell Signaling 8135) at 1:1000 dilution with 5% BSA, Caspase 3 (Santa Cruz Sc-7148) at 1:200 dilution, PARP (Sigma-Aldrich P7605) at 1:200 dilution, Bax (Santa Cruz Sc-65532) at 1:200 dilution, TM-3 (Cell Signaling D17B8) at 1:1000 dilution with 5% BSA, global P-Tyr (Santa Cruz Sc-7020) at 1:200 dilution with 5% BSA, global P-Ser/Thr (Antibodies-online, BD; ABIN968873) at 1:1000 dilution with 5% BSA, LMW-PTP (Thermo Scientific PA5-15545) at 1:200 dilution, LC3B antibody (NOVUS BIOLOGICALS NB600-1384) at 1:1000 dilution,  $\beta$ -actin (Abcam Ab6276) at 1:10,000 dilution, and  $\alpha$ -tubulin (Cell Signaling 2125) at 1:1000 dilution with 5% BSA. Polyclonal Rabbit Anti-Mouse (DakoCytomation P0260) and Goat Anti-Rabbit (DakoCytomation P0448) Immunoglobulins/HRP at 1:2000 dilution were used as secondary antibodies as appropriate and HRP-labelled proteins were detected by chemiluminescence (ECL-Amersham). Band intensities were quantified by Image Studio Software v 4.0.21 (LI-COR Biosciences, Lincoln, Nebraska, USA) and data are presented as the ratio of intensity for the protein of interest/housekeeping protein expressed as a % of the corresponding ratio under control conditions.

## **2.20 2-D Electrophoresis (2-DE)**

Cell lysates were desalted using Protein Desalting Spin Columns (Thermo Scientific). 2-DE was performed using a PROTEAN<sup>®</sup> IEF Cell (BIO-RAD) (Appendix B-22), followed by 12% SDS-PAGE. The 2-DE gels were stained by Silver Stain Plus (Bio-Rad) - or RAPIDstain<sup>™</sup> Reagent (Calbiochem) (if 2-DE was to be followed by mass spectrometry). In some experiments, proteins from 2-DE gels were blotted onto nitrocellulose membranes (Amersham) followed by probing with primary pan-specific antibody against P-Ser/Thr (Antibodies-online, BD).

## **2.21 Mass spectrometry**

Protein spots on 2-DE gels stained with RAPIDstain<sup>™</sup> Reagent (Calbiochem) were excised and subjected to proteomics analysis by trypsin digestion followed by Orbi-trap (LC MS/MS) or MALDI-TOF mass spectrometry (Voyager DE-STR). The resulting LC MS/MS data were analysed by Scaffold 3 software and MALDI-TOF MS data by the Mascot search engine.

## **2.22 Measurement of Cell Layer Pi**

Pi was determined in neutralised de-proteinised cell extracts as previously described (Challa *et al.*, 1985). Briefly, medium was aspirated and adherent cells rinsed three times in ice-cold 0.9% NaCl on ice. 150µl of 0.3M perchloric acid (PCA) was added per well and cells were scraped. Extracts were deproteinised by standing samples on ice for a 30min followed by centrifugation at 3000xg, 4°C for 10min. The protein pellet was dissolved in 200µl of 0.5M NaOH and stored at -80°C for total cell protein determination. 3µl of Universal Indicator was added to the deproteinised PCA supernatant and the pH was adjusted to approximately 7 by adding appropriate volumes of 4.3M KOH/0.6M Imidazole (Appendix B-16). Samples were snap-spun to precipitate potassium perchlorate and 145µl of neutralised deproteinised supernatant transferred to a clean tube and mixed with 655µl of H<sub>2</sub>O. 200µl of Acidified Molybdate (Challa *et al.*, 1985) (Appendix B-1), and 200µl of a mixture of 2-methyl propan-1-ol and light petroleum (IBPE; 4:1 v/v) (Challa *et al.*, 1985) was added. Samples were vortexed and briefly centrifuged to separate the phases. 75µl of the top pink

organic phase was transferred to a clean tube and mixed with 150  $\mu$ l of absolute ethanol and 10  $\mu$ l of 4% w/v SnCl<sub>2</sub>. The absorbance of the resulting blue species was determined at 750nm.

### **2.23 <sup>32</sup>Pi transport assays**

Pi transport into intact cell monolayers was assayed from the rate of uptake of <sup>32</sup>Pi as described in (Kemp *et al.*, 1993<sub>b</sub>) but the cells were incubated in HEPES Buffered Saline (HBS) (140mM NaCl, 20mM HEPES, 2.5mM MgSO<sub>4</sub>·7H<sub>2</sub>O, 5mM KCl, 1mM CaCl<sub>2</sub>·2H<sub>2</sub>O, 10mg/L Phenol Red) with <sup>32</sup>Pi at room temperature for only 5min, and the total Pi concentration in the assay was 0.1mM. To demonstrate the Na-dependence of Pi transport, NaCl in the HBS was replaced with 140mM Choline Chloride.

### **2.24 Determination of Inhibitory effect of Pi on Tyrosine and Serine/Threonine Phosphatase (PTPase and PSPase) Activity**

PTPase and PSPase activity in EAhy926 cell lysates were determined using Tyrosine and Serine/Threonine Phosphatase Assay Systems (Promega Ref V2471 and V2460 for PTPase and PSPase respectively) as described in the manufacturer's instructions.

### **2.25 Thrombin Generation Assay (TGA) using Calibrated Automated Thrombography (CAT)**

The ability of Pi-derived MPs to enhance thrombin generation was determined (Burton *et al.*, 2013) using CAT using PRP Reagent (Diagnostica Stago, UK) containing 1pM tissue factor. Briefly, 10<sup>6</sup> cells were seeded into a 75cm<sup>2</sup> culture plate and, at 60-70% confluence, were treated with 1mM and 2.5mM [Pi] for 24h. The medium was collected and microparticles isolated as described (Table 2.1) by serial centrifugation steps. One volume of the MP suspension (Fraction 2-Table 2.1) was mixed with 4 volumes of filtered pooled plasma. 20 $\mu$ l of PRP Reagent (Diagnostica Stago, UK) containing 1pM tissue factor was added to 80 $\mu$ l of MPs in PRP in Immulon 2HB round-bottomed microtitre plates and incubated for an hour at 37°C in a fluorescent plate reader equipped with

Thrombinoscope software (Thrombinoscope, Synapse BV, Netherlands) with continuous monitoring.

### **2.26 ATP measurement**

Intracellular ATP was determined by high-performance liquid chromatography as described in (Evans *et al.*, 2007). Briefly, cells on 35mm six-well plates were treated with 1mM and 2.5mM [Pi] for 90min, 8h, 24h and 48h. Test medium was removed and the monolayer rinsed three times in ice-cold 0.9% NaCl. 150µl of 0.3M perchloric acid (PCA) was added/well and cells scraped on ice to precipitate proteins. Samples were centrifuged at 3000xg, 4°C for 10min to sediment proteins. The protein pellet was used to determine total cell layer protein and an equal volume of Freon-Tri-Octylamine mixture (22% v/v Tri-n-octylamine: 78% v/v 1,1,2-trichlorotrifluoroethane) was added to the supernatant and agitated vigorously to neutralise the PCA. The neutralised aqueous-top phase was stored at -80°C for determination of ATP by HPLC.

### **2.27 Glycolytic rate (Lactate production measurement)**

The rate of glycolysis was determined in cells treated with 1mM Pi and 2.5mM Pi over time by measuring the rate of lactate production in culture medium from cells. Lactate was measured spectrophotometrically with lactate dehydrogenase. Briefly; 55µl of standards (0, 400, 800, 1200, 1600 nmoles Lactate/ml) (Table 2.5) and/or samples (medium from cells) was pipetted into 12mm diameter disposable tubes and to these 350µl of a glycine/hydrazine/NAD<sup>+</sup> mixture (comprising 10mg NAD<sup>+</sup> (Sigma N7004) mixed with 2ml of glycine/hydrazine (Sigma G5418) and 4ml of water) was added. Tubes were agitated and 190µl from each tube transferred to a cuvette and the OD read at 340nm. Lactate Dehydrogenase (LDH) suspension (4µl of Sigma L3916) was added to 215µl of the glycine/hydrazine/NAD<sup>+</sup> mixture above and incubated at room temperature until a new stable OD was obtained (about 30min). 190µl from each tube was transferred to a cuvette and the OD read again at 340nm. The increase in OD before and after adding LDH was used to estimate the concentration of lactate in the samples by comparison with a linear calibration curve obtained using lactate standards.

Final [Lactate] nmoles/ml	0	400	800	1200	1600
Vol of De-ionised water (ml)	2.50	2.275	2.050	1.825	1.600
Vol of 4.44mM Lactate standard (ml)	0	0.225	0.450	0.675	0.900

Table 2.5. Lactate calibration standards. Lactate standard (Sigma 826-10; 40mg/ml)

## 2.28 Determination of DNA content of protein particles from the medium

DNA assay (Burton DNA Assay) was carried out on 18,000xg protein particles pellet from the medium (Fraction 3-Table 2.1) to determine the total DNA content of particles. The 18,000xg protein pellets from 1ml of medium from cells were re-suspended in 300µl of 10% PCA. Samples were incubated on ice for about 30min to help the protein and DNA precipitation. DNA plus protein were sedimented by centrifugation at 10,000xg for 10min at 4°C. 100µl of supernatant was used to measure low-molecular weight deoxyribose compounds (this was essentially negligible) and the remaining supernatant plus pellet (i.e. DNA and protein) vortexed and incubated in the water bath at 70°C for 25 min with shaking of the sample tubes at intervals. Tubes were incubated in the fridge at 4°C overnight to precipitate the proteins. The next day, tubes were centrifuged at 10,000xg for 10 min to pellet the proteins. 100µl of supernatant containing the soluble digest of the DNA was transferred into new tubes to be processed further for DNA determination (see below) and the pellet dissolved in 100µl of 0.5M NaOH and used to determine the protein content.

To measure the content of DNA in the samples, 100µl of samples and/or standards (0-200µg/ml of calf thymus DNA) were pipetted into Eppendorf tubes and to this 100µl of diphenylamine (DPA) and 20µl of acetaldehyde (Waterborg & Matthews, 1984) added and vortexed to mix. Samples were incubated at room temperature overnight and the following day, 190µl of this mixture transferred onto 96-well plates and the OD read at 595nm and 710nm. The differences between two ODs was calculated and used to determine total DNA content.

## **2.29 RNA techniques**

### **2.29.1 Transfection with siRNA**

Transient silencing of phosphate transporters PiT-1/2 (slc20a1/a2) transporter expression in cells was performed by siRNA targeting the specific genes using Silencer<sup>®</sup> Select Validated siRNAs (Ambion) with a scrambled non-target Silencer<sup>®</sup> Select Negative Control siRNA (Ambion) as a negative control. siRNA oligonucleotides were incubated for 4h with the cultures at 10nM final concentration, as described in the manufacturer's instructions with some modifications using Lipofectamine<sup>®</sup> RNAiMAX Transfection Reagent (Invitrogen) (Detailed transfection mixture applied is summarised in Appendix C-4.1). Uptake of siRNA was confirmed using BLOCK-iT<sup>™</sup> Fluorescent oligonucleotides (Invitrogen) followed by quantification by flow cytometry. Gene silencing was confirmed by RT-qPCR using primers specific for PiT-1/2.

### **2.29.2 Primer design and DNA sequencing**

Slc20a2 primers were designed using gene sequence obtained from the NCBI nucleotide database and Primer-3 software v.0.4.0. and the amplified product was sequenced to confirm the result as previously described in this laboratory (Nima Abbasian, 2010). All primers (Slc20a1, Slc20a2, and reference GAPDH; see table 2.7) were optimised for qPCR efficiency. Briefly, three different annealing temperatures ( $T_A$ ) were run to obtain the optimal  $T_a$ . Having obtained the optimum  $T_a$ , qPCR efficiency was determined by performing qPCR using five descending concentrations of cDNA (1:5 dilution) to produce a standard curve. Primer efficiency was obtained from the slope on the standard curve ( $10^{(-1/\text{slope})} \times 100$ ).

### **2.29.3 Total RNA extraction from cell monolayer**

Total RNA was extracted from 70% confluent cultures (HUVECs, VSMCs. & EAhy926 Cells) and/or transfected EAhy cells (Section 2.29.1) using Trizol<sup>®</sup> Reagent (Invitrogen 15596-018). Briefly, Growth Medium/test medium was aspirated from the culture dishes and cells were washed with HBSS two times. Next, 1.5ml and 600 $\mu$ l Trizol reagent (pre-warmed to Room Temperature) was added into each culture vessels (25cm<sup>2</sup> flasks) or per well of 6-well plates

(35mm) respectively and cells were covered by the reagent by swirling the Trizol. Thereafter, the resulting cell suspension was transferred into an autoclaved (RNAase-free) 2ml screw-cap Sarstedt tube. In the next step, 200µl of Molecular Biology grade chloroform (Sigma-302432) was added per ml of the Trizol reagent and tubes were centrifuged at 14,000xg and 4°C for 15min. From top to bottom, three distinctive phases were obtained namely; an aqueous crystal clear phase containing RNA, the interface containing DNA, and the lower phase containing protein.

The lower phase (phenol/chloroform) was stored at (-80°C) for further protein extraction from Trizol (if necessary). The upper phase (RNA) was transferred into a new clean autoclaved 2ml Sarstedt and 500µl of molecular biology grade Isopropyl alcohol (Iso-2-propanol) (Sigma 19516) was added (per ml of Trizol reagent that had originally been used) to precipitate the RNA. After adding Iso-2-propanol, the tube was vortexed gently and allowed to stand on the bench for at least 10min for the precipitation to be completed, followed by centrifugation at 8,300xg for 10min on a refrigerated microcentrifuge at 4°C. Then, the supernatant (The isopropyl alcohol) was aspirated and the pellet (RNA; Barely visible) was washed by re-suspending in 1ml RNAase free 75% chilled ethanol. The tube was then vortexed and the RNA was spun down at 8,300xg at 4°C for 5min. In the following step, the supernatant (75% ethanol) was aspirated by gently inverting the tube and the RNA pellet was allowed to air dry for half an hour. 20µl of RNAase-free (DEPC) water was added to dissolve the RNA pellet and the concentration of RNA was measured by reading the optical density at 260nm on a Nano-Drop 1000 V3.71 spectrophotometer. RNA samples were stored at (-80°C).

#### **2.29.4 Total RNA extraction from Pi-derived MPs**

Total RNA was extracted from Pi-derived MPs (Fraction 2-Table 2.1) from the medium collected from phosphate treated cells in large (125cm<sup>2</sup>) culture plates (1mM control phosphate vs. 2.5mM in DMEM).

250µl of Trizol<sup>®</sup> Reagent (pre-warmed to Room Temperature) was added to the pellet of MP. In the next step, 50µl of Molecular Biology grade chloroform was added to this and then tubes were vortexed and then centrifuged at 10,000xg and 4°C for 15min. The upper clear phase (RNA phase) was transferred into new autoclaved tubes and 250µl Isopropyl alcohol was added to this to precipitate the RNA (NB: This is twice as much Isopropyl alcohol as was added to routine RNA extraction from cell monolayers. (This modification was made to increase the desired RNA precipitation). Tubes were agitated gently and the precipitation was completed by standing the tube at room temperature for 10min. Tubes were centrifuged at 10,000xg for 10min on a bench microcentrifuge followed by aspiration of the isopropyl alcohol supernatant and washing the pellet in 1ml of RNAase free 75% ethanol. In the following step the tubes were centrifuged at 10,000xg for 5min at 4°C and the supernatant was aspirated by gently inverting the tube and allowing the pellet to air dry for a few minutes. 20µl of DEPC water was added to the pellet and the concentration of RNA was calculated by measuring the optical density at 260nm on a Nano-Drop 1000 V3.71 spectrophotometer (Thermo Scientific). The presence of microRNA in samples was determined using an Agilent RNA 6000 Pico Kit (Agilent Technologies; 5067-1513). Extracted RNA (containing microRNA) was stored at -80°C for future use.

#### **2.29.5 Reverse Transcription (RT) reaction (cDNA synthesis)**

Using 1µg of total RNA, cDNA was synthesised using an AMV Reverse Transcription System (Promega) according to the manufacturer's instructions. Briefly, extracted RNA as described in Section 2.29.3 was diluted on ice with DEPC water to 1µg per 1µl in a total volume of 2µl in a thin walled PCR tube, followed by incubation in a water-bath at 70°C for 15 min and immediate chilling of the tube on ice, to remove secondary structure in the RNA. In the meantime the RT Master Mix was prepared by mixing reagents (Appendix B-17) from a Promega Reverse Transcription System kit (Promega A3500).

RT-Master Mix (18µl) was added to each cooled RNA+DEPC tube. Tubes were then placed in a PCR thermal cycler (Techne Genius or Techne Progene) and programmes were set up as follow;

- 1 Cycle, Segment 1, 42°C, Hold Time (1h) for synthesis time.
- Segment 2, 99°C, Hold Time (5min) for enzyme inactivation.
- Segment 3, 4°C, Hold Time (5min) or could be left over-night.

At the end of the programme samples (RT-Products) were stored at (-80°C) for future PCR or qPCR analysis.

### 2.29.6 PCR (Polymerase Chain Reaction)

Polymerase Chain Reaction (PCR) was performed on RT-Products to amplify with specific primers the cDNA followed by subsequent separation of the products of interest by Agarose gel electrophoresis.

PCR Master Mix was made up by mixing 22.5µl ReddyMix PCR Master Mix (ABgene AB-0575), 0.5µl of the Forward and the same volume of the Reverse primer (Table 2.6), and 0.5µl DEPC (RNase-free) water. To this 24µl of PCR Master Mix, 1µl of relevant RT-Product (Section 2.29.5) was added on ice and the content was mixed thoroughly by pipetting up and down in a pipette tip. PCR tubes were transferred to a thermal cycler (Techne Genius or Techne Progene) and programmes were set up as follows to achieve 25 to 38 amplification cycles.

94°C	4min for 1 Cycle	
94°C	30Sec	} 32 Cycles
58°C	1min	
68°C	1min	
68°C	7min for 1 Cycle	

Figure 2.8. Schematic diagram of applied PCR with 32 cycles.

At the end of these programmes PCR-Products were either immediately separated on Agarose Gel Electrophoresis or stored at (-20°C).

Primer		Sequence	Length	Product size (bp)	NCBI reference
<b>PiT-1</b>	F	TACCATCCTCATCTCGGTGG	20	410	NM_005415.4
	R	TGACGGCTTGACTGAACTGG	20		
<b>PiT-2</b>	F	TGGATGGTCATTTTGGGTTT	20	385	NM_006749.3
	R	GCACACCTTTGGTACCGATT	20		
<b>NaPi-IIb</b>	F	GATCGGAGTGAGTTCAGAAGAG	22	195	NM_001177999.1
	R	GGGCTTAGTGATGACTTTCAG	21		
<b>GAPDH</b>	F	TACATGTTCCAATATGATTCCACCC	25	310	NM_001289746.1
	R	TGATGATCTTGAGGCTGTTGTC	22		

Table 2.6. PCR Primers table. F: Forward primer and R: Reverse primer. PiT-1 and -2 (gene family; Slc20a1 and a2), and NaPi-IIb (gene family; Slc34a2).

### 2.29.7 Agarose Gel Electrophoresis

The gel bed chamber tray of an electrophoresis rig was filled with 1.5% w/v molecular biology grade Agarose (Sigma A9539) in 40mM Tris-Acetate, 1mM EDTA, pH 8.3 (1x TAE) by diluting the 10x stock (Sigma T-9650) with DEPC water and adding 0.3µg/ml Ethidium Bromide (Sigma E-1510). After the casting gel had cooled, 1x TAE was poured into the gel tank. A DNA Size Marker Ladder (ϕX174 Hae III Digest) (Sigma D-0672) and the PCR-Products were loaded into the wells of the gel and then subjected to electrophoretic separation at 100V for ~ 2hours, followed by UV visualisation of the bands on a Bio-Rad Gel Doc imaging system.

### 2.29.8 RT-qPCR

Total RNA was extracted using Trizol reagent (Section 2.29.3). Using 1µg of total RNA, cDNA was synthesised using an AMV Reverse Transcription System (Section 2.29.5). The q-RT-PCR Master Mix was made up by mixing 12.5µl of Power SYBER®Green PCR Master Mix (Applied Biosystems; Cat N. 4367659) with 1µl of either FWD or REV Slc20a1/Slc20a2 primer (or GAPDH qPCR primer as a house keeping gene) (Table 2.7). The total volume was adjusted to 24µl by adding autoclaved nano-pure water. To this 24µl Master Mix, 1µl of cDNA (Section 2.29.5) was added. Real-time PCR was performed using an

Applied Biosystems 7500 Fast Real-Time PCR System (Applied Biosystems, Life Technologies). Relative amounts of mRNA were normalised to the corresponding GAPDH signal for each sample and relative expression is presented as  $(2^{-\Delta\Delta CT})$  (Livak & Schmittgen, 2001).

Primer		Sequence	Length	Product size (bp)	NCBI reference
<b>PiT-1</b>	F	CCAACCTGTGCAGGCATAGAA	20	92	NM_005415.4
	R	TTCTTCCTGGTTCGTGCATT	20		
<b>PiT-2</b>	F	AGGATTCTCACTGGTTCGCAA	20	111	NM_001257181.1
	R	AGGCCAGACATGAAACCAGA	20		
<b>GAPDH</b>	F	CATGTAGTTGAGGTCAAGGA	20	151	NM_001289746.1
	R	CGAGCCACATCGCTCAG	17		

Table 2.7. Primers used for RT-qPCR. F: Forward primer and R: Reverse primer. PiT-1 and -2 (gene family; Slc20a1 and a2).

### 2.30 <sup>45</sup>Ca deposition on cell monolayer

<sup>45</sup>Ca deposition on EAhy926 endothelial cells was determined by measuring the <sup>45</sup>Ca deposition (cpm: counts per minute) in deproteinised extracts of phosphate-treated EAhy926 endothelial cells. Cells were seeded on 35mm diameter (6-well plates) at  $30 \times 10^4$  cells per well and allowed to reach confluence in normal Growth Medium. At confluence, growth media were aspirated and cultures were rinsed three times in HBSS to remove serum, then 2ml per well of relevant test media (Appendix C-Tables 3.1 and 3.2) were added on cells and cells incubated over 90min, 8h, 24h, and 48h. <sup>45</sup>Ca was added as stated in Appendix C-3.2.

After incubation of EAhy926 cells in test media with <sup>45</sup>Ca, the medium was aspirated, plates were then placed on ice and the cells were washed thrice in ice-cold 0.9% NaCl to remove extracellular <sup>45</sup>Ca and stored at -20°C. In the next step, plates were taken out of the -20°C freezer and cells were thawed and scraped in 150µl 0.3M PCA to make Perchloric Acid Extracts. PCA extracts were transferred into 1.5ml microcentrifuge tubes and then incubated on ice for 30min to allow as much protein as possible to precipitate. Tubes were centrifuged at 1,900xg for 10min at 4°C to sediment cell protein, then 150µl of supernatant above the pellet (cell protein) was removed, mixed with 4ml

Ecoscint A scintillant and counted on the LKB1219 Scintillation counter. Total cell protein in the protein pellet was dissolved in 200µl of 0.5M NaOH and the resulting digest was assayed using the Lowry assay described in Section 2.18.1.

The reading in un-used test media was also measured in triplicate by pipetting 50µl aliquots of each unused <sup>45</sup>Ca-labelled Test Medium sample into scintillant.

The effect of phosphonoformic acid (PFA) on <sup>45</sup>Ca deposition on EAhy926 cells was assayed in the same way, but some culture were treated in the presence of 1mM [PFA], a concentration which has been shown to blunt transport of Pi into the cells (Figure 4.7 A). Medium from cells was also saved to measure the protein particle release from the cells into the medium (Fraction 3-Table 2.1).

### **2.31 Statistical Analysis**

Data are presented as the Mean±SEM and were analysed using GraphPad Prism 6.0. Data normality was checked with the Kolmogorov-Smirnov test. Two group data comparisons were analysed by *t* test (for normally distributed data) or by Wilcoxon matched-pairs signed rank test (for nonparametric data). One-way ANOVA (combined with Tukey's *post hoc* test (for normally distributed data) or Dunn's (nonparametric) *post hoc* test) was applied for multiple comparison tests as appropriate. *P* values < 0.05 were considered statistically significant.

## Chapter 3. Effect of Pi on microparticle (MP) release from EAhy926 endothelial cells

---

### 3.1.1 High [Pi] acutely induces microparticle (MP) release from EAhy926 cells

Patients with Chronic Kidney Disease (CKD) are at high risk of cardiovascular complications and display endothelial cell (EC) dysfunction (Burton *et al.*, 2013; Foley *et al.*, 1998<sub>b</sub>). As explained in Section 1.16.5, upon cellular activation and/or apoptosis, microparticles (MPs) are shed from plasma membranes of cells (notably platelets, endothelial cells (ECs) and leucocytes) (Burton *et al.*, 2013; VanWijk, *et al.*, 2003; Boulanger & Dignat-George, 2011; Key *et al.*, 2010<sub>a,b</sub>). A growing body of evidence suggests that CKD leads to activation of ECs (Shuto *et al.*, 2009; Burton *et al.*, 2013) culminating in MP generation. MPs occurring in plasma of healthy subjects are mainly of platelet origin, but endothelial MPs are increasingly recognised as powerful markers for vascular dysfunction in CKD (Dursun *et al.*, 2009) and potential causes of thrombosis and cardiovascular disease (Bernal-Mizrachi *et al.*, 2004; Mallat *et al.*, 2000). Work from this laboratory has recently shown that endothelial and platelet MPs increase significantly in patients on haemodialysis or peritoneal dialysis compared to matched controls (Burton *et al.*, 2013).

Hyperphosphataemia, on the other hand, as explained in Section 1.5, is one of the commonest findings in patients with CKD (Bevington. A *et al.*, 1990; Shuto *et al.*, 2009) and has been implicated in induction of EC dysfunction (Shuto *et al.*, 2009; Di Marco *et al.*, 2008; Di Marco *et al.*, 2012; Peng *et al.*, 2011) and therefore MP formation.

In mammalian cells, hyperphosphataemia has been shown to result in Pi influx into the cells within 2 hours (Kemp *et al.*, 1988<sub>a,b</sub>; Kemp *et al.*, 1993<sub>b</sub>). This increase in intracellular Pi could in principle work as a signal triggering the MP release from the cells which has been reported in CKD patients (Burton *et al.*, 2013).

In principle the effect of hyperphosphataemia on endothelial cell dysfunction and loss of cell membrane integrity (regarding intracellular Pi as a stress stimulus) could result in release of a range of particles from the cells (Figure 3.1). These could vary from small membrane blebs ( $\leq 1\mu\text{m}$  diameter) to big apoptotic bodies (approximately 1-5 $\mu\text{m}$  diameter) (Section 1.16.5.3) or even bigger fragment(s) of the cells, and/or cell detachment or anoikis resulting in circulating intact cells (Erdbruegger *et al.*, 2006; Boos *et al.*, 2006; Mohamed *et al.*, 2005). Pi may also in principle exert direct physico-chemical effects on protein particles, enhancing their ability to sediment (Figure 3.1-mechanism 2).

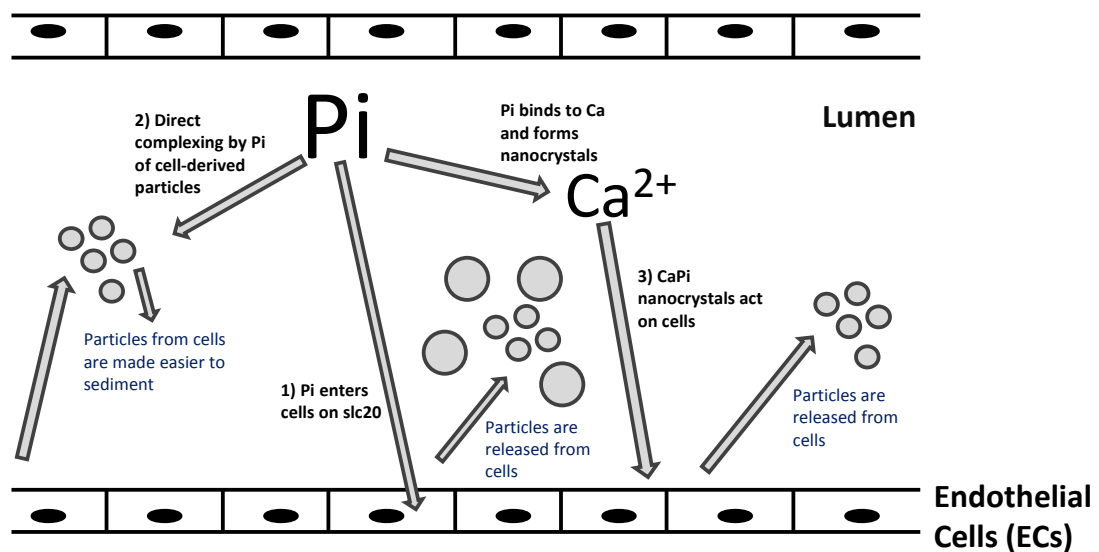


Figure 3.1. Schematic view of shedding membrane vesicles from endothelial cells (ECs) in response to hyperphosphataemia (see Section 1.18). The figure depicts three hypothetical mechanisms of Pi acting on ECs and MP formation (Section 1.Aims). Mechanism 1 indicates Pi influx into the cells through Pi transporters (i.e. PiT transporters) resulting in accumulation of Pi in the cells which signals MP release from the cells. Pi may also directly bind to  $\text{Ca}^{2+}$  and form calcium phosphate nanocrystals (mechanism 3) which could act in their own right act on cells (Sage *et al.*, 2011) and result in particle release. Moreover, Pi in solution may directly act on protein particles in the medium and exert physico-chemical effects (i.e. mechanism 2). Pi may complex with the particles and result in an enhanced particle sedimentation and/or aggregation.

### **3.1.2 Pi-derived MPs are strongly pro-coagulant**

As histones (Ammollo *et al.*, 2011) and the phosphatidylserine (Sinauridze *et al.*, 2007) expressed on the surface of MPs have been shown to be pro-coagulant, the possible pro-coagulant effect of the MP fraction derived from the Pi-stimulated cultures of EAhy926 cells was assayed in a Thrombin generation assay. This was done to determine whether Pi-derived MPs might be a possible contributor to the elevated levels of procoagulant plasma microvesicles in dialysis patients that have previously been reported from this laboratory (Burton *et al.*, 2013).

The aims of the work in this chapter were therefore;

- To investigate if cells (EAhy926 endothelial cells or HUVECs) exposed to a high extracellular Pi concentration lose membrane integrity and start budding off cell surface vesicles.
- To investigate if manipulating intracellular Pi concentration in the cells (i.e. by (i) metabolic trapping of intracellular Pi by fructose and (ii) blocking Pi entry into the cells using Pi transporter inhibitor (PFA)) results in a decrease and/or abolition of particle release from the cells.
- To investigate both acute and chronic Pi actions on cells and to check if an elevated Pi concentration in solution results in Ca/Pi nanocrystal formation.
- To investigate if Pi in solution results in enhanced protein particle sedimentation and/or aggregation.

## 3.2 Results

### 3.2.1 Acute (90min) hyperphosphataemia enhances EAhy926 cells' membrane blebbing

Perturbing extracellular Pi concentration typically leads to changes in intracellular Pi in mammalian cells within 90min (Kemp *et al.*, 1988<sub>a,b</sub>; Kemp *et al.*, 1993<sub>b</sub>). After 90min of exposure to an elevated extracellular Pi concentration of 2.5mM, significant membrane blebbing was detected on the surface of EAhy926 cells by scanning electron microscopy (Figure 3.2 A) and the resulting particles were approximately 100-200nm diameter (Figure 3.2 B).

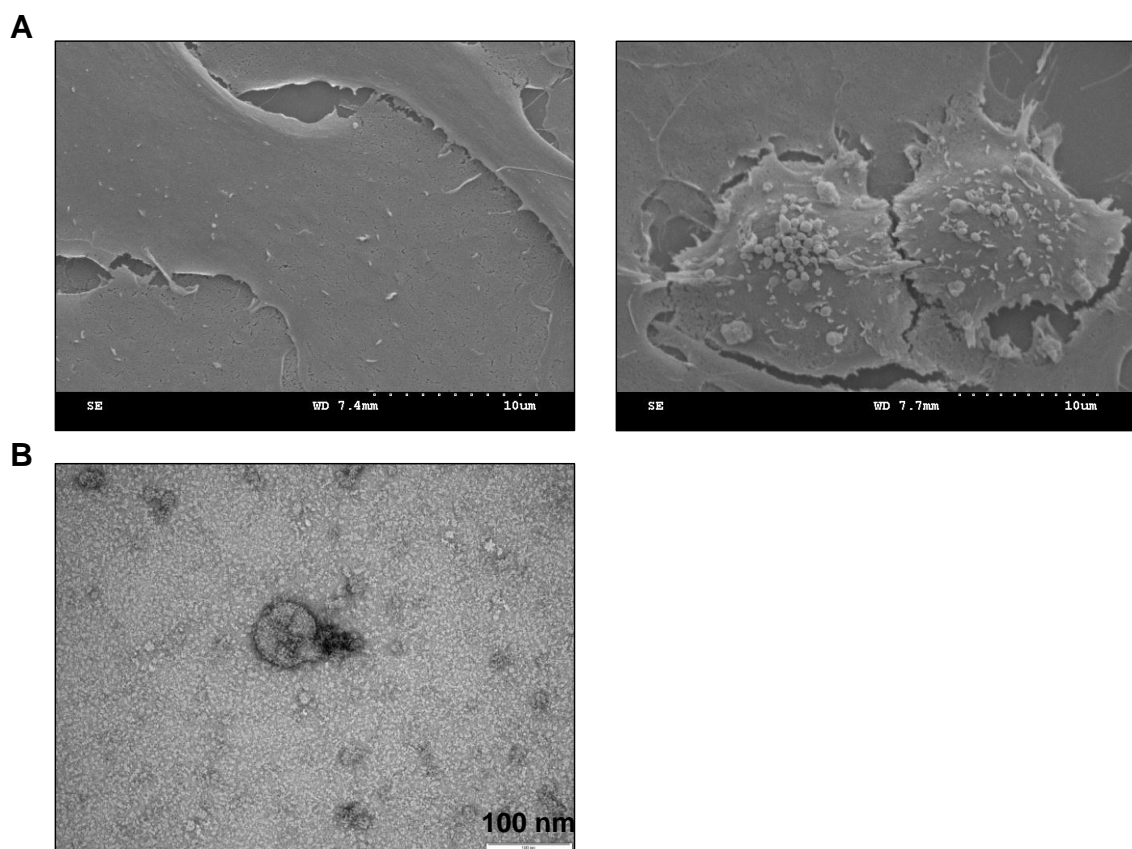


Figure 3.2. Acute release of microparticles from EAhy926 endothelial cells incubated for 90min with control (1mM) and high (2.5mM) [Pi] medium. (A) Scanning Electron Micrographs (SEM) showing microparticles budding off the cell surface (Original magnification x4000) (with 1mM Pi (Left)) or high phosphate milieu (2.5mM Pi (Right)) (B) Negatively stained Transmission Electron Micrographs (TEM) of microparticle fraction (Fraction 2-Table 2.1) from the medium, showing a Pi-derived MP of approximately 100-200nm diameter with an intact membrane (Original magnification x100,000). (NB: all micrographs are representative of three experiments)

### 3.2.2 Acute (90min) hyperphosphataemia increases microparticle release from EAhy926 cells

Examination of the culture medium by transmission electron microscopy (Figure 3.2 B), nanoparticle tracking analysis (NTA) (Figure 3.3 A, B, and E) and flow cytometry (Figure 3.3 C-D) showed that cell surface membrane blebbing was accompanied by a marked increase in release of particles resembling *in vivo* endothelial microparticles i.e. membrane-limited vesicles of 0.1-1.0 $\mu$ m diameter (Figure 3.2 B and Figure 3.3 B) expressing CD144 (VE-Cadherin) and phosphatidylserine on their surface (Figure 3.3 C-D).

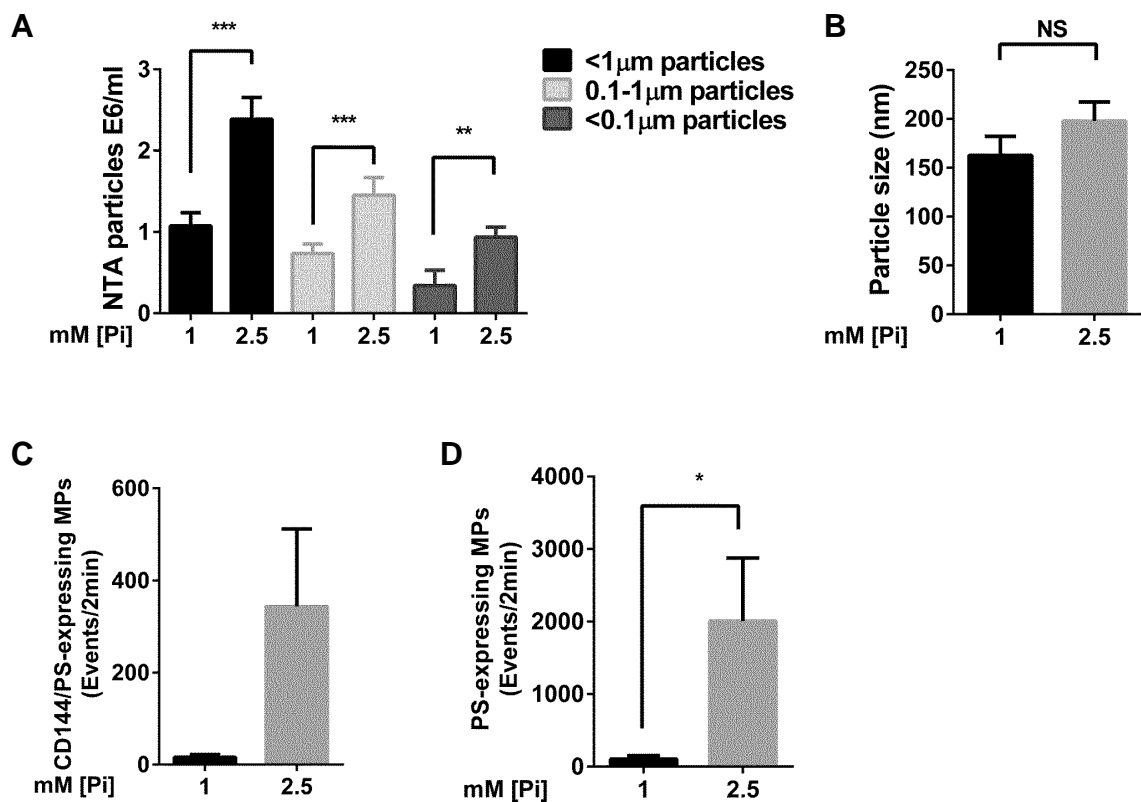


Figure 3.3. (Part 1 of 2) Acute release of microparticles from EAhy926 endothelial cells incubated for 90min with control (1mM) and high (2.5mM) [Pi] medium. (A, B) Nanoparticle Tracking Analysis (NTA) performed on uncentrifuged medium showing (A) particle concentration expressed as millions (E6) per ml; and (B) average particle size. (n=35), \*\*P<0.01, \*\*\*P<0.001; NS: Not Statistically Significant. (C, D) Flow cytometry data showing the number of particles (obtained after incubation of cells with medium for t = 90min at the specified Pi concentration) which dual-labelled with anti-CD144-PE antibody and Annexin V-FITC (C) and Annexin V-FITC only (D). Using medium from a 75cm<sup>2</sup> culture flask, particles were prepared (Fraction 2-Table 2.1; see General Methods section), suspended in 500 $\mu$ l MP-Buffer (145mM NaCl, 2.7mM KCl, 10mM Hepes, pH 7.4) and 38 $\mu$ l of this suspension was subjected to FACS analysis as described in General Methods section; (n=3), \*P<0.05 versus 1mM Pi control.

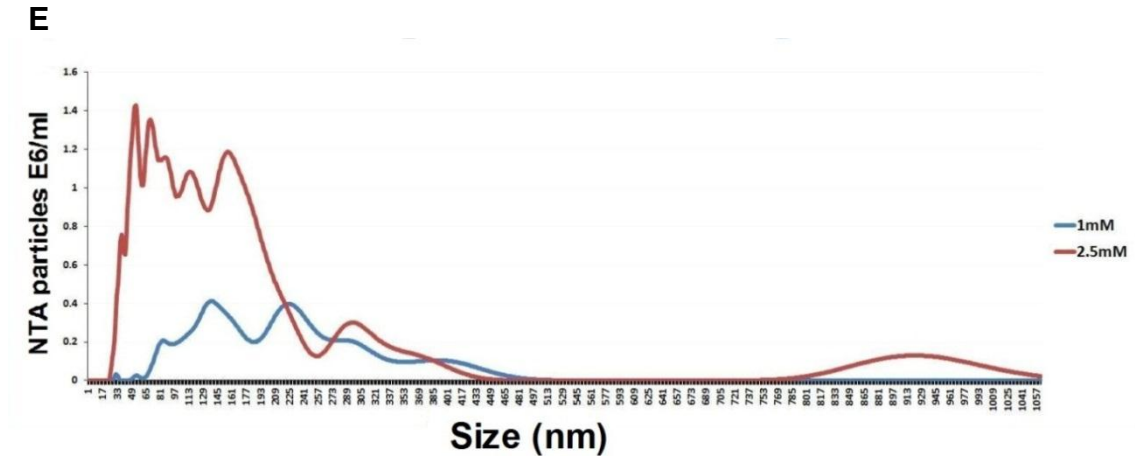


Figure 3.3. (Part 2 of 2) Acute release of microparticles from EAhy926 endothelial cells incubated for 90min with control (1mM) and high (2.5mM) [Pi] medium. (E) Comparison of the size/concentration of released MVs from ECs determined by NTA (particle size (x-axis) and concentration (y-axis)).

The effect of a wide range of extracellular Pi (i.e. 0.5, 1, 1.7, and 2.5mM) on the NanoSight detectable particle release from EAhy926 cells was studied after 90min of exposure of the medium to the cells. Whereas a modest increase in Pi concentration from 1.0mM to 1.7mM had no detectable effect, lowering the concentration to 0.5mM apparently blunted the particle release.

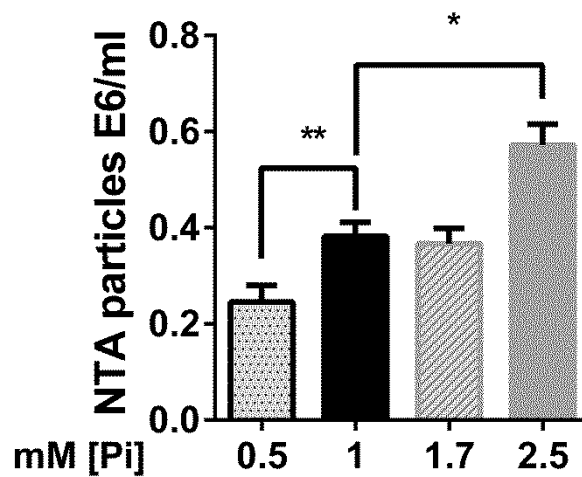


Figure 3.4. Effect of wide range of extracellular Pi on MP output from EAhy926 cells at 90min. EAhy926 cells were incubated in the medium containing 0.5, 1, 1.7, and 2.5mM Pi for 90min. Medium from cells was collected after 90min incubation and particles from the medium counted by NTA. Medium containing 1mM [Pi] was set up as the control. (n=3) \*P<0.05, \*\*P<0.01.

In an alternative culture model of human vascular endothelial cells (HUVECs), a similar acute (90min) effect of an elevated Pi concentration on particle release was detected by NTA (Figure 3.5).

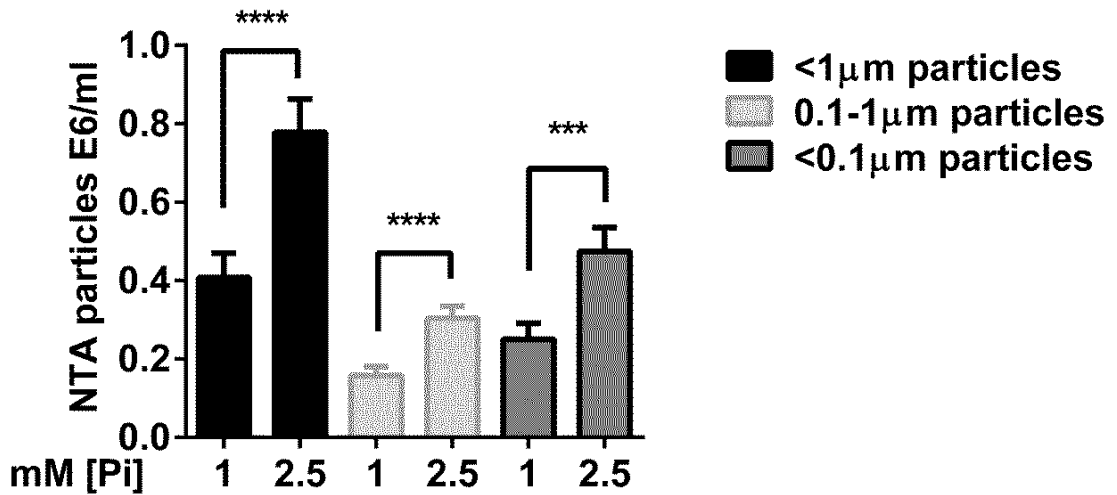


Figure 3.5. Acute release of microparticles from EAhy926 endothelial cells incubated for 90min with control (1mM) and high (2.5mM) [Pi] medium. Nanoparticle Tracking Analysis (NTA) was performed on uncentrifuged medium (particle concentration expressed as millions (E6) per ml) (n=3) \*\*\*P<0.001, \*\*\*\*P<0.0001.

In principle the Pi-induced light-scattering particles detected by NTA could be Calcium Phosphate nanocrystals rather than MPs. However, enhanced release of particles persisted even after the extracellular Pi concentration had been returned to the control value of 1mM (Figure 3.6 A-B). This would not have been expected if the particles were Calcium Phosphate nanocrystals. Enhanced release of microparticles containing protein was confirmed by centrifugation of the medium and analysis of the sedimentable protein pellet (Figure 3.6 B). Such enhanced release of sedimentable protein persisted even at 24h (see Section 3.2.4 below).

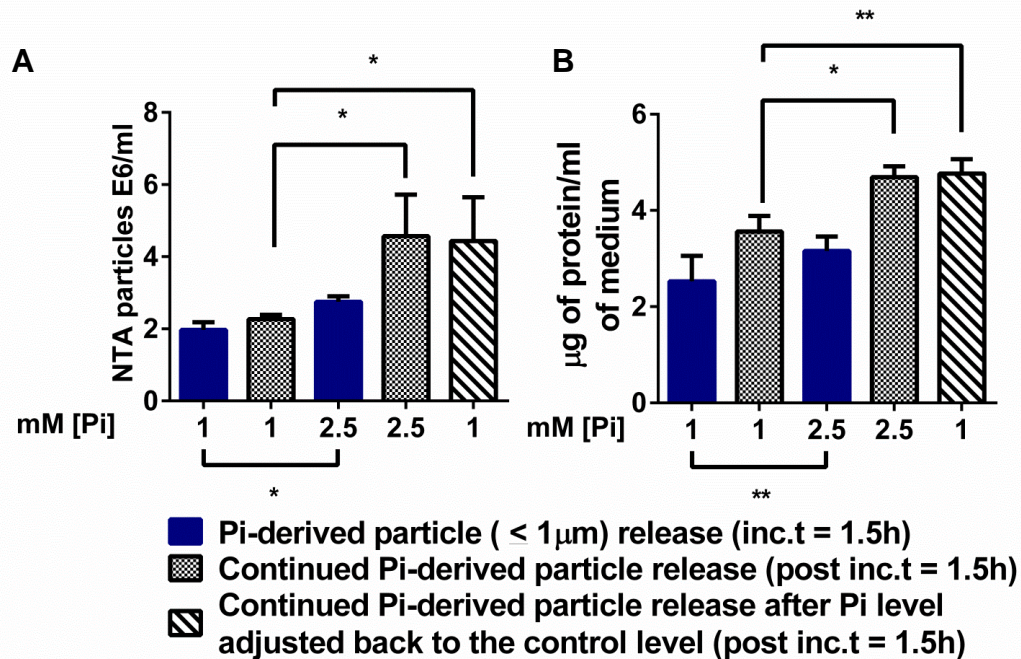


Figure 3.6. Acute release of microparticles from EAhy926 endothelial cells incubated for 90min with control (1mM) and high (2.5mM) [Pi] medium is not attributable to calcium phosphate crystallisation in the medium. (A, B) Continued particle release after the extracellular Pi concentration had been raised to 2.5mM for 1.5h then adjusted back to the control level of 1mM for a further 1.5h (an indication that Pi-derived particles are microparticles rather than Ca/Pi-nanocrystals forming in the medium as a direct result of the high Pi concentration). (A) particle concentration measured by NTA in uncentrifuged medium; and (B) total protein determined in particles sedimented from the medium at 18,000g (Fraction 3-Table 2.1) (n=3) \*P<0.05, \*\*P<0.01.(The design of this experiment is explained in detail in the schematic diagram in Appendix C-Figure 3.1).

### 3.2.3 Acute (90min) Pi-induced MP release from EAhy926 cells depends upon Pi influx into the cells

Depletion of intracellular Pi by metabolic trapping with the slowly metabolised sugar fructose (Woods *et al.*, 1970) (Figure 3.7 A), or by blocking Pi transporters with the Pi analogue PFA (Figure 3.7 B), significantly blunted release of MPs from the cells when they were exposed to an elevated extracellular Pi concentration of 2.5mM, suggesting that a rise in intracellular Pi concentration was the primary cause of the increase in MP output.

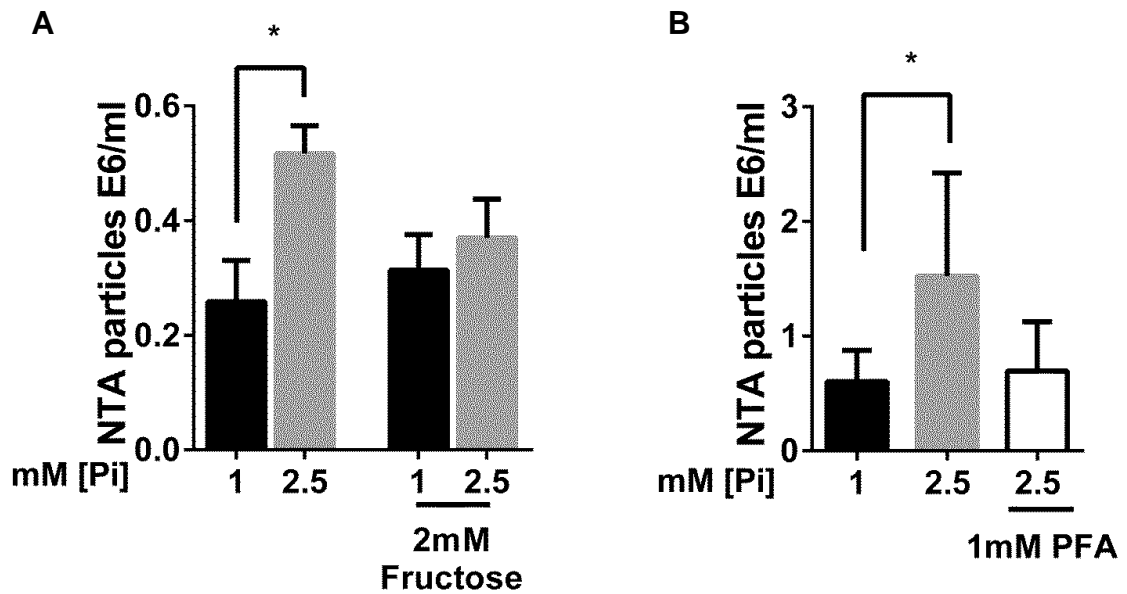


Figure 3.7. Acute release of microparticles from EAhy926 endothelial cells incubated for 90min with control (1mM) and high (2.5mM) [Pi] medium depends upon Pi influx into the cells. (A, B) Blunting of the Pi-induced microparticle release by loading the medium with fructose (A) or with Pi analogue PFA (B) (an inhibitor of sodium-dependent PiT-1/2 Pi transporters). (n=3) \*P<0.05.

### 3.2.4 Chronic (24h) hyperphosphataemia increases detachment of EAhy926 cells

Quantification by NTA of MP release during more prolonged ( $\geq 24$ h) exposure to 2.5mM Pi initially detected no stimulation of particle output (Figure 3.8). However, centrifugation of the resulting culture medium at 18,000g after 24h exposure of the cells to 2.5mM Pi led to a reproducible increase in sedimentable protein (Figure 3.8 A and 3.9 A) implying that the sedimented particles were whole cells or large cell fragments exceeding the NTA analyser's 1.0 $\mu$ m upper detection threshold. This was confirmed by subjecting the particles to fragmentation by freeze-thawing the medium from these experiments and then sedimenting and resuspending the particles. In this way NTA readily detected an increase in particle count following 24h 2.5mM Pi exposure (Figure 3.8 C). As with the acute particle release after 90min (Figure 3.7 B), this cell detachment effect of 2.5mM Pi was abolished by blocking Pi transport with PFA (Figure 3.9 B). Examination of the culture medium by flow cytometry again showed that these particles resembled *in vivo* endothelial microparticles (i.e. expressing CD144 (VE-Cadherin) and phosphatidylserine on their surface (Figure 3.9 C)).

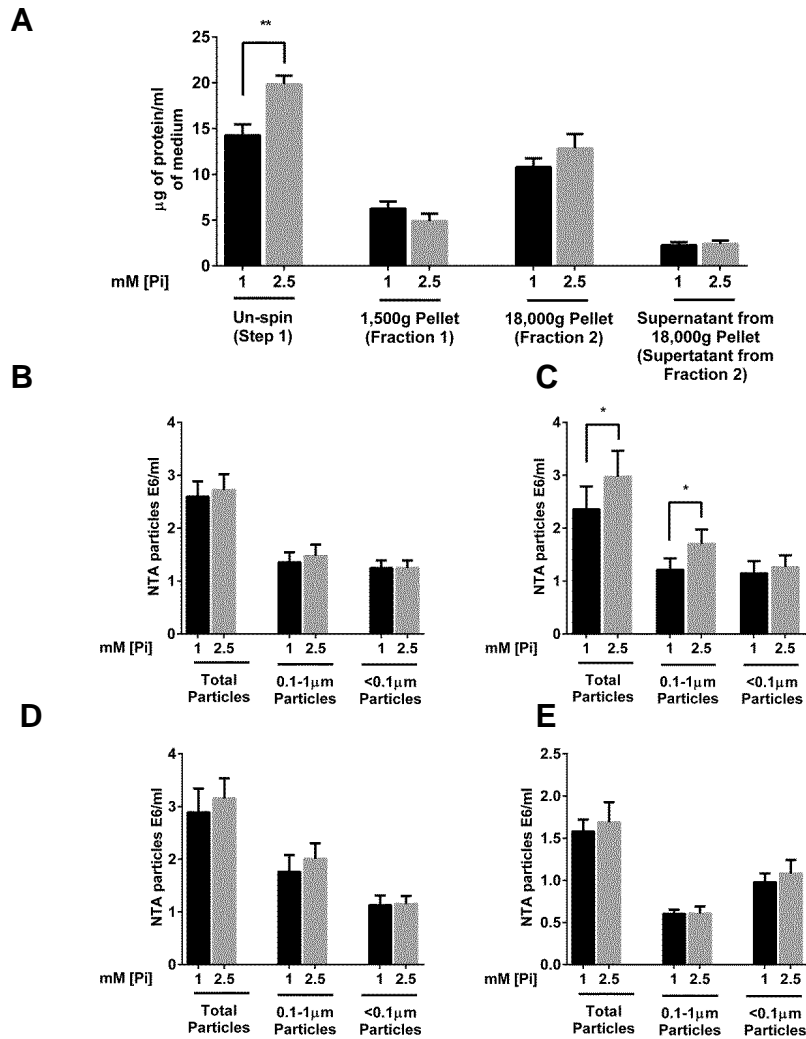


Figure 3.8. Chronic protein particle release/cell detachment from EAhy926 endothelial cells after exposure for 24h to medium (2ml per 35mm culture well) with control (1mM) Pi or high (2.5mM) Pi. (A) Protein particles from the medium (for Fractions definition see Table 2.1; General Methods chapter) determined by protein assay (B) Quantification by Nanoparticle Tracking Analysis (NTA) of MP release during prolonged ( $\geq 24$ h) exposure to 2.5mM Pi detected no stimulation of particle output (Fraction 3-Table 2.1; see General Methods chapter) (C) Detection of MP-size particles by Nanoparticle Tracking Analysis (NTA) by harvesting of the medium after incubation with the cells for 24h at the stated Pi concentration, followed by freeze-thaw and 1,500xg centrifugation cycle (see Table 2.1) followed by resuspension of the sedimented material in the same volume as the original medium. (Fraction 1-Table 2.1) (D) NTA on 18,000xg MP pellet (after removal of large particles by 1,500xg centrifugation as in (C)) detected no stimulation of particle output (Fraction 2-Table 2.1) (E) NTA on supernatant from 18,000xg MP pellet detected no stimulation of particle output (supernatant from Fraction 2-Table 2.1). (n=3) \*P<0.05.

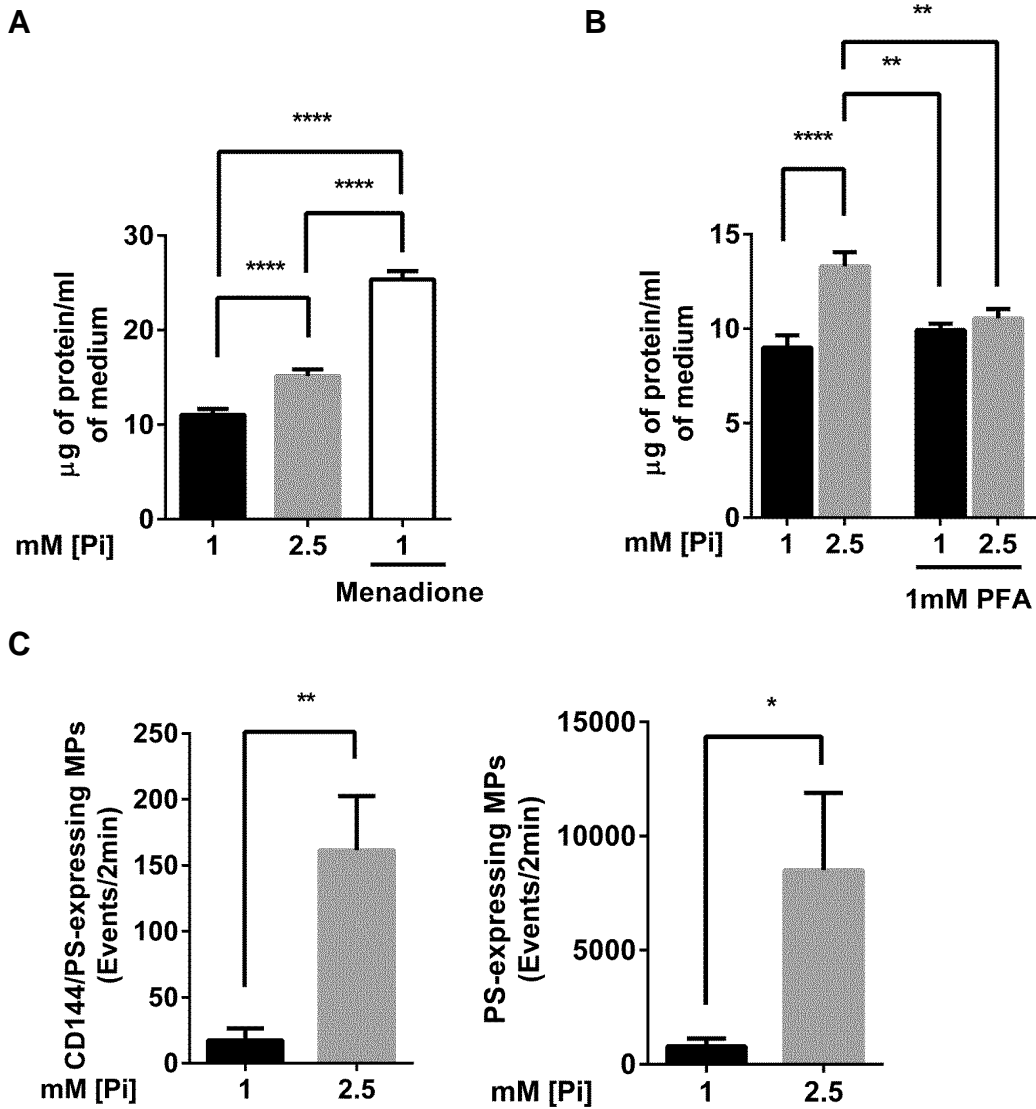


Figure 3.9. Chronic protein particle release/cell detachment from EAhy926 endothelial cells after exposure for 24h to medium (2ml per 35mm culture well) with control (1mM) Pi or high (2.5mM) Pi. (A) Total protein determined in particles sedimented from the medium at 18,000g (Fraction 3 -Table 2.1). 30µM Menadione was used as a positive control. (n=36) \*\*\*\*P<0.0001. (B) Blunting of the Pi-induced sedimentable protein particle release by loading the medium with Pi analogue PFA (an inhibitor of sodium-dependent-Pi transporters PiT-1/2) (Fraction 3 -Table 2.1). (n=4) \*\*P<0.01, \*\*\*\*P<0.01. (C) Flow cytometry data showing the number of particles (obtained after incubation of cells with medium for t = 24h at the specified Pi concentration) which dual-labelled with anti-CD144-PE antibody and Annexin V-FITC (Left) and Annexin V-FITC only (Right). Using medium from a 75cm<sup>2</sup> culture flask. particles were prepared (Fraction 2-Table 2.1), suspended in 500µl MP-Buffer (145mM NaCl, 2.7mM KCl, 10mM HEPES, pH 7.4) and 38µl of this suspension was subjected to FACS analysis as described in Methods (n=3), \*P<0.05, \*\*P<0.01 versus 1mM Pi control.

In principle this increase in sedimentable protein after 24h of exposure of cells to medium containing an elevated Pi concentration could arise because of a direct physico-chemical effect of Pi on the tendency of particles containing protein to sediment (i.e. hypothetical Mechanism 2 shown in Figure 3.1 above). In practice, control experiments performed by adding Pi to particle suspensions in culture medium *in the absence of cells* showed that, while Pi may slightly increase the ability of particles to sediment (Figure 3.10), this effect was not significantly decreased by PFA (unlike the result in the presence of cells in Figure 3.9 B) and does not fully account for the apparent Pi-induced increase in sedimentable protein particle output shown in Figures 3.9 A, B.

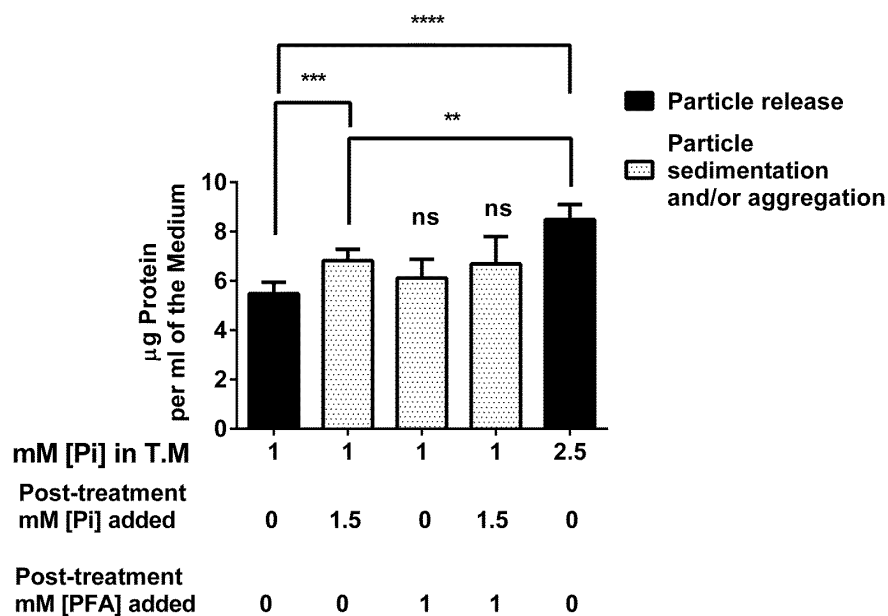


Figure 3.10. Association between extracellular phosphate and PFA concentrations and particle release, sedimentation and/or aggregation. EAhy926 treated with control 1mM [Pi] vs. High phosphate concentration of 2.5mM for 24h (x-axis first row) Test media harvested from cells were subjected to further post-treatment protocols to look at direct effect of phosphate on particle sedimentation and/or aggregation (x-axis middle row), and the effect of phosphonoformic acid (PFA) as a phosphate analogue (x-axis bottom row). (n=9) ns: not significant. \*\*P<0.01, \*\*\*P<0.001, \*\*\*\*P<0.0001.

In an alternative culture model of human vascular endothelial cells (HUVECs), a similar chronic (24h) effect of an elevated Pi concentration on sedimentable particle release was detected by centrifugation of the medium and analysis of the sedimentable protein pellet by protein assay (Figure 3.11).

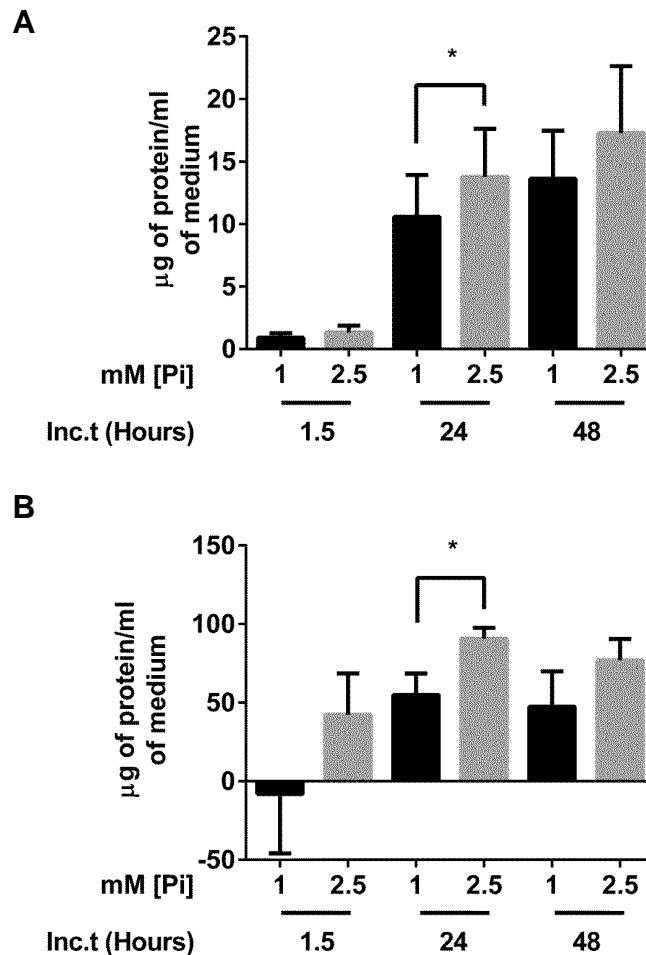


Figure 3.11. Protein particle release/cell detachment from EAhy926 endothelial cells and HUVECs after exposure for 24h to medium (2ml per 35mm culture well) with control (1mM) Pi or high (2.5mM) Pi. (A, B) Total protein determined in particles sedimented from the medium at 18,000xg (Fraction 3-Table 2.1; see General Methods section) (A) From EAhy926 cells over time (n=6) \*P<0.05 (B) From HUVECs over time (n=3) \*P<0.05.

### 3.2.5 Chronic (24h) microparticle output is not attributable to the action of Calcium Phosphate nanocrystals from the high Pi medium

In principle raising the Pi concentration in the medium to 2.5mM may lead to precipitation of Calcium Phosphate nanocrystals which may act on the cells (Sage *et al.*, 2011), possibly affecting cell signalling and contributing to MP output (hypothetical Mechanism 3 in Figure 3.1). Even though a detectable

increase in calcium precipitation in the cell layer was demonstrable in Pi-loaded cultures (by showing deposition of radio-activity from medium labelled with  $^{45}\text{Ca}^{2+}$ ) this effect was enhanced by the Pi analogue PFA (Figure 3.12 A). In contrast (as in Figure 3.12 B) PFA abolished chronic (24h) output of sedimentable protein particles into the medium in the same experiments, indicating that the calcium deposition was not the cause of the particle output (Figure 3.12 B).

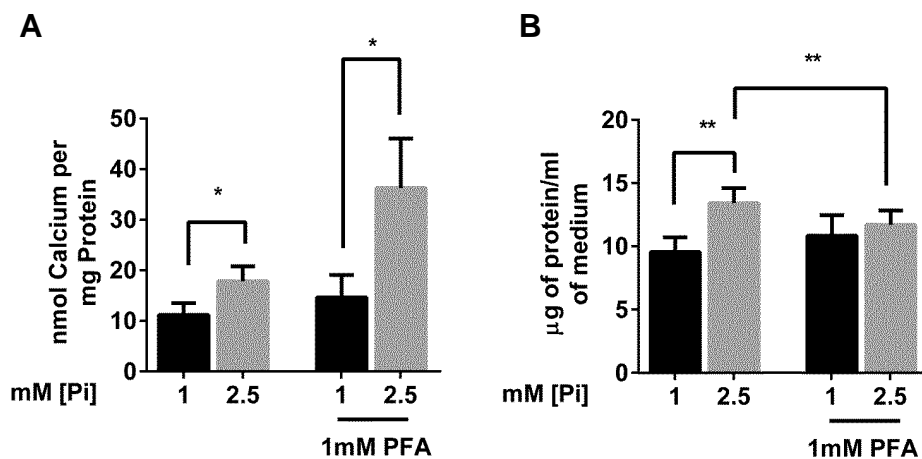


Figure 3.12. Particle release from Pi loaded EAhy926 endothelial cells in vitro is independent of Calcium Phosphate (CaPi) deposition on the cell monolayer. (A) Calcium ( $^{45}\text{Ca}$ ) deposition on EAhy926 cells after Pi loading;  $t=24\text{h}$ ;  $*P<0.05$  ( $n=6$ ) (B) Effect of Pi and PFA on protein particle release from the medium of Pi and PFA loaded EAhy926 cells (For the duration of the 24h incubation, the culture medium was supplemented with  $^{45}\text{Ca}$  at  $27\text{nCi/ml}$ );  $t=24\text{h}$ ;  $**P<0.001$  ( $n=3$ ).

### **3.2.6 Pi-derived MPs are strongly pro-coagulant**

In assays on the 18,000g MP fraction from the medium (after removal of apoptotic bodies, detached cells and other large fragments by serial centrifugation (Table 2.1)); MPs derived from the Pi-treated cultures of EAhy cells were found to be significantly more pro-coagulant than controls from cultures maintained at 1mM Pi (Figure 3.13 A-D), even though the total protein content of this particle fraction was similar at 1 and 2.5mM Pi (Figure 3.13 E). This pro-coagulant effect was completely abolished when MPs were removed by ultra-filtration (Figure 3.13 A).

This effect of an elevated Pi concentration only reached statistical significance after 24h of incubation of the Pi-loaded medium with the cells. Almost no effect was observed in Pi-derived particles after only 90min of cell incubation with 2.5mM Pi (data not shown).

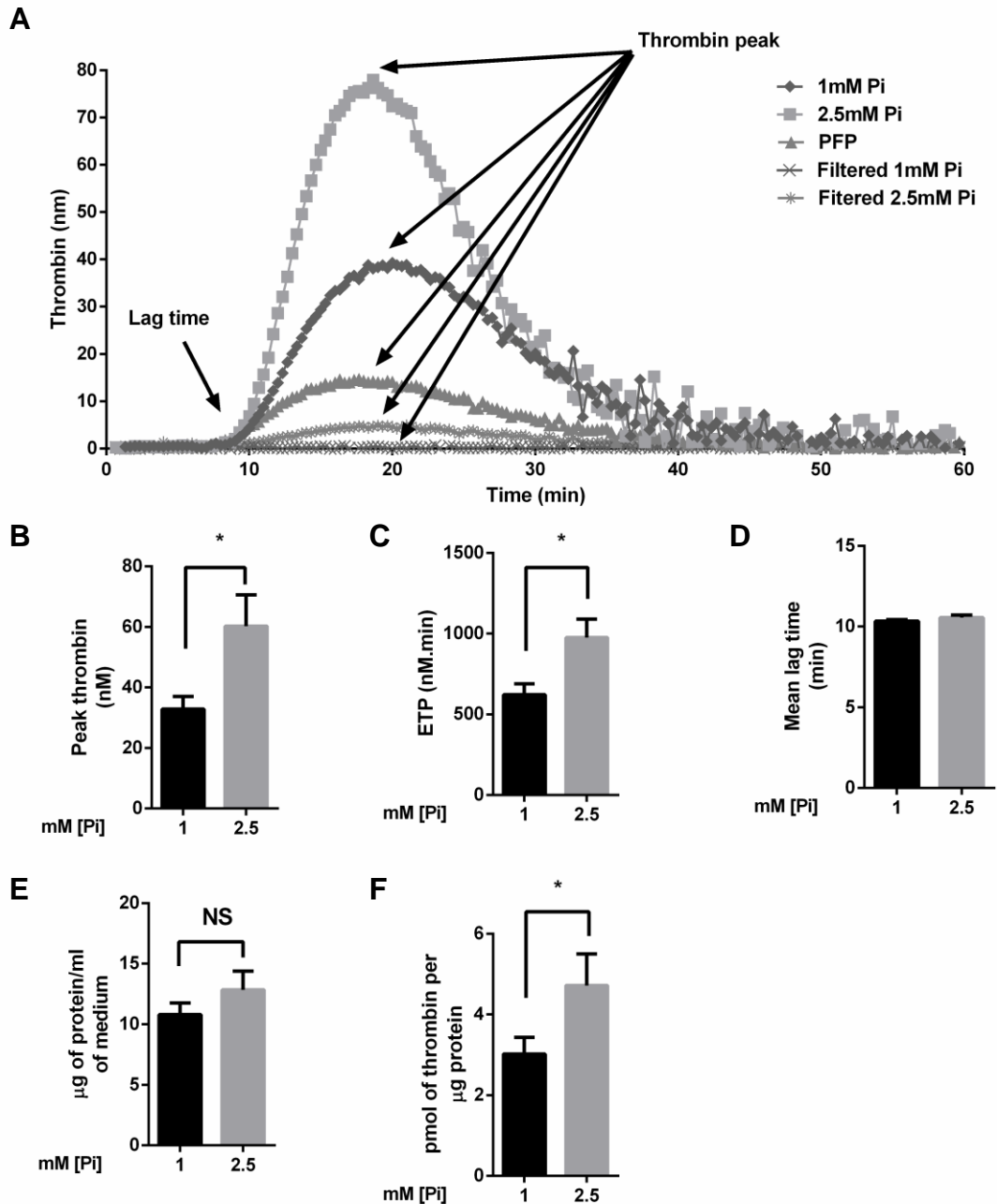


Figure 3.13. Effect in a thrombin-generation assay of microparticles sedimented at 18,000 x g from medium (with 1mM Pi or 2.5mM Pi) cultured for 24h with EAhy926 cells. Particle centrifugation was performed as described in Table 2.1. Sedimented particles (Fraction 2-Table 2.1) were resuspended in Pooled Filtered Plasma (PFP) prior to assay. Control curves are also shown for PFP alone and for particle preparations from which particles had been removed by ultra-filtration. (A) Representative thrombin generation curves (showing definitions of the Thrombogram parameters). (B, C, and D) Analysis of Peak thrombin, Endogenous thrombin potential (ETP), and Lag time of Control and Pi-derived microparticles showing significantly increased Peak Thrombin and ETP with MPs from Pi-treated cells even though the time at which thrombin burst commenced (Lag time) was not different between the two MP preparations. t=24h. (n=3) \*P<0.05. (E) Total protein concentration of the 18,000g sedimented MP pellet (Fraction 2-Table 2.1) from the control (1mM Pi) and Pi-loaded (2.5mM Pi) culture medium showing similar MP content. t=24h. (n=3) NS: Not Statistically Significant. (F) Analysis of thrombin generated per µg of protein indicating release of more pro-coagulant MP from high Pi medium. t=24h. (n=3) \*P<0.05.

The presence of a similar pro-coagulant effect of a 24h Pi-derived particle fraction could not be tested in particles derived from the alternative cultured endothelial cell model (HUVECs) cultured in similar serum-free medium, because HUVEC cell viability was found to decline significantly during 24h incubations in such serum-free medium.

### **3.3 Discussion**

#### **3.3.1 Hyperphosphataemia enhances CD144/PS positive MP release from EAhy926 endothelial cells**

The work in this chapter has shown that a higher extracellular Pi (2.5mM) results in an enhanced cell surface vesiculation (Figure 3.2 A). Further characterisation by NTA (Figure 3.3 A, B, and E), Flow Cytometry (Figure 3.3 C-D), and TEM (Figure 3.2 B) indicated that these released surface particles are  $\leq 1\mu\text{m}$  diameter and expressing CD144 (VE-Cadherin) and PS on their surface. Furthermore, even though a modest increase in extracellular Pi concentration from 1mM to 1.7mM had no effect on NTA detectable particle release from EAhy926 cells, lowering Pi concentration from 1mM to 0.5mM (i.e. hypophosphataemia) apparently blunted particle release from cells (Figure 3.4).

#### **3.3.2 Particle output from high Pi medium does not arise from Ca/Pi deposition on the cells or nanocrystal formation in high Pi medium**

The observed persistent elevated protein particle release from the cells after transient exposure to high Pi indicates that released particles detected by NTA are MPs triggered by high Pi trapped inside the cells, rather than Ca/Pi nanocrystals crystallising outside the cells (Figure 3.6). Moreover, as mentioned in Section 3.1.1 (also see Figure 3.1 Mechanism 3), there is a possibility that Pi in high Pi medium binds to calcium so that Ca/Pi complexes are deposited on the cell monolayer, activating them to release particles. As can be seen in Figure 3.12, even though there was an increase in calcium deposition on cells under high Pi medium, this increase became even bigger after loading the high Pi medium with PFA (which blocks Pi transport into the cells: Figure 4.4 C and 4.7 A). Interestingly, PFA blunted rather than enhanced the effect of Pi on protein particle release from the cells (Figure 3.12). From this it can be

concluded that the cause of particle release from the cells is unlikely to be calcium deposition on the cells activating the cells to release particles.

### **3.3.3 High intracellular Pi drives particle release from EAhy926 cells**

Depletion of intracellular Pi by fructose and by PFA blunted acute 90min release of MP from the cells in response to elevated extracellular Pi (Figure 3.7). Furthermore, chronic 24h protein particle release was also blunted by PFA (Figure 3.9). These indicate that Pi-induced particle release from EAhy926 endothelial cells (both acute and chronic) depends upon Pi influx into the cells.

The observed effect of high Pi on particle release from EAhy926 cells persisted after prolonged (24h) incubation of the cells with 2.5mM Pi (Figure 3.9). This fraction also expressed CD144 (VE-Cadherin) and PS, thus resembling *in vivo* endothelial MPs. Running this fraction on the NanoSight NTA system detected no increase in MP numbers or particle size (Figure 3.8) however after a freeze-thaw cycle followed by centrifugation at 1,500g, an elevated MP count was detected by NTA (Figure 3.8 C) implying that after prolonged incubation with Pi the released particles are bigger than the threshold of NTA detection ( $\leq 1\mu\text{m}$ ) but after the freeze-thaw-centrifugation the resulting fragments from the big particles are countable on the NTA.

### **3.3.4 Pi enhances particle sedimentation and/or aggregation**

Incubating particles in medium with Pi supplementation (an attempt to investigate the feasibility of Mechanism 2 in the hypothesis diagram (Figure 3.1)) indicated that raising the Pi concentration of the medium per se results in some increase in particle sedimentation (possibly via increased aggregation) (Figure 3.10); however this effect was not sufficient to account fully for the effect of Pi on the release of sedimentable particles from the cells during 24h incubations (Figure 3.9).

The work in this chapter demonstrated that hyperphosphataemia induces both acute and chronic effects on particle release from endothelial cells (Figure 3.14) which depends upon Pi entry into the cells, but the precise mechanism through

which Pi acts on the cells was not determined and is further investigated in the following chapters.

## Lumen

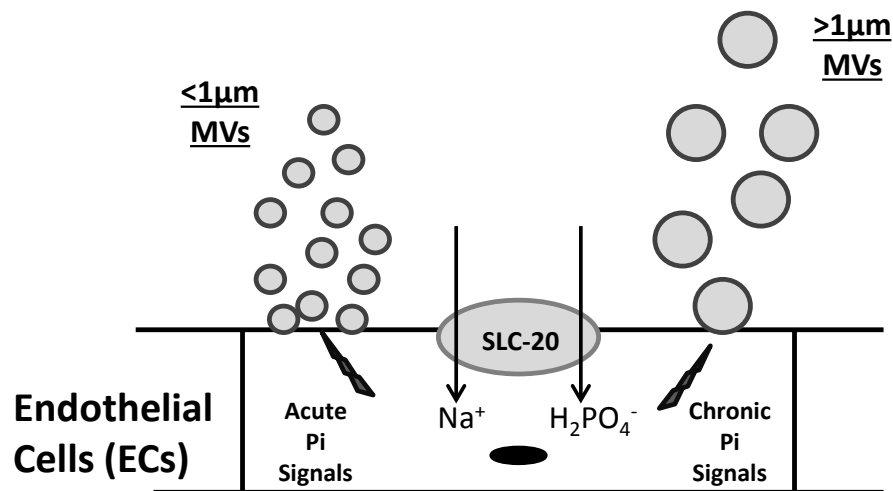


Figure 3.14. Hyperphosphataemia enhances both acute and chronic particle release from endothelial cells *in vitro*. Hyperphosphataemia culminates in influx of Pi into the cells and this stimulates cells acutely to release MPs and/or chronically release bigger particles (e.g. apoptotic bodies and big cell fragments/detached cells (resulting in sedimentable protein particles (see mechanism 2-Figure 3.1)).

### 3.3.5 High [Pi]-derived MPs are strongly pro-coagulant

Histones (Ammollo *et al.*, 2011) and the phosphatidylserine (Sinauridze *et al.*, 2007) expressed on the surface of the MPs have been shown to be pro-coagulant. It should be noted that the effect of histones is to accelerate thrombin generation via the intrinsic (contact) pathway rather than the extrinsic pathway. Here it has been shown that Pi-derived MPs express both the phosphatidylserine (Figure 3.3 C-D and 3.9 C) and histones (Figure 5.14 A-E) indicating that there might be at least two distinct mechanisms contributing to the observed pro-coagulant activity of Pi-derived MPs. The observed effect of Pi-derived MPs in Figure 3.13 is unlikely to be mediated only by expression of negatively-charged PS on the surface of the MPs (Figure 3.3 C-D and 3.9 C) because PS expression was already significant at 90min even though no significant increase in thrombin generation by the particles was detected at that time point.

The presence of some other pro-thrombotic factor(s) on the Pi-derived MPs from 24h onwards seems likely. Enrichment of Pi-derived MPs in histones may exert a part of this effect, whereby histone-positive Pi-derived MPs stimulate activation of the contact pathway (Ammollo *et al.*, 2011) and inhibit fibrinolysis (Longstaff *et al.*, 2013) and hence accelerate and stabilise thrombin generation. However, the fact that clear histone enrichment in the particles seems to need 48h of incubation with 2.5mM Pi (Figure 5.14 and Appendix C-Figure 5.6) suggests that histones are not the only biochemical factors involved.

The possible clinical significance of these observations of a pro-coagulant effect of Pi-derived MPs is discussed in more detail in the General Discussion chapter (Sections 6.1.5 and 6.1.6).

## Chapter 4. High [Pi] raises intracellular Pi concentration by transport through active Na<sup>+</sup>-linked PiT-1 (slc20a1) Pi transporters

---

### 4.1 Introduction

In mammalian cells, it has been shown that within 90min, changes in extracellular Pi concentration can result in alteration in intracellular Pi concentration (Kemp *et al.*, 1988<sub>a,b</sub>; Kemp *et al.*, 1993<sub>b</sub>; Villa-Bellosta *et al.*, 2007). As discussed in Sections 1.10.2, the transport of Pi across the plasma membrane is mediated by special trans-membrane active solute carrier proteins belonging to the SLC17, SLC34, and SLC20 gene families (Reimer, 2013; Werner *et al.*, 1998; Forster *et al.*, 2013). In endothelial cells the latter (i.e. transporter proteins Slc20a1 or PiT-1 and Slc20a2 or PiT-2) have been implicated in Pi transport, and in initial characterisation experiments both PiT-1 and PiT-2 were shown to be expressed in EAhy926 endothelial cells (Figure 4.3). These transporters of Pi have been demonstrated to transport Pi into the cells in a sodium dependent manner (Section 1.10.2.3.5).

In the previous chapter (Chapter 3) it was shown that a higher extracellular Pi concentration (2.5mM) induces a rapid cell surface vesiculation from EAhy926 cells (Figure 3.2), an observation which was further shown to be continued even after prolonged incubation of the cells with high Pi medium (Figure 3.9 & 3.12) and was blunted by (i) the Pi transport inhibitor PFA (Figure 3.7 B, 3.9 B and 3.12 B), and by metabolic trapping of intracellular Pi with slowly metabolised fructose (Figure 3.7 A) (Woods *et al.*, 1970; Cox, 2002). It was not fully understood whether the cause of acute and chronic particle release from the cells that was shown in the previous chapter arose from an increase in intracellular Pi concentration or was possibly mediated by elevation in extracellular Pi, acting directly on the cell surface and resulting in subsequent changes in signalling pathways.

As discussed in Section 1.8, Oubain (Figure 4.1), PFA, and fructose can result in inhibition of active Na<sup>+</sup>-linked Pi transport and/or depletion of intracellular Pi

or blunting in the incremental increase in intracellular Pi concentration during hyperphosphataemia.

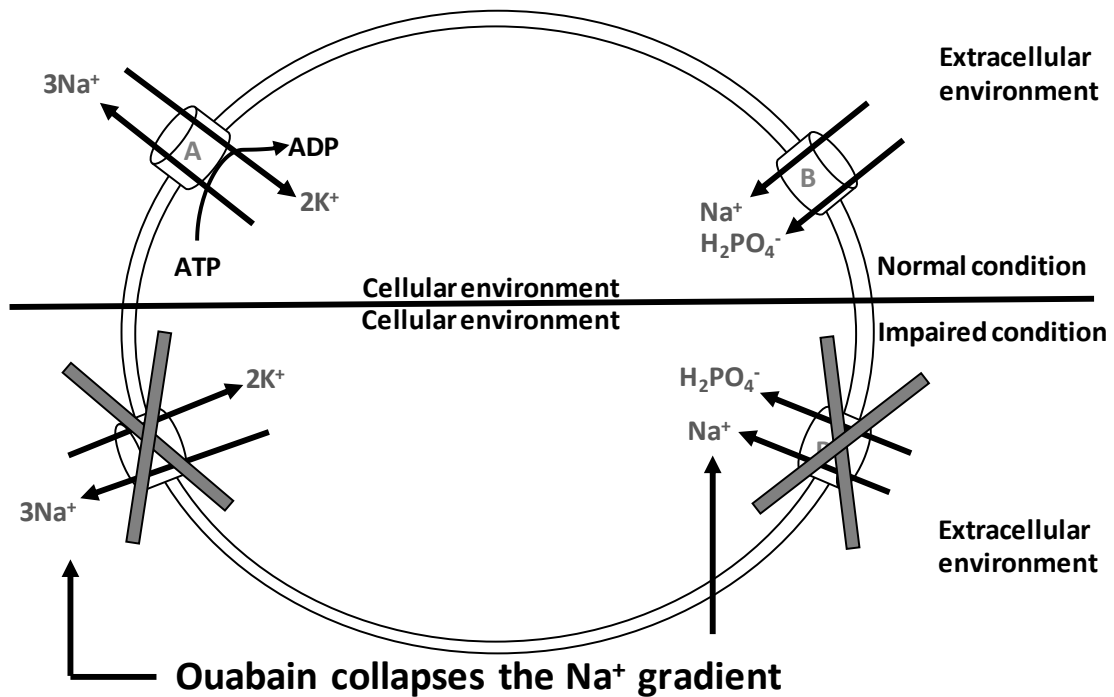


Figure 4.1. Diagram showing the inhibitory indirect effect of Oubain on Slc20 (Sodium-dependent Pi transporters) and blockade of Pi influx into the cells. (A) Membrane sodium pump (Na/K-ATPase) and (B) Slc20 (i.e. PiT-1 & -2); Note that Ouabain removes the trans-membrane Na<sup>+</sup> gradient which acts as the driving force pumping phosphate into the cells.

Therefore by administering these probes the work in this chapter aimed:

- To investigate if collapsing trans-membrane sodium gradient with Ouabain blunts the increase in cell layer Pi when extracellular Pi concentration is elevated to 2.5mM.
- To investigate if PFA inhibits transport of Pi into the cells.
- To investigate if fructose depletes intracellular Pi in endothelial cells.
- To further characterise the transport of Pi into the cells through siRNA silencing of PiT transporters.

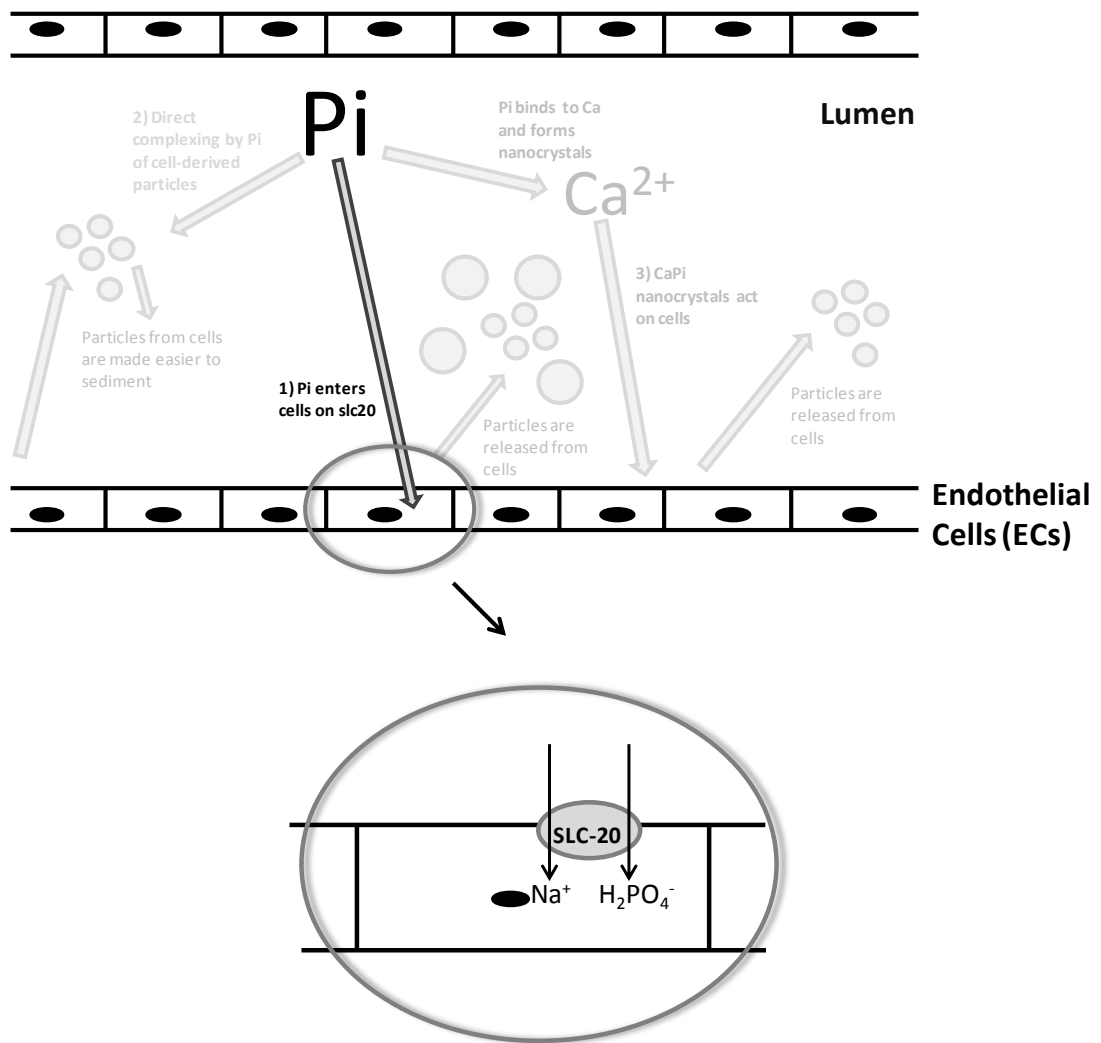


Figure 4.2. A schematic view of the hypothesis tested in this chapter. In this picture Mechanism 1 of the three hypothetical mechanisms of  $\text{Pi}^i$  action on the cells is emphasised i.e. (1)  $\text{Pi}^i$  enters cells on Slc20 (i.e. PiT-1 and PiT-2) in a sodium dependent manner (based on the kinetics of substrate interdependence of Slc20  $\text{Na}^+ : \text{H}_2\text{PO}_4^-$  transporters according to (Ravera *et al.*, 2007; Mune *et al.*, 2009)).

## **4.2 Results**

### **4.2.1 Pi transporter characteristics of EAhy926 endothelial cells**

EAhy926 cells, like HUVECs, exhibit cobblestone morphology and are 20-70 $\mu$ m in diameter (Figure 4.3 B). As described in the method section 2.2, EAhy926 cell line is a permanent human endothelial cell line which is a hybrid of HUVECs with lung epithelial cell line (A549). To determine whether this hybridization of HUVECs with a lung epithelial cell line has introduced non-physiological epithelial Pi transporters (rather than endothelium origin (i.e. SLC20/PiT) transporters), gel RT\_PCR was performed to screen for the expression of PiT transporters and a key lung epithelium Pi transporter (i.e. SLC34A2) in this cell line and several control cell lines (i.e. RNA from EAhy926 endothelial cells, HUVECs, hVSMCs, and as a comparison RNA from HK2 human renal proximal tubular epithelial cells and human podocytes were extracted and RT-PCR performed to look at the the phosphate transporter expression profile (i.e. Slc20a1, Slc20a2, and Slc34a2) (Figure 4.3 A). The expression of CD144 VE-cadherin and CD146 was also confirmed in these cells by Flow Cytometry (Figure 4.3 C). Results indicate that EAhy cells express CD144 and (to a negligible extent) CD146 (Figure 4.3 C) and express both PiT transporters (PiT-1 and PiT-2) but not the epithelial transporter (SCL34A2) (Figure 4.3 A).

A

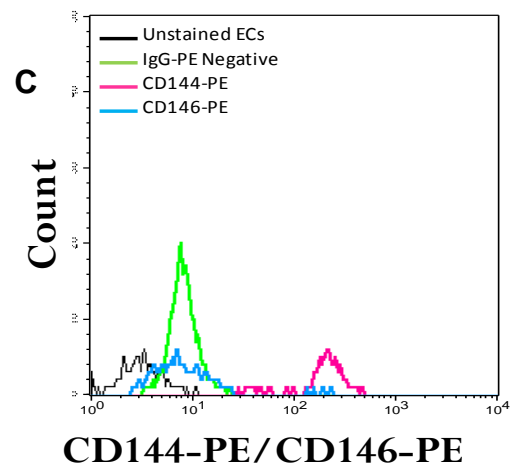
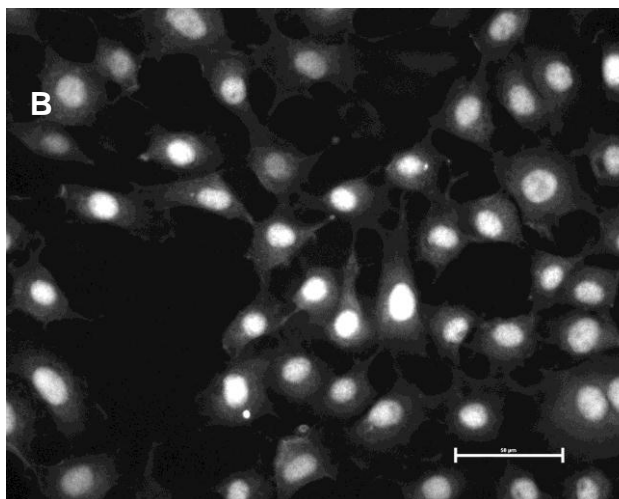
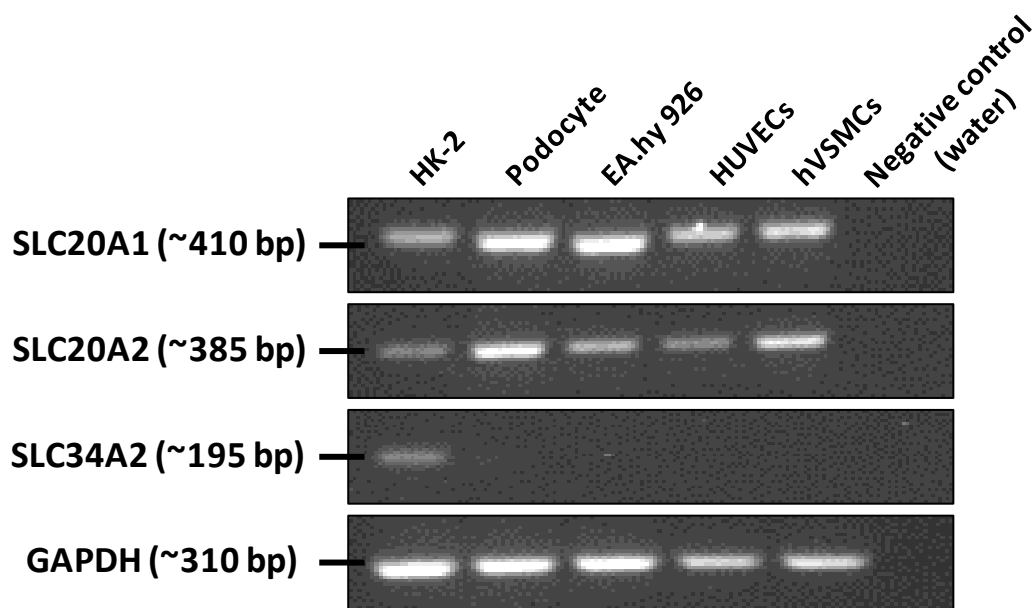


Figure 4.3. Characteristics of EAhy926 endothelial cells. (A) representative gel PCR (32 amplification cycles) demonstrating the expression of different phosphate transporters in HK-2 (Human kidney epithelial cells), podocytes, EAhy cells, HUVECs, and hVSMCs showing detection of PiT-1 (Slc20a1) and PiT-2 (Slc20a2) but not NaPi-IIc (Slc34a2) expression in EAhy926, HUVECs, and hVSMCs by RT-PCR using oligonucleotide primers (Table 2.6). Note that endothelial cells (EAhy926 and HUVECs) express both Slc20a1 and Slc20a2, possibly with a higher level of expression for Slc20a1. hVSMCs, on the other hand, express both transporters (i.e. Slc20a1 and Slc20a2). HK-2 were used as epithelial positive control cells, shown to express the epithelial transporter (i.e. Slc34a2) whose expression is absent in endothelial cells and smooth muscle cells. (Note: Podocytes also express Slc34a2, but at a very low level). GAPDH was used a house-keeping gene. (B) Fluorescence photomicrograph of Hoechst-stained EAhy cells showing cells of 20-70 μm with a centrally located nucleus and distinct cell borders; *Scale bar is 50 μm* (40x Magnification). (C) Flow Cytometric analysis of intact EAhy cells using anti-CD144-Phycoerytherin (PE) and CD146-PE antibodies indicating the level of expression of these two endothelial cell markers on EAhy926 endothelial cells. IgG-PE was used as isotype control.

#### **4.2.2 Hyperphosphataemia increases cell layer Pi in EAhy926 cells**

To confirm that a rise in intracellular Pi concentration was the signal triggering the acute increase in MP release observed in response to elevated extracellular Pi concentration in Chapter 3, Pi was directly measured in the cell layer and shown to increase significantly within 90min of exposure to medium with 2.5mM Pi, achieving particularly high levels after 48h (Figure 4.4 A). This Pi was shown to be intracellular, and dependent on inwardly-directed active Na<sup>+</sup>-dependent Pi transporters, since it could be blocked by (i) collapsing the plasma membrane Na<sup>+</sup> gradient with ouabain (which removes the thermodynamic driving force for these Pi pumps) (Figure 4.4 B), (ii) blockade of the Pi transporters with PFA (Figure 4.4 C), or (iii) metabolic trapping of intracellular phosphate with fructose (Figure 4.4 D).

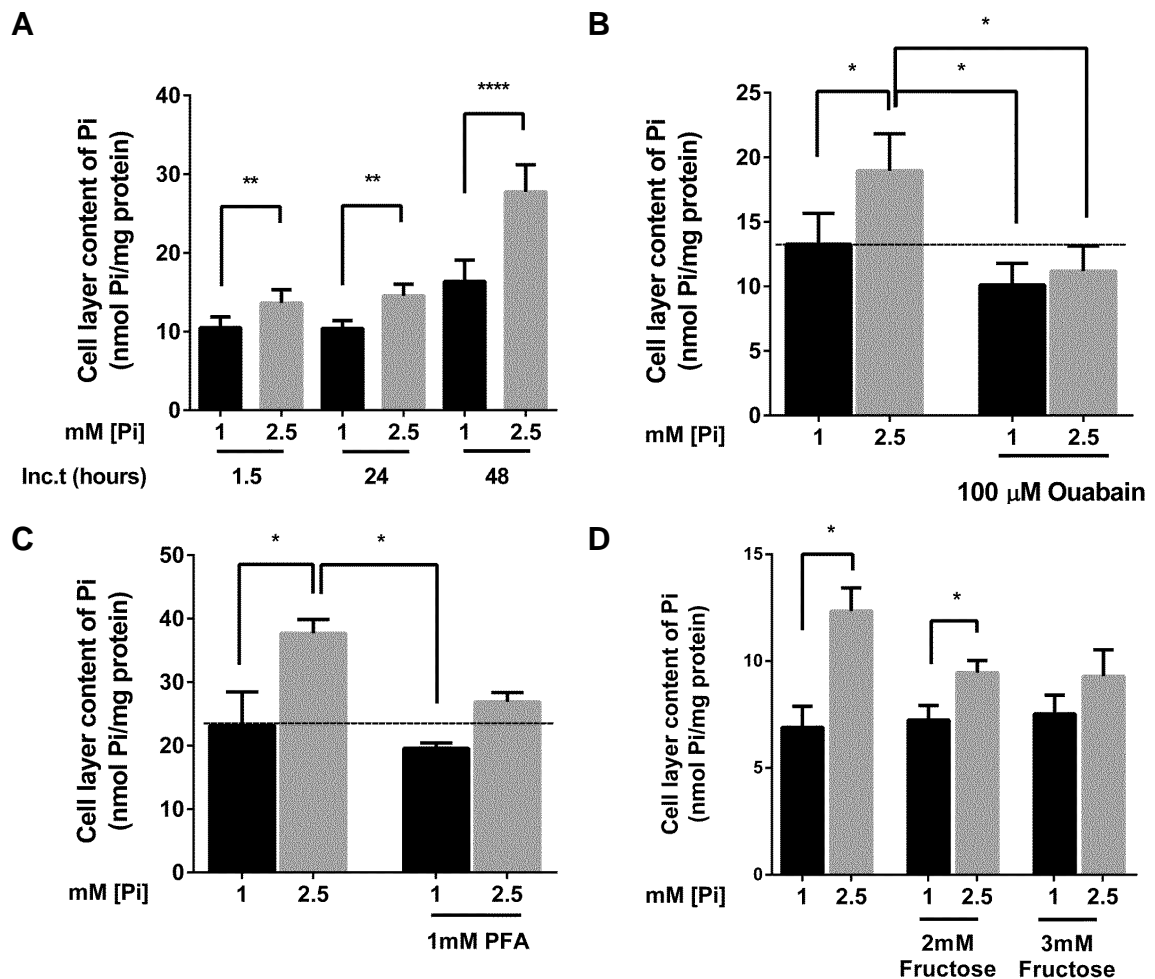


Figure 4.4. Relationship between extracellular Pi concentration, Pi transport inhibition and Pi detected in the cell layer in EAhy926 endothelial cells. (A) Time course of the increase in intracellular Pi. (n=6) \*\*P<0.01, \*\*\*\*P<0.0001 (B, C, D) Blunting of the hyperphosphataemia-induced rise in intracellular Pi at t = 1.5h (B) by collapsing the plasma membrane sodium-gradient with Na<sup>+</sup>/K<sup>+</sup>-ATPase inhibitor ouabain (n=6); (C) by blocking Pi transport with Pi analogue PFA (n=4); (D) by metabolic trapping of intracellular Pi with fructose (n=3), \*P<0.05.

In an alternative culture model of human vascular endothelial cells (HUVECs), a similar acute (90min) effect of a high extracellular Pi concentration (i.e. 2.5mM [Pi]) on cell layer Pi concentration was observed (Figure 4.5 A); indeed the effect was even more marked than that observed with EAhy926 cells (Figure 4.5 A). Such a clear acute increase in cell layer Pi was not observed however in 2 control cell lines: human vascular smooth muscle cells (Figure 4.5 B) and L6 rat skeletal muscle cells (Figure 4.5 C).

In some cell types decreasing extracellular pH can increase intracellular Pi concentration (Bevington *et al.*, 1995). In principle the addition of extra

NaH<sub>2</sub>PO<sub>4</sub> to the culture medium to model hyperphosphataemia might lower the pH either directly or by stimulating glycolytic lactic acid production in the cells (Bevington *et al.*, 1995). Direct measurement of the pH of the medium (Figure 4.6) showed however that adding NaH<sub>2</sub>PO<sub>4</sub> had little effect on pH and could not explain the effect on cellular Pi shown in Figure 4.4 A.

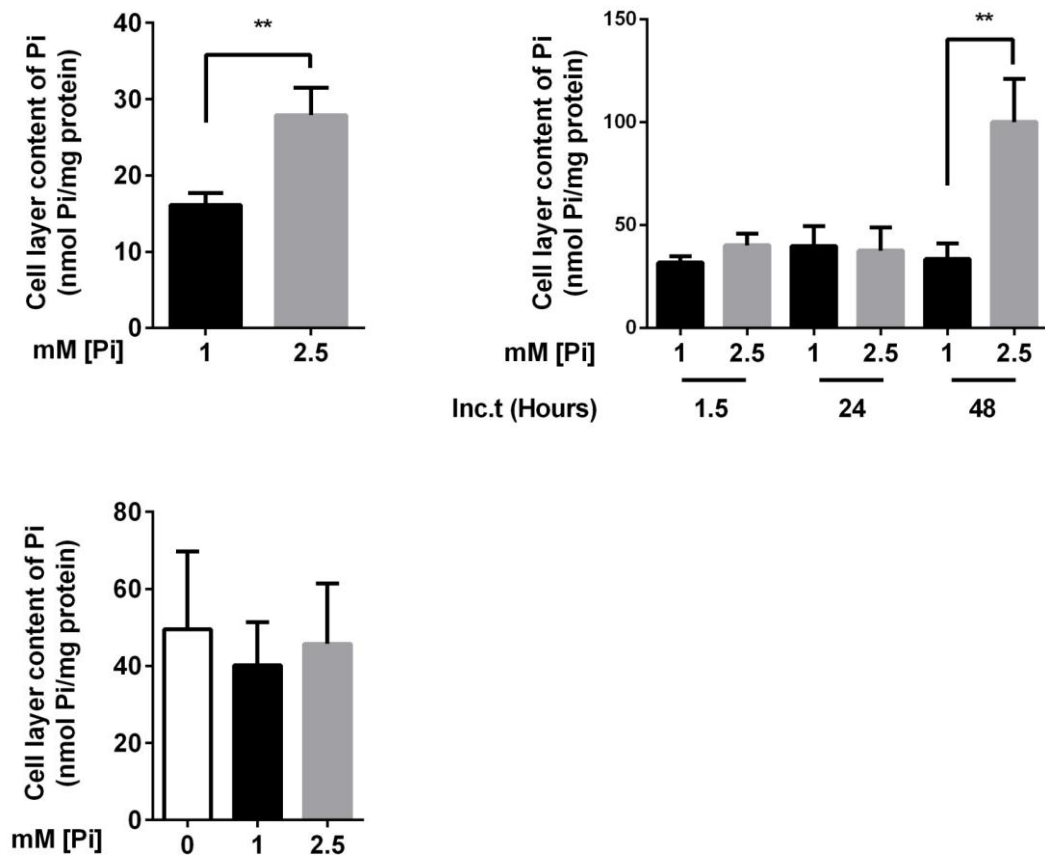


Figure 4.5. Relationship between extracellular Pi concentration and Pi detected in the cell layer in HUVECs, human VSMC and Rat skeletal muscle cells (L6). (A) HUVECs incubated for 90min with control (1mM) and high (2.5mM) [Pi] medium. This indicates an acute increase in intracellular Pi. (n=3) \*\*P<0.01. (B) hVSMCs incubated over time with control (1mM) and high (2.5mM) [Pi] medium. Cellular content of Pi tended to be elevated when cells were incubated with a higher extracellular [Pi] particularly after longer incubation time (n=3), \*\*P<0.01. (C) L6 cells incubated with 0, 1, and 2.5mM [Pi] for 2hours. (Note that the Test Medium applied to this experiment was Hepes Buffered Saline (HBS)) (n=3).

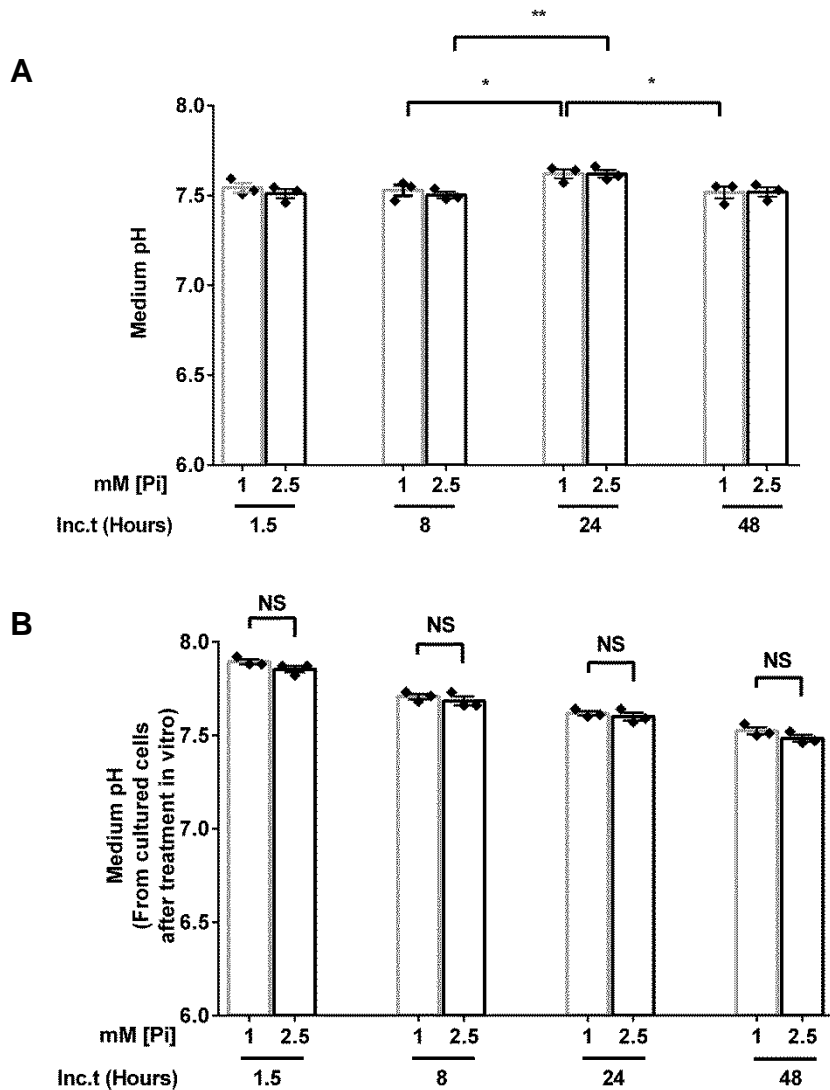


Figure 4.6. Medium pH from culture dishes. The pH of the medium from (A) culture dishes without cells and (B) culture dishes with cells collected after 90min, 8h, 24h, and 48h into 1ml plastic syringes followed by injection into 1.5ml tubes pre-warmed to 37°C in a water bath and incubated under a 5% CO<sub>2</sub> atmosphere. The pH was measured using a Mettler Toledo SevenEasy pH meter.

### 4.2.3 Hyperphosphataemia raises intracellular Pi concentration by transport through active Na<sup>+</sup>-linked PiT-1 (Slc20a1) Pi transporters

Further characterisation of Pi transport into these cells using <sup>32</sup>Pi confirmed that transport depended on extracellular Na<sup>+</sup> (Figure 4.7 A), and was efficiently blocked by PFA (Figure 4.7 A) or by selective siRNA silencing of expression of slc20a1 (PiT-1) Pi transporters leading to depletion of intracellular Pi (Figure 4.7 B) in spite of compensatory up-regulation of slc20a2 (PiT-2) transporters (Figure 4.7 C).

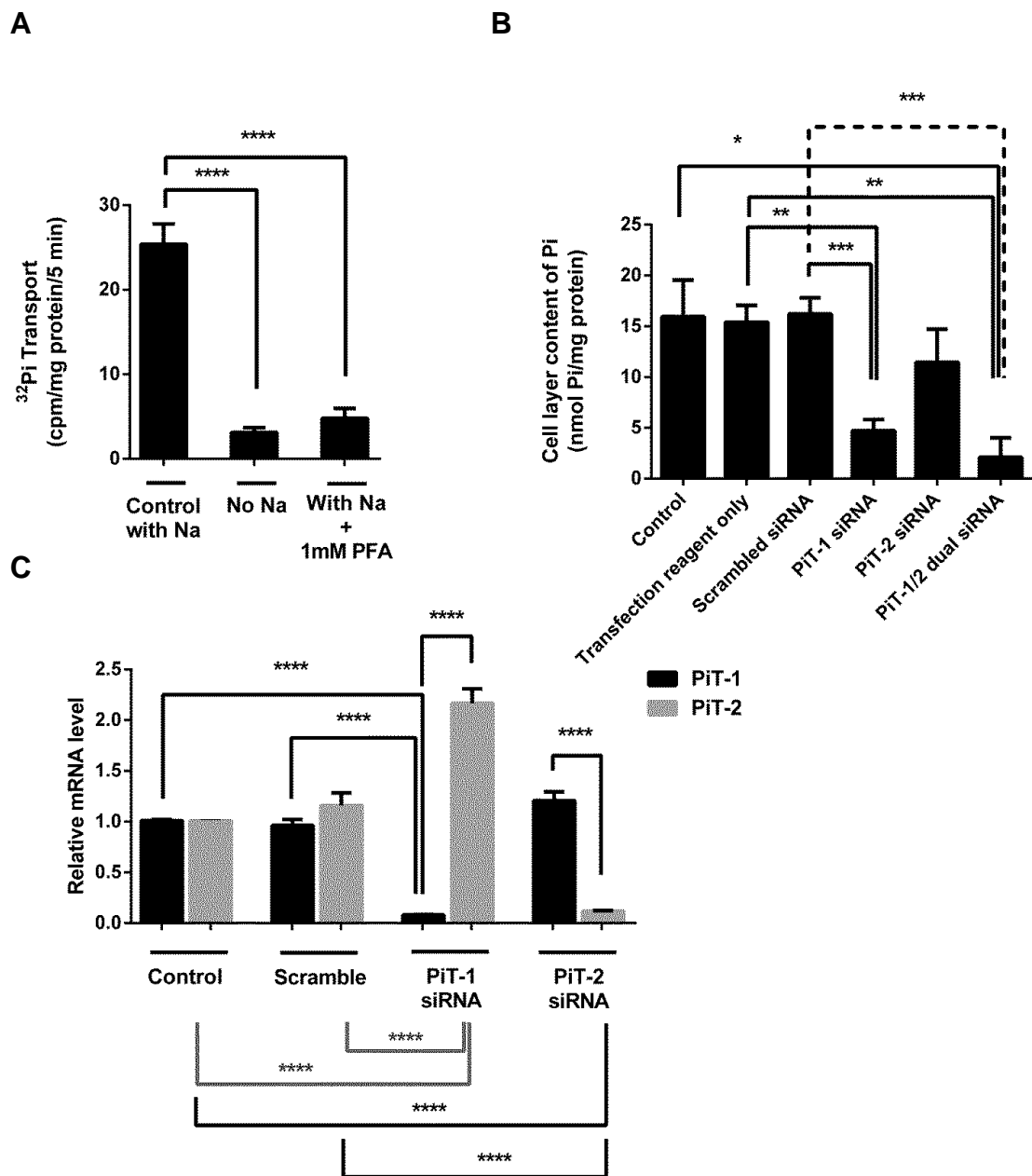


Figure 4.7. Characterisation of sodium-dependent active Pi transport in EAhy926 endothelial cells. (A) Effect of replacing Na in the HEPES-buffered saline (HBS) medium with Choline or blocking Pi transporters with 1mM PFA on transport of <sup>32</sup>Pi. Cells were incubated to steady state for 90min in HBS with 1mM Pi at 37°C under air, followed immediately by assay of <sup>32</sup>Pi transport by incubating for exactly 5 min at 20°C in medium with 0.1mM <sup>32</sup>Pi at 2μCi/ml. (n=3) \*\*\*\*P<0.0001. (B) Effect of siRNA silencing of PiT-1 and/or PiT-2 and/or PiT-1/2 dual siRNA silencing on total cell layer Pi. After removal of the transfection medium and allowing a further 24h recovery period in Growth Medium, cells were incubated in HEPES-buffered saline with 1mM Pi for 90min at 37°C under air. (n=3) \*P<0.05, \*\*P<0.003, \*\*\*P<0.0009. (C) Relative mRNA levels of PiT-1 and PiT-2 in EAhy926 cells transfected with scrambled/non targeting siRNA, PiT-1 siRNA, and PiT-2 siRNA for 24h. After removal of the transfection medium and allowing a further 24h recovery period in Growth Medium, RNA was extracted from the cells, reverse transcribed and subjected to RT-qPCR. (n=5) \*\*\*\*P<0.0001.

## **4.3 Discussion**

### **4.3.1 Hyperphosphataemia acutely enhances cell layer Pi in EAhy926 endothelial cells**

Within 90min of exposure of EAhy926 cells or HUVEVs to 2.5mM Pi (Figure 4.4 A and Figure 4.5 A) a significant increase in cell layer Pi was observed. This effect became even more significant after prolonged incubation of cells with high Pi loaded medium for 48h. In contrast to endothelial cells, incubation of vascular smooth muscle cells (Figure 4.5 B) and rat skeletal muscle cell line (L6 cells) (Figure 4.5 C) with high Pi medium resulted in almost no detectable increase in cell layer Pi. Similar to VSMCs and L6 cells in this study, no significant increase in intracellular Pi in response to hyperphosphataemia was observed in earlier studies of other cells such as erythrocytes (Kemp *et al.*, 1988<sub>a,b</sub>) and skeletal myocytes (Bevington *et al.*, 1986). The molecular basis for this difference is still unclear. In addition to Na<sup>+</sup>-linked PiT-1 (slc20a1) Pi transporters which carry Pi into the cells, mathematical modelling of the regulation of intracellular Pi concentration suggests that the hitherto uncharacterised Pi transporter which carries Pi out of mammalian cells could also have a marked influence on the relationship between intracellular and extracellular Pi concentration (Kemp & Bevington, 1993<sub>a</sub>). This difference between ECs and other cell types may therefore reside in this Pi efflux transporter.

### **4.3.2 Transport of Pi depends on extracellular sodium concentration in EAhy926 cells and is mediated predominantly by PiT-1**

Here it was shown that the normal increase in cell layer Pi that was observed when raising the extracellular Pi to 2.5mM, was abolished after loading the medium with Ouabain (which collapses the trans-membrane sodium gradient) (Figure 4.4 B). Similarly, in transport experiments using <sup>32</sup>Pi, this transport was confirmed to be dependent on extracellular Na<sup>+</sup> (Figure 4.7 A), as replacing the extracellular sodium with choline resulted in blockade of <sup>32</sup>Pi transport into EAhy926 cells (Figure 4.7 A). Furthermore, PFA was shown to blunt the increase in cell layer Pi (Figure 4.4 C) and in a parallel experiment looking at <sup>32</sup>Pi transport into the cells in PFA loaded medium (Figure 4.7 A) or when

slc20a1 (PiT-1) was selectively siRNA silenced (Figure 4.7 B), both approaches resulted in depletion of intracellular Pi. This confirmed two important points. Firstly it indicated that PFA is a suitable drug for inhibiting transport of Pi into endothelial cells and secondly it showed that most of the active transport of Pi into the cells is mediated through PiT-1 but not PiT-2 transporters in endothelial cells. In Chapter 1- Section 1.8.1.2 it was noted that in some cell types PFA is a poor inhibitor of slc20 transporters such as PiT1. In contrast the similar effects of PFA and of siRNA silencing of PiT1 shown here (Figure 4.7) suggest that in EAhy926 cells PFA is an effective inhibitor. The reason for this difference between the inhibitor sensitivity of PiT1 in EAhy926 cells compared with other cell types is unclear.

## **Chapter 5. Mechanism of Pi-induced microparticle release**

---

### **5.1.1 Pi induces global changes in protein phosphorylation**

The data presented in Chapters 3 and 4 showed that in endothelial cells increasing extracellular Pi concentration resulted in an increase in intracellular Pi concentration, an effect which was accompanied by both acute (90min) and chronic (24h) particle release from the cells. Blockade of Pi influx into the cells resulted in blunted particle output, implying that release of particles arises from a signalling effect of intracellular Pi on endothelial cells. Previous reports indicated that hyperphosphataemia induces generation of reactive oxygen species (ROS) in endothelial cells (Shuto *et al.*, 2009), a signal leading to apoptosis in endothelial cells (Di Marco *et al.*, 2008) which culminates in MP formation (Section 1.16.5).

Apart from Pi-induced generation of reactive oxygen species and consequent apoptosis that has been reported previously in endothelial cells; elevated intracellular Pi concentration may also exert other forms of cellular stress effects, including cellular activation which might work as an alternative signal in triggering MP formation (Section 1.16.5.2). There is no evidence indicating that Pi exerts direct regulatory effects on protein kinases in mammalian cells, however there is strong evidence indicating that Pi can inhibit a wide range of phosphotyrosine and phosphoserine/threonine protein phosphatases (Szajerka & Kwiatkowska, 1984; Buzalaf *et al.*, 1998; Zhang & VanEtten, 1991) (Section 1.7). In micro-organisms and plants such Pi-sensing through protein phosphatases is regarded as functionally important in intracellular signalling (Dick *et al.*, 2011).

### **5.1.2 Proteomic analysis demonstrates Pi-induced changes in Tropomyosin expression and Histone distribution**

From the data presented in the previous chapter, significant changes in protein phosphorylation were detected in EAhy cells and HUVECs in response to elevated extracellular Pi concentration, with a possible role in the increased MP output observed in Chapter 3. However, the proteins involved in these effects

were not identified. The protein composition of the endothelial cells and the composition of the microparticles released into the medium were therefore examined by 1-dimensional and 2-dimensional gel electrophoresis with 2 aims:

1) To determine whether any proteins in the cells were showing rapid and reproducible responses to Pi which might be functionally important in stimulating MP output (for example because of changes in cytoskeletal or plasma membrane-associated proteins).

2) To examine whether the protein composition of the MPs released in response to Pi differed from that in particles from control cultures, and (if so) to identify the proteins involved and investigate whether these might be relevant to the functional effects of the particles (for example on coagulation).

The aims of the work presented in this chapter were therefore:

- To investigate the possible effect of elevated Pi concentration on ROS generation and apoptosis induction in EAhy926 cells.
- To investigate whether Pi inhibits EAhy926 endothelial cells' phosphoprotein phosphatases and, if it does, whether this results in a significant change in global protein phosphorylation.

## **5.2 Results**

### **5.2.1 Pi has little effect on oxidative stress and cell death**

Elevated Pi concentration has previously been reported to influence endothelial production of labile nitroxide and oxygen species; decreasing nitric oxide synthase activity (Shuto *et al.*, 2009; Peng *et al.*, 2011) and increasing production of reactive oxygen species (ROS) (Shuto *et al.*, 2009), the latter being a potential cause of apoptosis and consequent MP production. Inducing ROS production in EAhy926 cells with menadione did induce a marked increase in particle output (shown as a positive control in Figure 3.9 A). However, even though decreased nitric oxide synthase activity was readily detected after 90min of exposure to 2.5mM Pi (Figure 5.1 C), no effect of Pi was observed on ROS production. Three independent ROS probes: CM-H2DCFDA (Figure 5.1 A and B), Dihydroethidium (DHE) (Figure 5.1 D) and Nitro-blue Tetrazolium (NBT) (Figure 5.1 E), readily detected a ROS signal within 30 min using a Menadione positive control, but no reproducible response to elevated Pi concentration.

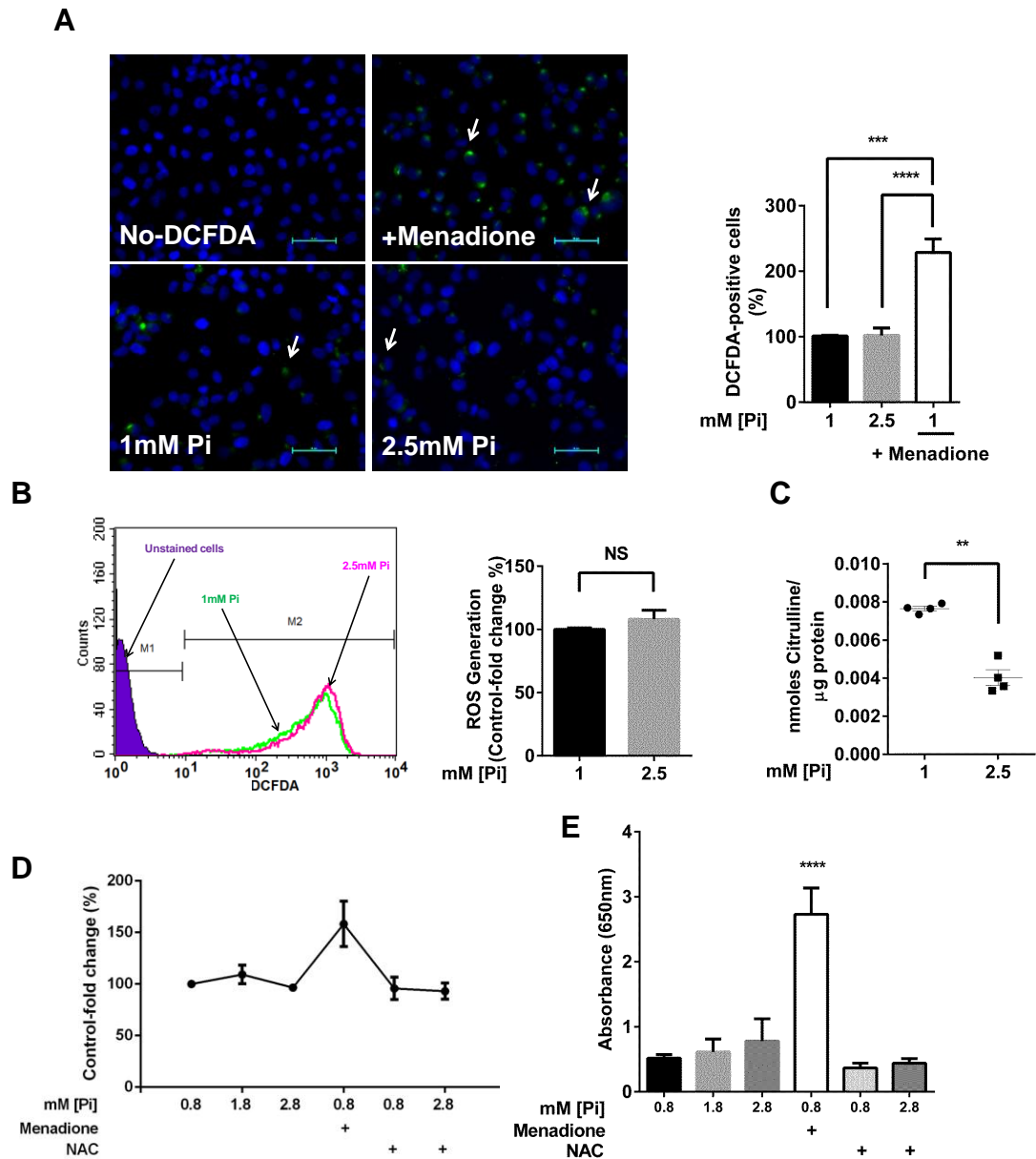


Figure 5.1. Effect of hyperphosphataemia on ROS generation in EAhy926 endothelial cells. (A) Representative fluorescent microscopy images (Left) and analysis (Right) of ROS DCFDA positive cells (Green fluorescence *Arrows*). Nuclei were counterstained with Hoechst dye (Blue). Cells were treated (t=90min) with 1mM Pi, or 2.5mM Pi, or 1mM Pi + 30μM Menadione as a positive control in the presence and absence of DCFDA probe; Scale Bar: 50μm; (n=3) \*\*\*P<0.001, \*\*\*\*P<0.0001. (B) Representative histogram (Left) and corresponding analysis (Right) of the effect of high Pi on intracellular ROS generation using DCFDA probe analysed by Flow Cytometry; t=90min, (n=3). NS: Not Statistically Significant. (C) HPLC analysis of citrulline generation by cells treated with control and high phosphate for 90min. (Citrulline measured as a by-product of the conversion of L-arginine to nitric oxide (NO)): data are from four replicate cultures from one experiment; \*\*P<0.01. (D) Detection of ROS using DHE fluorescence as a probe. Cells were treated in medium at the stated Pi concentration for 90min. Menadione (30μM) and ROS scavenger N-Acetyl Cysteine (10mM) were used as positive and negative controls respectively. Data are pooled from two independent experiments. (E) Colorimetric detection of ROS using Nitro Blue Tetrazolium (NBT) in cells treated in medium at the stated Pi concentration for 90min. (n=3) \*\*\*\*P<0.0001 (Menadione and NAC were added as in (D)).

At all time points studied (90min to 48h), exposure of the cells to 2.5mM Pi induced only a small apparent decline in cell viability assessed by MTT staining (Figure 5.2 A); consistent with small increases in pro-apoptotic signals including Caspase-3 cleavage (Figure 5.2 B and C), Bax (Figure 5.2 B and D), PARP cleavage (Figure 5.2 E and F) and DNA laddering (Figure 5.2 L). However, more detailed analysis by Propidium iodide/Annexin V flow cytometry, failed to detect significant apoptosis or necrosis (Figure 5.2 G, H and I), or cell shrinkage (Figure 5.2 J and K) in the cell population as a whole when averaged over 13 independent experiments. Similarly cell death and apoptosis measured by the TUNEL-coupled Hoechst assay (Figure 5.2 M, N), cellular ATP concentration (Figure 5.3 A) and glycolytic rate (lactate output – Figure 5.3 B) were also unaffected by elevated Pi, confirming that only minor effects on cell viability were occurring and that the pro-apoptotic signals in Figures 5.2 B-F and L were confined to a small fraction of the total cells.

Further investigation of apoptosis using Annexin V binding and PI staining of cells, or measurement of apoptotic cell shrinkage, at time points up to 48 hours also failed to detect any significant effect of elevated Pi concentration (Figure 5.2 O-V).

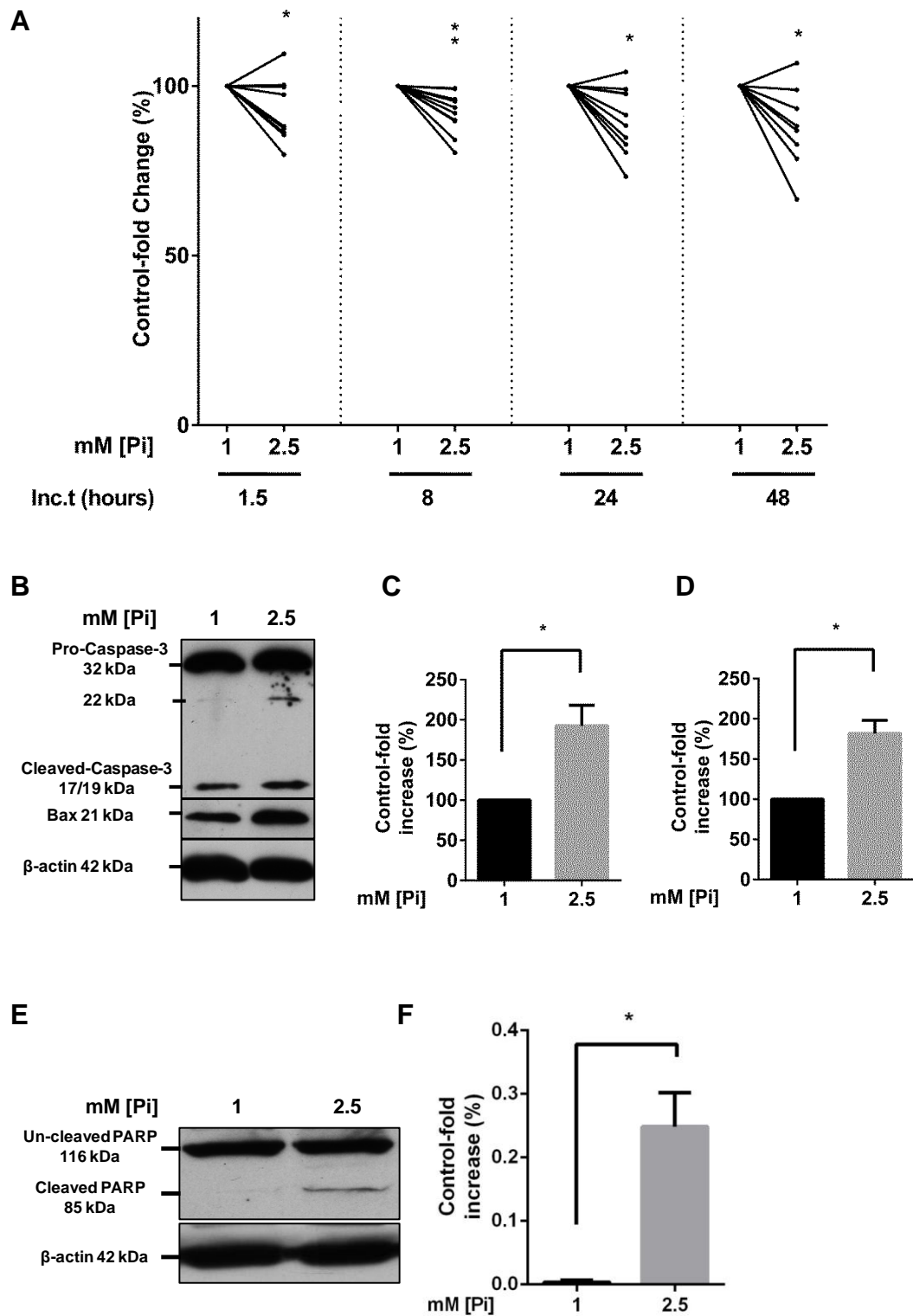


Figure 5.2. (Part 1 of 5). Effect of hyperphosphataemia on cell viability, apoptosis and pro-apoptotic signals in EAhy926 cells. (A) Time course of MTT cell viability staining of control (1mM Pi) and 2.5mM Pi-treated cells. (n=4)  $\hat{P}$ <0.05,  $\hat{\hat{P}}$ <0.01. (B) Representative immunoblots showing cleavage of caspase-3 and increase in pro-apoptotic Bax expression in cells treated with 2.5mM Pi; t=24h. (C and D) Densitometry analysis of cleaved 17/19kDa caspase-3 fragment (C) and Bax expression (D); t=24h (n=3)  $\hat{P}$ <0.05. (E and F) Representative immunoblot and corresponding densitometry analysis showing increased cleavage of PARP at 85kDa; t=24h, (n=3)  $\hat{P}$ <0.05.

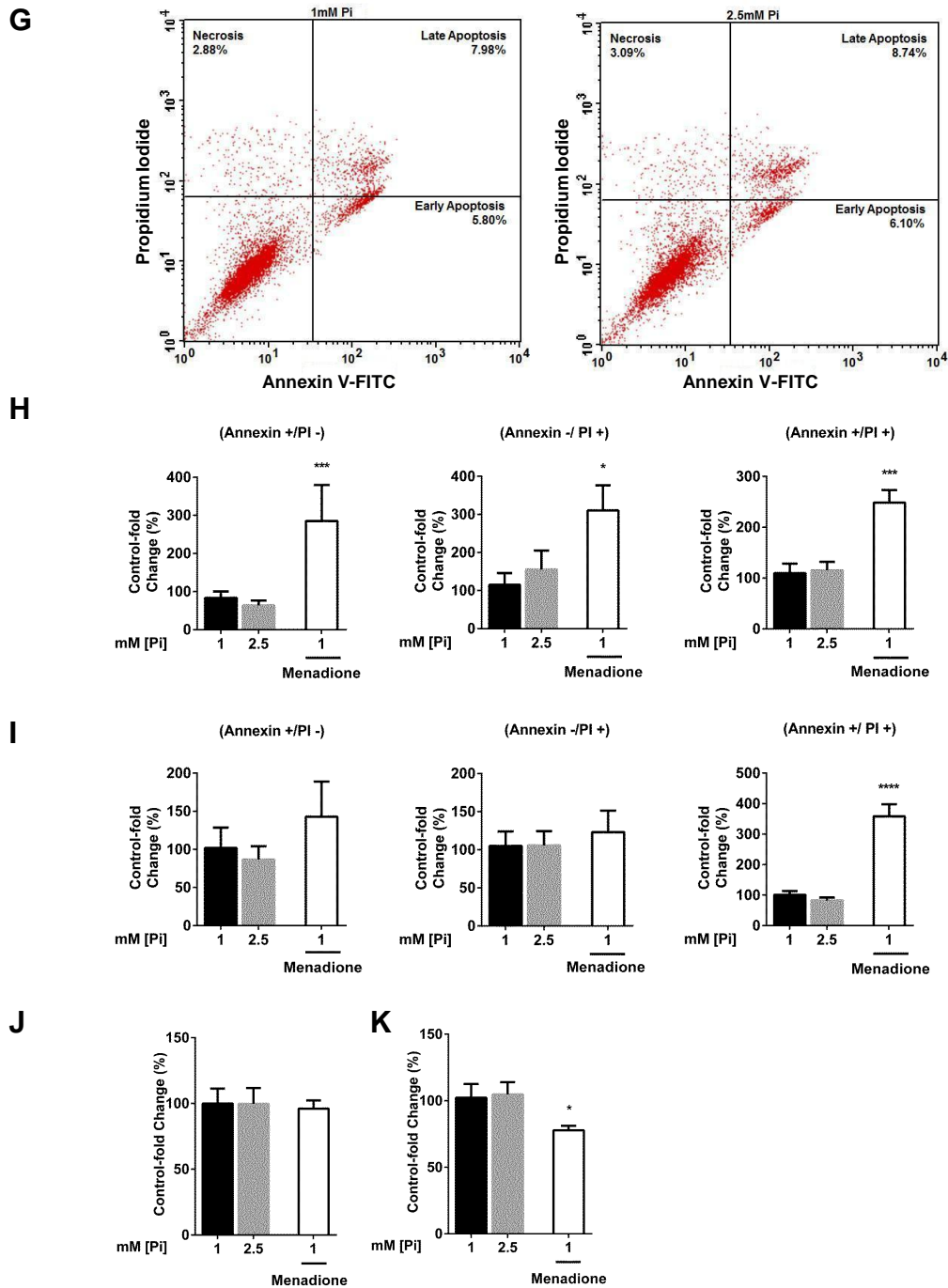
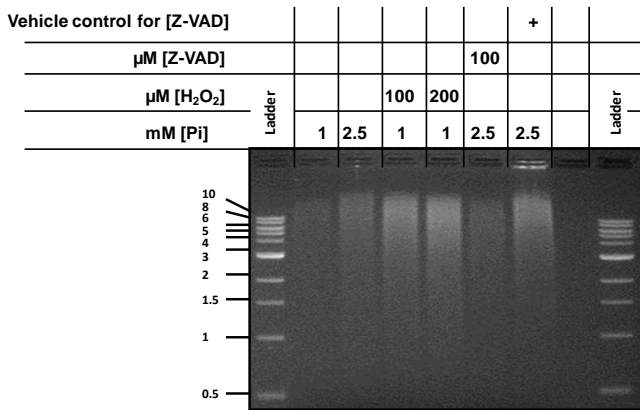
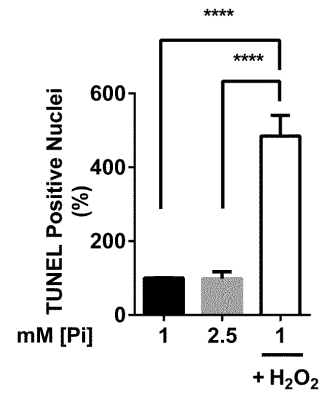


Figure 5.2. (Part 2 of 5). Effect of hyperphosphataemia on cell viability, apoptosis and pro-apoptotic signals in EAhy926 cells. (G-I) Representative Flow Cytometry cytograms (G) and analysis of Annexin V binding and PI staining of cells (H-I) exposed to 1mM and 2.5mM Pi for 90min and 24h showing failure to detect an effect of Pi-loading on necrosis, early apoptosis or late apoptosis in spite of clear effects with a 30 $\mu$ M Menadione positive control. (H: Different apoptosis stages at 90min and I: at 24h) (n=13) \*P<0.05, \*\*\*P<0.001, \*\*\*\*P<0.0001. (J, K) Forward angle light scatter (an indication of cell size) detects apoptotic cell shrinkage in response to 30 $\mu$ M Menadione positive control (n=5) but no response to Pi loading (neither at 90min: J nor at 24h: K). \*P<0.05.

L



N



M

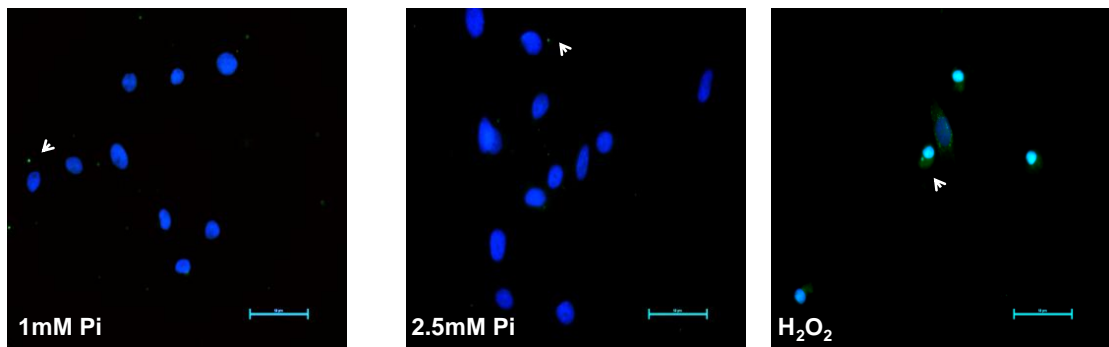


Figure 5.2. (Part 3 of 5). Effect of hyperphosphataemia on cell viability, apoptosis and pro-apoptotic signals in EAh926 cells. (L) Representative agarose gel electrophoresis from 3 experiments showing the presence of DNA fragmentation in 2.5mM Pi-treated and Positive control ( $\text{H}_2\text{O}_2$ -treated) cells. Caspase inhibitor Z-VAD-FMK prevented the effect of high Pi; t=24h. (Note that the pattern observed indicates DNA fragmentation but Pi does not induce a clear DNA laddering like that observed in classical apoptosis) (M and N) Representative Fluorescent Microscopy images (M) and analysis (N) of apoptosis index in Pi treated cells as determined by TUNEL assay (Green: Arrows). Nuclei were counterstained (Blue) and cells treated with  $\text{H}_2\text{O}_2$  as a positive control; Scale Bar 50 $\mu\text{m}$ , t=24h (n=3) \*\*\*\* P<0.0001.

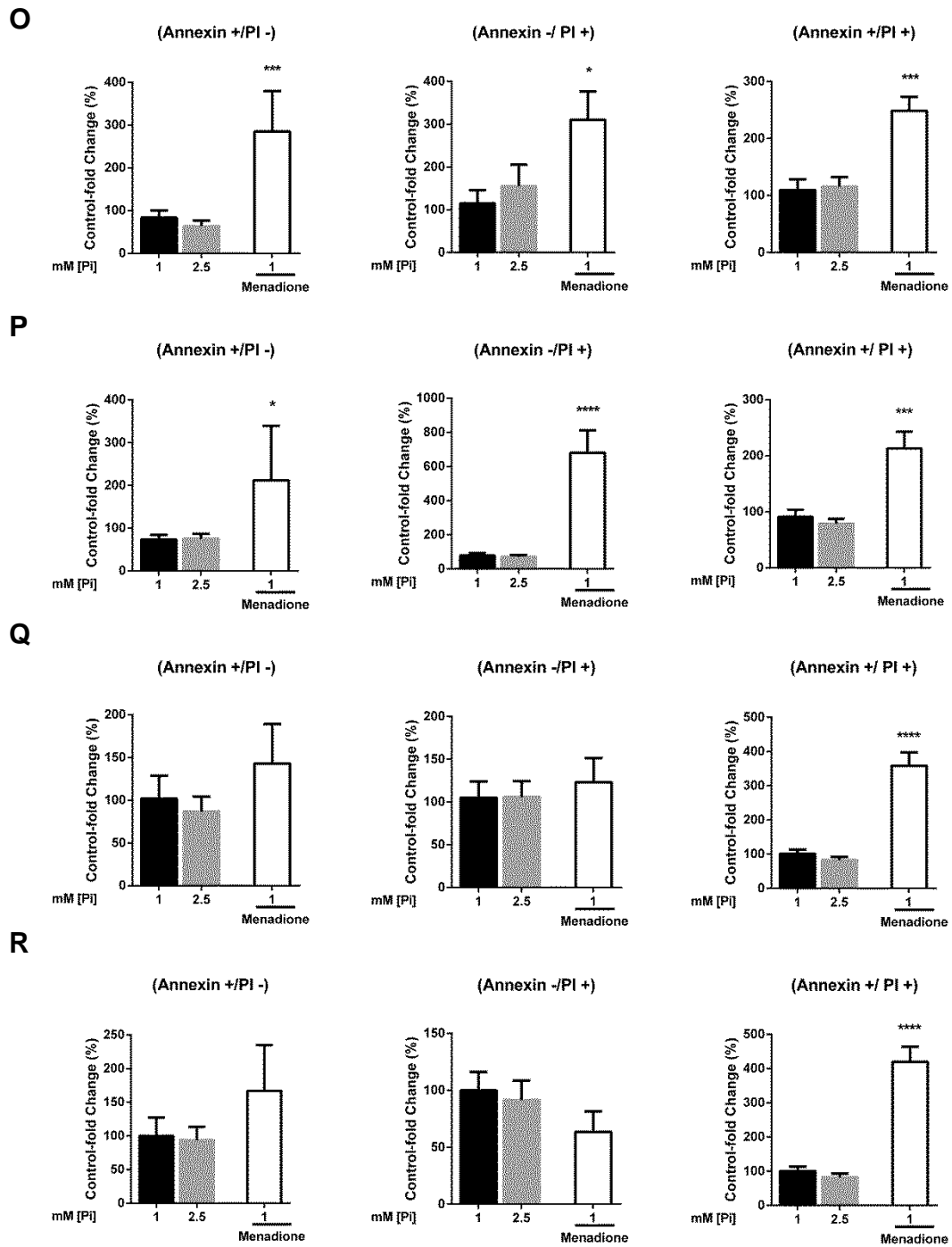


Figure 5.2. (Part 4 of 5). Effect of hyperphosphataemia on cell viability, apoptosis and pro-apoptotic signals in EAhy926 cells. (O-R) Analysis of Annexin V binding and PI staining of cells exposed to 1mM and 2.5mM Pi for 90min, 8h, 24h and 48h showing failure to detect an effect of Pi-loading on necrosis, early apoptosis or late apoptosis in spite of clear effects with a 30µM Menadione positive control. (O: Different apoptosis stages (see Figure 2.6) at 90min and P: at 8h, Q: at 8h, R: at 48h) (n=13) \*P<0.05, \*\*\*P<0.001, \*\*\*\*P<0.0001.

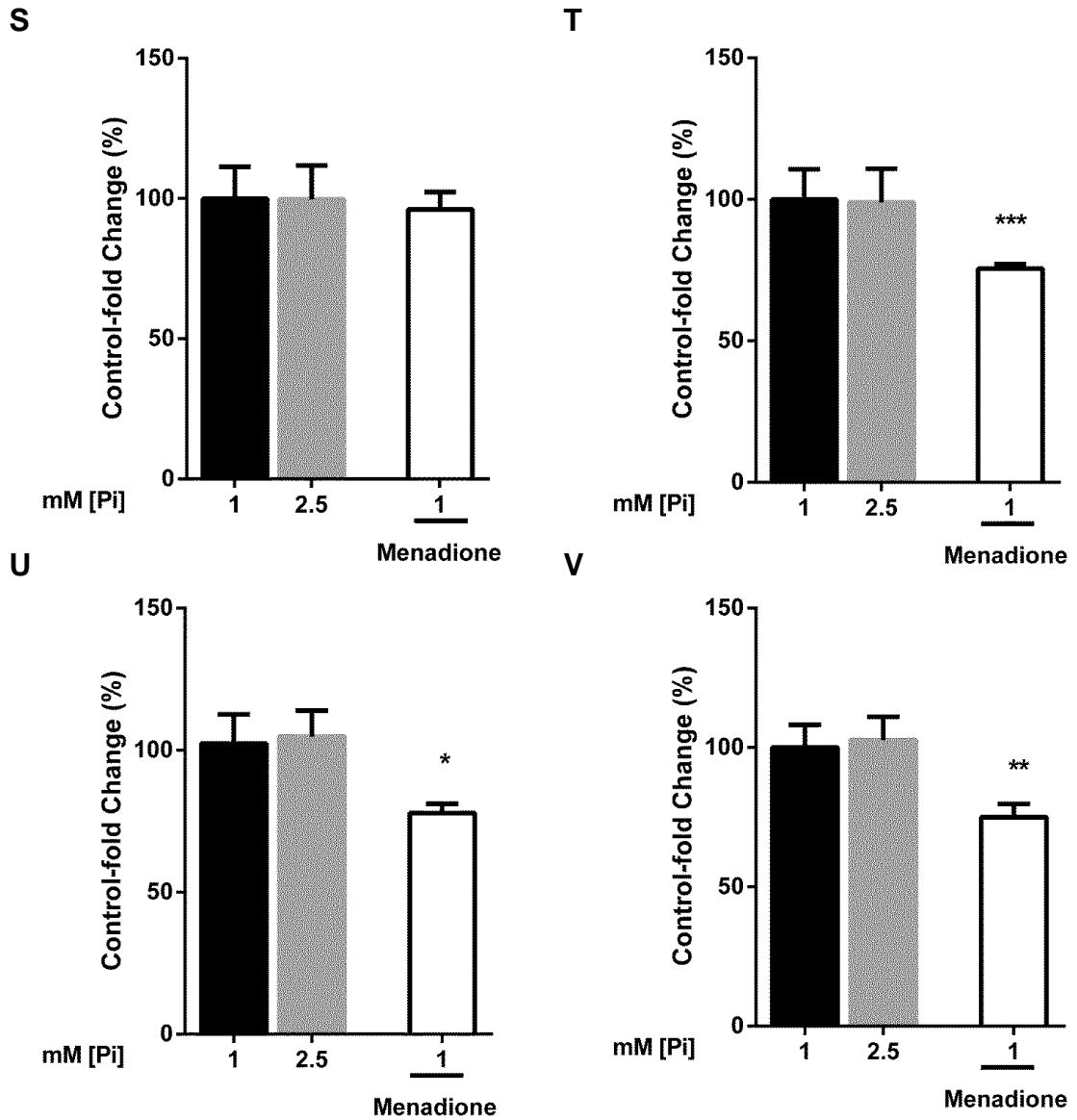


Figure 5.2. (Part 5 of 5) Effect of hyperphosphataemia on cell viability, apoptosis and pro-apoptotic signals in EAhy926 cells. (S- V) Forward angle light scatter (an indication of cell size) detects apoptotic cell shrinkage in response to 30μM Menadione positive control (n=5) but no response to Pi loading (neither at 90min: S nor at 8h: T nor at 24h: U nor at 48h: V). \*P<0.05, \*\*P<0.01, \*\*\*P<0.001.

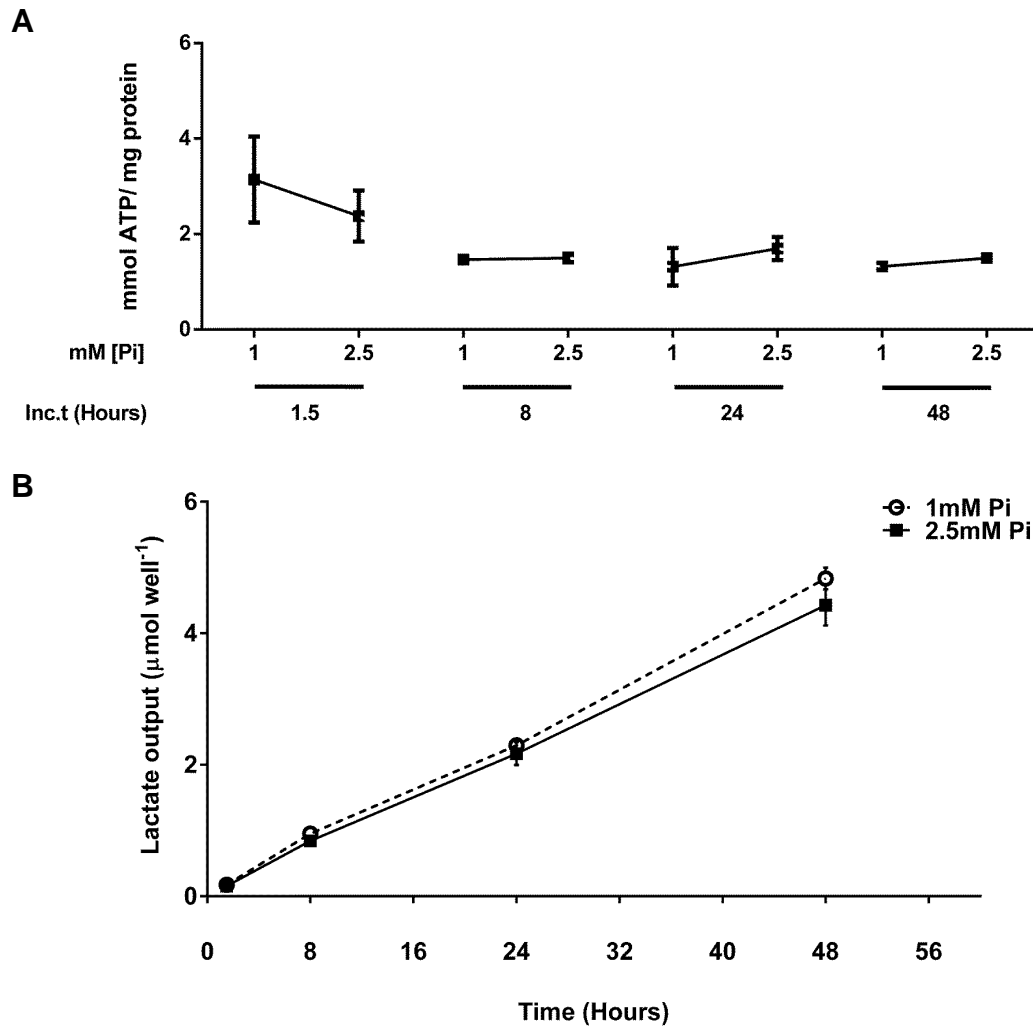


Figure 5.3. *In vitro* effect of Pi on intracellular adenosine triphosphate (ATP) and glycolytic rate (Lactate production). (A) Time course of the effect of extracellular Pi load on intracellular ATP level in EAhy926 cells determined by HPLC (Three replicates from a representative experiment in culture wells of 35mm diameter) (B) Glycolytic rate (Lactate production) in Pi loaded EAhy926 endothelial cells over time (Three replicates from a representative experiment in culture wells of 35mm diameter).

### 5.2.2 Effect of Z-VAD-FMK Caspase-3 inhibitor on Pi-induced EMP output

The effect of a Caspase 3 inhibitor on the acute (90min) and chronic (24h) effect of elevated extracellular Pi (i.e. 2.5mM [Pi]) on NTA detectable particle release from EAhy926 ECs was studied. Cultures were treated with vehicle alone (DMSO) or Z-VAD-FMK (100 $\mu$ M) (Figure 5.4). Even though Z-VAD-FMK apparently abolished the effect of Pi, a similar blunting was also observed with the DMSO vehicle alone.

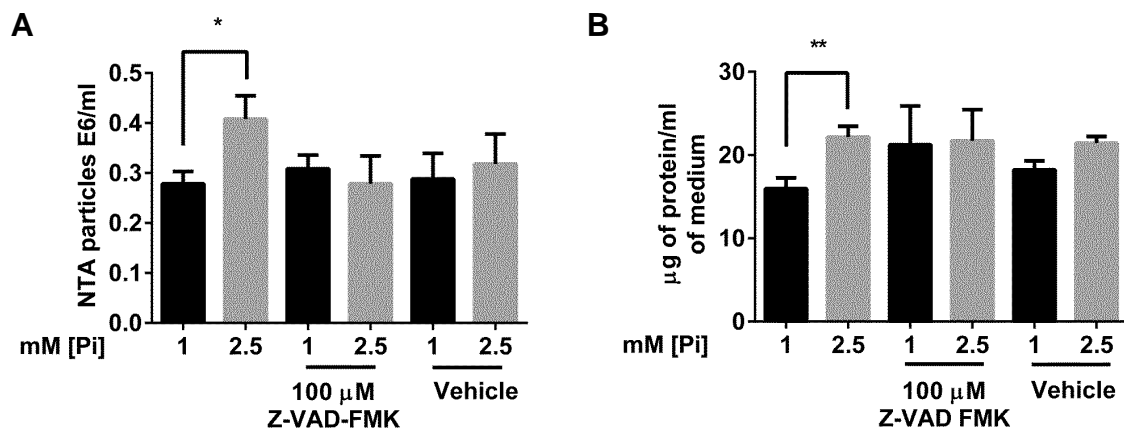


Figure 5.4. Effect of Pi and caspase-3 inhibitor Z-VAD-FMK on EAhy926 ECs function and membrane integrity. (A) Nanoparticle Tracking Analysis (NTA) performed on uncentrifuged medium showing particle concentration expressed as millions (E6) per ml indicating that both Z-VAD-FMK and vehicle (0.5% v/v DMSO) blunt Pi-induced MP output at t = 90min. (n=3) \*P<0.05. (B) Chronic protein particle release from Pi treated cells at t = 24h in the presence or absence of inhibitor or vehicle showing abolition of the Pi-induced increase in sedimentable protein particles from the medium with both Z-VAD-FMK and vehicle alone \*\*P<0.01 (n=3).

### 5.2.3 Effect of Rho Kinase inhibitors on Pi-induced EMP output

As caspase-mediated activation of the Rho/ROCK pathway has been implicated in the activation of microparticle output accompanying apoptosis (Sebbagh *et al.*, 2001), the effect of an inhibitor of this pathway (Y-27632) on the acute effect of a high extracellular Pi concentration (i.e. 2.5mM [Pi]) on NTA detectable particle release from EAhy926 ECs was studied. Some cultures were treated with ROCK inhibitor Y-27632 (10 $\mu$ M as described in (Ark *et al.*, 2010; Li *et al.*, 2013)) for 1hour before Pi treatment. Control cultures were treated with 1mM [Pi] in the absence of Y-27632. The Rho-kinase inhibitor did not blunt Pi-induced MP release from EAhy926 endothelial cells but did result in a higher base line of MP output into the medium (Figure 5.5).

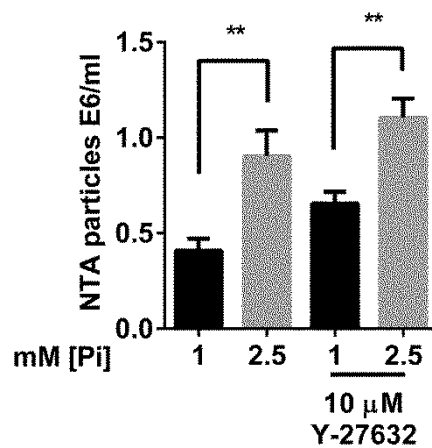


Figure 5.5. Acute release of microparticles from EAhy926 endothelial cells incubated for 90min with control (1mM) and high (2.5mM) [Pi] medium in the presence or absence of Rho kinase inhibitor (ROCK; Y-27632-10  $\mu$ M). Nanoparticle Tracking Analysis (NTA) was performed on uncentrifuged medium showing no inhibitory effect of the inhibitor on MP output at 90min (particle concentration expressed as millions (E6) per ml) (n=3) \*\*P<0.01.

#### **5.2.4 Inhibitory effect of Pi on phosphoprotein phosphatases**

Even though elevated Pi concentration has previously been reported to increase endothelial production of reactive oxygen species (Shuto *et al.*, 2009; Peng *et al.*, 2011), a potential cause of apoptosis and consequent MP production (Di Marco *et al.*, 2008), no significant oxidative stress or apoptosis was detected in response to 2.5mM Pi in the present study (Figures 5.1 - 5.5), suggesting that Pi-induced MP output arose from some alternative cell stress or signalling induced by Pi. At physiological concentrations, Pi is a potent inhibitor of a wide range of Phosphotyrosine protein phosphatases (PTPases) and Phosphoserine/threonine protein phosphatases (PSPases) in mammalian cells (Buzalaf *et al.*, 1998; Szajerka & Kwiatkowska, 1984; Zhang & VanEtten, 1991) – an inhibitory effect confirmed here for PTPases with as little as 100µM Pi by assaying catalytic activity in lysates from EAhy926 cells (Figure 5.6 A and B). (Similar attempted assays of PSPase activity in EAhy lysates are presented in Figure 5.7).

If this inhibition is functionally important in eliciting the MP output observed with 2.5mM Pi, applying other inhibitors capable of affecting a wide range of these phosphatases should exert a similar effect (i.e. with orthovanadate as a PTPase inhibitor (Huyer *et al.*, 1997) and fluoride as a PSPase inhibitor (Jaumot & Hancock, 2001)). PTPase inhibition was found to mimic the acute (90min) effect of Pi on MP output (Figure 5.6 C), whereas PSPase inhibition mimicked the chronic (24h) Pi effect on particle output (Figure 5.6 D).

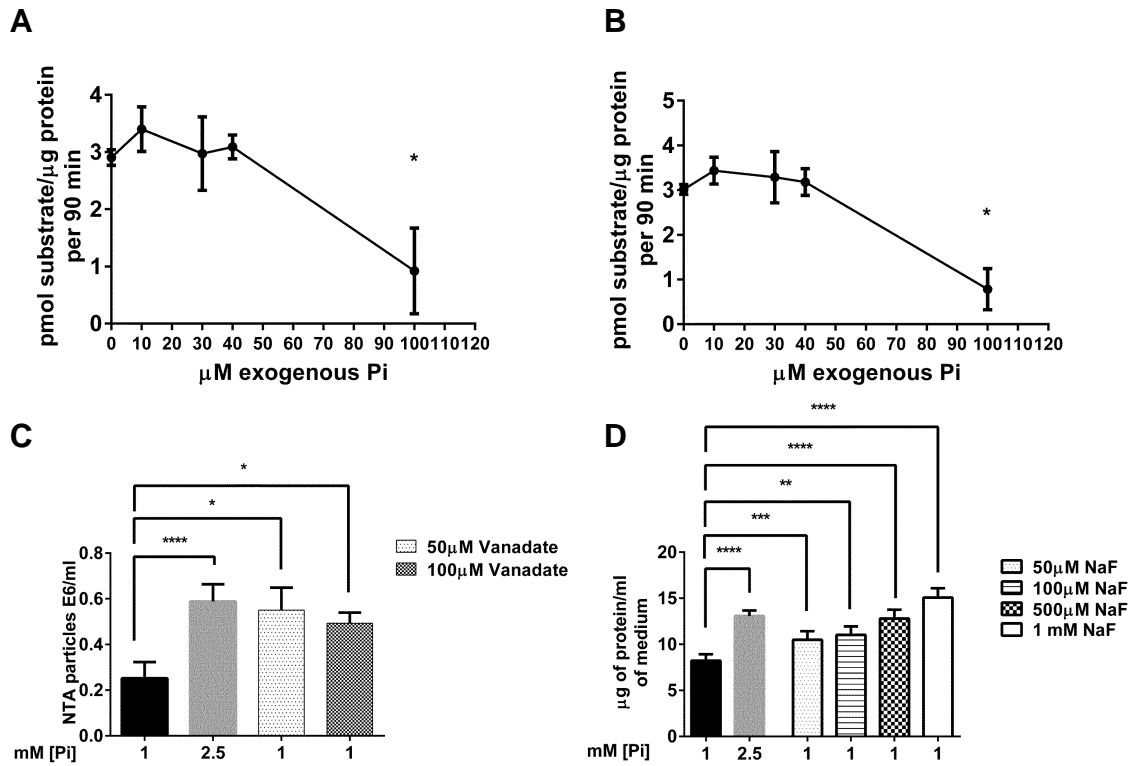


Figure 5.6. Inhibitory effects of Pi on phosphoprotein phosphatases. (A and B) Direct inhibition by Pi of tyrosine protein-phosphatase catalytic activity in lysates of EAhy926 cells assayed *in vitro* in the presence of exogenous Pi at the stated concentration using two different tyrosine-phosphatase substrates (Promega Ref V2471 substrate-1 (Left) and Promega Ref V2471 substrate-2 (Right)) (n=3), \*P<0.05. (C) Mimicry by broad-spectrum tyrosine protein phosphatase inhibitor (Vanadate) of the acute (90min) Pi-induced increase in particle output detected by NTA in uncentrifuged medium from EAhy926 cells. (n=3) \*P<0.05, \*\*\*\*P<0.0001. Particle concentration is expressed as millions (E6) per ml. (D) Mimicry by broad-spectrum serine/threonine protein phosphatase inhibitor (sodium fluoride, NaF) of the chronic (24h) Pi-induced increase in particle output detected by measuring total sedimentable protein after centrifugation at 18,000xg. (Fraction 3-Table 2.1). (n=3) \*\*P<0.01, \*\*\*P<0.001, \*\*\*\*P<0.0001.

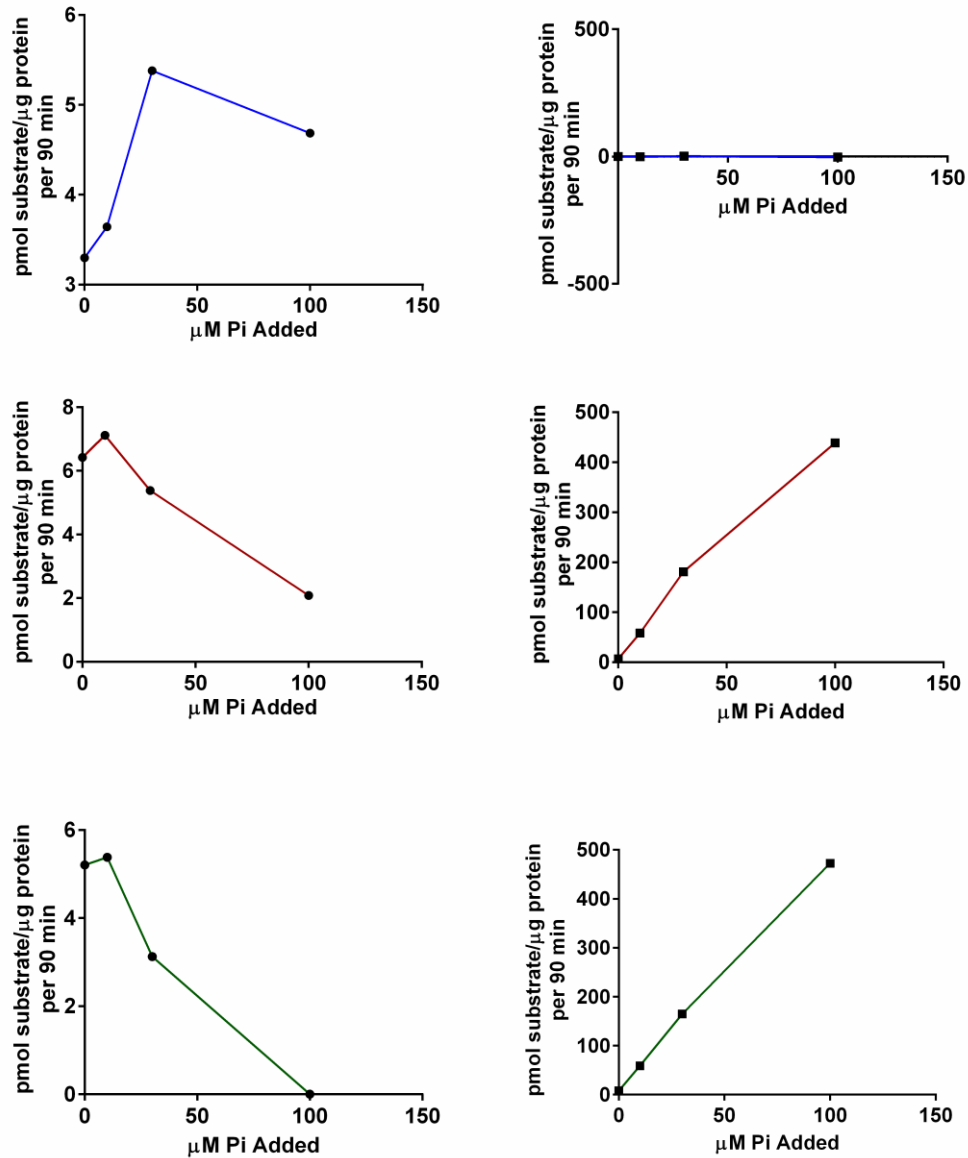


Figure 5.7. Effect of Pi on phosphoprotein Serine/Threonine phosphatase (PSPase) catalytic activity in cell lysates. Unlike positive controls (i.e. HeLa cell lysate; graphs indicated with (●) in the left hand panels) no catalytic activity was detectable under basal (i.e. Pi-free) conditions in assays for PSPase 2A (Blue lines), PSPase 2B (Red lines), and PSPase 2C (Green lines) in lysates from EAhy926 cells (indicated with (■) in the right hand panels). The apparent stimulatory effect of Pi on PSPase 2B and 2C activity in EAhy926 lysates may arise from a previously described Pi-activated phospho-histone phosphatase activity (Khandelwal & Kamani, 1980).

### 5.2.5 Hyperphosphataemia alters global protein phosphorylation and/or de-phosphorylation

If intracellular Pi accumulation inhibits phosphoprotein phosphatases in intact cells, global increases in protein phosphorylation should be observed in Pi-loaded cells. On probing cell lysates with pan-specific anti-phospho-Tyrosine or

anti-phospho-Serine/Threonine antibodies, such global increases in phosphorylation were detectable within 90min of exposure to 2.5mM Pi (Figure 5.8 A-D) and were reversed by siRNA silencing of PiT-1/slc20a1 gene expression (Figure 5.8 E-H). The increased phosphorylation induced by 2.5mM extracellular Pi was sustained for at least 48h (Figure 5.8 A and C) in spite of compensatory up-regulation of at least one major cellular protein phosphatase (the Low Molecular Weight PTPase – Figure 5.8 I and J). Similar global phosphorylation increases were observed on treating cells with orthovanadate and fluoride (data not shown).

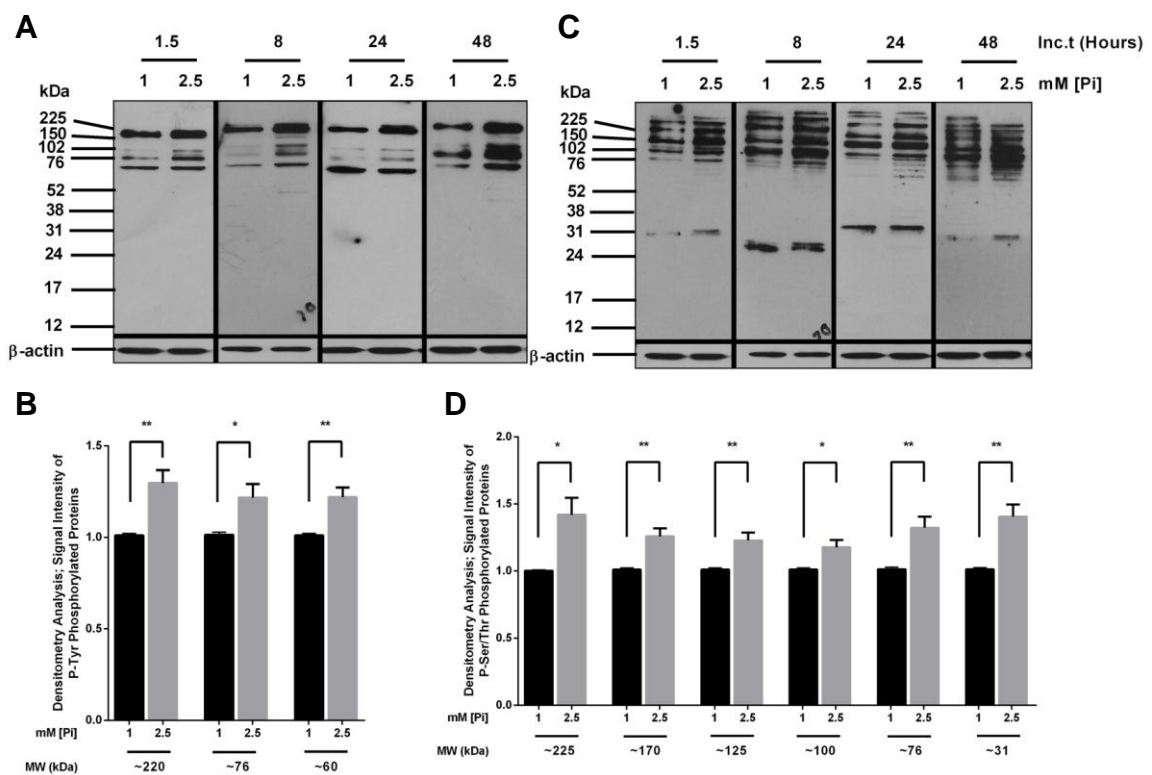


Figure 5.8. (Part 1 of 2) Net global effects of hyperphosphataemia on protein phosphorylation and/or de-phosphorylation in EAhy926 endothelial cells. (A-D) Representative immunoblots and quantitative analysis by densitometry of protein tyrosine phosphorylation probed with pan-specific anti-phosphotyrosine antibody (A, B) and of protein serine/threonine phosphorylation probed with pan-specific anti-phosphoserine/threonine antibody (C, D). Densitometry is shown for cells incubated for 1.5h in medium with 1 or 2.5mM Pi. For tyrosine phosphorylation. (n=4), \*P<0.05, \*\*P<0.01. For serine/threonine phosphorylation. (n=4), \*P<0.05, \*\*P<0.01.

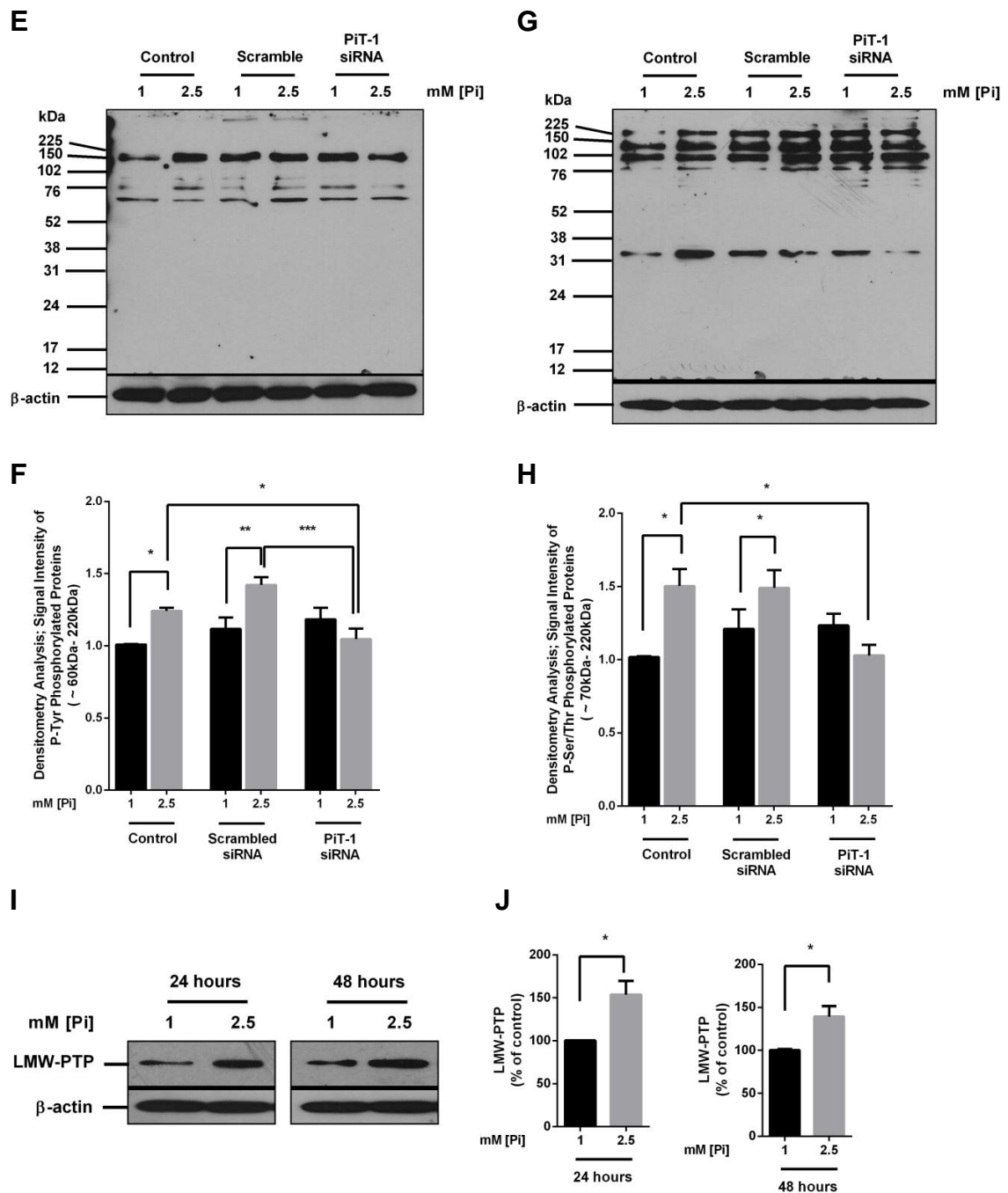


Figure 5.8. (Part 2 of 2) Net global effects of hyperphosphataemia on protein phosphorylation and/or dephosphorylation in EAhy926 endothelial cells. (E-H) Effect of siRNA silencing of PiT-1 transporter expression during 1.5h incubations of cells with 1 or 2.5mM Pi. Representative immunoblots and quantitative analysis by densitometry of protein tyrosine phosphorylation (E, F) and of protein serine/threonine phosphorylation (G, H). "Control" denotes cultures treated with transfection agent only. In (F) the densitometry analysis was performed on all bands in the 60-220kDa region of the blots. (n=3) \*P<0.05, \*\*P<0.01, \*\*\*P<0.001. In (H) densitometry was performed at 70-220kDa. (n=4) \*P<0.05. (I and J) Effect of 24 or 48h of hyperphosphataemia on expression of Low Molecular Weight Protein Tyrosine Phosphatase; LMW-PTP) determined by immunoblotting and densitometry. (n=3) \*P<0.05.

In an alternative culture model of human vascular endothelial cells (HUVECs), a similar acute (90min) effect of a high extracellular Pi concentration (i.e. 2.5mM [Pi]) on **global protein phosphorylation** was observed; (Figure 5.9).

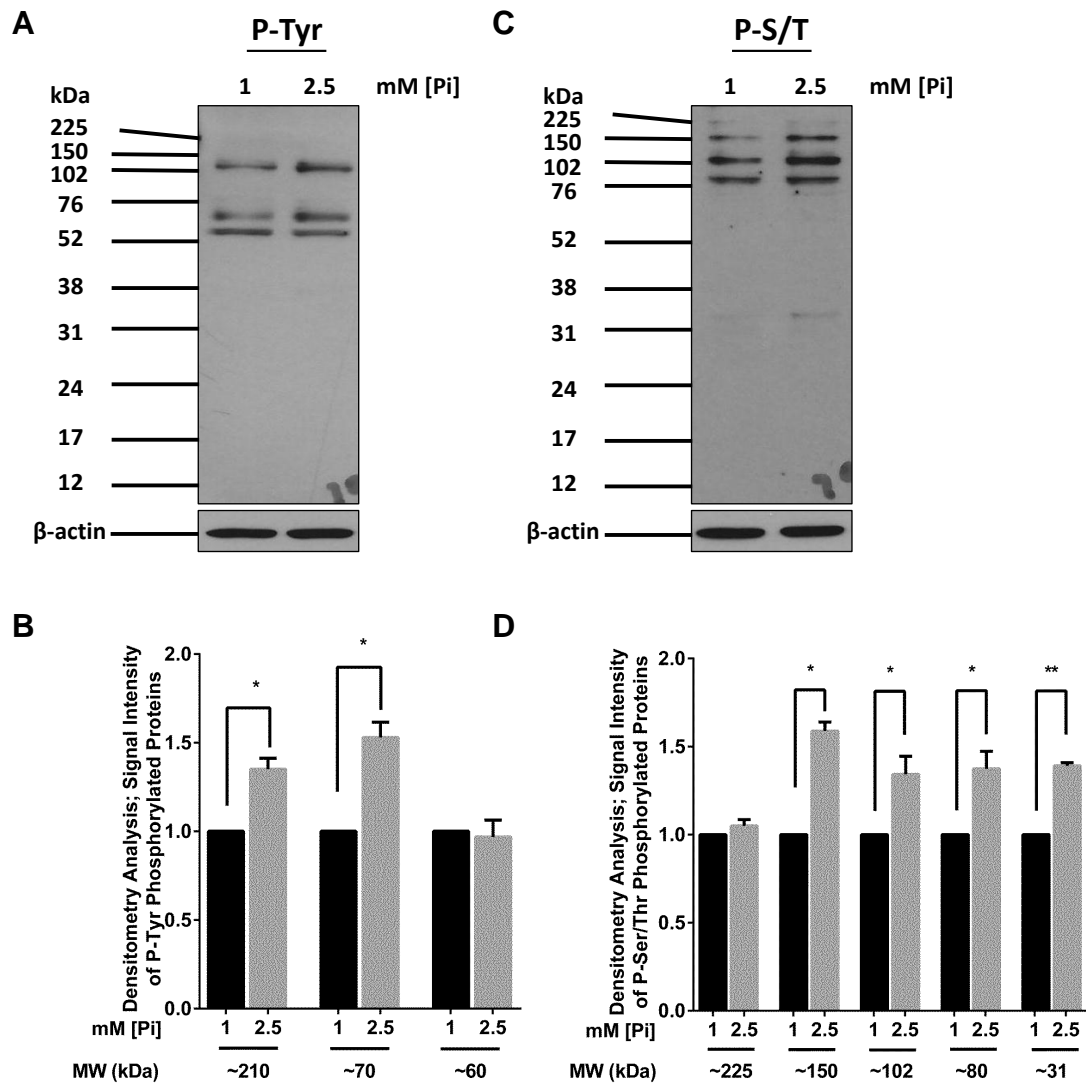


Figure 5.9. Net global effects of hyperphosphataemia on protein phosphorylation and/or de-phosphorylation in HUVECs. (A, B) Representative immunoblots and quantitative analysis by densitometry of protein tyrosine phosphorylation probed with pan-specific anti-phosphotyrosine antibody. (C, D) Corresponding immunoblots and densitometry of protein serine/threonine phosphorylation probed with pan-specific anti-phosphoserine/threonine antibody. Densitometry is shown for cells incubated for 1.5h in medium with 1 or 2.5mM Pi. For tyrosine phosphorylation (n=3), \*P<0.05, \*\*P<0.01. For serine/threonine phosphorylation (n=3), \*P<0.05, \*\*P<0.01.

### 5.2.6 Acute and chronic effect of fructose on protein phosphorylation and/or dephosphorylation

If fructose depletes intracellular Pi, it would be expected that this would reverse the effect of higher intracellular Pi concentration on net global protein phosphorylation events (Figure 5.8) and particle release from the cells (Figure 3.7 A). Even though fructose loading the medium blunted the *acute* particle release from the cells (Figure 3.7 A), which was accompanied by a reversed (i.e. blunted) phosphorylation signal (Figure 5.10 A-D), *chronic* loading of the medium with fructose, if anything, resulted in (i) more sedimentable particle release from the cells (Figure 5.11 E) and (ii) an enhanced effect on net global phosphorylation events (Figure 5.11 A-D).

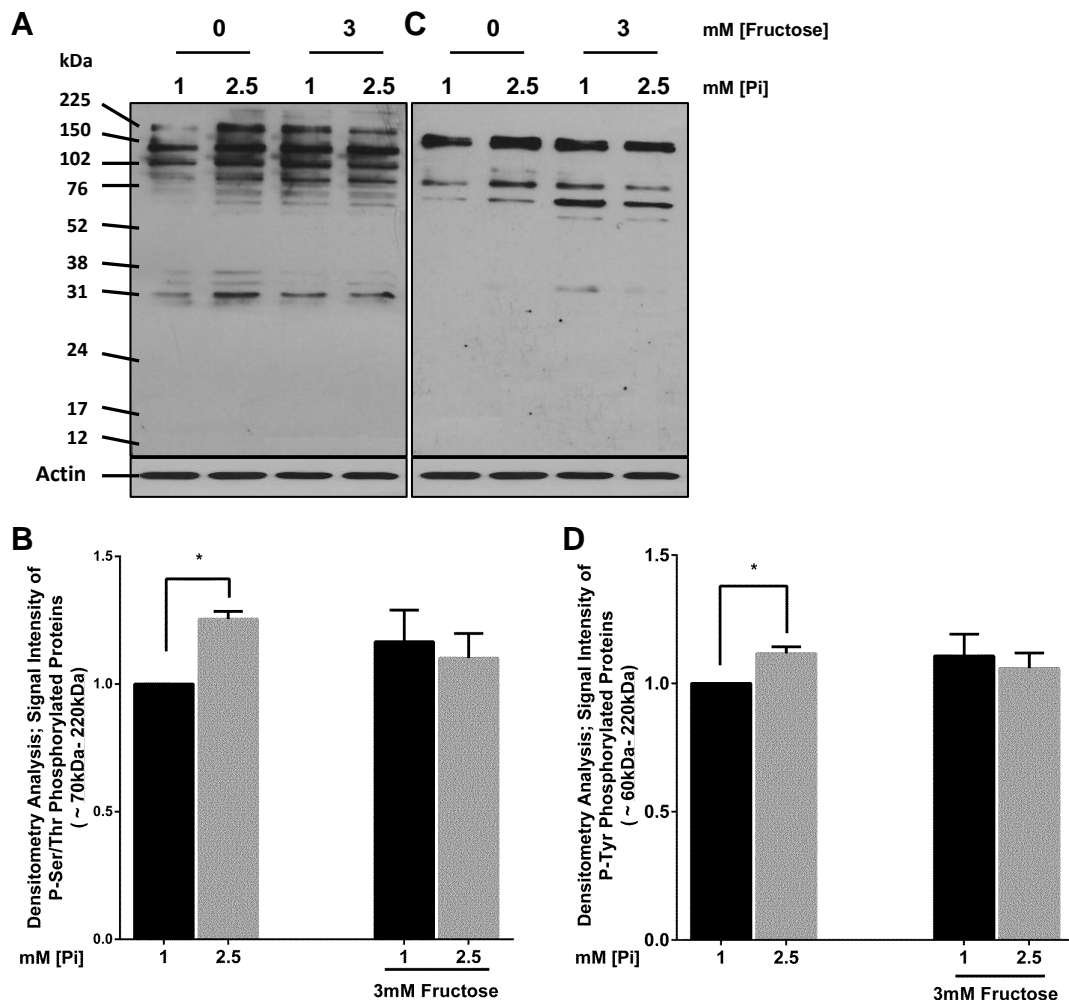


Figure 5.10. Acute (90min) net global effects of hyperphosphataemia in the presence or absence of Fructose on protein phosphorylation and/or de-phosphorylation in EAhy926 endothelial cells. (A, B) Representative immunoblots and quantitative analysis by densitometry of protein serine/threonine

phosphorylation probed with pan-specific anti-phosphoserine/threonine antibody; and (C, D) of protein tyrosine phosphorylation probed with pan-specific anti-phosphotyrosine antibody (B, D). Densitometry is shown for cells incubated for 1.5h in medium with 1 or 2.5mM Pi in the presence or absence of 3mM Fructose. For tyrosine phosphorylation. (n=3), \*P<0.05. For serine/threonine phosphorylation. (n=3), \*P<0.05.

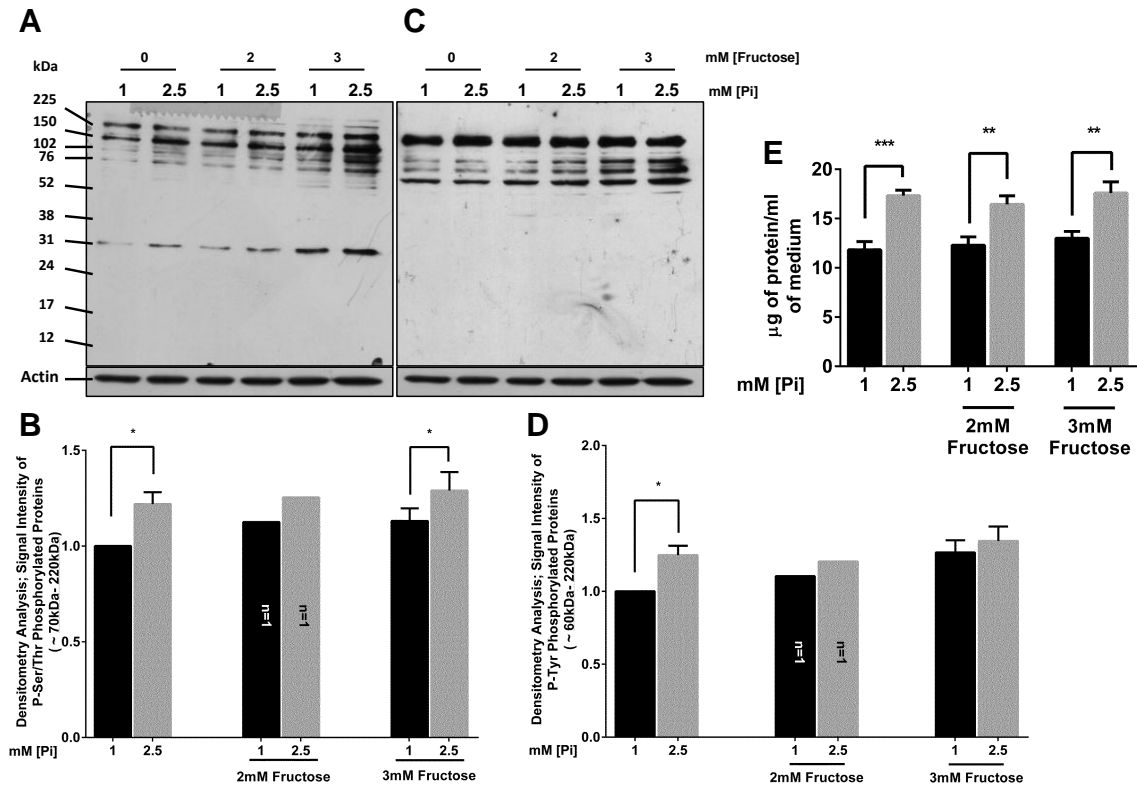
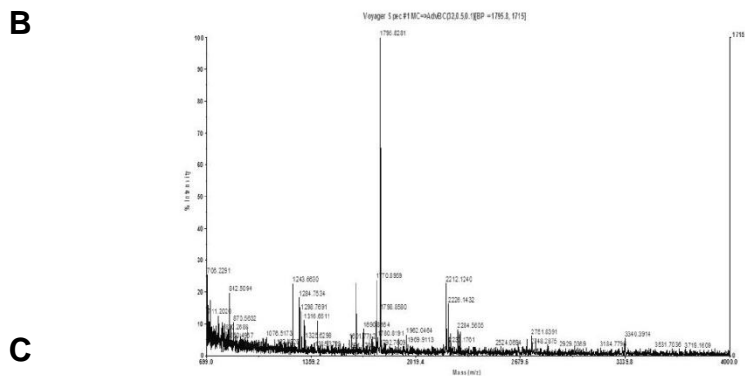
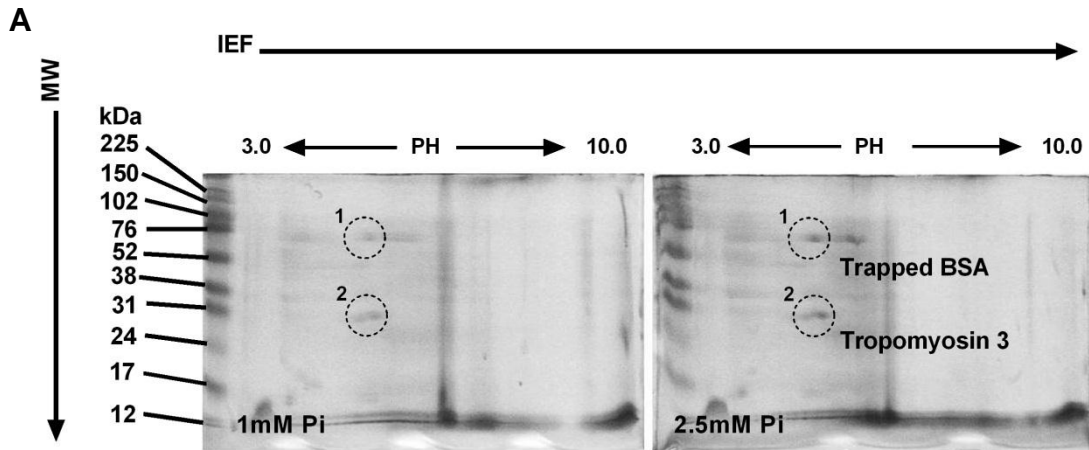


Figure 5.11. Chronic (24h) net global effects of hyperphosphataemia in the presence or absence of Fructose on protein phosphorylation and/or de-phosphorylation in EAhy926 endothelial cells. (A, B) Representative immunoblots and quantitative analysis by densitometry of protein serine/threonine phosphorylation probed with pan-specific anti-phosphoserine/threonine antibody (C, D) and of protein tyrosine phosphorylation probed with pan-specific anti-phosphotyrosine antibody (B, D). Densitometry is shown for cells incubated for 24h in medium with 1 or 2.5mM Pi in the presence or absence of 3mM Fructose. For tyrosine phosphorylation. (n=4), \*P<0.05. For serine/threonine phosphorylation. (n=4), \*P<0.05. (E) Chronic protein particle release/cell detachment from EAhy926 endothelial cells after exposure for 24h to medium (2ml per 35mm culture well) with control (1mM) Pi or high (2.5mM) Pi in the presence or absence of Fructose (n=3) \*P<0.01, \*\*\*P<0.001.

### **5.2.7 Effect of intracellular Pi on cytoskeletal regulatory protein (TM-3)**

The cytoskeletal regulatory protein Tropomyosin and its phosphorylation have been implicated in regulation of endothelial membrane blebbing and microparticle formation (Houle *et al.*, 2007). Analysis of Pi-treated EAhy926 cells by 2-dimensional gel electrophoresis revealed a prominent ~30kDa protein accumulating within 90min of exposure to 2.5mM Pi (Figure 5.12 A) and immuno-staining with anti-phospho-Serine/Threonine antibody (Figure 5.12 I). Excision and mass spectrometry of the protein spot identified it as Tropomyosin-3 (TM-3) (Figure 5.12 B and C) and its rapid up-regulation was subsequently confirmed by immuno-blotting with antibody specific for TM-3 (Figure 5.12 D-H). In spite of marked up-regulation of this protein, the intensity of its anti-phospho-Serine/Threonine immuno-staining decreased in Pi-treated cells (Figure 5.12 I and J) indicating that it was profoundly hypophosphorylated.



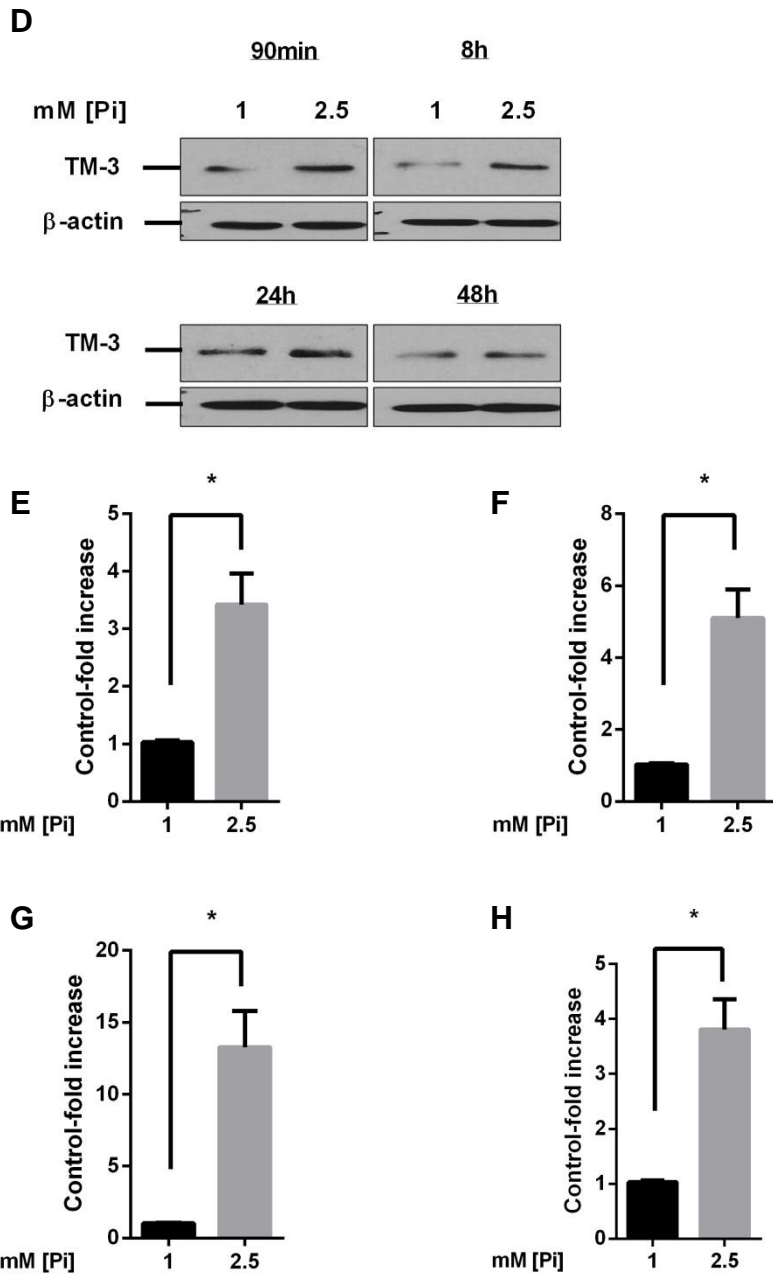


Figure 5.12. (Part 2 of 3) Effect of hyperphosphataemia on the concentration and phosphorylation of Tropomyosin-3 (TM-3) in EAhy926 cells. (D) Tropomyosin immunoblots (representative of 3 independent experiments) obtained from cells incubated as in (A), probed using anti-TM-3 antibody to confirm the accumulation of TM-3 in cells treated with 2.5mM Pi over a time course from 90min to 48h. (E - H) Corresponding densitometry analysis on TM-3 immunoblots at (E) 90min, (F) 8h, (G) 24h, and (H) 48h respectively. (n=3) \*P<0.05.

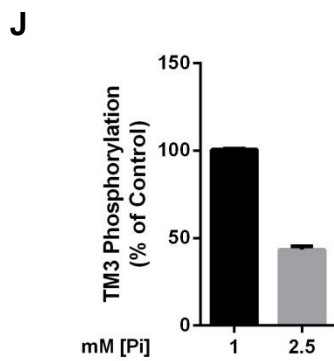
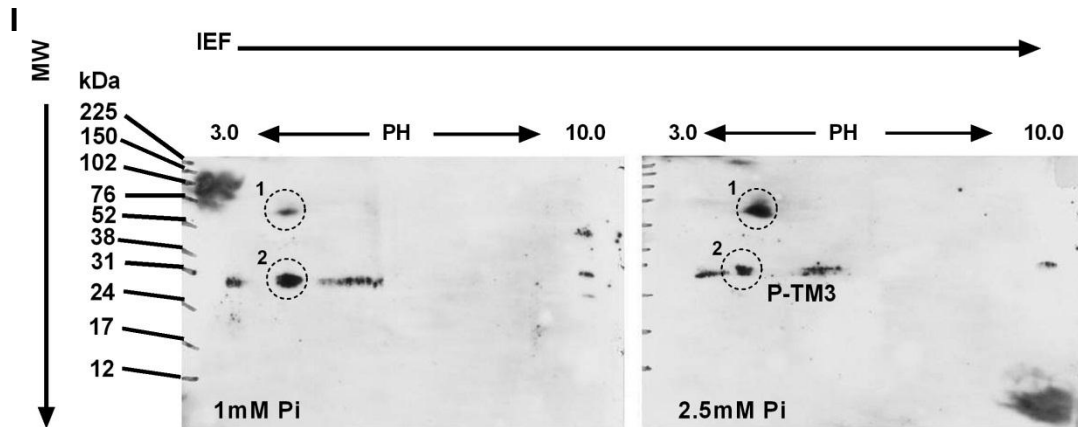


Figure 5.12. (Part 3 of 3) Effect of hyperphosphataemia on the concentration and phosphorylation of Tropomyosin-3 (TM-3) in EAhy926 cells. (I and J) Tropomyosin phosphorylation. Immunoblotting and densitometry analysis of 2-DE gels blotted on nitrocellulose membranes and probed with pan-specific anti-P-Ser/Thr antibody. (Spot 2 designated P-TM3 denotes phosphorylated Tropomyosin).

In an alternative culture model of human vascular endothelial cells (HUVECs), a similar acute (90min) effect of a high extracellular Pi concentration (i.e. 2.5mM [Pi]) on Tropomyosin accumulation was observed (Figure 15.13).

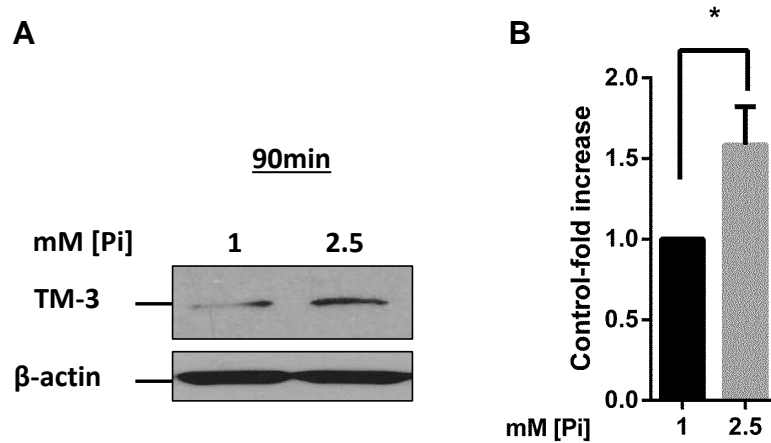


Figure 15.13. Acute effect of high Pi in the medium on on the expression of Tropomyosin-3 (TM-3) in HUVECs. (A) Tropomyosin immunoblots (representative of 3 independent experiments) obtained from cells incubated in medium with 1 or 2.5mM Pi for 1.5h, probed using anti-TM-3 antibody (B) Corresponding densitometry analysis on TM-3 immunoblots at 1.5h. (n=3) \*P<0.05.

### 5.2.8 High Pi-derived MPs are enriched in Histones

Analysis of acid-extractable proteins from EAhy926 lysates (extracted as described in Section 2.18.3.2) also demonstrated depletion of a prominent ~17kDa protein (Figure 5.14 F and G) after prolonged exposure (i.e. 24-48h) of the cells to 2.5mM Pi. In spite of this depletion in the intact cells, a similar protein correspondingly accumulated after 48h in the 18,000g MP fraction sedimented from the medium (Figure 5.14 A and B and Appendix C-Figure 5.6). Analysis of the 17kDa band by mass spectrometry identified Histone H2B (Figure 5.14 C) and this was confirmed by immuno-blotting with specific anti-Histone H2B antibody (Figure 5.14 A, B, F and G). A detailed table summarising detected candidate proteins in the 17kDa band has been shown in (Appendix C-5.10).

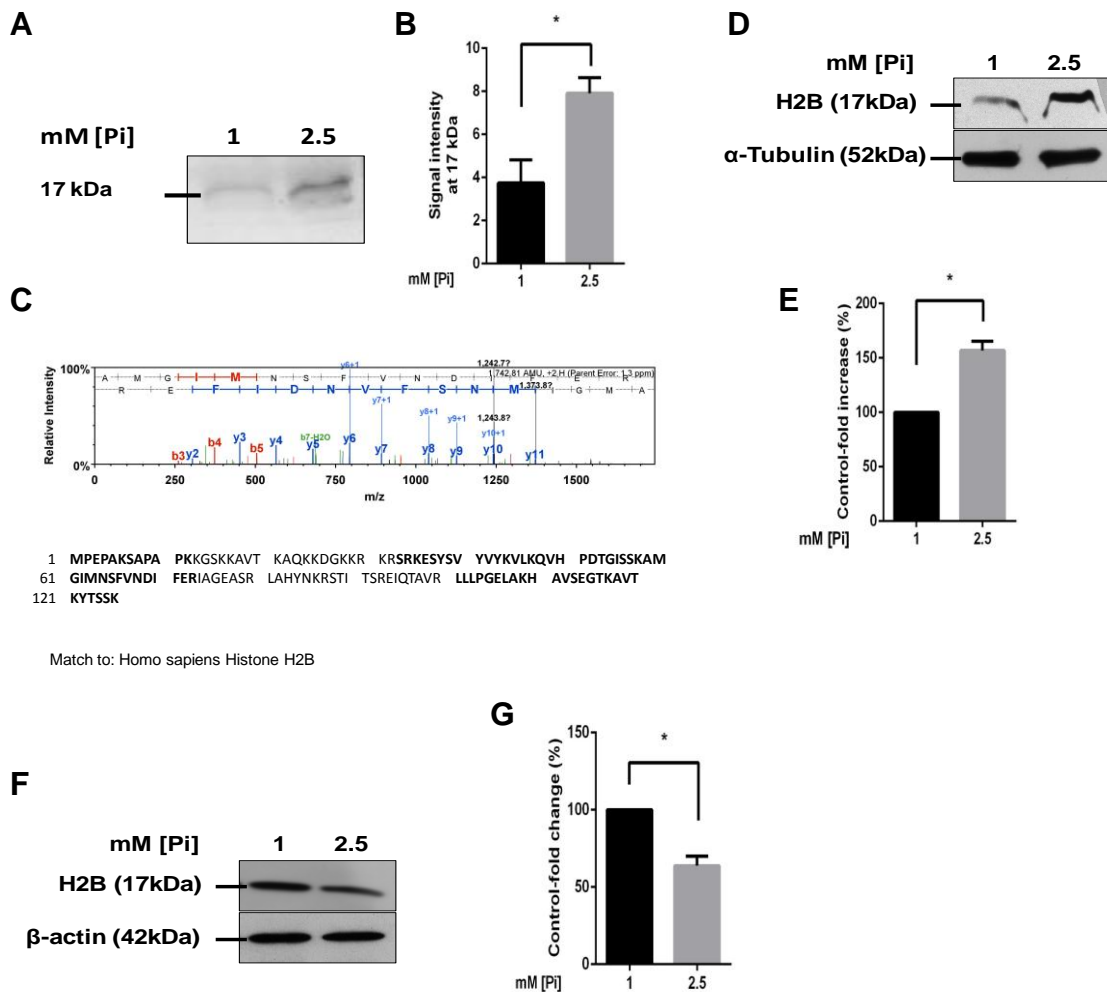


Figure 5.14. Effect of high [Pi] in the medium on Histone H2B expression/distribution in cell layer and sedimentable particles from EAhy926 endothelila cells. (A) Silver Stained SDS-PAGE gel (representative of 4 independent experiments) showing a prominent ~17kDa protein band that increases in intensity in particles sedimented from the medium at 18,000g (Fraction 3-Table 2.1) after 48h treatment of cells in medium with 1 or 2.5mM Pi. (B) Densitometry analysis of the 17kDa band (n=4) \*P<0.05 (C) Orbi-TRAP LC MS/MS analysis of the ~17kDa protein band excised from SDS-PAGE as in (A) showing mass spectrum (Top) and peptide sequence homology with Homo sapiens Histone H2B (bold letters) identified by LC MS/MS and database search (Bottom). The sequence coverage of Histone H2B reached 67%. Similar results were also obtained from the 17kDa protein band of the 18,000g particle fraction derived from cells treated with 1mM Pi (Data not shown). (D and E) Representative immunoblot (D) of particles sedimented as in (A) probed using anti-H2B antibody; and densitometry analysis (E) confirming that Histone H2B is enriched in high Pi-derived sedimentable particles at 48h. (n=3) \*P<0.05. (F and G) Immunoblot (representative of 3 independent experiments) and densitometry analysis of the effect on total cell layer Histone H2B expression of incubating the cells for 48h in medium with 2.5mM Pi; (n=3) \*P<0.05.

## **5.3 Discussion**

### **5.3.1 Elevated Pi has no significant effect on ROS and cell apoptosis in EAhy926 cells**

In contrast to earlier reports indicating that elevated Pi concentration induces ROS generation and apoptosis in endothelial cells (Di Marco *et al.*, 2008; Shuto *et al.*, 2009) the work presented in this chapter indicated a negligible effect of higher extracellular Pi on ROS generation (Figure 5.1 A-E) and apoptosis (Figure 5.2). In addition using an inhibitor of Rho/ROCK pathway (i.e. Y-27632) (Figure 5.5) failed to abolish the Pi-induced increment in MP release, suggesting that the effect of Pi on MP output (Chapter 3) cannot convincingly be attributed to membrane blebbing secondary to classical apoptosis (Section 1.16.5.3).

### **5.3.2 High Pi modulates protein phosphorylation**

In Chapter 3 it was shown that elevated Pi concentration gave rise to an enhanced MP output from endothelial cells. A possible mechanism for this MP formation is cell apoptosis (Section 1.16.5.3) however the work presented in this chapter indicated that in EAhy926 cells apoptosis cannot explain the observed MP release (Section 5.2.2). If ROS generation and apoptosis is not involved in the observed MP release from EAhy926 cells, this suggests a distinct form of cellular stress inducible by elevation in Pi concentration. It was shown that Pi directly inhibits phosphotyrosine protein phosphatase catalytic activity in EAhy cell lysates (Figure 5.6 A-B) and also two well known broad-spectrum inhibitors of phosphotyrosine protein phosphatases (Vanadate) (Figure 5.6 C) and phosphoserine/threonine protein phosphatases (Fluoride) (Figure 5.6 D) respectively mimic the acute and chronic effect of high Pi on particle output. This led to the important question of whether this inhibition of phosphoprotein phosphatases results in accumulation of phosphoprotein within the cells. Western blotting with pan-specific phosphotyrosine (Figure 5.8 A-B) and phosphoserine/threonine (Figure 5.8 C-D) antibodies demonstrated that added Pi from 90min onwards results in accumulation of some phosphoproteins in EAhy926 endothelial cells. This effect of Pi on incremental accumulation of phosphoprotein was reversed by selective siRNA silencing of *slc20a1* (PiT-1)

transporters (Figure 5.8 E-H) indicating that this effect of elevated Pi concentration depended on Pi influx into the cells.

Phospho-serine/threonine protein phosphatases (PSPases) are also known to be inhibited directly by Pi. However, even though catalytic activity of PSPases 2A, 2B and 2C was readily detectable in positive control cell lysates (from HeLa cells), no similar basal catalytic activity was detected in EAhy cell lysates (Figure 5.7). For that reason a direct inhibitory effect of Pi on PSPase activity in EAhy lysates was not demonstrable, and the major Pi-inhibitable PSPases that Figure 5.8 C suggests are present in these cells remain to be identified.

The data presented in this chapter suggest that Pi effects on protein phosphatases and global changes in protein phosphorylation play a role in Pi-induced MP production in endothelial cells, but the individual proteins involved were not identified. In the next chapter a proteomic analysis was performed to try to identify candidate protein(s).

It was shown that fructose reverses the effect of high (2.5mM) Pi on (i) the acute (90min) increase in intracellular Pi (Figure 4.4 D), and (ii) the acute (90min) NTA-detected particle release from the medium (Figure 3.7 A), However, there was no corresponding effect on chronic (24h) protein particle release into the medium (Figure 5.11 E). To investigate why this was happening, parallel studies were performed on the effect of extracellular Pi on net global protein phosphorylation. It was shown that added Pi increases protein phosphorylation on both tyrosine (Figure 5.8 A-B) and serine/threonine (Figure 5.8 C-D) in EAhy926 cells. Further investigation looking at the effect of Pi loaded medium with/without addition of fructose demonstrated that fructose acutely reverses the effect of high (2.5mM) Pi on both protein tyrosine (Figure 5.10 C and D) and serine/threonine phosphorylation (Figure 5.10 A and B). However, chronic (24h) loading of the medium with fructose in the presence or absence of addition of Pi to the medium was shown to be associated with a paradoxical enhanced protein tyrosine (Figure 5.11 C and D) and serine/threonine (Figure 5.11 A and B) phosphorylation. (This effect was

accompanied by enhanced chronic release of sedimentable protein particles from the medium (Figure 5.11 E)). These observations may be partly explained by the fact that fructose loading the medium acutely depletes intracellular Pi (Figure 4.4 D) and therefore blunts the effect of high (2.5mM) Pi on MP release from the medium (Figure 3.7 A). However, at later times (24h), a significant accumulation of fructose-1-phosphate (F-1-P) may occur in the cells. This might result in direct inhibition of phospho-protein tyrosine and serine/threonine phosphatases by F-1-P itself (similar to the effect observed with high Pi) hence enhancing the net global protein phosphorylation which works as a signal resulting in an enhanced sedimentable protein particle release into the medium.

### **5.3.3 High [Pi] alters in Tropomyosin expression and Histone distribution**

The initial proteomic analysis in this chapter of the effect of an elevated Pi concentration on some of the proteins which occur at the highest concentration in cultured endothelial cells, and in the particles derived from them, detected at least two significant proteins whose concentration seemed to respond to Pi.

Firstly incubation of EAhy926 cells and HUVECs in medium with 2.5mM Pi led to rapid accumulation of a Ser-Thr-phosphorylated protein of about 30kDa within 90min, which was identified as Tropomyosin. The possible functional importance of this cytoskeletal regulator protein (and its phosphorylation) in the effect of Pi on MP output from these cells is discussed in detail in the General Discussion chapter (Section 6.1.4).

Secondly prolonged incubation of EAhy926 cells with 2.5mM Pi was found to lead to release of an 18,000g MP fraction that was enriched in Histone H2B (and possibly also other histones (Appendix C-5.10)). The mechanism of release of these nuclear proteins from the cells is unknown. Extracellular nucleosomes are detectable in circulation in humans and their numbers increase in several diseases (Holdenrieder & Stieber, 2009). However, a much higher g force than 18,000g is normally needed to sediment free nucleosomes (Näslund & von der Decken, 1981), so it is unlikely that the histones occurred in this form in the MP fraction described here. The presence of nucleosomes

within larger cell fragments released into the culture medium might have contributed to the Histone enrichment observed in Figure 5.14 D, nevertheless the presence of these extracellular histones is of interest because these proteins have been reported to be pro-coagulant (Ammollo *et al.*, 2011) and this was one of the reasons why the Pi-derived MPs from EAhy cells were studied in a Thrombin generation assay in the next chapter.

## Chapter 6. General Discussion and Future work

---

### 6.1 General Discussion

#### 6.1.1 Rapid Pi-stimulation of MP output implies a direct "Pi signal" within endothelial cells

There has been only one previous report that elevated extracellular Pi can induce MP production from cultured endothelial cells (Di Marco *et al.*, 2012). This study has now made the important observation that *intracellular* Pi is the crucial signal generating potential pathological events in ECs during hyperphosphataemia. Using a selective and well characterised assay for intracellular Pi (Challa *et al.*, 1985) it was shown that, unlike other cell types (Kemp *et al.*, 1993<sub>b</sub>; Bevington *et al.*, 1986), human vascular endothelial cells experience an acute increase in intracellular Pi concentration when extracellular Pi is elevated as in hyperphosphataemia.

The concept of a powerful effect of intracellular Pi signalling on cytoskeletal and MP biology is strongly supported by the demonstration that the intracellular Pi can be depleted by silencing of SLC20 Pi transporters (Figure 4.7), by collapse of the trans-membrane Na<sup>+</sup>-gradient with ouabain (Figure 4.4 B), by Pi transport inhibitor PFA (Figure 4.4 C) and by phosphate-trapping with fructose (Figure 4.4 D); Pi depletion effects which blunt the subsequent release of MPs in response to elevated extracellular Pi (Figure 3.9 A and B).

It is also worth noting that there is wide expression of SLC20 Pi transporters in cells other than endothelial cells (which have been the subject of this thesis), for example in vascular smooth muscle cells (SMCs) underlying the endothelial cells (Figure 4.3 A). It has been shown that the VSMCs under hyperphosphataemic conditions undergo phenotypic changes from SMC to osteogenic phenotypes (Giachelli *et al.*, 2001; Giachelli, 2003). This osteochondrogenic differentiation of VSMC in hyperphosphataemic milieu has been shown to be partly PiT-dependent, as PiT-depletion ameliorates these transformational changes in SMC *in vitro* (Lau *et al.*, 2011; Crouthamel *et al.*, 2013). However, it has been reported that these phosphate transporter proteins

may exert biological effects by mechanisms other than Pi transport. For instance depletion of PiT-1 in HeLa cells and HepG2 cells has been shown to decrease cell proliferation, delay the cell cycle and impair mitosis and cytokinesis, independent of its transport activity (Beck *et al.*, 2009). A similar transport-independent involvement of PiT-1 has also been reported in TNF-induced apoptosis in HeLa cells (Salaun *et al.*, 2010).

### **6.1.2 Pi induced particle release is independent of apoptosis**

Treatment of EAhy926 cells with either caspase inhibitor (Figure 5.4) or Rho/ROCK pathway inhibitor (Figure 5.5) failed to give a convincing reversal of the effect of high (2.5mM) Pi on particle output. This implies that the observed effect of Pi on MP output is derived from a distinct mechanism rather than fully developed apoptosis in whole cells (i.e. not through ROCK activation and ROCK-mediated myosin-light chain phosphorylation and particle formation (Sebbagh *et al.*, 2001) but from for example impaired Tropomyosin phosphorylation and loss of stress fibre formation and therefore MP formation as proposed in Sections 6.1.3 and 6.1.4 below). Even though this study showed some effect of higher Pi on apoptosis signals in EAhy cells such as Caspase-3 activation and its substrate PARP's cleavage, Bax abundance and DNA fragmentation, this did not necessarily induce fully developed apoptosis and cell death. Possible explanations for this are that firstly caspase-3 activation is not always associated with apoptosis and cell death (Abraham & Shaham, 2004; Portela & Richardson, 2013) and it has also been suggested that hyperphosphataemia induces protective autophagy in ECs which prevents the occurrence of apoptosis even though caspase-3 and PARP cleavage occur (Hsu *et al.*, 2014). In the present study assessment of autophagy by immunoblot assay of the conversion of the microtubule-associated protein light chain 3 (LC-3-I) to the autophagosome marker LC-3-II also suggested that hyperphosphataemia may induce some autophagy in EAhy926 endothelial cells (Appendix C-Figure 5.5). However caution is needed in using this method because LC-3-II itself is degraded by autophagy (Mizushima & Yoshimori, 2007).

Another indication that high Pi does not induce apoptosis (as detected with Annexin-V-FITC/Pi dual labelling (Figure 5.2 G-I)) is that regardless of possible false positive or negative interpretations with this labelling, the alternative technique of forward angle scattering of the light, which reflects the size of the cells, failed to detect any effect of elevated Pi concentration (Figure 5.2 K and Figure 5.2 S-V). From this it can be concluded that higher Pi does not result in the cell shrinkage which is a hallmark of apoptosis.

### **6.1.3 Pi induces a distinct and sustained form of cell stress through global changes in protein phosphorylation**

No significant Pi-induced oxidative stress or apoptosis was detected in this study but, in spite of this, a rapid Pi-induced increase in MP output was observed. The MP formation reported here is associated with a distinct and novel form of metabolic stress characterised by global changes in protein phosphorylation. The intracellular Pi “signal” is sensed in EAhy926 cells through the potent direct inhibition of phosphotyrosine protein phosphatases (Figure 5.6 A and B) and phosphoserine/threonine phosphatases by Pi ions that occurs in response to pathological intracellular Pi concentrations (Buzalaf *et al.*, 1998; Szajerka & Kwiatkowska, 1984; Zhang & VanEtten, 1991); culminating in global accumulation of Tyr-phosphorylated and Ser-Thr phosphorylated proteins that is readily demonstrated using pan-specific P-Tyr and P-Ser/Thr antibodies (Figure 5.8 A-D). This effect is reversed by siRNA silencing of Pi transporter PiT-1/slc20a1 (Figure 5.8 E-H) confirming that Pi translocation into cells is needed for the effect. Similar global inhibition of phosphotyrosine protein phosphatases by the Pi analogue orthovanadate; and of phospho-serine/threonine phosphatases by fluoride (Figure 5.6 C and D) closely mimicked the generation of MPs observed with Pi (Figure 3.2, 3.3 and 3.9).

The predicted increases in protein phosphorylation on exposure to Pi were observed for some but not all of the major protein bands that stained with pan-specific anti-phospho antibodies (Figure 5.8 A-H), resulting in total cellular increases in protein phosphorylation of the order of 30 – 50%. There are several reasons for the failure of Pi to affect all phosphoproteins. Firstly global inhibition

of phosphatases by Pi may result in hyperphosphorylation of some protein kinases at inhibitory phosphorylation sites, thus leading to *hypo*-phosphorylation of that kinase's substrates. (The hypophosphorylation of TM3 in Figure 5.12 I and J is presumably an example of this, possibly through the previously reported inhibitory Ser-308 phosphorylation of death-associated protein kinase-1 (DAPK) (Jin *et al.*, 2006) inhibiting the reported ability of DAPK to phosphorylate Tropomyosin on Ser-283 (Houle *et al.*, 2007) (shown schematically in Figure 6.1)). Secondly, even though most phosphoprotein phosphatases whose Pi-sensitivity has been reported are inhibited by Pi, at least one such enzyme is activated by Pi (Khandelwal & Kamani, 1980) and such Pi-activated enzymes may be detectable in lysates of EAhy926 cells as shown in Figure 5.7. Thirdly compensatory up-regulation of phosphoprotein phosphatase expression may occur in response to prolonged inhibition with Pi or orthovanadate (Figure 5.8 I and J). Finally, even though exposure of cells to 2.5mM Pi was shown to increase total Pi in the cell layer (probably initially in the cytosol), the Pi concentration may not increase immediately in all sub-cellular compartments, resulting in negligible protein phosphorylation changes in any unaffected compartments.

## In the cytoplasm

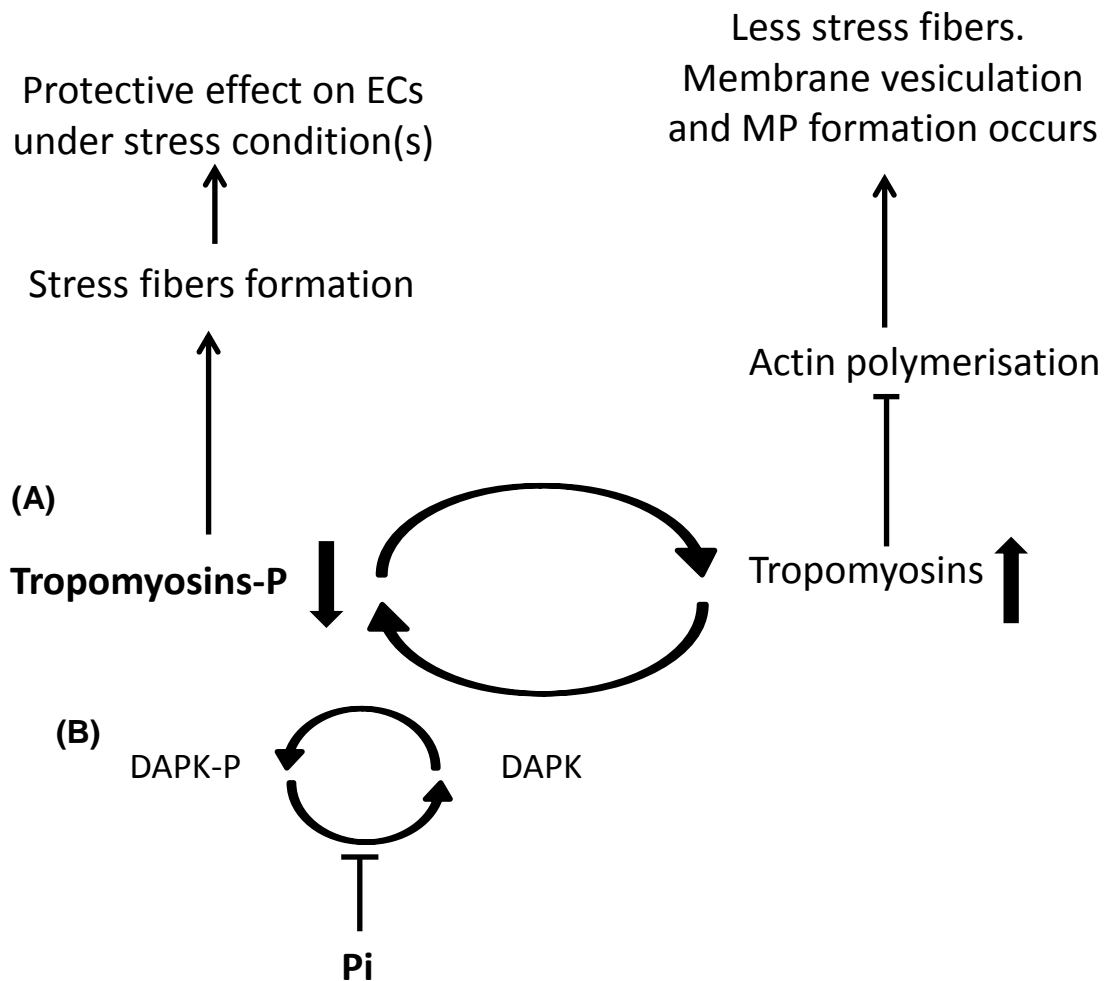


Figure 6.1. Schematic view showing a proposed mechanism of Pi signalling to cytoskeletal protein Tropomyosin-3 (TM-3) and MP formation, based on data from the following references: (A) (Houle *et al.*, 2007) (B) (Jin *et al.*, 2006).

### **6.1.4 Phosphate stress is associated with rapid changes in the cytoskeletal regulator Tropomyosin**

A proteomic screen of EAhy926 cells demonstrated that, following initial Pi-induced phosphorylation events that were seen in these cells (Figure 5.8 A-H), a reproducible and rapid (90min onwards) accumulation of Tropomyosin (TM3) was readily visible on 2D gels, and was confirmed by immunoblotting cell lysates with a specific anti-TM3 antibody (Figure 5.12 D-H). In spite of the approximately 4-fold increase in total concentration of TM3, probing of 2D gels with anti-phospho-Ser/Thr antibody indicated that, in Pi-treated cells, this

protein was *hypo*-phosphorylated (Figure 5.12 I and J). It has been reported that, at least in ECs subjected to oxidative stress, hypophosphorylation of Tropomyosin leads to membrane blebbing and hence MP formation (Houle *et al.*, 2007), suggesting that the rapid changes affecting TM3 in the present study are functionally important in the MP response to Pi (Figure 6.1).

The mechanism of the rapid (possibly compensatory) 90min increase in total TM3 (Figure 5.12 D and E) is at present unknown, but is apparently too rapid for *de novo* synthesis of the protein. However the Pi analogue orthovanadate which closely mimicked the acute MP effect of Pi in this study (Figure 5.6 C) is an inhibitor of proteasomal protein degradation (Hoffman & Rechsteiner, 1996), a mechanism that may contribute not only to the increase in TM but also to the reproducible accumulation of previously absorbed albumin that was observed in the same Pi-loaded EAhy cells (Figure 5.12 A).

#### **6.1.5 Clinical implications of these effects of Pi**

Evidence has been presented here linking three important areas of research relevant to cardiovascular risk in CKD: hyperphosphataemia, MPs and thrombotic risk. It should be emphasised that the MPs mediate this link (rather than the elevated Pi concentration itself through being carried over into the thrombin generation assay). This was clearly demonstrated by the observation that the pro-coagulant effect of the cell-derived particles in Figure 3.13 A-D was abolished by removal of MPs by ultra-filtration. The occurrence of phosphatidylserine on the surface of MPs is regarded as an important contributor to their pro-coagulant effect (Sinauridze *et al.*, 2007). However, the new observation here that Pi-derived endothelial MPs are significantly enriched in histone (which can both promote activation of the contact pathway (Ammollo *et al.*, 2011) and inhibit fibrinolysis (Longstaff *et al.*, 2013)) suggests a further important and previously unsuspected mechanism whereby hyperphosphataemia may lead to a pro-thrombotic state. Whether additional biochemical features of specifically Pi-derived endothelial MPs also promote coagulation remains to be determined.

In principle, biomarkers are species (including particular proteins or peptides, cells, particles, metabolites, hormones, lipids, miRNA etc.) which can be isolated in the laboratory from serum, urine and/or other body fluids, and can be used as an indicator of the existence or the severity of a disease state or to assess the effectiveness of a particular therapy (Wang *et al.*, 2015; Zhao *et al.*, 2014). In terms of biomarker-discovery, Pi-derived MPs can be regarded as potentially strong biomarkers of early changes leading to cardiovascular disease in CKD patients. In CKD patients abnormalities in serum Pi metabolism, FGF-23, and some uraemic toxins like ADMA, advanced glycation end products (AGE), p-cresol and indoxyl sulphate have been regarded as useful biomarkers to define disease stage and monitor the effectiveness of therapies (Molony & Stephens, 2011; Isoyama *et al.*, 2015; Liabeuf *et al.*, 2014). As the renal function declines and Pi retention starts occurring, compensatory mechanisms are in place to adjust serum Pi level back within the physiological normal range after the post-prandial increase that follows a Pi-rich meal. These include an increase in phosphaturic hormone secretion (for example FGF-23) which in turn increases Pi wasting through the urine by decreasing the activity of renal Pi transporters performing Pi reabsorption (see section 1.6.3.3). Therefore within a few hours the serum phosphate level is regulated and cannot be solely used as an indication of the presence or severity of CKD, except in more advanced CKD stages where kidney damage results in overt hyperphosphataemia. This implies the need for identifying Pi-related biomarkers that might be used at an earlier stage in the progression of CKD.

Unlike some other biomarkers in CDK, Pi-induced increase in the plasma level of microparticles can start occurring acutely within minutes (i.e. as early as 90min) and may persist for some time after plasma Pi concentration has declined. This provides the possibility that such particles may have value as markers beyond what can currently be achieved by measurements of plasma Pi alone.

### **6.1.6 Hyperphosphataemic states, independent of kidney disease, are also associated with thrombotic and/or embolic events**

Tumour lysis syndrome during cancer chemotherapy provides another possible example of thrombosis associated with hyperphosphatemia. While a number of forms of cancer are associated with increased risk of thrombosis (Bick, 2003) in which MPs expressing tissue factor play a role, this effect is significantly increased during the marked hyperphosphatemia that arises as part of the so-called tumour lysis syndrome during chemotherapy (Date *et al.*, 2013). At least in its early stages this hyperphosphataemia is independent of renal impairment, occurs without accompanying azotaemia, and can arise directly from phosphate release from the dying tumor cells (Cohen *et al.*, 1980).

### **6.1.7 Broader implications of these findings**

Finally it should be emphasised that, in view of the ubiquitous role of protein phosphorylation in regulating mammalian cells and its dependence on phosphoprotein phosphatases which are almost universally responsive to Pi (Figure 5.6 A and B and Figure 5.8 and (Zhang & VanEtten, 1991; Szajerka & Kwiatkowska, 1984; Buzalaf *et al.*, 1998)) the intracellular effects reported here should be widely applicable in understanding the pathological effects of hyperphosphataemia or indeed of any factor which stimulates Pi uptake into cells. This should be true not only in hyperphosphataemia in CKD, but also in other disorders such as hypoxia and ischaemia which are associated with an elevated intracellular Pi concentration arising from impaired energy metabolism with resulting large-scale Pi generation from cytosolic organophosphorus metabolites such as ATP and phosphocreatine (Rath *et al.*, 1995). Clearly such effects would be expected to be particularly severe during cardiovascular events in CKD in which hyperphosphataemia and ischaemia/hypoxia co-exist.

## **6.2 Summary of the Present Position and Future Work**

The precise mechanism underlying the molecular basis for generation of acutely pro-coagulant endothelial microparticles (e.g. from vascular endothelial cells and blood platelets) in uraemic cardiovascular disease is still elusive. Previous data from this laboratory have demonstrated that circulating MPs in patients

with advanced CKD exert a potent pro-coagulant effect (Burton *et al.*, 2013) (thereby contributing to cardiovascular risk). The present study has shown that hyperphosphataemia (elevated plasma inorganic phosphate (Pi)) which is an almost universal finding in advanced CKD, is a potent signal triggering pro-coagulant MP generation in cultured human VECs (Figure 3.13). It was also shown that hyperphosphataemia elevates intracellular Pi concentration in cultured VECs (Figure 4.4), resulting in an apparent direct global inhibition by Pi ions of both Tyr phosphoprotein phosphatases (Figure 5.8 A-B) and Ser/Thr phosphoprotein phosphatases (Figure 5.8 C-D).

For future work, the hypothesis is that the resulting accumulation of phosphorylated proteins includes an inhibitory phosphorylation at Ser-308 (Jin *et al.*, 2006) on death-associated protein kinase-1 (DAPK) which normally phosphorylates the cytoskeletal regulatory protein Tropomyosin on Ser-283 (Houle *et al.*, 2007). The resulting hypo-phosphorylation of Tropomyosin (in spite of an apparent compensatory increase in total Tropomyosin) leads to impairment of protective stress fibre formation in the face of Pi-induced metabolic stress. These changes in the cytoskeleton result in increased cell surface membrane blebbing and acute release of a strongly pro-coagulant isoform of EMPs which contributes to elevated cardiovascular risk in CKD. A proteomic screen of EAhy926 cells has already demonstrated that, following the initial Pi-induced phosphorylation events that have been demonstrated in these cells (Figure 5.8 A-H), a reproducible acute (90min onwards) accumulation of Tropomyosin is readily visible on 2D gels, which has been confirmed by immunoblotting cell lysates with a specific anti-Tropomyosin antibody (Figure 5.12 D-H). In spite of the increased total concentration of Tropomyosin, probing of the 2D gels with anti-P-Ser/Thr antibody indicated that, in Pi-treated cells, this protein is markedly *hypo*-phosphorylated (Figure 5.12 I and J) strongly suggesting that the stress-fibre-mediated protective mechanism that has been described in oxidative stress in VECs (Houle *et al.*, 2007) is inactivated by intracellular Pi accumulation during Pi-stress of VECs, and that this is the probable mechanism of the observed Pi-induced MP formation.

In future this can be tested in two ways:

- 1- By incubating human VECs with an elevated concentration of Pi *in vitro* to mimic hyperphosphataemia, measuring the resulting rise in intracellular Pi, and determining the protein phosphorylation signals downstream from Pi to Tropomyosin which result in cytoskeletal changes and MP generation.
- 2- By varying plasma [Pi] (by dietary Pi manipulation) *in vivo* in the rat remnant kidney model of CKD to determine the resulting effects on endothelial protein phosphorylation signals to Tropomyosin, circulating MPs, and thrombin generation, to confirm that the Pi-induced generation of pro-coagulant MPs is also functionally significant *in vivo*.

By studying the profile of circulating microparticles in relation to hyperphosphataemia, the suggested future work above offers a realistic prospect of developing powerful biomarkers that could be used to identify CKD patients at greatest risk. In addition, through studying the effect of manipulating plasma phosphate on microparticle formation and thrombotic risk, this suggested future work may identify a key step in the development of uraemic cardiovascular disease at which therapy aimed at reducing plasma phosphate may be particularly effective.

## Appendix

### Appendix A (Culture & Test Medium composition)

#### A-1 DMEM (Invitrogen 11880-028/500ml) components

COMPONENTS	Molecular Weight	Concentration (mg/L)	mM
<b>Amino Acids</b>			
Glycine	75	30	0.4
L-Arginine hydrochloride	211	84	0.398
L-Cystine 2HCl	313	63	0.201
L-Histidine hydrochloride-H <sub>2</sub> O	210	42	0.2
L-Isoleucine	131	105	0.802
L-Leucine	131	105	0.802
L-Lysine hydrochloride	183	146	0.798
L-Methionine	149	30	0.201
L-Phenylalanine	165	66	0.4
L-Serine	105	42	0.4
L-Threonine	119	95	0.798
L-Tryptophan	204	16	0.0784
L-Tyrosine	181	72	0.398
L-Valine	117	94	0.803
<b>Vitamins</b>			
Choline chloride	140	4	0.0286
D-Calcium pantothenate	477	4	0.00839
Folic Acid	441	4	0.00907
Niacinamide	122	4	0.0328
Pyridoxine hydrochloride	204	4	0.0196
Riboflavin	376	0.4	0.00106
Thiamine hydrochloride	337	4	0.0119
i-Inositol	180	7.2	0.04
<b>Inorganic Salts</b>			
Calcium Chloride (CaCl <sub>2</sub> ·2H <sub>2</sub> O)	147	264	1.8
Ferric Nitrate (Fe(NO <sub>3</sub> ) <sub>3</sub> ·9H <sub>2</sub> O)	404	0.1	0.000248
Magnesium Sulfate (MgSO <sub>4</sub> ·7H <sub>2</sub> O)	246	200	0.813
Potassium Chloride (KCl)	75	400	5.33
Sodium Bicarbonate (NaHCO <sub>3</sub> )	84	3700	44.05
Sodium Chloride (NaCl)	58	6400	110.34
Sodium Phosphate monobasic (NaH <sub>2</sub> PO <sub>4</sub> ·2H <sub>2</sub> O)	154	141	0.916
<b>Other Components</b>			
D-Glucose (Dextrose)	180	1000	5.56
Sodium Pyruvate	110	110	1

URL: [http://www.invitrogen.com/site/us/en/home/support/Product-Technical-Resources/media\\_formulation.183.html](http://www.invitrogen.com/site/us/en/home/support/Product-Technical-Resources/media_formulation.183.html)  
Last access date 02/08/2011.

## A-2 MEM (Invitrogen 21090-022/500ml) components

COMPONENTS	Molecular Weight	Concentration (mg/L)	mM
<b>Amino Acids</b>			
L-Arginine hydrochloride	211	126	0.597
L-Cystine	240	24	0.1
L-Histidine hydrochloride-H <sub>2</sub> O	210	42	0.2
L-Isoleucine	131	52	0.397
L-Leucine	131	52	0.397
L-Lysine hydrochloride	183	73	0.399
L-Methionine	149	15	0.101
L-Phenylalanine	165	32	0.194
L-Threonine	119	48	0.403
L-Tryptophan	204	10	0.049
L-Tyrosine	181	36	0.199
L-Valine	117	46	0.393
<b>Vitamins</b>			
Choline chloride	140	1	0.00714
D-Calcium pantothenate	477	1	0.0021
Folic Acid	441	1	0.00227
Niacinamide	122	1	0.0082
Pyridoxal hydrochloride	204	1	0.0049
Riboflavin	376	0.1	0.000266
Thiamine hydrochloride	337	1	0.00297
i-Inositol	180	2	0.0111
<b>Inorganic Salts</b>			
Calcium Chloride (CaCl <sub>2</sub> ·2H <sub>2</sub> O)	147	264	1.8
Magnesium Sulfate (MgSO <sub>4</sub> ·7H <sub>2</sub> O)	246	200	0.813
Potassium Chloride (KCl)	75	400	5.33
Sodium Bicarbonate (NaHCO <sub>3</sub> )	84	2200	26.19
Sodium Chloride (NaCl)	58	6800	117.24
Sodium Phosphate monobasic (NaH <sub>2</sub> PO <sub>4</sub> ·2H <sub>2</sub> O)	156	158	1.01
<b>Other Components</b>			
D-Glucose (Dextrose)	180	1000	5.56
Phenol Red	376.4	10	0.0266

URL: [http://www.invitrogen.com/site/us/en/home/support/Product-Technical-Resources/media\\_formulation.197.html](http://www.invitrogen.com/site/us/en/home/support/Product-Technical-Resources/media_formulation.197.html)  
 Last access date 02/08/2011.

### A-3 HBSS (Invitrogen 24020-133/500ml) components

COMPONENTS	Molecular Weight	Concentration (mg/L)	mM
<b>Inorganic Salts</b>			
Calcium Chloride (CaCl <sub>2</sub> ) (anhyd.)	111	140	1.26
Magnesium Chloride (MgCl <sub>2</sub> ·6H <sub>2</sub> O)	203	100	0.493
Magnesium Sulfate (MgSO <sub>4</sub> ·7H <sub>2</sub> O)	246	100	0.407
Potassium Chloride (KCl)	75	400	5.33
Potassium Phosphate monobasic (KH <sub>2</sub> PO <sub>4</sub> )	136	60	0.441
Sodium Bicarbonate (NaHCO <sub>3</sub> )	84	350	4.17
Sodium Chloride (NaCl)	58	8000	137.93
Sodium Phosphate dibasic (Na <sub>2</sub> HPO <sub>4</sub> ) anhydrous	142	48	0.338
<b>Other Components</b>			
D-Glucose (Dextrose)	180	1000	5.56
Phenol Red	376.4	10	0.0266

URL: [http://www.invitrogen.com/site/us/en/home/support/Product-Technical-Resources/media\\_formulation.152.html](http://www.invitrogen.com/site/us/en/home/support/Product-Technical-Resources/media_formulation.152.html)  
 Last access date 02/08/2011.

### A-4 <sup>45</sup>Ca Radio isotope data sheet (Physical half-life 163 days)

	Days									
	0	5	10	15	20	25	30	35	40	45
0	1.000	0.979	0.958	0.938	0.918	0.899	0.880	0.862	0.844	0.826
50	0.808	0.791	0.775	0.759	0.743	0.727	0.712	0.697	0.682	0.668
100	0.654	0.640	0.626	0.613	0.600	0.588	0.575	0.563	0.551	0.540
150	0.528	0.517	0.506	0.496	0.485	0.475	0.465	0.455	0.446	0.436
200	0.427	0.418	0.409	0.401	0.392	0.384	0.376	0.368	0.360	0.353
250	0.345	0.338	0.331	0.324	0.317	0.311	0.304	0.298	0.291	0.285
300	0.279	0.273	0.268	0.262	0.257	0.251	0.246	0.241	0.236	0.231
350	0.226	0.221	0.216	0.212	0.207	0.203	0.199	0.195	0.191	0.186

URL: <http://www.perkinelmer.com/Catalog/Product/ID/NEZ013001MC> Last access date 22/12/2012

## **Appendix B (Reagents & Buffers)**

### **B-1 Acidified Molybdate**

To 2.098 g of Ammonium Molybdate Tetrahydrate (BDH AR 10028) add 50 ml of Nanopure water and swirl to dissolve. In the meantime, add 4.18 ml of concentrated Sulphuric Acid (BDH AR 10276 SG 1.84) to the mixture on ice (Through this step heat may be produced). In the final step, add 8.33 ml of water to the mixture and mix thoroughly. Store the solution at Room temperature.

### **B-2 0.5M NaOH**

Weigh out 2 g of Sodium hydroxide pellets (Sigma S-8045 FW: 40.00) in a 100 ml pot. Add 50ml Nanopure water to that to dissolve the pellets and then increase the volume to 100 ml in a 100 ml volumetric flask. Store the solution at room temperature.

### **B-3 Lowry (Folin) Reagent A**

Weigh out 20.00 g, 4.00 g, and 0.2 g of Sodium Carbonate “Anhydrous” (Sigma S-2127 FW 106.0), Sodium hydroxide (Sigma S-8045 FW: 40.00), and Potassium Sodium (+)-tartrate (BDH AR 10219 FW: 282.22) respectively in a 1 Litre Duran bottle. Add 500 ml Nanopure water to that to dissolve the pellets and then increase the volume to a litre in a 1000 ml volumetric flask. Store the solution at 4°C.

### **B-4 Lowry (Folin) Reagent B**

Weigh out 5 g of Cupric Sulphate (BDH AR 10091 FW: 249.68) in a 1000 ml Duran bottle. Add 500 ml Nanopure water to that to dissolve it and then increase the volume to 1000 ml in a Litre volumetric flask. Store the solution at 4°C.

## B-5 Folin Standards Preparation

Final (BSA) ( $\mu\text{g/ml}$ )	0	50	100	150	200	300	400	500
Volume of stock S. <sup>1</sup> ( $\mu\text{l}$ )	0	50	100	150	200	300	400	500
Volume of 0.5M NaOH (ml)	2.5	2.45	2.4	2.35	2.3	2.2	2.1	2.0

<sup>1</sup>Stock S: Weigh out 0.05 g of Bovine Serum Albumin (BSA: Sigma A-7638) in a 100 ml pot and add to this 20 ml of 0.5M NaOH and mix completely to dissolve.

## B-6 Reducing Lysis Buffer

Stock Solutions	For 5ml	Final Concentration
1M pH 7.4 beta glycerophosphate	50 $\mu\text{l}$	10mM
0.5M pH 8 EDTA	10 $\mu\text{l}$	1mM
40mM EGTA	125 $\mu\text{l}$	1mM
1M pH 7.5 Tris-HCl	250 $\mu\text{l}$	50mM
10mM Na Orthovanadate	500 $\mu\text{l}$	1mM
1M Benzamidine	5 $\mu\text{l}$	1mM
100mM PMSF	10 $\mu\text{l}$	0.2mM
5mg/ml Pepstatin A	5 $\mu\text{l}$	
5mg/ml Leupeptin	5 $\mu\text{l}$	
Beta-Mercaptoethanol	5 $\mu\text{l}$	0.1%
10% Triton X-100	500 $\mu\text{l}$	1%
500mM Na Fluoride	500 $\mu\text{l}$	50mM
Nano-Pure Water	3035 $\mu\text{l}$	

## B-7 Resolving & Stacking Gel (Western Blotting & SDS-PAGE)

Component	Resolving Gel 8%	Resolving Gel 12%	Stacking Gel 4%
Water (Nano-pure)	4.6ml	3.35ml	3.03ml
Acrylamide <sup>1</sup> (30 x/v)	2.7ml	4.00ml	0.65ml
1.5M Tris HCL, pH 8.8	2.5ml	2.5ml	-
0.5M Tris HCL, pH 6.8	-	-	1.25ml
SDS (10% w/v)	0.1ml	0.1ml	0.05ml
10% APS <sup>2</sup>	0.1ml	0.05ml	0.025ml
TEMED <sup>3</sup>	0.006ml	0.005ml	0.005ml

Table 2.4 Components to prepare one SDS-PAGE Gel.

<sup>1</sup> Acrylamide: Sigma A3699-100ml

<sup>2</sup> APS: Ammonium persulphate.

<sup>3</sup> N,N,N',N'- Tetramethylene diamine (Sigma T9281-25ml).

## B-8 Running Buffer for Western Blotting & SDS-PAGE (10x)

Component	For 1 Litre
Trizma Base	30.3g
Glycine	144g
Water	800ml
Swirl to mix	
SDS	10g
Water (Nano-pure)	200ml

**\*For (1x) Running Buffer as required in Western Blotting**

Components	For 1 Litre
10x Running Buffer	100ml
Water (Nano-pure)	900ml

### **B-9 Sample Buffer (Reducing Sample Buffer for Western Blotting)**

<b>Component</b>	<b>For 8ml</b>
Water (Nano-pure)	4ml
0.5m TRIS HCL pH6.8	1ml
Glycerol	0.8ml
10% (w/v) SDS	1.6ml
2-β-mercaptoethanol	0.4ml
0.05% (w/v) Bromophenol blue	0.2ml of 2% stock

### **B-10 De-Staining Buffer (following Coomassie Blue SDS-PAGE Gel Staining)**

Mix the following to make up 1000 ml;

- |                              |                              |
|------------------------------|------------------------------|
| A. Reagent grade Methanol    | 400ml 40% v/v (BDH AR 20807) |
| B. Reagent grade Acetic acid | 100ml 10% v/v (Sigma 695092) |
| C. Nanopure Water            | 500ml 50% v/v                |

### **B-11 Equilibration Buffer (Silver and Coomassie Blue; SDS-PAGE Gel Staining Approaches)**

Mix the following to make up 1000 ml;

- |                              |                              |
|------------------------------|------------------------------|
| D. Reagent grade Methanol    | 400ml 40% v/v (BDH AR 20807) |
| E. Reagent grade Acetic acid | 100ml 10% v/v (Sigma 695092) |
| F. Glycerol                  | 30ml 3% v/v (BDH AR 101184K) |
| G. Nanopure Water            | 470ml 47% v/v                |

### **B-12 Fixative (Silver; SDS-PAGE Gel Staining Approaches)**

According to Silver Stain Plus protocol (Bio-Rad 161-0449), briefly;

Mix the following to make up 400ml 100% v/v Fixative solution for 2 gels (8x10cm & 0.75-1.0mm thick);

- |                                  |                               |
|----------------------------------|-------------------------------|
| A. Reagent grade Methanol        | 200ml 50% v/v (BDH AR 20807)  |
| B. Reagent grade Acetic acid     | 40ml 10% v/v (Sigma 695092)   |
| C. Fixative Enhancer Concentrate | 40ml 10% v/v (Bio-Rad 72587A) |
| D. Nanopure Water                | 120ml 30% v/v                 |

### **B-13 Staining & Developing (Silver; SDS-PAGE Gel Staining)**

According to Silver Stain Plus protocol (Bio-Rad 161-0449), briefly;

Make up 5 min before use.

To 35 ml deionised distilled water add the following and label "D":

- A. 5 ml of the Silver Complex Solution. (Bio-Rad 73818A)
- B. 5 ml of the Reduction Moderator Solution. (Bio-Rad 72181A)
- C. 5 ml of the Image Development Reagent. (Bio-Rad 12333)

**Caution:** Just before use add **50 ml** of the room temperature Development Accelerator Reagent (Bio-Rad 162809C), which has been pre-prepared by adding 500 ml of nanopure water to 25 g of Development Accelerator Reagent and kept at 4<sup>0</sup>C, to the prepared solution above (D) and swirl to mix.

### **B-14 Stock (2mg/ml) solution of MTT**

MTT: FW=414.3. Add 30 µl of the prepared 2 mg/ml stock into each culture well containing 0.5 ml Test Medium. This gives rise to the final concentration of 0.29mM. Weigh out 0.002 gr of MTT (Sigma M-5655-1g) into a 30 ml Universal and add to this 1 ml MEM. (NB: The MTT solution should be added into the wells 45min before ending of each incubation, therefore filter sterilising the MTT solution is not crucial).

**NB:** this solution is Light sensitive therefore should be covered and sealed with aluminium foil.

### **B-15 KOH (2M)**

Weigh out 11.222 g of Potassium hydroxide pellets (BDH 10210 FW: 56.11) in a 100 ml pot. Add 50 ml Nanopure water to that to dissolve the pellets and then increase the volume to 100 ml in a 100 ml volumetric flask. Store the solution at Room temperature.

### **B-16 (4.3M) KOH/(0.6M) Imidazole**

Weigh out 12.064 g and 2.043 of Potassium hydroxide pellets (BDH AR 10210 FW: 56.11) and Imidazole (BDH GP 28546 FW: 68.08) respectively in a 500ml Duran bottle. Add 40 ml Nanopure water to that to dissolve the pellets (this step

should be carry out on ice since the solution becomes very hot) and then increase the volume to 50 ml in a 50 ml volumetric flask. Store the solution at Room temperature.

### **B-17 Reverse Transcription System Master Mix recipe**

<b>Component</b>	<b>Volume needed (µl)</b>
MgCl <sub>2</sub> , 25mM	4
Reverse Transcription 10X Buffer	2
dNTP Mixture, 10mM	2
Recombinant RNasin Ribonuclease Inhibitor	0.5
AMV Reverse Transcriptase (High Conc.) (15U)	0.75
Oligo (dT)15	1
DEPC Water	7.75
Final volume	18

### **B-18 Calcium ionophore A23187 (SIGMA C7522-1MG) (100x)**

Weigh out 0.0052g of A23187 into a 30ml Universal and add to this 10ml of DMSO (sigma D-8779) to dissolve the calcium ionophore. This yields the 100x stock of 1mM A23187.

### **B-19 Annexin V Binding buffer and control buffer**

#### **B-19.1 Annexin V binding buffer (10x) (MP Analysis) (0.1M HEPES/ 1.4M NaCl/ 25mM CaCl<sub>2</sub> pH.7.4)**

Weigh out 1.1915g of HEPES Acid (Sigma H.3375), 4.0915g NaCl (Sigma S9888), and 0.183g CaCl<sub>2</sub> (C/1500/20 Anal.R) in a 100ml Universal. Add about 40ml of Nanopure water and put on a magnetic stirrer to mix. Adjust the pH to 7.4 by titrating in 47% w/v NaOH (HPLC Electrochemical Grade from Fisher Ref. S/4940/17). Make up the buffer mixture to 50ml in a volumetric flask. Mix well. Then filter sterilise the buffer through a 0.2µ Acrodisc.

**B-19.2 Annexin V binding buffer (10x)\_(Apoptosis Analysis) (0.1M Hepes/  
1.4M NaCl/ 25mM CaCl<sub>2</sub>, 0.5% FCS, 0.5% NaN<sub>3</sub>, pH.7.4)**

**B-19.3 Control Buffer B (10x) (Ca-free) (1.4 M NaCl/ 0.1 M HEPES/ PH 7.4)**

This is the same as Annexin V-binding buffer but without CaCl<sub>2</sub>

**NB:** Working solution: On use, prepare just before use as required (1x) solution of the Annexin V-Binding Buffer and Buffer B by diluting the 10x stock with filtered Nanopure water.

**B-20 MP Buffer (10x) (145mM NaCl/ 2.7mM KCl/ 10mM HEPES/ pH 7.4)**

Weigh out 0.2383 g of Hepes Acid (Sigma H3375), 0.84738 g NaCl (Sigma S9888), and 0.0201 g KCl (BDH AnalaR 10198) in a 100ml container. Add about 70ml of Nanopure water and put on a magnetic stirrer to mix. Adjust the pH to 7.4. Make up the buffer mixture to 30ml in a volumetric flask. Mix well. Then filter sterilise the buffer through a 0.2u Acrodisc.

**NB:** Working solution is (1x)

## **B-21 Composition of Buffers and Solutions for Tyrosine (i.e. PTP) and Serine/Threonine (i.e. PSP) Phosphatases Assays**

### **B-21.1 Sephadex® G-25 storage buffer**

10mM Tris (pH 7.5)  
1mM EDTA  
0.02% sodium azide

### **B-21.2 Phosphate Standard**

1mM KH<sub>2</sub>PO<sub>4</sub>

### **B-21.3 PPase-2A 5X reaction buffer (For PSP Assay)**

250mM imidazole (pH 7.2)  
1mM EGTA  
0.1% β-mercaptoethanol  
0.5mg/ml BSA

### **B-21.4 PPase-2B 5X reaction buffer (For PSP Assay)**

250mM imidazole (pH 7.2)  
1mM EGTA  
50mM MgCl<sub>2</sub>  
5mM NiCl<sub>2</sub>  
250μg/ml calmodulin  
0.1% β-mercaptoethanol

### **B-21.5 PPase-2C 5X reaction buffer (For PSP Assay)**

250mM imidazole (pH 7.2)  
1mM EGTA  
25mM MgCl<sub>2</sub>  
0.1% β-mercaptoethanol  
0.5mg/ml BSA

## **B-22 Composition of Buffers and Solutions for 2-DG**

### **B-22.1 Rehydration Buffer (Make up to 2ml)**

7 M Urea (0.850 g), 2 M Thiourea (0.304 g), 65mM CHAPS (0.08 g), 0.5% Ampholytes (10 μl), 1.2% Destreak (24 μl), 0.00125% Bromophenol Blue (10 μl of 0.25% solution)

### **B-22.2 Equilibration Buffer (I) (Make up to 15ml)**

7 M Urea (5.40 g), 3.75 ml 1.5M TRIS-HCl pH 8.8, 3 ml 10% SDS, 3 ml glycerol, 129.65mM DTT (0.3 gr)

### **B-22.3 Equilibration Buffer (II) (Make up to 15ml)**

This is the same as Buffer (I) but instead of DTT, the Buffer (II) contains 135mM Iodoacetamide (0.375 gr).

### **B-23 Additional Fixative Step schedule (Silver Staining)**

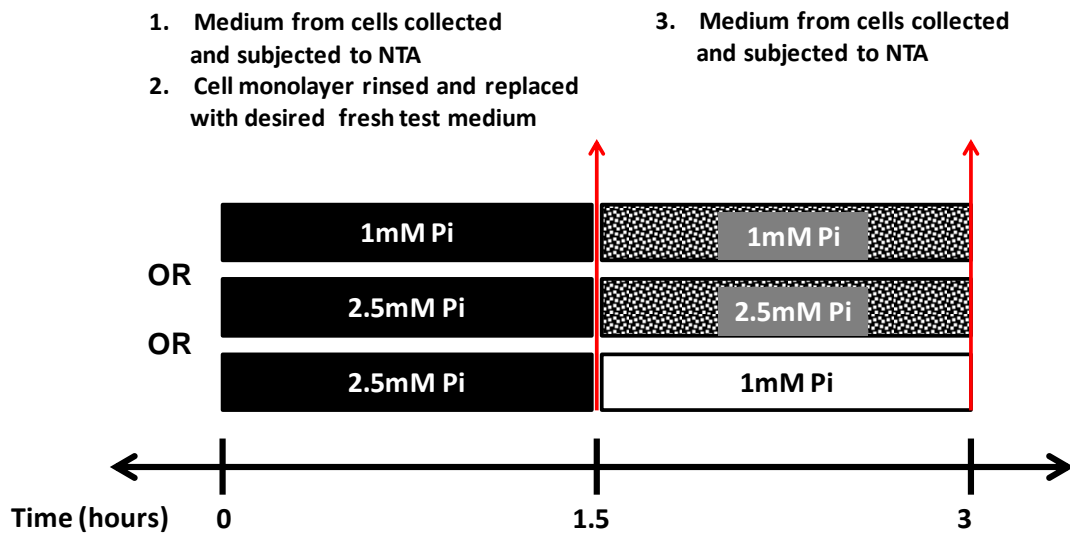
According to Silver Stain Plus protocol (Bio-Rad 161-0449):

Step	Gel Thickness 0.75mm-1.0mm			Gel Thickness 1.5mm-3mm		
	Time	Mini gel	Large gel	Time	Mini gel	Large gel
<b>Fixative</b>	20min	400ml	800ml	30min	400ml	800ml
<b>Water wash</b>	10min	400ml	800ml	20min	400ml	800ml
<b>Water wash</b>	10min	400ml	800ml	20min	400ml	800ml
<b>Stain</b>	20min	100ml	300ml	20min	100ml	300ml
<b>Stop</b>	15min	400ml	400ml	15min	400ml	400ml

## Appendix C (Supporting data)

### Supporting Data to Chapter 3

#### C-3.1 Protocol for the study of the effect of Pi on particle release after returning the Pi concentration to the control (1mM) level



Appendix C-Figure 3.1. Study Design illustrating the treatment protocol applied to test the effect of Pi on NTA detected particles – to show that these are not CaPi nanocrystals. Cells ( $30 \times 10^4$  cells) were seeded on each well of a 6-well culture plate (diameter 35mm) and grown to confluence. At confluence, growth medium was removed and cell monolayer washed three times with HBSS to remove serum and detached cells. 2ml Test Medium was added per well (Test Medium containing 1mM and 2.5mM [Pi]) as appropriate (I.e in the sequence that is indicated in diagram above) and cells incubated in the cell culture incubator for 90min. At the end of this first 90min period, the medium from cells was collected and saved for NTA analysis and the cell monolayer replaced with new/fresh test medium (hashed black bars in the diagram above). In some cultures the Pi level was adjusted back to the control level (white bar in the diagram above) and then the culture plates returned in the incubator for the second 90min incubation. At the end of this second 90min period the medium from cells was collected and saved for NTA analysis and determination of total sedimentable protein from the medium by protein assay.

### C-3.2 Solution and mixtures used for <sup>45</sup>Ca measurements

Medium Label	Final [Pi] in the Medium (mM)	Basal Medium <sup>1</sup> (ml)	100mM NaHPO <sub>4</sub> added (μl)	H <sub>2</sub> O (μl)	WS <sup>45</sup> Ca (μl) <sup>2</sup>
A	0	10	-----	500	10
B	0.3	10	30	470	10
C	0.5	10	50	450	10
D	1	10	100	400	10
E	2.5	10	250	250	10
F	5	10	500	-----	10

<sup>1</sup>Basal Medium: Pi-free MEM (Appendix)

<sup>2</sup>WS (Working Solution <sup>45</sup>Ca: approx. 1 kBq per μl): On the day of the experiment, the remaining fraction "F" of the original <sup>45</sup>Ca activity was calculated from the <sup>45</sup>Ca decay table (Appendix A-4). To 1ml of sterile serum/Pi-free MEM (1/F μl of the Perkin Elmer NEZ013001MC stock was added, and swirled to mix. e.g. on day 1 the fraction remaining is 0.996 therefore  $(1) / (0.996) = 1.004\mu\text{l}$  of stock 1MBq should be added to 1ml serum/Pi-free MEM to give the required working solution of 1 kBq per μl (almost 10<sup>6</sup> fold diluted).

Appendix C-Table 3.1. Test Medium detailed components used for cell incubation conditions (<sup>45</sup>Ca experiment).

Note: In some experiments, the effect of adding the Pi analogue PFA was also investigated as follows:

Medium Label	Final [Pi] in the Medium (mM)	Basal Medium <sup>1</sup> (ml)	100mM NaHPO <sub>4</sub> added (μl)	50mM PFA added (μl)	H <sub>2</sub> O (μl)	WS <sup>45</sup> Ca (μl) <sup>2</sup>
A	1	10	100	-----	600	10
B	2.5	10	250	-----	750	10
C	5	10	500	-----	200	10
D	1	10	100	200	400	10
E	2.5	10	250	200	250	10
F	5	10	500	200	-----	10

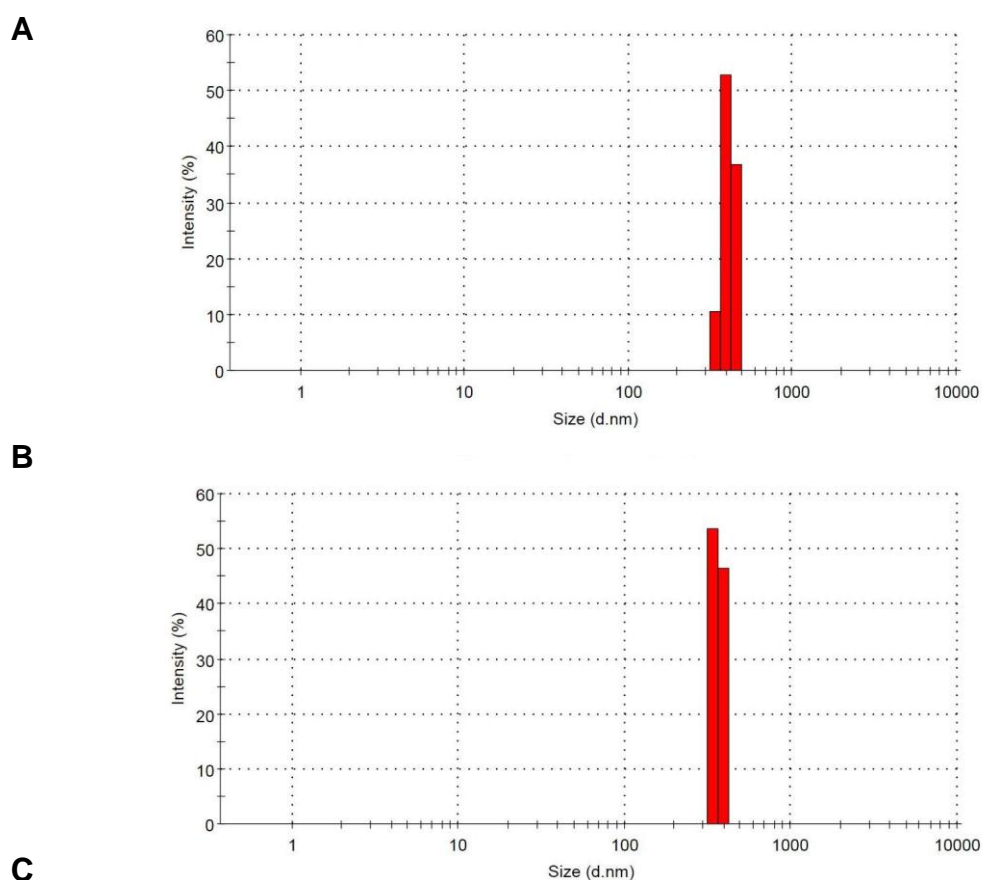
<sup>1</sup>Basal Medium: Pi-free MEM (Appendix)

<sup>2</sup>WS (Working Solution <sup>45</sup>Ca: approx. 1 kBq per μl): On the day of the experiment, the remaining fraction "F" of the original <sup>45</sup>Ca activity was calculated from the <sup>45</sup>Ca decay table (Appendix A-4). To 1ml of sterile serum/Pi-free MEM (1/F μl of the Perkin Elmer NEZ013001MC stock was added, and swirled to mix. e.g. on day 1 the fraction remaining is 0.996 therefore  $(1) / (0.996) = 1.004\mu\text{l}$  of stock 1MBq should be added to 1ml serum/Pi-free MEM to give the required working solution of 1 kBq per μl (almost 10<sup>6</sup> fold diluted).

Appendix C-Table 3.2. Test Medium detailed components used for cell incubation conditions (Effect of PFA on <sup>45</sup>Ca deposition).

### C-3.3 Size distribution of released MPs from EAhy926 cells studied by (DLS)

Analysis of MPs (released from EAhy926 endothelial cells) by DLS demonstrated the release of three predominant MP fractions regarding size from the control medium with 1mM Pi (Panel A). The fraction containing the largest particles tended to be absent in cells treated in higher phosphate (2.5mM Pi) medium (Panel B).

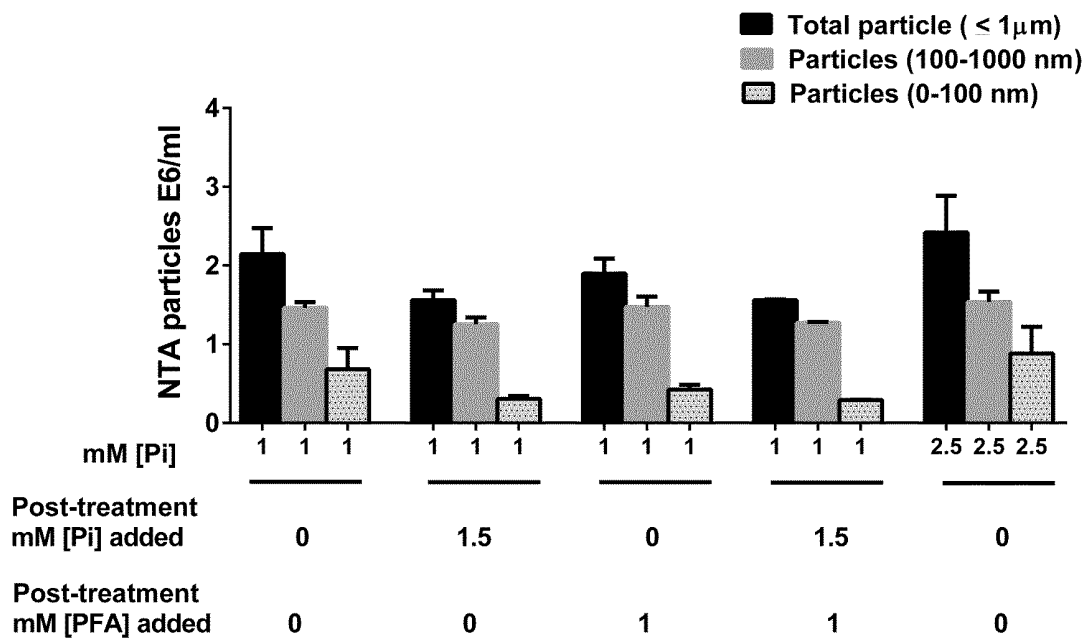


Sample	Z-Ave (nm)	PdI	Peak-1 (nm)/Intensity (%)	Peak-2 (nm)/Intensity (%)	Peak-3 (nm)/Intensity (%)
1mM [Pi]	666.5	0.646	342/10.4	396/52.8	458/36.8
2.5mM [Pi]	1346	0.861	342/53.6	396/46.4	N/A

Appendix C-Figure 3.2. Size distribution from DLS measurement of phosphate treated EAhy926 cells exposed to control (1mM) and high phosphate (2.5mM) for 90min. Particle intensity detected on DLS (x-axes) and particle size in nm (y-axes). (A) Particle release from test medium containing 1mM [Pi] and (B) from 2.5mM [Pi]. (C) Data summary showing Z-average diameter (nm), Polydispersity index (PdI), and detected size distribution (Peaks).

### C-3.4 Physicochemical effect of Pi/PFA on Pi-derived MPs by NTA

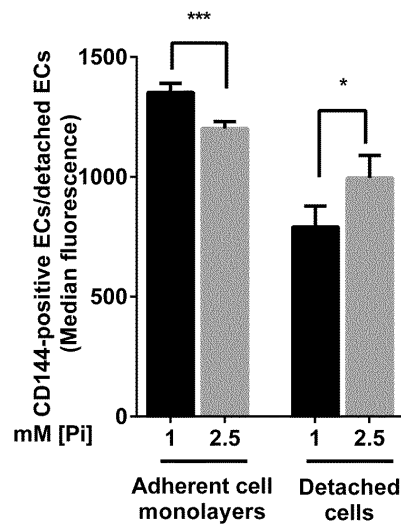
This experiment was similar to that shown in Figure 3.10, but the particles were analysed by NTA instead of centrifugation followed by total protein analysis of the pellet. NanoSight NTA analysis was applied to the medium from EAhy926 cells treated with phosphate for 24h and the collected medium from the cells was further incubated with/without extra phosphate and/or PFA to check for the possibility a direct effect of phosphate and/or phosphate analogues on particle sedimentation and aggregation. This indicated no such direct physicochemical effect of phosphate and PFA on NTA detectable counts.



Appendix C-Figure 3.3. No detectable physicochemical effects of extracellular phosphate and PFA concentrations on particles from media analysed by NTA. Particle intensity (y-axes) and phosphate/PFA concentration (x-axes) (n=9).

### C-3.5 Pi does not enhance CD144 expression in adherent EAhy926 cells

Even though 24h of exposure to elevated Pi concentration enhanced CD144 expression in MPs (Chapter 3-Figure 3.9 C) and in detached cells (Appendix C-Figure 3.4) that were released from the cultures, a small decrease in CD144 expression was observed in intact adherent cells (Appendix C-Figure 3.4).



Appendix C-Figure 3.4. Reciprocal modulatory effect of Pi on CD144 level in adherent EAhy926 endothelial cells vs. detached cells *in vitro* sedimented after centrifugation at 1,500g for 30min. Flow Cytometry performed on intact adherent EAhy926 cells in high Pi and control Pi medium showed a phosphate-induced decrease in CD144-positive cells (n=3 at t=24h) \*P<0.05, contrasting with the increase observed in detached cells \*\*\*P<0.001.

## Supporting Data to Chapter 4

### C-4.1 Transfection Mixtures for siRNA silencing of PiT-1 and PiT-2 in EAhy926 cells

Experimental Condition	Tube 1 (for 1 transfection)	Tube 2 (for 1 transfection)			
	Lipofectamine (μl) + Opti-MEM (μl)	PiT-1 siRNA (μl) + Opti-MEM (μl)	PiT-2 siRNA (μl) + Opti-MEM (μl)	Scrambled siRNA (μl) + Opti-MEM (μl)	Nuclease Free H <sub>2</sub> O (μl) + Opti-MEM (μl)
Control	0 + 50	-	-	-	0.6 + 199.4
Transfection Reagent Only	10 + 40	-	-	-	0.6 + 199.4
Scrambled siRNA	10 + 40	-	-	0.6 + 199.4	-
PiT-1 siRNA	10 + 40	0.6 + 199.4	-	-	-
PiT-2 siRNA	10 + 40	-	0.6 + 199.4	-	-
Dual PiT-1/-2 siRNA	10 + 40	0.6 (PiT-1 siRNA) + 0.6 (PiT-2 siRNA) + 198.8 (Opti-MEM)		-	-

## Supporting Data to Chapter 5

### C-5.1 Solutions for Nitro Blue Tetrazolium (NBT) Assay to measure ROS in Pi treated cells

Medium Label	Final [Pi] in the Medium (mM)	Basal Medium <sup>1</sup> (NBT) (ml)	Sterile 100mM NaHPO <sub>4</sub>	Sterile 1.1M NaCl	Ethanol (Absolute) to be added	NAC (g) 10mM	30mM Menadione <sup>2</sup> to be added (ul)
A	0.8	4ml	-----	7.2ul	4ul	-----	-----
B	1.8	4ml	40ul	3.68ul	4ul	-----	-----
C	2.8	4ml	80ul	-----	4ul	-----	-----
D	0.8+M	4ml	-----	7.2ul	-----	-----	4ul
E	0.8+NAC	4ml	-----	7.2ul	4ul	~0.006 5	-----
F	2.8+NAC	4ml	80ul	-----	4ul	~0.006 5	-----

<sup>1</sup>For 8ml of the Basal Medium (0.2%NBT), 0.016g of NBT dissolved in 8ml of HBSS and wrapped to prevent light exposure.

<sup>2</sup>For 1ml of 30mM stock Menadione, 0.0052g of Menadione added to 1ml of absolute Ethanol and mixed thoroughly and wrapped to prevent light exposure.

NB: NAC denotes wells incubated with antioxidant, pre-incubated for two hours in 1ml of 10mM N-Acetyl-L-Cysteine (NAC).

Appendix C-Table 5.1. Test Medium detailed components used for cell incubation conditions (NBT assay).

### C-5.2 Solutions: MTT to measure effect of albumin species on cell viability

Test Medium	B.M (ml) <sup>1</sup>	HSA <sup>2</sup> (g)	BSA <sup>3</sup> (g)	0.893M NaHCO <sub>3</sub> (ml)	P/S (ml)	L-Gln (ml)
Control	50	-----	-----	0.465	0.50	0.50
HSA	50	0.25	-----	0.465	0.50	0.50
BSA	50	-----	0.25	0.465	0.50	0.50

<sup>1</sup>Basal Medium: Serum-free MEM, 1% PS, 2mM L-Gln, pH 7.4

<sup>2</sup>HSA: Albumin from Human Serum, (Sigma A-8763-5G)

<sup>3</sup>BSA: Globulin-free Bovine Serum Albumin (Sigma A-7638)

Appendix C-Table 5.2. Test Medium detailed components used for cell incubation conditions (MTT assay).

**C-5.3 Solutions: MTT to measure effect of acute phosphate level on cell viability**

Test Medium	B.M (ml) <sup>1</sup>	Final [Pi] mM	100mM [Pi] <sup>2</sup> to be added (ml)	0.893M NaHCO <sub>3</sub> (ml)	P/S (ml)	L-Gln (ml)	H <sub>2</sub> O (ml)
Control	50	1	-----	0.465	0.50	0.50	-----
1mM [Pi]	20	1	-----	0.465	0.50	0.50	0.3
2.5mM [Pi]	20	2.5	0.3	0.465	0.50	0.50	-----

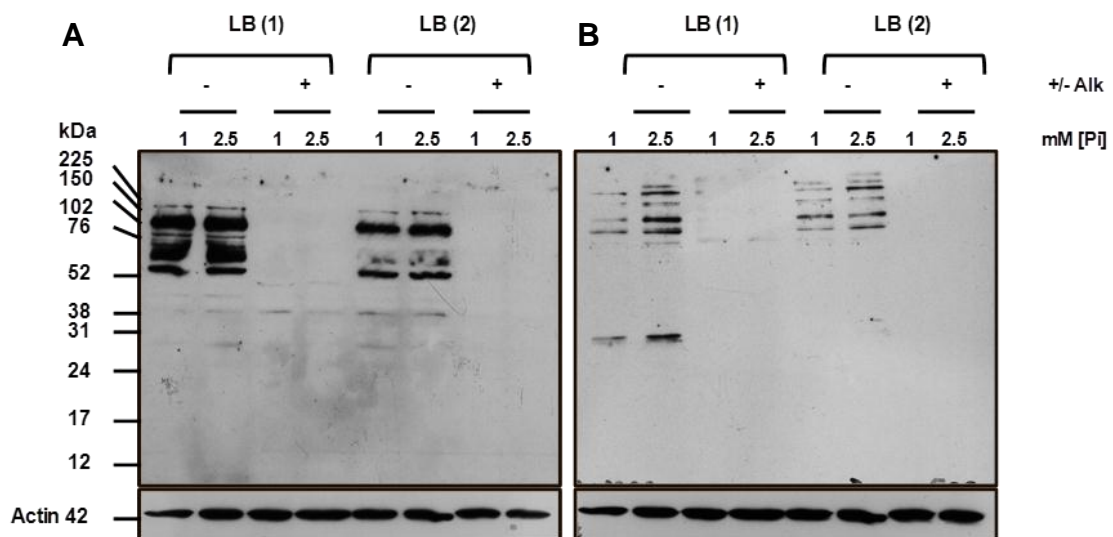
<sup>1</sup>Basal Medium: Serum-free DMEM, 1% PS, 2mM L-Gln, pH 7.4

<sup>2</sup>100mM [Pi]: NaH<sub>2</sub>PO<sub>4</sub>·2H<sub>2</sub>O

Appendix C-Table 5.3. Basal Test Medium detailed components used for cell incubation conditions (MTT assay).

### C-5.4 Alkaline Phosphatase treatment of EAhy926 cells lysate

To check the specificity of anti-phospho antibodies (P-Tyrosine and P-Serine/Threonine) to detect phospho-Tyr and –Ser/Thr phosphorylated proteins the EAhy926 lysate underwent alkaline phosphatase treatment. Results (Appendix C-Figure 5.1) show that these antibodies efficiently/effectively detect targeted phosphoproteins in cell lysates, as following treatment of lysates with alkaline phosphatase the signals detected by the antibodies were abolished. Furthermore when cell lysates were prepared in modified Lysis Buffers (LB 1; containing complete proteases and phosphatases inhibitors and LB 2: without inhibitors) it was demonstrated that LB 1 maintained phosphorylated proteins in the cell lysate whereas the phosphoprotein signal was blunted on the blots in LB 2.

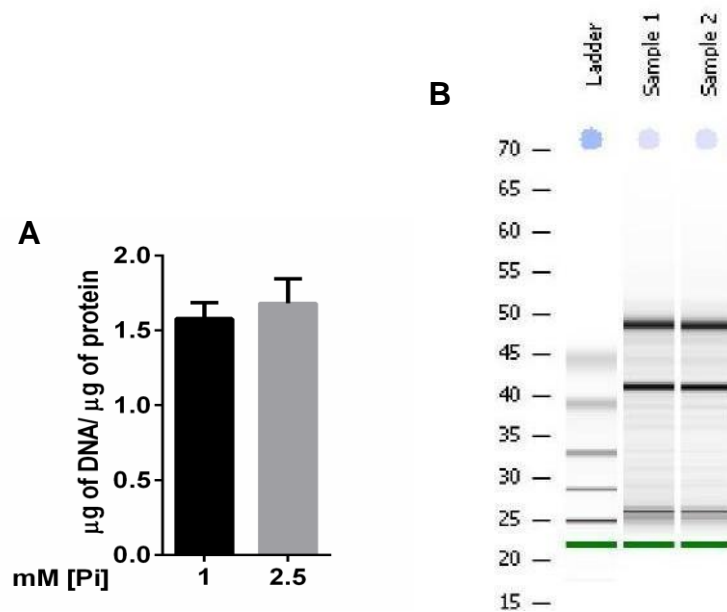


Appendix C-Figure 5.1. Detection of protein phosphorylation and/or de-phosphorylation in EAhy926 endothelial cell lysates with pan-specific anti-phosphoserine/threonine and tyrosine antibodies. (A, B) Representative immunoblots of protein tyrosine phosphorylation probed with pan-specific anti-phosphotyrosine antibody (A) and of protein serine/threonine phosphorylation probed with pan-specific anti-phosphoserine/threonine antibody (B). In each set, cell lysates were treated with (+) or without (-) alkaline phosphatase (AP, New England Biolabs- M0290S at 50U/ml) for 30min at 37°C. (Alk: Alkaline Phosphatase; LB1: Lysis Buffer 1; LB2: Lysis Buffer 2 (without phosphatase inhibitors))

### C-5.5 Phosphate-derived MPs contain DNA and RNA

An increasing body of evidence indicates the importance of miRNA for a number of cell processes including cell proliferation, apoptosis, and growth (Emilian *et al.*, 2012). The level of this novel biomarker has been shown to undergo changes in a number of physio-/pathophysiological conditions such as myocardial damage (Emilian *et al.*, 2012), monocytes abnormalities (Li *et al.*, 2011), and acute kidney injuries (Lorenzen *et al.*, 2011; Neal *et al.*, 2011). No evidence to date shows whether or not the circulating (i.e. shed from cells into the extracellular milieu) levels of miRNA are affected in hyperphosphataemia.

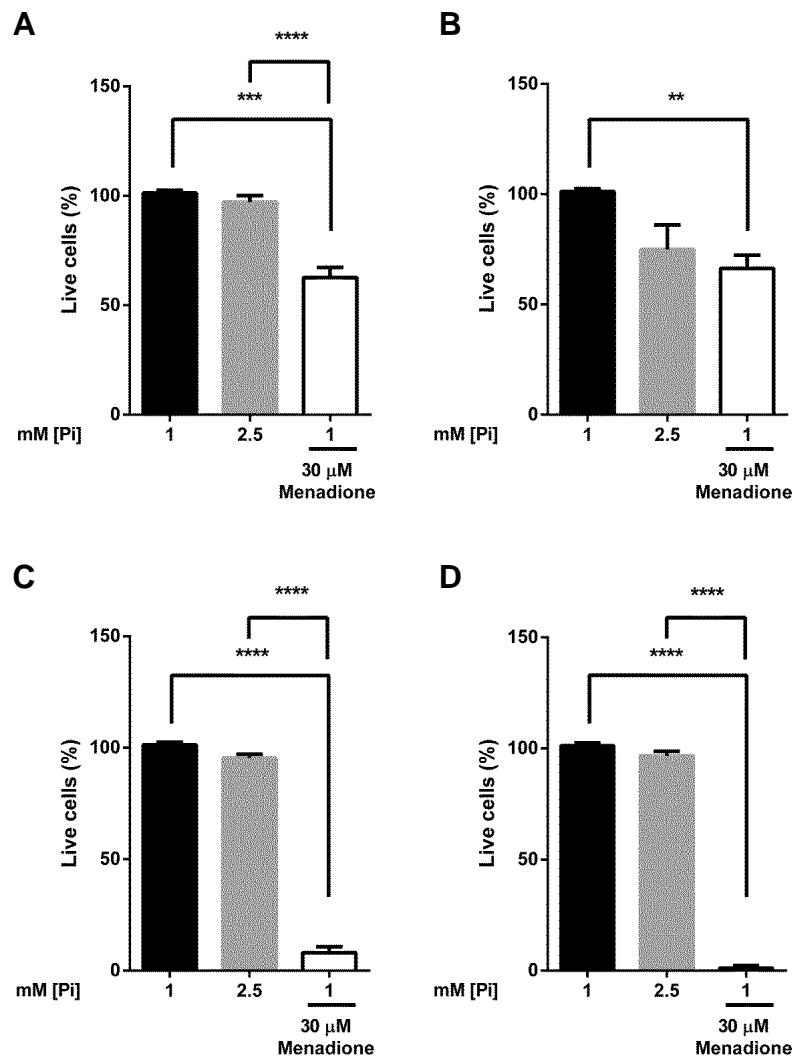
In this preliminary experiment, MPs from EAhy926 cells were shown to contain DNA (panel A), RNA and miRNAs (panel B) (determined as described in Methods Chapter Sections 2.29.4). However, Pi loading of the culture medium had no obvious effect on these parameters.



Appendix C-Figure 5.2. Presence of DNA and RNA (and possibly miRNA) in MPs derived from phosphate treated endothelial cells. EAhy926 cells were treated with control 1mM phosphate vs. 2.5mM and medium harvested and centrifuged to collect phosphate-derived MP from the media (Fraction 2- Table 2.1; see Chapter 2). The total RNA was extracted from the MP pellet and subjected to screening for the presence of miRNA as described in Section 2.29.4. (Sample 1) 1mM Pi-derived MP, (Sample 2) 2.5mM Pi-derived MP. NB: Vertical axis in panel B denotes ladder (bp).

### C-5.6 Effect of Pi on EAhy926 ECs viability by Trypan-blue exclusion (TBE)

TBE showed no statistically significant reduction on the cell viability after 90min ( $P=0.6319$ ), 8h ( $P=0.1285$ ), 24h ( $P=0.0554$ ), and 48h ( $P=0.3086$ ) exposure to higher phosphate milieu comparing 1mM Pi with 2.5mM Pi treated cells, while Menadione positive control resulted in a significant reduction in cell viability over the whole time course ( $P<0.05$ ).

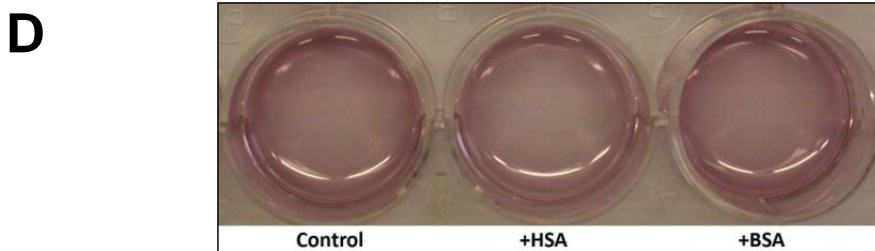
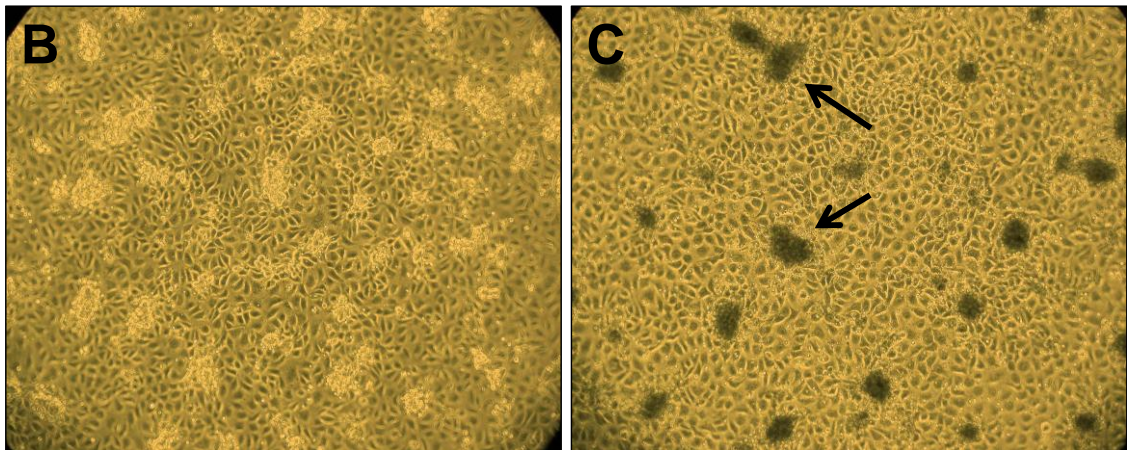
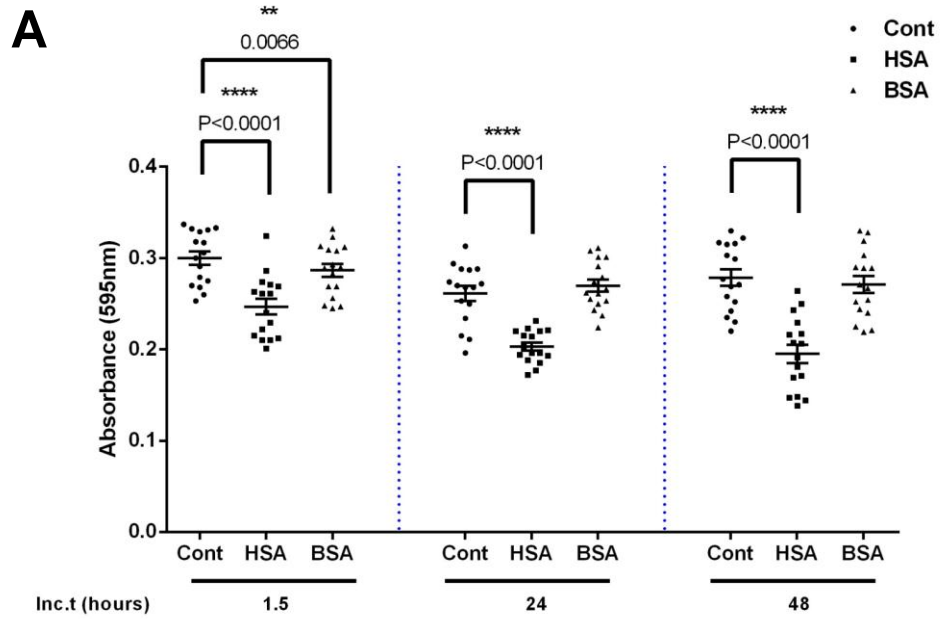


Appendix C-Figure 5.3. Trypan Blue Exclusion as determinant of viable cells. EAhy926 cells were treated with control (1mM) Pi medium vs. high (2.5mM) Pi medium on 35mm culture plates for (A) 90min, (B) 8h, (C) 24h, and (D) 48h. Cells were treated with 30µM Menadione used as positive control. No statistically significant effect of Pi on cell death was observed. Note that the Menadione positive control resulted in a significant cell death. (A) 90min, (B) 8h, (C) 24h, and (D) 48h. ( $n=3$ ) \*\* $P<0.01$ , \*\*\* $P<0.001$ , \*\*\*\* $P<0.0001$ .

### **C-5.7 Effect of Albumin load on cells proliferation/viability in vitro**

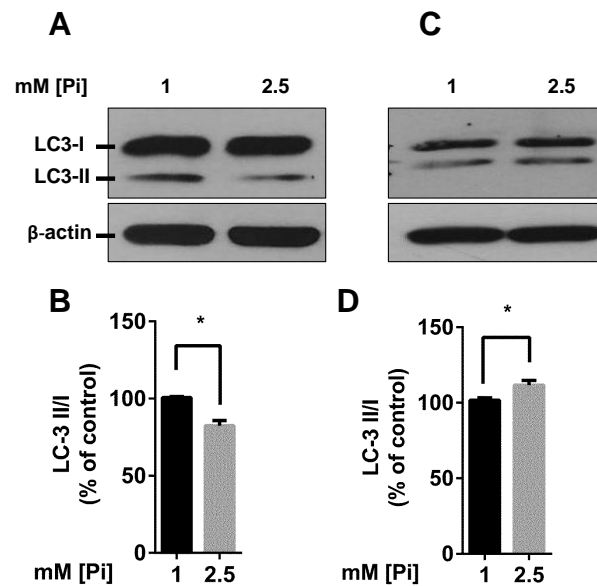
To evaluate whether ECs can tolerate serum-free, or BSA, or HSA, or other growth factor-free conditions a control study was set up. Cells were seeded in 12-well plates and Test Media added on cells when cells reached 70% confluence. Just before adding Test Medium on cells, Growth Medium was aspirated and cells were washed to remove any remaining serum or growth factor by 3 steps washing with HBSS. MEM containing 2mM (v/v) L-Glutamine, 1% (v/v) penicillin/streptomycin, and and additional 0.93% (v/v) NaHCO<sub>3</sub> to give final pH of 7.4 was set as the control. In treatment groups, control medium was supplemented with 5mg/ml HSA or 5mg/ml BSA. Cells treatments were studied over a time course up to 48h. At the termination of each incubation, MTT cell viability assay was performed to determine cell viability and proliferation in response to albumin species.

At each indicated incubation time, comparing the control condition vs. treated groups, ECs tended to show a decreased formazan production implying less viable cells in the presence of albumin. Albumin was not therefore added routinely to the Test Medium in the experiments in this thesis (\*\*\*\* P<0.001, & \*\* P=0.01).



Appendix C-Figure 5.4. Effect of albumin species on cell viability by MTT assay. (A) Relationship between MTT-formazan production and presence/absence of 5 mg/ml human serum albumin (HSA) or bovine serum albumin (BSA). (Cont) denotes serum-free control condition. (B) EAhy926 cells after 48 hours incubation with control test medium (serum-free) without having MTT added on cells. (C) EAhy926 cells after 48 hours incubation with control test medium containing 0.29mM MTT. Arrows indicated formazan production. (D) Purple colour species produced after adding DMSO on cells to solubilise the Formazan. (Inverted Microscopic images are zoomed in shots of an original microscopic magnification of x100).

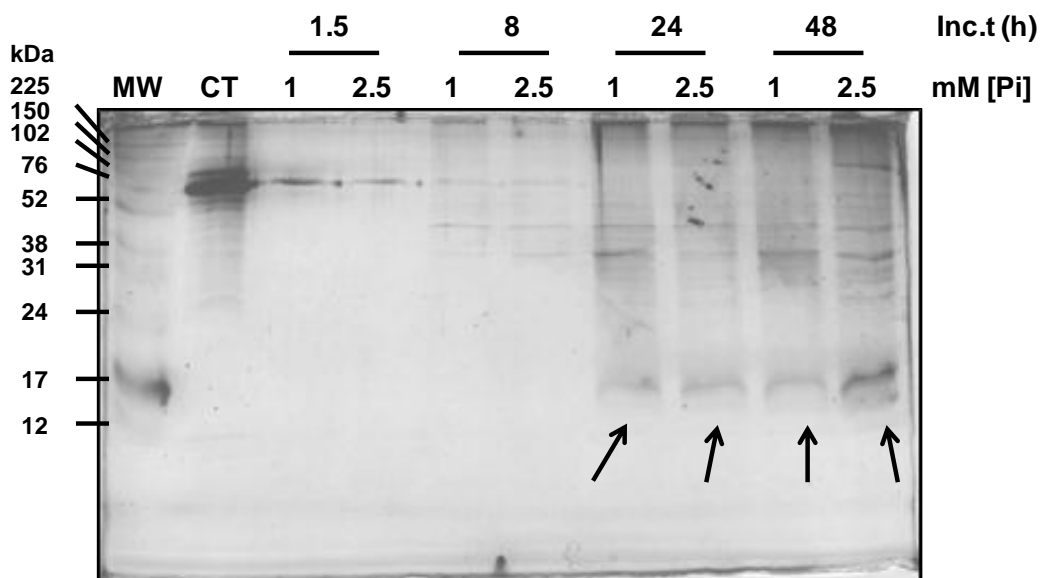
## C-5.8 Pi induces protective autophagy in EAhy926 cells



Appendix C-Figure 5.5. High Pi induces autophagy in EAhy926 cells. Cells treated with control (1mM) Pi vs. high (2.5mM) Pi for (A, B) 90min and (C, D) 24h on 35mm cell culture plates. Test medium from cells was decanted and cell monolayer probed for LC-3 with an anti-LC3 antibody. This implies that high Pi chronically induces slight autophagy at 24h in EAhy926 ECs. (A) Representative immunoblotting with anti-LC-3 antibody at 90min and (B) Corresponding densitometry analysis at 90min, (n=3) \* $P < 0.05$  (C) Representative immunoblotting with anti-LC-3 antibody at 24h and (D) Corresponding densitometry analysis at 24h, (n=6) \* $P < 0.05$ .

### C-5.9 SDS-PAGE profiling of particles released from EAhy926 into the Test Medium

Staining particle released from cells on SDS-PAGE with Coomassie blue seemed not to be a sensitive approach to stain as little as nanogram amounts of proteins (data not shown) therefore, released particles from phosphate treated EAhy926 cells were separated in a similar way on SDS-PAGE gel electrophoresis but stained using a more sensitive in gel protein stain (Silver Staining). Separating particle fractions on SDS-PAGE followed by the Silver staining revealed higher band intensity at ~17kDa detected in samples from higher phosphate treated cells (Appendix C-Figure 5.6; Note arrows). Running a densitometry analysis on the observed 17kDa band from four individual experiments showed a significant increase in the intensity of this marker/biomarker in cells treated in higher phosphate solution, with a maximal response after 48h (2.5mM [Pi] vs. Control 1mM [Pi], Mean  $\pm$  SEM, \*\*P=0.0017, n=4) (Figure 5.14 A and B).



Appendix C-Figure 5.6. Representative Silver staining of particles released from EAhy926 endothelial cells separated on SDS-PAGE gel electrophoresis. Lysates of sedimented particles from cells incubated with test media with 1 or 2.5mM Pi for the times shown *Lanes 2 is used complete growth medium from cells containing FBS Lane 1 is coloured molecular weight markers (Amersham APM800E)*. Arrows showing reproducible ~17 kDa (possible hyperphosphataemic biomarker) bands which have been observed in four experiments on EAhy926 cells.

### C-5.10 Table of Proteomics Analysis of Pi-derived EAhy926 MPs by orbi-trap (LC MS/MS).

\*. Indicates the trend (abundance) of nominated protein comparing control Pi-derived MP to high (2.5mM) Pi-derived MP by Scaffold3 software.

Protein name	Accession code	Sequence coverage%/Mowse score	N.peptides	sequence	MW (kDa)	1 vs 2.5*
<b>Nucleosome</b>						
Histone H2B	P62807	58/67	10/12	1 mpepaksapa pkkgskkavt kaqkkdgkkr krsrkesysv yvyvlkqvh pdtgisskam 61 gimnsfvndi feriageasr lahynkrsti tsreiqtavr llpgelakh avsegtkavt 121 kytssk	14	UP
Histone H3.2	Q71DI3	60/60	10/11	1 martkqtark stggkaprkq latkaarksa patggvkkph ryrpgtvalr eirryqkste 61 llirklpfqr lvreiaqdfk tdlrfqssav malqeaseay lvgfedtnl caihakrvti 121 mpkdiqlarr irgera	15	UP
Histone H2A	Q16777	38/58	9/8	1 msgrgkqggk arakaksrss raglqfpvgr vhrllrkghy aervgagapv ymaavleylt 61 aeilelagna ardnkktrii prhlqlairn deelnlkllgk vtiaqggvlp niqavllpkk 121 teshkaks	14	DOWN
Histone H4	P62805	51/52	6/9	1 msgrgkqggk lgkggahrhr kvlrndiqgi tkpairrlar rggvkrisgl iyeetrgvlk 61 vflenvirda vtytehakrk tvtamdvvya lkrqgrtlyg fgg	11	UP
H2A.x	P16104	41/38	4/3	1 msgrgkqggk arakaksrss raglqfpvgr vhrllrkghy aervgagapv ylaavleylt 61 aeilelagna ardnkktrii prhlqlairn deelnlkllgg vtiaqggvlp niqavllpkk 121 tsatvgpkap sggkakatqas qey	15	DOWN
<b>Cytoskeleton</b>						
Vimentin	P08670	53/57	31/33	1 mstrsvssss yrrmfggpgt asrpssrsy vttstrtysl gsalrpstsr slyasspggv 61 yatrssavrl rsvpgvrrll qdsvdflad aintefkntnr nekvelqel ndranyidk 121 vrfleqqnki llaeleqlkg qgksrgldly eeemrelrrq vdqitndkar veverdnlæ 181 dimrlreklq eemlqreeae ntlqsrqdv dnaslarldl erkveslqee iaflkklhee 241 eiqlqaciq eqhvqidvdv skpdltaalr dvrqqyesva aknlqaeew ykskfadlse 301 aanrndaalr qakqesteyr rqvqsltecv dalkgtneal erqmremeen faveaanyqd 361 tigrldiq nmkeemarhl reyqdllnk maldieiaty rkllgeesr islplnfss 421 lnretnlds lplvdthskr tlliktvetr dgqvinetsq hhdle	54	UP

<b>Actin</b>	P63261	59/67	16/18	1 meeeiaalvi dngsgmckag fagddapprav fpsivgrprh qgvvmvngmqk dsyvgdeaqs 61 krgiltkyp iehgivtnwd dmekiwhtf ynelrvapee hpvllteapl npanrekmt 121 qimfetfntp amyvaiqavl slyasgrttg ivmdsgdgv htvpiyegya lphailrldl 181 agrldtdylm kiltergysf ttaereivr dikeklcyva ldfeqemata assssleksy 241 elpdgqviti gnerfrcepa lfqpsflgme scgihettfn simkcdvdir kdlyantvls 301 ggttmypgia drmqkeital apstmkikii apperkysvw iggsilasls tfqqmwiskq 361 eydesgpsiv hrkcf	42	-
<b>Cofilin-1</b>	P23528	78/72	14/15	1 masgvavsdg vikvndmkv rksstpeevk krkkavfcl sedkkniiile egkeilvgdv 61 ggtvddpyat fvkmlpkdc ryalydatye tkeskkedlv fifwapesap lkskmiyass 121 kdaikkkltg ikhelqancy eevkdrctla eklggsavis legkpl	19	DOWN
<b>Tubulin beta chain</b>	P07437	55/51	16/17	1 mreivhiqag qcgnqigakf wevisdehgi dptgtyhgds dlqldrisvy yneatggkyy 61 prailvlep gtmdsvrsgp fgqifrdnf vfgqsgagnn wakghytega elvdsldvv 121 rkeaescdcl qgfqlthslg ggtgsgmgtl liskireeyp drimntfsvv pspkvsdtvv 181 epynatlsvh qlventdety cidnealydi cfrtlkltp tygdlnhlvs atmsgvtcl 241 rfpqqlnadl rklavnmpvf prlhffmpgf apltsrgsqq yraltvpelt qqvfdaknmm 301 aacdprhgry ltvaavfrgr msmkeveqem Invqknssy fvewipnnvk tavcdipprg 361 lkmavtfign staiqelfkr iseqtamfr rkafhlwytg egmdemefte aesnmdnlvs 421 eyqqyqdata eeeedfgeea eeea	50	-
<b>Myosin light polypeptide</b>	P60660	87/84	12/11	1 mcdftedqta efkeafqlfd rtgdgkily qcgdvmlalg qnptnaevlk vlgnpksdem 61 nvkvldefh lpmlqtvakn kdqgtyedyv eglrvfdkeg ngvtmgaeir hlvltlgekm 121 teeevemlva ghedsngcin yeafvrhils g	17	UP
<b>Tubulin alpha-1B chain</b>	P68363	32/51	10/16	1 mrecisihvg qagvqignac welyclehgi qpdgqmpsdk tiggdddsfn tffsetgagk 61 hvpravvdl eptvidevrt gtyrqlfhpe qlitgkeda nnyarghyti gkeiidlvld 121 rirkladqct glqgflvfhs fgggtsgft silmerlsvd ygkksklefs iypapqvsta 181 vvepynsilt thtlehsdc afmvdneaiy dicrrndie rptynlrnl isqivssita 241 slrfdgalnv dltefqtnlv pyprihfpla tyapvisaek ayheqlsvae itnacfeapan 301 qmvkcdprhg kymaccllyr gdvvpkdvna aiatiktks iqfvdwcpdg fkvginypqp 361 tvpvgdlak vqravcmisn ttaiaeawar ldhkfdlmya krafvhwvyg egmeegefse 421 aredmaalek dyeevqvdsv egegeeegee y	50	-
<b>Actin-regulated protein</b>	P59998	50/55	6/8	1 mtatlrpys avratlqaal clenfssqv erhknpevev rskellqp vtisrnekek 61 vliegsinsv rsviavkqad eiekilchkf mrfmmraen ffilrrkpvpe gydisflitn 121 fhteqmykhk lvdfvihfme eidkeisemk lsvnarariv aeeflknf	20	UP
<b>Elongation factor 1-alpha</b>	P68104	11/15	3/5	1 mgkekthini vvighvdsdg stttghlyk cggidkrtie kfekeaaemg kgsfkyawvl	50	DOWN

				61 dklkaererg itidislwkf etskyvvtii dapghrdfik nmitgtsqad cavliavaagv 121 gefeagiskn gqtrehalla ytlgvkqliv gvnkmdstep pysqkryeei vkeestyikk 181 igynpdtvaf vprisgwngdn mlepsanmpw fkgwkvtrkd gnasgttle aldclpptr 241 ptdkplrpl qdvykiggig tvpvgrvetg vlkpgmvvtf apvnttevk svemhheals 301 ealpgdngvf nvknsvkdv rrgnvagdsd ndppmeaagf taqviilnhp gqisagyapv 361 ldchtahiac kfaelkekid rrsqkkledg pkflksgdaa ivdmvpgkpm cvesfsdypp 421 lgrfavrdmr qtvavgvika vdkkaagagk vtsaqkaqk ak		
<b>Microtubule-associated protein</b>	Q15691	19/18	4/4	1 mavnvystsv tsdnlsrhdm lawineslql nltkieqlcs gaaycqfmdm lfpgsialkk 61 vkfqaklehe yiqnfkilqa gfkrmgvdkl ipvdklvkgk fqdnfefvqw fkkffdannd 121 gkdydpvaar qqgetavaps lvapalnkp kpltsssaap qrpistqrta aapkagpgvv 181 rknpgvngnd deaaelmqqv nvlklvedl ekerdfyfgk lmielicqe negendpvlq 241 rivdilyatd egfvipdegg pqeeqeeey	30	UP
<b>Tubulin beta-2C</b>	P68371	55/52	4/4	1 mreivhlqag qcgnqigakf wevisdehgi dptgtyhgds dlqlerinvy yneatggkyy 61 pravldlep gtmdivsrsgp fgqifrdnf vfgqsagann wakghytega elvdsvidvv 121 rkeaesdcl qgfqlthslg ggtgsgmgtl liskireeyp drimntfsv pspkvsdtvv 181 epynatlsvh qlventdety cidnealydi cfrtlkltp tygdlnhlvs atmsgtvtcl 241 rfpqqnladi rklavnmpvf prlhffmpgf apltsrgsqq yraltvpelt qqmfdaknmm 301 aacdprhgry ltvaavfrgr msmkevedeqm Invqknssy fvewipnnvk tavcdipprg 361 lkmsatfign staiqelfkr iseqftamfr rkafllhwytg egmdemefte aesnmndlvs 421 eyqqyqdata eeegefueea eeeva	50	-
<b>Vesiculation</b>						
<b>Annexin A2</b>	P07355	23/25	6/7	1 mstvheilck lslegdhstp psaygsvkay tnfaerdal nietaiktg vdevtivnil 61 tnrsnaqrqd iafayqrrtk kelasalksa lsgkletvil gllktpaqyd aselkasmkg 121 lgtdeedslie iicsrtngel qeinrvkem yktdlekdii sdtsgdfrkl mvalakgrra 181 edgsvdyel idqdardlyd agvkrkgtdv pkwisimter svphlqvfd ryksyspydm 241 lesirkevkg dlenafnlv qciqnkplyf adrltdsmkg kgtrdkvlir imvrssevdn 301 lkirsefkrk ygkslyyyiq qdtkgdyqka llylccgdd	39	UP
<b>Annexin A5</b>	P08758	38/32	9/8	1 maqvlrgvtv dfpgfderad aetlrkamkg lgtdeesilt lltsrnaqr qeisaafktl 61 fgrdllddk seltgkfekl ivalmkpsrl ydayelkhal kgagtnekvl teiiasrpe 121 elraikqvye eeygssledd vvgdtsgyyq rmlvllqan rdpdagidea qveqdaqalf 181 qagelkwgtd eekfiiiftg rsvshlrkvf dkymtisfgq ietidrets gnleqllav 241 vksirsipay laetlyyamk gagtdhdhli rvmvrsleid lfnirkefrk nfatslysmi 301 kgdtsedykk alllccgedd	36	UP

Signaling						
Ras-related protein Rab-1B	Q9H0U4	29/33	4/4	1 mnpeydylfk lligdsgvg kscllrfad dtyesyist igvdfkirti eldgktiklq 61 iwdtagqerf rtiitssyrg ahgiiivydv tdqesyavnk qwlqeidrya senvnkllvg 121 nksdlttkkv vdnntakefa dslgipflet saknatnveq afmtmaaeik krmgpgaasg 181 gerpnlkids tpvkpagggc c	22	UP
Ras-related protein Rab-7a	P51149	27/28	4/4	1 mtsrkkvllk viilgdsgvg ktslmnqyvn kkfsnqykat igadfltkv mvddrlvtmq 61 iwdtagqerf qslgvafyrg adccvlvfdv tapntfktd swrdefliqa sprdpenfpf 121 vvlgnkidle nrqvatraq awcysknnip yfetsakeai nveqafqtia rnalkqetev 181 elynefpepi kldkndraka saescsc	23	UP
Signal recognition particle 19 kDa protein	P09132	36/45	3/5	1 macaaarspa dqdrficiyp aylnnkktia egrripiska venptateiq dvcsavglv 61 fleknmysr ewnrdrvqyrg rrvqqlkqed gslclvqfps rksvmyaae mipklktrtq 121 ktggadqslq qgegskkgkg kkkk	16	UP
Apoptosis regulator BAX	Q07812	41/41	8/8	1 mdgsgeqprg ggptsseqim ktgallqgf iqdragrmgg eapelaldpv pqdastkkls 61 eclkrigdel dsnmelqrm i aavtdspre vffrvaadm sdgnfnwgrv valyfaskl 121 vikalctkv elirtimgwt ldfirerllg wiqdqggwdg llsyfgtpw qvtifvagv 181 ltsltiwkk mg	21	UP
Low molecular weight phosphotyrosine protein phosphatase	P24666	61/63	8/9	1 maeqatksvl fvlcgnicrs piaevfrkl vtdqnisenw rvdsaatsgy eignppdyrg 61 qscmkrhgip mshvarqitk edfatfdyil cmdesnrlrd nrksnqvktc kakiellgsy 121 dpqkqliied pyygnsdse tvyqqcvcrc raflekeh	18	UP
Enzymes						
Pyruvate kinase PKM	P14618	20/28	6/8	1 mskphseagt afiqtqqlha amadtflehm crididsppi tarntgiict igpasrsvet 61 lkemiksgmn varlnfshgt heyhaetkn vrtatesfas dpilyrpvav aldtkgpeir 121 tglkgsqga evelkkgatl kitldnayme kdenilwld yknickvvev gskiyvddgl 181 islqvkkqga dflvtevang gslgskkgvn lpgaavdlpa vsekdiqdlk fgveqdvdmv 241 faskirkasd vhevrvlge kgkniikiisk ienhegvrrf deileasdgi mvargdlgie 301 ipaekvflaq kmmigrncra gkpvcicatqm lesmikkrp traegsdvan avldgacim 361 lsgetakgdy pleavrmqhl iareaeaaiy hlqlfeelrr lapitsdpte atavgaveas 421 fkccsgaiiv ltkgrsahq varyrprapi iavtrnpqta rqahlyrgif pvckdpvqe 481 awaedvdlrv nfamnvqkar gffkkgdvvi vltgwrpgsg fntmrvvpv p	58	UP
Nucleoside diphosphate kinase B	P22392	69/57	8/8	1 manlertfia ikpdgvqrgl vgeiikrfeq kgfrlvamkf lraseehlkq hyidlkdrpf 61 fpglvkymns gpvavamweg lnvktgrvm lgetnpadsk pgtirgdfci qvgrniihgs 121 dsvksaekei slwfkpeelv dykscahdwv ye	17	DOWN
GAPDH	P04406	39/59	11/11	1 mgkvkvgvng fgrigrivr aafnsgkvdv vaindpfidl nymvymfyd sthgkfhgtv 61 kaengklvin gnpitifer dpskikwga gaeyvvestg vftmekaga hlqggakrvi 121 isapsadapm fvmgvnheky dnsliksna scttnclapl akvihdnfji veglmttvha	36	DOWN

				181 itatqktvdg psgklwrdr galqniipas tgaakavgv ipelngklgt mafvrptanv 241 svldtcrle kpakyddikk vvkqasegpl kgilgytehq vssdfnsdt hstfdagag 301 ialndhfvkl iswydnefgy snrvdlmah maske		
<b>Triosephosphate isomerase</b>	P60174	35/40	6/7	1 maedgeeaeef hfaalyisgq wprlraddl qrlgssamap srkffvgnw kmngrkqslg 61 eligtlnaak vpadtevca pptayidfar qkldpkiava aqncykvtng aftgeispgm 121 ikdcgatwvv lghserrhvf gesdeligqk vahalaeglg viacigekld ereagitek 181 vfeqtkviad nvkdwskvvl ayepvwaigt gktatpqqaq evheklrgwl ksnvsdavaq 241 striiyggsv tgatckelas qpdvdgflvg gaslkpefvd iinakq	27	DOWN
<b>Cytochrome c oxidase subunit 4 isoform 1</b>	P13073	41/53	9/12	1 mlatrsvslv gkraistsvc vrahsvvks edfslpaymd rrdhplpeva hvkhlsasqk 61 alkekekasw sslsmdekve lyrikkesf aemnrgsnew ktvvggamff igftalvimw 121 qkhyvygplp qsfdekewvak qtkrmlmkv npigglaskw dyeknewkk	20	DOWN
<b>Caspase-14</b>	P31944	13/16	3/3	1 msnprselee kydmgarla lilcvtkare gseeddale hmfrqlrfes tmkrdptaeg 61 fqeekfqq aidsredpvs cafvvlmahg regflkgedg emvklenlfe alnnkncqal 121 rakpkvyyiq acrgearpdg etvggdeivm vikdspqtip tytdalhvsy tvegyiayrh 181 dqkgsfiqt lvdvftkrkg hilelltevt rmaaealvq egkarktnpe iqstlrkrl 241 lq	28	DOWN
<b>Chaperones</b>						
<b>Heat shock protein beta-1</b>	P04792	46/52	6/5	1 mterrvpfsl lrgpswdpfr dwyphsrld qafglprlpe ewsqwlggss wpgyvrplpp 61 aaiespavaa paysralsrq lssgvseirh tadrwrslid vnhfapdelt vktkdgvvei 121 tgkheerqde hgyisrcfr kytppgvdp tqvsslspe gtlteamp klatqsneit 181 ipvfesraq lggpeaaksd etaak	23	DOWN
<b>Heat shock cognate 71 kDa protein</b>	P11142	48/53	3/3	1 mskgpavid lgttyscvgv fqhgveia ndqgnrtts yvaftderl igdaaknva 61 mnptntvda krligrrfd avvqsdmkhw pfmvndagr pkvqveykge tksfypeevs 121 smvltkmei aeaylgkvt navvtvpayf ndsqrqatkd agtiaglnvl riineptaaa 181 iaygldkkvg aernvlifdl gggtdvsil tiedgifevk stagdthlgg edfdrmvnh 241 fiaefkrkhk kdisenkrav rrltacera krtlsstqa sieidslyeg idfytsitra 301 rfeelnadlf rgtldpveka lrdakldksq ihdivlvgs tripkiqkl qdffngkeln 361 ksinpdeava ygaavqaail sgdksevad lllldvtpls lgietaggyv tvlikrntti 421 ptkqtqftt ysdnqpgvli qvyegeramt kdnnllgkfe ltgippaprg vpqievtfdi 481 dangilnva vdkstgkenk ititndkgrl skediermvq eaekyaede kqrkvsskn 541 slesyafnmk atvedeklqg kinedkqki ldkcneiinw ldknqtaeke efehqkele 601 kvcnpiitkl yqsaggmpgg mppggfpggga ppsggassgp tieevd	71	-
<b>Caveolin-2</b>	P51636	26/26	3/3	1 mgletekad vqlfmdsys hsgleyadp ekfadsqdr dphrlnshlk lgedviaep 61 vtthsfdkvw icshalfais kyvmykfltv flaiplafia gilfatscl hiwilmfvk 121 tclmvlpsvq tiwksvtdvi iaplctsvgr cfssvslqls qd	18	DOWN
<b>Thioredoxin domain-containing protein 12</b>	O95881	30/36	4/3	1 metrprlgat clgfsfll visdghngl gkgfgdhiw rtedgkkea aasglplmvi 61 ihswcwgack alpkfaest eiselsnhfv mvnledeeeep kdedspdg yiprllfdp 121 sgkvhpeiin engnpsykyf yvsaeqvvg mkeaqerltg dafrkkhled el	19	DOWN

<b>Microsomal glutathione S-transferase 3</b>	O14880	34/52	3/6	1 mavlskeygf vlltgaasfi mvahlainvs karkkykvey pimystdpen ghifnciqra 61 hqntlevypp flfflavggv yhpriasglg lawivgrlv aygyytgeps krsrgalgsi 121 allglvgttv csafqhlgwv ksglsgspkc ch	17	DOWN
<b>Microsomal glutathione S-transferase 1</b>	P10620	20/27	4/4	1 mvdltqvmdd evmfafasya tiilskmmlm statafyrlt rkvanpedc vafgkgenak 61 kylrtddrve rvrrahlnl eniipflgig llyslsgdpd stailhrfl vgariyhtia 121 yltplqpnr alsffvgygv tismayrllk sklyl	18	DOWN
<b>Protein Folding</b>						
<b>Peptidyl-prolyl cis-trans isomerase NIMA-interacting 1</b>	Q13526	47/26	5/3	1 madeeklppg wekrmsrsg rvyvfnhitn asqwerpsgn sssggkngqg eparvrcshl 61 lvkhsqsrp sswrqekitr tkeaelelin gyiqkiksge edfeslasqf sdcssakarg 121 dlgafrsqm qkpfedasfa lrtgemsgpv ftdsgihil rte	18	DOWN
<b>Translocon-associated protein subunit delta</b>	P51571	36/36	5/5	1 maamaslga alllsslsr csaeaclepq itpsytttd avistetvfi veislctknr 61 vqnmalyadv ggkqfpvtrg qdvgrqvsw sldhksahag tyevrffdee sysllrkaqr 121 nnedisiipp lftsvdhrng twngpwwste vlaaiglvi yylafsaksh iqa	19	UP
<b>Other proteins</b>						
<b>Voltage-dependent anion-selective channel protein 1</b>	P21796	15/15	3/3	1 mavpptyadl gksardvftk gygfglikld lktsengle ftssgsante tktvgslet 61 kyrwteyglf ftekwntdnt lgeitvedq larglkltd sfspsntgkk nakiktgykr 121 ehinlgcdmd fdiagpsirg alvlyegwl agyqmnfeta ksrvtqsnfa vgyktdefql 181 htnvndgtef ggsiyqkvnk kletavnlaw tagnsntrfg iaakyqidpd acfsakvnns 241 sliglytqt lkpgiklts alldgknvna gghklglgle fqa	31	DOWN
<b>CD59 glycoprotein</b>	P13987	28/28	5/6	1 mgiqggsvlf gllvlavfc hshslqcyn cpnptadckt avncssdfa clitkaglv 61 ynkckwfehcnfndvtrlr eneltyyck kdlcnfneql enggtlslek tvllvtpfl 121 aaawslhp	14	DOWN
<b>40S ribosomal protein S18</b>	P62269	37/53	8/12	1 mslvipekfq hilrvlntni dgrrkiafai taikgvrry ahvvlrkadi dltrkragelt 61 edeverviti mqnrqykip dwflnrqkdv kdgkysqlva ngldnkred lerlkkirah 121 rglrhfwglr vrgqhtktg rrgrtvgvsk kk	18	DOWN
<b>60S ribosomal protein L22</b>	P35268	59/69	7/9	1 mapvkklvk ggkkkkqvlk fltdcthpve dgimdaanfe qflqerikvn gkagnlgggy 61 vtierskski tvtsevpfsk rykyltkky lkknrlrdwl rvvanskesy elryfqinqd 121 eeeeeed	15	UP

## References

---

- Abbasian, N., Herbert, K., Bevington, A., Brunskill, N., and Burton, J., 2012. Hyperphosphataemia and microvesicle formation: a novel mechanism for cardiovascular risk in chronic kidney disease. *Nephrology Dialysis Transplantation*. **27**, ii227-ii251.
- Abcam, 2014 [online]. Available at: <http://www.abcam.com/ps/pdf/protocols/histone%20western%20blotting.pdf> [accessed 16/07/2014].
- Abraham, M.C. & Shaham, S., 2004. Death without caspases, caspases without death. *Trends in Cell Biology*. **14**, 184-193.
- Adler, A.J., Ferran, N., Berlyne, G.M., 1985. Effect of inorganic phosphate on serum ionized calcium concentration in vitro: A reassessment of the " trade-off hypothesis". *Kidney International*. **28**, .
- Agouni, A., Lagrue-Lak-Hal, A.H., Ducluzeau, P.H., Mostefai, H.A., Draunet-Busson, C., Leftheriotis, G., Heymes, C., Martinez, M.C., Andriantsitohaina, R., 2008. Endothelial dysfunction caused by circulating microparticles from patients with metabolic syndrome. *American Journal of Pathology*. **173**, 1210-1219.
- Aharon, A., Katzenell, S., Tamari, T., Brenner, B., 2009. Microparticles bearing tissue factor and tissue factor pathway inhibitor in gestational vascular complications. *Journal of Thrombosis and Haemostasis : JTH*. **7**, 1047-1050.
- Ahmed, N. & Behzad, F., 2011. Disorders of calcium, phosphate, and magnesium homeostasis. In Ahmed, N., ed, *Clinical Biochemistry*. First ed. United States: Oxford University Press. 255-296.
- Alessio, M., De Monte, L., Scirea, A., Gruarin, P., Tandon, N.N., Sitia, R., 1996. Synthesis, processing, and intracellular transport of CD36 during monocytic differentiation. *Journal of Biological Chemistry*. **271**, 1770-1775.
- Alkhatatbeh, M., Enjeti, A., Acharya, S., Thorne, R., Lincz, L., 2013. The origin of circulating CD36 in type 2 diabetes. *Nutrition & Diabetes*. **3**, e59.
- Amabile, N. & Boulanger, C.M., 2011. Circulating microparticle levels in patients with coronary artery disease: a new indicator of vulnerability? *European Heart Journal*. **32**, 1958-1960.
- Amabile, N., Guerin, A.P., Leroyer, A., Mallat, Z., Nguyen, C., Boddaert, J., London, G.M., Tedgui, A., Boulanger, C.M., 2005. Circulating endothelial microparticles are associated with vascular dysfunction in patients with end-stage renal failure. *Journal of the American Society of Nephrology : JASN*. **16**, 3381-3388.
- Amabile, N., Guerin, A.P., Tedgui, A., Boulanger, C.M., London, G.M., 2012. Predictive value of circulating endothelial microparticles for cardiovascular mortality in end-stage renal failure: a

pilot study. *Nephrology, Dialysis, Transplantation : Official Publication of the European Dialysis and Transplant Association - European Renal Association*. **27**, 1873-1880.

Ammollo, C., Semeraro, F., Xu, J., Esmon, N., Esmon, C., 2011. Extracellular histones increase plasma thrombin generation by impairing thrombomodulin-dependent protein C activation. *Journal of Thrombosis and Haemostasis*. **9**, 1795-1803.

Andriantsitohaina, R., Gaceb, A., Vergori, L., Martínez, M.C., 2012. Microparticles as regulators of cardiovascular inflammation. *Trends in Cardiovascular Medicine*. **22**, 88-92.

Ardoin, S., Shanahan, J., Pisetsky, D., 2007. The role of microparticles in inflammation and thrombosis. *Scandinavian Journal of Immunology*. **66**, 159-165.

Arici, M., Brown, J., Walls, J., Bevington, A., 2004. Free amino acids mimic the anabolic but not the proliferative effect of albumin in OK proximal tubular cells. *Cell Biochemistry and Function*. **22**, 1-7.

Ark, M., Özdemir, A., Polat, B., 2010. Ouabain-induced apoptosis and Rho kinase: a novel caspase-2 cleavage site and fragment of Rock-2. *Apoptosis*. **15**, 1494-1506.

Arking, D.E., Becker, D.M., Yanek, L.R., Fallin, D., Judge, D.P., Moy, T.F., Becker, L.C., Dietz, H.C., 2003. < i> KLOTTHO Allele Status and the Risk of Early-Onset Occult Coronary Artery Disease. *The American Journal of Human Genetics*. **72**, 1154-1161.

Ayers, L., Kohler, M., Harrison, P., Sargent, I., Dragovic, R., Schaap, M., Nieuwland, R., Brooks, S.A., Ferry, B., 2011. Measurement of circulating cell-derived microparticles by flow cytometry: sources of variability within the assay. *Thrombosis Research*. **127**, 370-377.

Bacconi, A., Virkki, L.V., Biber, J., Murer, H., Forster, I.C., 2005. Renouncing electroneutrality is not free of charge: switching on electrogenicity in a Na<sup>+</sup>-coupled phosphate cotransporter. *Proceedings of the National Academy of Sciences of the United States of America*. **102**, 12606-12611.

Bachetti, T., Comini, L., Curello, S., Bastianon, D., Palmieri, M., Bresciani, G., Callea, F., Ferrari, R., 2004. Co-expression and modulation of neuronal and endothelial nitric oxide synthase in human endothelial cells. *Journal of Molecular and Cellular Cardiology*. **37**, 939-945.

Banfi, C., Brioschi, M., Wait, R., Begum, S., Gianazza, E., Pirillo, A., Mussoni, L., Tremoli, E., 2005. Proteome of endothelial cell-derived procoagulant microparticles. *Proteomics*. **5**, 4443-4455.

Bansal, V.K., 1990. Serum Inorganic Phosphorus. In Walker, H. K., Hall, W. D. and Hurst, J. W., eds, *Clinical Methods: The History, Physical, and Laboratory Examinations*. 3rd ed. Boston: Butterworth Publishers, a division of Reed Publishing.

Bardin, N., Anfosso, F., Masse, J.M., Cramer, E., Sabatier, F., Le Bivic, A., Sampol, J., Dignat-George, F., 2001. Identification of CD146 as a component of the endothelial junction involved in the control of cell-cell cohesion. *Blood*. **98**, 3677-3684.

- Batool, S., Abbasian, N., Burton, J.O., Stover, C., 2013. Microparticles and their Roles in Inflammation: A Review. *Open Immunology Journal*. **6**, 1-14.
- Beck, L., Leroy, C., Salaun, C., Margall-Ducos, G., Desdouets, C., Friedlander, G., 2009. Identification of a novel function of PiT1 critical for cell proliferation and independent of its phosphate transport activity. *The Journal of Biological Chemistry*. **284**, 31363-31374.
- Beg, Z.H., Stonik, J.A., Brewer, H.B., Jr, 1978. 3-Hydroxy-3-methylglutaryl coenzyme A reductase: regulation of enzymatic activity by phosphorylation and dephosphorylation. *Proceedings of the National Academy of Sciences of the United States of America*. **75**, 3678-3682.
- Bellocchio, E.E., Reimer, R.J., Fremeau, R.T., Jr, Edwards, R.H., 2000. Uptake of glutamate into synaptic vesicles by an inorganic phosphate transporter. *Science (New York, N.Y.)*. **289**, 957-960.
- Berckmans, R.J., Nieuwland, R., Boing, A., Romijn, F., Hack, C.E., Sturk, A., 2001. Cell-derived microparticles circulate in healthy humans and support low grade thrombin generation. *THROMBOSIS AND HAEMOSTASIS-STUTTGART*. **85**, 639-646.
- Bergwitz, C. & Jüppner, H., 2011. Phosphate sensing. *Advances in Chronic Kidney Disease*. **18**, 132-144.
- Bergwitz, C., Roslin, N.M., Tieder, M., Loredó-Osti, J., Bastepe, M., Abu-Zahra, H., Frappier, D., Burkett, K., Carpenter, T.O., Anderson, D., 2006. SLC34A3 Mutations in Patients with Hereditary Hypophosphatemic Rickets with Hypercalciuria Predict a Key Role for the Sodium-Phosphate Cotransporter NaP<sub>IIc</sub> in Maintaining Phosphate Homeostasis. *The American Journal of Human Genetics*. **78**, 179-192.
- Bernal-Mizrachi, L., Jy, W., Fierro, C., Macdonough, R., Velazques, H.A., Purow, J., Jimenez, J.J., Horstman, L.L., Ferreira, A., de Marchena, E., 2004. Endothelial microparticles correlate with high-risk angiographic lesions in acute coronary syndromes. *International Journal of Cardiology*. **97**, 439-446.
- Berne, R.M., Levy, M.N., Stanton, B.A. and Koeppen, B.M., 2000. Principles of physiology. In Koeppen, B.M. and Stanton, B.A., ed, 3rd ed. Mosby St. Louis, Missouri, USA. 408-478.
- Bevington, A., Kemp, G., Graham, R., RUSSEL, G., 1992. Phosphate-sensitive enzymes: a possible molecular basis for cellular disorders of phosphate metabolism. *Clinical Chemistry and Enzymology Communications*. **4**, 235-257.
- Bevington, A., Mundy, K., Yates, A., Kanis, J., Russell, R., 1986. A study of intracellular orthophosphate concentration in human muscle and erythrocytes by <sup>31</sup>P nuclear magnetic resonance spectroscopy and selective chemical assay. *Clinical Science (1986)*. **71**, 129-735.
- Bevington, A., Brough, D., Baker, F.E., Hattersley, J., Walls, J., 1995. Metabolic acidosis is a potent stimulus for cellular inorganic phosphate generation in uraemia. *Clinical Science*. **88**, 405-412.

- Bevington, A, Kemp, G.J and Russell, R.G.G., 1990. ACQUIRED DISORDERS OF PHOSPHATE METABOLISM. In R.D.COHEN, B.LEWIS, K.G.M.M.ALBERTI, A.M.DENMAN, BAILLIERE TINDALL, ed, *The Metabolic and Molecular Basis of Acquired Disease*. 1st ed. Suffolk: Bailliere Tindall. 1097-1117.
- Bian, A., Xing, C., Hu, M., 2014. Alpha Klotho and phosphate homeostasis. *Journal of Endocrinological Investigation*. **37**, 1121-1126.
- Biber, J., Caderas, G., Stange, G., Werner, A., Murer, H., 1993. Effect of low-phosphate diet on sodium/phosphate cotransport mRNA and protein content and on oocyte expression of phosphate transport. *Pediatric Nephrology*. **7**, 823-826.
- Bick, R.L., 2003. Cancer-associated thrombosis. *New England Journal of Medicine*. **349**, 109-110.
- Blann, A., Shantsila, E., Shantsila, A., 2009. Microparticles and arterial disease. *Seminars in Thrombosis and Hemostasis*. **35**, 488-496.
- Boger, R.H., 2004. Asymmetric dimethylarginine, an endogenous inhibitor of nitric oxide synthase, explains the "L-arginine paradox" and acts as a novel cardiovascular risk factor. *The Journal of Nutrition*. **134**, 2842S-2847S; discussion 2853S.
- Boos, C.J., Lip, G.Y., Blann, A.D., 2006. Circulating endothelial cells in cardiovascular disease. *Journal of the American College of Cardiology*. **48**, 1538-1547.
- Bose, S., French, S., Evans, F.J., Joubert, F., Balaban, R.S., 2003. Metabolic network control of oxidative phosphorylation: multiple roles of inorganic phosphate. *The Journal of Biological Chemistry*. **278**, 39155-39165.
- Bottger, P. & Pedersen, L., 2011. Mapping of the minimal inorganic phosphate transporting unit of human PiT2 suggests a structure universal to PiT-related proteins from all kingdoms of life. *BMC Biochemistry*. **12**, 21-2091-12-21.
- Boulanger, C.M., Amabile, N., Guerin, A.P., Pannier, B., Leroyer, A.S., Mallat, Z., Nguyen, C., Tedgui, A., London, G.M., 2007. In vivo shear stress determines circulating levels of endothelial microparticles in end-stage renal disease. *Hypertension*. **49**, 902-908.
- Boulanger, C.M. & Dignat-George, F., 2011. Microparticles: an introduction. *Arteriosclerosis, Thrombosis, and Vascular Biology*. **31**, 2-3.
- Bovellan, M., Fritzsche, M., Stevens, C., Charras, G., 2010. Death-associated protein kinase (DAPK) and signal transduction: blebbing in programmed cell death. *FEBS Journal*. **277**, 58-65.
- Boyd, R.D., Pichaimuthu, S.K., Cuenat, A., 2011. New approach to inter-technique comparisons for nanoparticle size measurements; using atomic force microscopy, nanoparticle tracking analysis and dynamic light scattering. *Colloids and Surfaces A: Physicochemical and Engineering Aspects*. **387**, 35-42.
- Brand, I. & Söling, H., 1975. Activation and inactivation of rat liver phosphofructokinase by phosphorylation—dephosphorylation. *FEBS Letters*. **57**, 163-168.

- Bright, R., 1837. *Cases and observations illustrative of renal disease accompanied with the secretion of albuminous urine*. A. Waldie.
- Brill, A., Dashevsky, O., Rivo, J., Gozal, Y., Varon, D., 2005. Platelet-derived microparticles induce angiogenesis and stimulate post-ischemic revascularization. *Cardiovascular Research*. **67**, 30-38.
- Brodsky, S.V., Zhang, F., Nasjletti, A., Goligorsky, M.S., 2004. Endothelium-derived microparticles impair endothelial function in vitro. *American Journal of Physiology. Heart and Circulatory Physiology*. **286**, H1910-5.
- Brogan, P., Shah, V., Brachet, C., Harnden, A., Mant, D., Klein, N., Dillon, M., 2004. Endothelial and platelet microparticles in vasculitis of the young. *Arthritis & Rheumatism*. **50**, 927-936.
- Brunet, P., Gondouin, B., Duval-Sabatier, A., Dou, L., Cerini, C., Dignat-George, F., Jourde-Chiche, N., Argiles, A., Burtey, S., 2011. Does uremia cause vascular dysfunction? *Kidney & Blood Pressure Research*. **34**, 284-290.
- Brunskill, N.J., 2004. Albumin signals the coming of age of proteinuric nephropathy. *Journal of the American Society of Nephrology*. **15**, 504.
- Buesing, K.L., Densmore, J.C., Kaul, S., Pritchard Jr, K.A., Jarzembowski, J.A., Gourlay, D.M., Oldham, K.T., 2011. Endothelial microparticles induce inflammation in acute lung injury. *Journal of Surgical Research*. **166**, 32-39.
- Burger, D., Schock, S., Thompson, C.S., Montezano, A.C., Hakim, A.M., Touyz, R.M., 2013. Microparticles: biomarkers and beyond. *Clinical Science*. **124**, 423-441.
- Burger, D., Thibodeau, J.F., Holterman, C.E., Burns, K.D., Touyz, R.M., Kennedy, C.R., 2014. Urinary Podocyte Microparticles Identify Prealbuminuric Diabetic Glomerular Injury. *Journal of the American Society of Nephrology : JASN*.
- Burnier, L., Fontana, P., Kwak, B.R., Angelillo-Scherrer, A., 2009. Cell-derived microparticles in haemostasis and vascular medicine. *Thrombosis and Haemostasis*. **101**, 439-451.
- Burnouf, T., Goubran, H.A., Chou, M., Devos, D., Radosevic, M., 2014. Platelet microparticles: Detection and assessment of their paradoxical functional roles in disease and regenerative medicine. *Blood Reviews*.
- Burton, J.O., Hamali, H.A., Singh, R., Abbasian, N., Parsons, R., Patel, A.K., Goodall, A.H., Brunskill, N.J., 2013. Elevated Levels of Procoagulant Plasma Microvesicles in Dialysis Patients. *PLoS One*. **8**, e72663.
- Buzalaf, M.A., Taga, E., Granjeiro, J.M., Ferreira, C.V., Lourença, V.A., Ortega, M.M., Poletto, D.W., Aoyama, H., 1998. Kinetic characterization of bovine lung low-molecular-weight protein tyrosine phosphatase. *Experimental Lung Research*. **24**, 269-272.
- Caen, J.P. & Rosa, J.P., 1995. Platelet-vessel wall interaction: from the bedside to molecules. *Thrombosis and Haemostasis*. **74**, 18-24.

- Camus, S.M., Gausseres, B., Bonnin, P., Loufrani, L., Grimaud, L., Charue, D., De Moraes, J.A., Renard, J.M., Tedgui, A., Boulanger, C.M., Tharaux, P.L., Blanc-Brude, O.P., 2012. Erythrocyte microparticles can induce kidney vaso-occlusions in a murine model of sickle cell disease. *Blood*. **120**, 5050-5058.
- Capella, L.S., Gefé, M., Silva, E.F., Morales, M.M., Affonso-Mitidieri, O., Lopes, A.G., Rumjanek, V.M., Capella, M.A., 2001. Reduced glutathione protect cells from ouabain toxicity. *Biochimica Et Biophysica Acta (BBA)-General Subjects*. **1526**, 293-300.
- Carr, B. & Malloy, A., *NanoParticle Tracking Analysis–The NANOSIGHT System*.
- Cecil, D.L., Rose, D.M., Terkeltaub, R., Liu-Bryan, R., 2005. Role of interleukin-8 in PiT-1 expression and CXCR1-mediated inorganic phosphate uptake in chondrocytes. *Arthritis & Rheumatism*. **52**, 144-154.
- Cerini, C., Dou, L., Anfosso, F., Sabatier, F., Moal, V., Glorieux, G., De Smet, R., Vanholder, R., Dignat-George, F., Sampol, J., 2004. P-cresol, a uremic retention solute, alters the endothelial barrier function in vitro. *THROMBOSIS AND HAEMOSTASIS-STUTTGART-*. **92**, 140-150.
- Challa, A., Bevington, A., Angier, C., Asbury, A., Preston, C., Russell, R., 1985. A technique for the measurement of orthophosphate in human erythrocytes, and some studies of its determinants. *Clinical Science*. **69**, 429-434.
- Chargaff, e. & West, r., 1946. The biological significance of the thromboplastic protein of blood. *The Journal of Biological Chemistry*. **166**, 189-197.
- Chi, J.T., Chang, H.Y., Haraldsen, G., Jahnsen, F.L., Troyanskaya, O.G., Chang, D.S., Wang, Z., Rockson, S.G., van de Rijn, M., Botstein, D., Brown, P.O., 2003. Endothelial cell diversity revealed by global expression profiling. *Proceedings of the National Academy of Sciences of the United States of America*. **100**, 10623-10628.
- Chironi, G.N., Boulanger, C.M., Simon, A., Dignat-George, F., Freyssinet, J.M., Tedgui, A., 2009. Endothelial microparticles in diseases. *Cell and Tissue Research*. **335**, 143-151.
- Chironi, G.N., Simon, A., Boulanger, C.M., Dignat-George, F., Hugel, B., Megnien, J.L., Lefort, M., Freyssinet, J.M., Tedgui, A., 2010. Circulating microparticles may influence early carotid artery remodeling. *Journal of Hypertension*. **28**, 789-796.
- Choi, K., Kennedy, M., Kazarov, A., Papadimitriou, J.C., Keller, G., 1998. A common precursor for hematopoietic and endothelial cells. *Development (Cambridge, England)*. **125**, 725-732.
- Classics Lowry, O., Rosebrough, N., Farr, A., Randall, R., 1951. Protein measurement with the Folin phenol reagent. *J Biol Chem*. **193**, 265-275.
- Cohen, L.F., Balow, J.E., Magrath, I.T., Poplack, D.G., Ziegler, J.L., 1980. Acute tumor lysis syndrome: a review of 37 patients with Burkitt's lymphoma. *The American Journal of Medicine*. **68**, 486-491.

- Cole, A., Frame, S., Cohen, P., 2004. Further evidence that the tyrosine phosphorylation of glycogen synthase kinase-3 (GSK3) in mammalian cells is an autophosphorylation event. *Biochem.J.* **377**, 249-255.
- Collins, J.F., Bai, L., Ghishan, F.K., 2004. The SLC20 family of proteins: dual functions as sodium-phosphate cotransporters and viral receptors. *Pflügers Archiv.* **447**, 647-652.
- Covic, A., Kothawala, P., Bernal, M., Robbins, S., Chalian, A., Goldsmith, D., 2009. Systematic review of the evidence underlying the association between mineral metabolism disturbances and risk of all-cause mortality, cardiovascular mortality and cardiovascular events in chronic kidney disease. *Nephrology, Dialysis, Transplantation : Official Publication of the European Dialysis and Transplant Association - European Renal Association.* **24**, 1506-1523.
- Cox, T.M., 2002. The genetic consequences of our sweet tooth. *Nature Reviews Genetics.* **3**, 481-487.
- Crescitelli, R., Lässer, C., Szabo, T.G., Kittel, A., Eldh, M., Dianzani, I., Buzás, E.I., Lötvall, J., 2013. Distinct RNA profiles in subpopulations of extracellular vesicles: apoptotic bodies, microvesicles and exosomes. *Journal of Extracellular Vesicles.* **2**, .
- Crouthamel, M.H., Lau, W.L., Leaf, E.M., Chavkin, N.W., Wallingford, M.C., Peterson, D.F., Li, X., Liu, Y., Chin, M.T., Levi, M., Giachelli, C.M., 2013. Sodium-dependent phosphate cotransporters and phosphate-induced calcification of vascular smooth muscle cells: redundant roles for PiT-1 and PiT-2. *Arteriosclerosis, Thrombosis, and Vascular Biology.* **33**, 2625-2632.
- Custer, M., Lotscher, M., Biber, J., Murer, H., Kaissling, B., 1994. Expression of Na-P(i) cotransport in rat kidney: localization by RT-PCR and immunohistochemistry. *The American Journal of Physiology.* **266**, F767-74.
- Dai, X., Zhao, M., Cai, Y., Guan, Q., Zhao, Y., Guan, Y., Kong, W., Zhu, W., Xu, M., Wang, X., 2013. Phosphate-induced autophagy counteracts vascular calcification by reducing matrix vesicle release. *Kidney International.* **83**, 1042-1051.
- Danziger, J., 2008. Importance of low-grade albuminuria, *Mayo Clinic Proceedings*, 2008, Elsevier pp806-812.
- Date, K., Hall, J., Greenman, J., Maraveyas, A., Madden, L.A., 2013. Tumour and microparticle tissue factor expression and cancer thrombosis. *Thrombosis Research.* **131**, 109-115.
- David, S., Kumpers, P., Lukasz, A., Fliser, D., Martens-Lobenhoffer, J., Bode-Boger, S.M., Kliem, V., Haller, H., Kielstein, J.T., 2010. Circulating angiopoietin-2 levels increase with progress of chronic kidney disease. *Nephrology, Dialysis, Transplantation : Official Publication of the European Dialysis and Transplant Association - European Renal Association.* **25**, 2571-2576.
- Dawson, D.W., Pearce, S.F., Zhong, R., Silverstein, R.L., Frazier, W.A., Bouck, N.P., 1997. CD36 mediates the In vitro inhibitory effects of thrombospondin-1 on endothelial cells. *The Journal of Cell Biology.* **138**, 707-717.

De Lorenzo, A., Noce, A., Bigioni, M., Calabrese, V., Della Rocca, D., Daniele, N., Tozzo, C., Renzo, L.D., 2010. The effects of Italian Mediterranean organic diet (IMOD) on health status. *Current Pharmaceutical Design*. **16**, 814-824.

Dejana, E., Orsenigo, F., Lampugnani, M.G., 2008. The role of adherens junctions and VE-cadherin in the control of vascular permeability. *Journal of Cell Science*. **121**, 2115-2122.

Del Conde, I., Cruz, M.A., Zhang, H., Lopez, J.A., Afshar-Kharghan, V., 2005. Platelet activation leads to activation and propagation of the complement system. *The Journal of Experimental Medicine*. **201**, 871-879.

Denison, T.A., Koch, C.F., Shapiro, I.M., Schwartz, Z., Boyan, B.D., 2009. Inorganic phosphate modulates responsiveness to 24, 25 (OH) 2D3 in chondrogenic ATDC5 cells. *Journal of Cellular Biochemistry*. **107**, 155-162.

Dey-Hazra, E., Hertel, B., Kirsch, T., Woywodt, A., Lovric, S., Haller, H., Haubitz, M., Erdbruegger, U., 2010. Detection of circulating microparticles by flow cytometry: influence of centrifugation, filtration of buffer, and freezing. *Vascular Health and Risk Management*. **6**, 1125.

Di Marco, G.S., König, M., Stock, C., Wiesinger, A., Hillebrand, U., Reiermann, S., Reuter, S., Amler, S., Köhler, G., Buck, F., 2012. High phosphate directly affects endothelial function by downregulating annexin II. *Kidney International*. **83**, 213-222.

Di Marco, G.S., Hausberg, M., Hillebrand, U., Rustemeyer, P., Wittkowski, W., Lang, D., Pavenstadt, H., 2008. Increased inorganic phosphate induces human endothelial cell apoptosis in vitro. *American Journal of Physiology.Renal Physiology*. **294**, F1381-7.

Dick, C.F., Dos-Santos, A.L., Meyer-Fernandes, J.R., 2011. Inorganic phosphate as an important regulator of phosphatases. *Enzyme Research*. **2011**, 103980.

Distler, J., Huber, L., Hueber, A., Reich III, C., Gay, S., Distler, O., Pisetsky, D., 2005. The release of microparticles by apoptotic cells and their effects on macrophages. *Apoptosis*. **10**, 731-741.

Donadee, C., Raat, N.J., Kanas, T., Tejero, J., Lee, J.S., Kelley, E.E., Zhao, X., Liu, C., Reynolds, H., Azarov, I., Frizzell, S., Meyer, E.M., Donnenberg, A.D., Qu, L., Triulzi, D., Kim-Shapiro, D.B., Gladwin, M.T., 2011. Nitric oxide scavenging by red blood cell microparticles and cell-free hemoglobin as a mechanism for the red cell storage lesion. *Circulation*. **124**, 465-476.

Dragovic, R.A., Gardiner, C., Brooks, A.S., Tannetta, D.S., Ferguson, D.J., Hole, P., Carr, B., Redman, C.W., Harris, A.L., Dobson, P.J., 2011. Sizing and phenotyping of cellular vesicles using Nanoparticle Tracking Analysis. *Nanomedicine: Nanotechnology, Biology and Medicine*. **7**, 780-788.

Duranton, F., Cohen, G., De Smet, R., Rodriguez, M., Jankowski, J., Vanholder, R., Argiles, A., European Uremic Toxin Work Group, 2012. Normal and pathologic concentrations of uremic toxins. *Journal of the American Society of Nephrology : JASN*. **23**, 1258-1270.

Dursun, I., Poyrazoglu, H.M., Gunduz, Z., Ulger, H., Yykylmaz, A., Dusunsel, R., Patyroglu, T., Gurgoze, M., 2009. The relationship between circulating endothelial microparticles and arterial

stiffness and atherosclerosis in children with chronic kidney disease. *Nephrology, Dialysis, Transplantation : Official Publication of the European Dialysis and Transplant Association - European Renal Association*. **24**, 2511-2518.

Edelstein, C.L., 2010. *Biomarkers of kidney disease*. Academic Press.

Edgell, C.J., McDonald, C.C., Graham, J.B., 1983. Permanent cell line expressing human factor VIII-related antigen established by hybridization. *Proceedings of the National Academy of Sciences of the United States of America*. **80**, 3734-3737.

Edmund Lamb, 2011. Kidney disease. In Nessar Ahmed, ed, *Clinical Biochemistry*. 1st ed. United States: Oxford University Press. 59-98.

Eilertsen, K. & Østerud, B., 2004. Tissue factor:(patho) physiology and cellular biology. *Blood Coagulation & Fibrinolysis*. **15**, 521-538.

Eisenreich, A., Malz, R., Pepke, W., Ayril, Y., Poller, W., Schultheiss, H., Rauch, U., 2009. Role of the phosphatidylinositol 3-kinase/protein kinase B pathway in regulating alternative splicing of tissue factor mRNA in human endothelial cells. *Circ J*. **73**, 1746-1752.

El-Andaloussi, S., Lee, Y., Lakhali-Littleton, S., Li, J., Seow, Y., Gardiner, C., Alvarez-Erviti, L., Sargent, I.L., Wood, M.J., 2012. Exosome-mediated delivery of siRNA in vitro and in vivo. *Nature Protocols*. **7**, 2112-2126.

Ellam, T.J. & Chico, T.J., 2012. Phosphate: the new cholesterol? The role of the phosphate axis in non-uremic vascular disease. *Atherosclerosis*. **220**, 310-318.

Emilian, C., Goretti, E., Prospert, F., Pouthier, D., Duhoux, P., Gilson, G., Devaux, Y., Wagner, D.R., 2012. MicroRNAs in Patients on Chronic Hemodialysis (MINOS Study). *Clinical Journal of the American Society of Nephrology*. **7**, 619-623.

Enjeti, A.K., Lincz, L.F., Seldon, M., 2008. Microparticles in health and disease. *Seminars in Thrombosis and Hemostasis*. **34**, 683-691.

Erdbruegger, U., Haubitz, M., Woywodt, A., 2006. Circulating endothelial cells: a novel marker of endothelial damage. *Clinica Chimica Acta*. **373**, 17-26.

Essayagh, S., Brisset, A., Terrisse, A., Dupouy, D., Tellier, L., Navarro, C., Arnal, J., Sié, P., 2005. Microparticles from apoptotic vascular smooth muscle cells induce endothelial dysfunction, a phenomenon prevented by beta3-integrin antagonists. *THROMBOSIS AND HAEMOSTASIS-STUTTGART*. **94**, 853.

Evans, K., Nasim, Z., Brown, J., Butler, H., Kauser, S., Varoqui, H., Erickson, J.D., Herbert, T.P., Bevington, A., 2007. Acidosis-sensing glutamine pump SNAT2 determines amino acid levels and mammalian target of rapamycin signalling to protein synthesis in L6 muscle cells. *Journal of the American Society of Nephrology : JASN*. **18**, 1426-1436.

Ewence, A.E., Bootman, M., Roderick, H.L., Skepper, J.N., McCarthy, G., Epple, M., Neumann, M., Shanahan, C.M., Proudfoot, D., 2008. Calcium phosphate crystals induce cell death in

human vascular smooth muscle cells: a potential mechanism in atherosclerotic plaque destabilization. *Circulation Research*. **103**, e28-34.

Fang, S.H., Yuan, Y.M., Peng, F., Li, C.T., Zhang, L.H., Lu, Y.B., Zhang, W.P., Wei, E.Q., 2009. Pranlukast attenuates ischemia-like injury in endothelial cells via inhibiting reactive oxygen species production and nuclear factor-kappaB activation. *Journal of Cardiovascular Pharmacology*. **53**, 77-85.

Farrell, K.B., Russ, J.L., Murthy, R.K., Eiden, M.V., 2002. Reassessing the role of region A in Pit1-mediated viral entry. *Journal of Virology*. **76**, 7683-7693.

Farrell, K.B., Tusnady, G.E., Eiden, M.V., 2009. New structural arrangement of the extracellular regions of the phosphate transporter SLC20A1, the receptor for gibbon ape leukemia virus. *The Journal of Biological Chemistry*. **284**, 29979-29987.

Faure, V., Dou, L., Sabatier, F., Cerini, C., Sampol, J., Berland, Y., Brunet, P., Dignat-George, F., 2006. Elevation of circulating endothelial microparticles in patients with chronic renal failure. *Journal of Thrombosis and Haemostasis*. **4**, 566-573.

Feehally, J., Floege, J. and Johnson, R.J., 2008. Renal Anatomy and Renal Physiology. In Kriz, W., Elger, M., Shirley, G. D., Capasso, G. and Unwin, J. R., eds, *Comprehensive clinical nephrology*. Third Edition ed. China: Mosby, Inc., an affiliate of Elsevier Inc. 1-34.

Festing, M.H., Speer, M.Y., Yang, H., Giachelli, C.M., 2009. Generation of mouse conditional and null alleles of the type III sodium-dependent phosphate cotransporter PiT-1. *Genesis*. **47**, 858-863.

Fink, K., Feldbrügge, L., Schwarz, M., Bourgeois, N., Helbing, T., Bode, C., Schwab, T., Busch, H., 2011. Circulating annexin V positive microparticles in patients after successful cardiopulmonary resuscitation. *Crit Care*. **15**, R251.

Fliser, D., Kielstein, J.T., Haller, H., Bode-Böger, S.M., 2003. Asymmetric dimethylarginine: A cardiovascular risk factor in renal disease? *Kidney International*. **63**, S37-S40.

Fliser, D., Kollerits, B., Neyer, U., Ankerst, D.P., Lhotta, K., Lingenhel, A., Ritz, E., Kronenberg, F., MMKD Study Group, Kuen, E., Konig, P., Kraatz, G., Mann, J.F., Muller, G.A., Kohler, H., Riegler, P., 2007. Fibroblast growth factor 23 (FGF23) predicts progression of chronic kidney disease: the Mild to Moderate Kidney Disease (MMKD) Study. *Journal of the American Society of Nephrology : JASN*. **18**, 2600-2608.

Flynn, P.D., Byrne, C.D., Baglin, T.P., Weissberg, P.L., Bennett, M.R., 1997. Thrombin generation by apoptotic vascular smooth muscle cells. *Blood*. **89**, 4378-4384.

Foley, R.N., Parfrey, P.S., Sarnak, M.J., 1998<sub>a</sub>. Clinical epidemiology of cardiovascular disease in chronic renal disease. *American Journal of Kidney Diseases*. **32**, S112-S119.

Foley, R.N., Collins, A.J., Herzog, C.A., Ishani, A., Kalra, P.A., 2009. Serum phosphorus levels associate with coronary atherosclerosis in young adults. *Journal of the American Society of Nephrology : JASN*. **20**, 397-404.

- Foley, R.N., Parfrey, P.S., Sarnak, M.J., 1998<sub>b</sub>. Epidemiology of cardiovascular disease in chronic renal disease. *Journal of the American Society of Nephrology : JASN.* **9**, S16-23.
- Forster, I.C., Hernando, N., Biber, J., Murer, H., 2013. Phosphate transporters of the SLC20 and SLC34 families. *Molecular Aspects of Medicine.* **34**, 386-395.
- Forster, I.C., Loo, D.D., Eskandari, S., 1999. Stoichiometry and Na<sup>+</sup> binding cooperativity of rat and flounder renal type II Na<sup>+</sup>-Pi cotransporters. *The American Journal of Physiology.* **276**, F644-9.
- Freyssinet, J.M., 2003. Cellular microparticles: what are they bad or good for? *Journal of Thrombosis and Haemostasis.* **1**, 1655-1662.
- Freyssinet, J. & Toti, F., 2010. Formation of procoagulant microparticles and properties. *Thrombosis Research.* **125**, S46-S48.
- Galley, H.F. & Webster, N.R., 2004. Physiology of the endothelium. *British Journal of Anaesthesia.* **93**, 105-113.
- Gansevoort, R.T., Correa-Rotter, R., Hemmelgarn, B.R., Jafar, T.H., Heerspink, H.J.L., Mann, J.F., Matsushita, K., Wen, C.P., 2013. Chronic kidney disease and cardiovascular risk: epidemiology, mechanisms, and prevention. *The Lancet.* **382**, 339-352.
- Gardiner, C., Ferreira, Y.J., Dragovic, R.A., Redman, C.W., Sargent, I.L., 2013. Extracellular vesicle sizing and enumeration by nanoparticle tracking analysis. *Journal of Extracellular Vesicles.* **2**, .
- Gattineni, J., Bates, C., Twombly, K., Dwarakanath, V., Robinson, M.L., Goetz, R., Mohammadi, M., Baum, M., 2009. FGF23 decreases renal NaPi-2a and NaPi-2c expression and induces hypophosphatemia in vivo predominantly via FGF receptor 1. *American Journal of Physiology.Renal Physiology.* **297**, F282-91.
- Gawaz, M., 2001. Blood platelets. Thieme. 1-41.
- Ge, S., Hertel, B., Emden, S.H., Beneke, J., Menne, J., Haller, H., von Vietinghoff, S., 2012. Microparticle generation and leucocyte death in Shiga toxin-mediated HUS. *Nephrology, Dialysis, Transplantation : Official Publication of the European Dialysis and Transplant Association - European Renal Association.* **27**, 2768-2775.
- George, F.D., 2008. Microparticles in vascular diseases. *Thrombosis Research.* **122 Suppl 1**, S55-9.
- Gerhard Giebisch and Erich Windhager, 2005. The Urinary System. In Walter F.Boron and Emile L.Boulpaep, ed, *Medical Physiology.* UPDATED EDITION of 2003 ed. United States of America: ELSEVIER. 737-876.
- Giachelli, C.M., Jono, S., Shioi, A., Nishizawa, Y., Mori, K., Morii, H., 2001. Vascular calcification and inorganic phosphate. *American Journal of Kidney Diseases.* **38**, S34-S37.

- Giachelli, C.M., 2003. Vascular calcification: in vitro evidence for the role of inorganic phosphate. *Journal of the American Society of Nephrology : JASN*. **14**, S300-4.
- Giachelli, C.M., Speer, M.Y., Li, X., Rajachar, R.M., Yang, H., 2005. Regulation of vascular calcification: roles of phosphate and osteopontin. *Circulation Research*. **96**, 717-722.
- GIL, G., CALVET, V.E., FERRER, A., HEGARDT, F.G., 1982. Inactivation and reactivation of rat liver 3-hydroxy-3-methylglutaryl-CoA-reductase phosphatases: effect of phosphate, pyrophosphate and divalent cations. *Hoppe-Seyler's Zeitschrift Für Physiologische Chemie*. **363**, 1217-1224.
- Giral, H., Caldas, Y., Sutherland, E., Wilson, P., Breusegem, S., Barry, N., Blaine, J., Jiang, T., Wang, X.X., Levi, M., 2009. Regulation of rat intestinal Na-dependent phosphate transporters by dietary phosphate. *American Journal of Physiology.Renal Physiology*. **297**, F1466-75.
- Glushakova, O., Kosugi, T., Roncal, C., Mu, W., Heinig, M., Cirillo, P., Sanchez-Lozada, L.G., Johnson, R.J., Nakagawa, T., 2008. Fructose induces the inflammatory molecule ICAM-1 in endothelial cells. *Journal of the American Society of Nephrology : JASN*. **19**, 1712-1720.
- González-Parra, E., Gracia-Iguacel, C., Egido, J., Ortiz, A., 2012<sub>a</sub>. Phosphorus and nutrition in chronic kidney disease. *International Journal of Nephrology*. **2012**, .
- Gonzalez-Parra, E., Tuñón, J., Egido, J., Ortiz, A., 2012<sub>b</sub>. Phosphate: a stealthier killer than previously thought? *Cardiovascular Pathology*. **21**, 372-381.
- González-Quintero, V.H., Jiménez, J.J., Jy, W., Mauro, L.M., Hortman, L., O'Sullivan, M.J., Ahn, Y., 2003. Elevated plasma endothelial microparticles in preeclampsia. *American Journal of Obstetrics and Gynecology*. **189**, 589-593.
- Greenberg, A. & Cheung, A.K., 2005. *Primer on kidney diseases*. Saunders.
- Harambat, J., van Stralen, K.J., Kim, J.J., Tizard, E.J., 2012. Epidemiology of chronic kidney disease in children. *Pediatric Nephrology*. **27**, 363-373.
- Hayes, G., Busch, A.E., Lang, F., Biber, J., Murer, H., 1995. Protein kinase C consensus sites and the regulation of renal Na/Pi-cotransport (NaPi-2) expressed in XENOPUS laevis oocytes. *Pflugers Archiv : European Journal of Physiology*. **430**, 819-824.
- Hediger, M.A., Cléménçon, B., Burrier, R.E., Bruford, E.A., 2013. The ABCs of membrane transporters in health and disease (SLC series): introduction. *Molecular Aspects of Medicine*. **34**, 95-107.
- Hladky, S.B. & Rink, T.J., 1986. *Body fluid and kidney physiology*. 1st ed. London: Edward Arnold.
- Hoffman, L. & Rechsteiner, M., 1996. Nucleotidase activities of the 26 S proteasome and its regulatory complex. *The Journal of Biological Chemistry*. **271**, 32538-32545.
- Holdenrieder, S. & Stieber, P., 2009. Clinical use of circulating nucleosomes. *Critical Reviews in Clinical Laboratory Sciences*. **46**, 1-24.

- Horstman, L.L. & Ahn, Y.S., 1999. Platelet microparticles: a wide-angle perspective. *Critical Reviews in Oncology/Hematology*. **30**, 111-142.
- Houle, F., Poirier, A., Dumaresq, J., Huot, J., 2007. DAP kinase mediates the phosphorylation of tropomyosin-1 downstream of the ERK pathway, which regulates the formation of stress fibers in response to oxidative stress. *Journal of Cell Science*. **120**, 3666-3677.
- Hoyer, F.F., Nickenig, G., Werner, N., 2010. Microparticles--messengers of biological information. *Journal of Cellular and Molecular Medicine*. **14**, 2250-2256.
- Hsu, C., Huang, P., Chiang, C., Leu, H., Huang, C., Chen, J., Lin, S., 2013. Increased circulating endothelial apoptotic microparticle to endothelial progenitor cell ratio is associated with subsequent decline in glomerular filtration rate in hypertensive patients. *PloS One*. **8**, e68644.
- Hsu, Y., Hsu, S., Huang, S., Lee, H., Lin, S., Tsai, C., Shih, C., Lin, C., 2014. Hyperphosphatemia induces protective autophagy in endothelial cells through the inhibition of Akt/mTOR signaling. *Journal of Vascular Surgery*.
- Huang, P.H., Huang, S.S., Chen, Y.H., Lin, C.P., Chiang, K.H., Chen, J.S., Tsai, H.Y., Lin, F.Y., Chen, J.W., Lin, S.J., 2010. Increased circulating CD31+/annexin V+ apoptotic microparticles and decreased circulating endothelial progenitor cell levels in hypertensive patients with microalbuminuria. *Journal of Hypertension*. **28**, 1655-1665.
- Huyer, G., Liu, S., Kelly, J., Moffat, J., Payette, P., Kennedy, B., Tsaprailis, G., Gresser, M.J., Ramachandran, C., 1997. Mechanism of inhibition of protein-tyrosine phosphatases by vanadate and pervanadate. *The Journal of Biological Chemistry*. **272**, 843-851.
- Ikushima, M., Rakugi, H., Ishikawa, K., Maekawa, Y., Yamamoto, K., Ohta, J., Chihara, Y., Kida, I., Ogihara, T., 2006. Anti-apoptotic and anti-senescence effects of Klotho on vascular endothelial cells. *Biochemical and Biophysical Research Communications*. **339**, 827-832.
- Isakova, T., Gutierrez, O.M., Smith, K., Epstein, M., Keating, L.K., Juppner, H., Wolf, M., 2011. Pilot study of dietary phosphorus restriction and phosphorus binders to target fibroblast growth factor 23 in patients with chronic kidney disease. *Nephrology, Dialysis, Transplantation : Official Publication of the European Dialysis and Transplant Association - European Renal Association*. **26**, 584-591.
- Isoyama, N., Leurs, P., Qureshi, A.R., Bruchfeld, A., Anderstam, B., Heimbürger, O., Barany, P., Stenvinkel, P., Lindholm, B., 2015. Plasma S100A12 and soluble receptor of advanced glycation end product levels and mortality in chronic kidney disease Stage 5 patients. *Nephrology, Dialysis, Transplantation : Official Publication of the European Dialysis and Transplant Association - European Renal Association*. **30**, 84-91.
- Ito, K. & Adcock, I.M., 2002. Histone acetylation and histone deacetylation. *Molecular Biotechnology*. **20**, 99-106.
- Jaffe, E.A., Nachman, R.L., Becker, C.G., Minick, C.R., 1973. Culture of human endothelial cells derived from umbilical veins. Identification by morphologic and immunologic criteria. *The Journal of Clinical Investigation*. **52**, 2745-2756.

- James, M.T., Hemmelgarn, B.R., Tonelli, M., 2010. Early recognition and prevention of chronic kidney disease. *Lancet*. **375**, 1296-1309.
- Jamison, R.L., 1987. Short and long loop nephrons. *Kidney Int*. **31**, 597-605.
- Jaumot, M. & Hancock, J.F., 2001. Protein phosphatases 1 and 2A promote Raf-1 activation by regulating 14-3-3 interactions. *Oncogene*. **20**, 3949-3958.
- Jha, V., Garcia-Garcia, G., Iseki, K., Li, Z., Naicker, S., Plattner, B., Saran, R., Wang, A.Y., Yang, C., 2013. Chronic kidney disease: global dimension and perspectives. *The Lancet*. **382**, 260-272.
- Jin, Y., Blue, E.K., Gallagher, P.J., 2006. Control of death-associated protein kinase (DAPK) activity by phosphorylation and proteasomal degradation. *The Journal of Biological Chemistry*. **281**, 39033-39040.
- Jobbagy, Z., Olah, Z., Petrovics, G., Eiden, M.V., Leverett, B.D., Dean, N.M., Anderson, W.B., 1999. Up-regulation of the Pit-2 phosphate transporter/retrovirus receptor by protein kinase C epsilon. *The Journal of Biological Chemistry*. **274**, 7067-7071.
- Johann, S.V., Gibbons, J.J., O'Hara, B., 1992. GLVR1, a receptor for gibbon ape leukemia virus, is homologous to a phosphate permease of *Neurospora crassa* and is expressed at high levels in the brain and thymus. *Journal of Virology*. **66**, 1635-1640.
- Jung, K.H., Chu, K., Lee, S.T., Bahn, J.J., Kim, J.H., Kim, M., Lee, S.K., Roh, J.K., 2011. Risk of Macrovascular Complications in Type 2 Diabetes Mellitus: Endothelial Microparticle Profiles. *Cerebrovascular Diseases (Basel, Switzerland)*. **31**, 485-493.
- Jy, W., Horstman, L.L., Jimenez, J.J., Ahn, Y.S., Biro, E., Nieuwland, R., Sturk, A., Dignat-George, F., Sabatier, F., Camoin-Jau, L., Sampol, J., Hugel, B., Zobairi, F., Freyssinet, J.M., Nomura, S., Shtet, A.S., Key, N.S., Hebbel, R.P., 2004. Measuring circulating cell-derived microparticles. *Journal of Thrombosis and Haemostasis : JTH*. **2**, 1842-1851.
- Kasai, K. & Field, J.B., 1983. Discrimination of multiple forms of phosphoprotein phosphatase in bovine thyroid. *Metabolism*. **32**, 296-307.
- Kavanaugh, M.P. & Kabat, D., 1996. Identification and characterization of a widely expressed phosphate transporter/retrovirus receptor family. *Kidney International*. **49**, 959-963.
- Kavanaugh, M.P., Miller, D.G., Zhang, W., Law, W., Kozak, S.L., Kabat, D., Miller, A.D., 1994. Cell-surface receptors for gibbon ape leukemia virus and amphotropic murine retrovirus are inducible sodium-dependent phosphate symporters. *Proceedings of the National Academy of Sciences of the United States of America*. **91**, 7071-7075.
- Kehrel, B., Flicker, E., Wigbels, B., Osterfeld, M., Van de Loo, J., Lüscher, E., 1996. Thrombospondin measured in whole blood-an indicator of platelet activation. *Blood Coagulation & Fibrinolysis*. **7**, 202-205.
- Keller, S., Ridinger, J., Rupp, A., Janssen, J., Altevogt, P., 2011. Body fluid derived exosomes as a novel template for clinical diagnostics. *J Transl Med*. **9**, 240.

Keller, S., Sanderson, M.P., Stoeck, A., Altevogt, P., 2006. Exosomes: from biogenesis and secretion to biological function. *Immunology Letters*. **107**, 102-108.

Kemp, G. & Bevington, A., 1993<sub>a</sub>. The regulation of intracellular orthophosphate concentration. *Journal of Theoretical Biology*. **161**, 77-94.

Kemp, G.J., Bevington, A., Khodja, D., Graham, R., Russell, G., 1988<sub>a</sub>. Net fluxes of orthophosphate across the plasma membrane in human red cells following alteration of pH and extracellular P<sub>i</sub> concentration. *Biochimica Et Biophysica Acta (BBA)-Molecular Cell Research*. **969**, 148-157.

Kemp, G.J., Bevington, A., Khodja, D., Graham, R., Russell, G., 1988<sub>b</sub>. Regulation of phosphate metabolism in human red cells following prolonged incubation to steady state in vitro. *Biochimica Et Biophysica Acta (BBA)-Molecular Cell Research*. **969**, 139-147.

Kemp, G.J., Khouja, H.I., Ahmado, A., Graham, R., Russell, G., Bevington, A., 1993<sub>b</sub>. Regulation of the phosphate (Pi) concentration in UMR 106 osteoblast-like cells: effect of Pi, Na<sup>+</sup> and K<sup>+</sup>. *Cell Biochemistry and Function*. **11**, 13-23.

Kemper, C., Atkinson, J.P., Hourcade, D.E., 2010. Properdin: emerging roles of a pattern-recognition molecule. *Annual Review of Immunology*. **28**, 131-155.

Ketteler, M., Wolf, M., Hahn, K., Ritz, E., 2012. Phosphate: a novel cardiovascular risk factor. *European Heart Journal*.

Key, N.S., 2010<sub>a</sub>. Analysis of tissue factor positive microparticles. *Thrombosis Research*. **125**, S42-S45.

Key, N.S., Chantrathammachart, P., Moody, P.W., Chang, J., 2010<sub>b</sub>. Membrane microparticles in VTE and cancer. *Thrombosis Research*. **125**, S80-S83.

Khandelwal, R.L. & Kamani, S.A., 1980. Studies on inactivation and reactivation of homogeneous rabbit liver phosphoprotein phosphatases by inorganic pyrophosphate and divalent cations. *Biochimica Et Biophysica Acta (BBA)-Enzymology*. **613**, 95-105.

Kim, H.K., Song, K.S., Chung, J., Lee, K.R., Lee, S., 2004. Platelet microparticles induce angiogenesis in vitro. *British Journal of Haematology*. **124**, 376-384.

Kobayashi, H., Saito, T., Tanaka, S., 2014. Mineralization of cartilage in growth plate. *Clinical Calcium*. **24**, 177-184.

Koeppen, B.M. & Stanton, B.A., 2007. *Renal physiology*. 4th ed. Philadelphia: Mosby Elsevier.

Koeppen, B.M. & Stanton, B.A., 2009. Overview of Circulation. *Berne & Levy Physiology*. Sixth ed. Canada: Elsevier Health Sciences. 289-291.

Koga, H., Sugiyama, S., Kugiyama, K., Watanabe, K., Fukushima, H., Tanaka, T., Sakamoto, T., Yoshimura, M., Jinnouchi, H., Ogawa, H., 2005. Elevated levels of VE-cadherin-positive endothelial microparticles in patients with type 2 diabetes mellitus and coronary artery disease. *Journal of the American College of Cardiology*. **45**, 1622-1630.

- Kotamraju, S., Konorev, E.A., Joseph, J., Kalyanaraman, B., 2000. Doxorubicin-induced apoptosis in endothelial cells and cardiomyocytes is ameliorated by nitron spin traps and ebselen. Role of reactive oxygen and nitrogen species. *The Journal of Biological Chemistry*. **275**, 33585-33592.
- Kumar, R., 2009. Phosphate sensing. *Current Opinion in Nephrology and Hypertension*. **18**, 281-284.
- Kuriki, C., Tanaka, T., Fukui, Y., Sato, O., Motojima, K., 2002. Structural and functional analysis of a new upstream promoter of the human FAT/CD36 gene. *Biological & Pharmaceutical Bulletin*. **25**, 1476-1478.
- Kuro-o, M., 2010. Klotho. *Pflügers Archiv-European Journal of Physiology*. **459**, 333-343.
- Lacroix, R. & Dignat-George, F., 2012. Microparticles as a circulating source of procoagulant and fibrinolytic activities in the circulation. *Thrombosis Research*. **129**, S27-S29.
- Landray, M.J., Wheeler, D.C., Lip, G.Y., Newman, D.J., Blann, A.D., McGlynn, F.J., Ball, S., Townend, J.N., Baigent, C., 2004. Inflammation, endothelial dysfunction, and platelet activation in patients with chronic kidney disease: the chronic renal impairment in Birmingham (CRIB) study. *American Journal of Kidney Diseases*. **43**, 244-253.
- Larson, M.C., Luthi, M.R., Hogg, N., Hillery, C.A., 2013. Calcium-phosphate microprecipitates mimic microparticles when examined with flow cytometry. *Cytometry Part A*. **83**, 242-250.
- Larson, M.C., Woodliff, J.E., Hillery, C.A., Kearl, T.J., Zhao, M., 2012. Phosphatidylethanolamine is externalized at the surface of microparticles. *Biochimica Et Biophysica Acta (BBA)-Molecular and Cell Biology of Lipids*. **1821**, 1501-1507.
- Lau, W.L., Pai, A., Moe, S.M., Giachelli, C.M., 2011. Direct effects of phosphate on vascular cell function. *Advances in Chronic Kidney Disease*. **18**, 105-112.
- Lawler, P.R. & Lawler, J., 2012. Molecular basis for the regulation of angiogenesis by thrombospondin-1 and -2. *Cold Spring Harbor Perspectives in Medicine*. **2**, a006627.
- Lechner, D., Kollars, M., Gleiss, A., Kyrle, P., Weltermann, A., 2007. Chemotherapy-induced thrombin generation via procoagulant endothelial microparticles is independent of tissue factor activity. *Journal of Thrombosis and Haemostasis*. **5**, 2445-2452.
- Lee, H., Oh, S.W., Heo, N.J., Chin, H.J., Na, K.Y., Kim, S., Chae, D.W., 2012. Serum phosphorus as a predictor of low-grade albuminuria in a general population without evidence of chronic kidney disease. *Nephrology Dialysis Transplantation*. **27**, 2799-2806.
- Lee, S., Chu, K., Jung, K., Kim, J., Moon, H., Bahn, J., Im, W., Sunwoo, J., Moon, J., Kim, M., 2012. Circulating CD62E microparticles and cardiovascular outcomes. *PLoS One*. **7**, e35713.
- Leone, A., Moncada, S., Vallance, P., Calver, A., Collier, J., 1992. Accumulation of an endogenous inhibitor of nitric oxide synthesis in chronic renal failure. *The Lancet*. **339**, 572-575.

- Leong, H., Podor, T., Manocha, B., Lewis, J., 2011. Validation of flow cytometric detection of platelet microparticles and liposomes by atomic force microscopy. *Journal of Thrombosis and Haemostasis*. **9**, 2466-2476.
- Leung, L., Li, W., McGregor, J., Albrecht, G., Howard, R., 1992. CD36 peptides enhance or inhibit CD36-thrombospondin binding. A two-step process of ligand-receptor interaction. *Journal of Biological Chemistry*. **267**, 18244-18250.
- Levey, A.S., Coresh, J., Balk, E., Kausz, A.T., Levin, A., Steffes, M.W., Hogg, R.J., Perrone, R.D., Lau, J., Eknoyan, G., 2003. National Kidney Foundation practice guidelines for chronic kidney disease: evaluation, classification, and stratification. *Annals of Internal Medicine*. **139**, 137-147.
- Levi, M. & Popovtzer, M., 1999. Disorders of phosphate balance. *Atlas of Diseases of the Kidney. Philadelphia: Current Medicine*. 7.2-7.14.
- Li, L.M., Hou, D.X., Guo, Y.L., Yang, J.W., Liu, Y., Zhang, C.Y., Zen, K., 2011. Role of MicroRNA-214–Targeting Phosphatase and Tensin Homolog in Advanced Glycation End Product-Induced Apoptosis Delay in Monocytes. *The Journal of Immunology*. **186**, 2552-2560.
- Li, S., Wang, C., Dai, Y., Yang, Y., Pan, H., Zhong, J., Chen, J., 2013. The stimulatory effect of ROCK inhibitor on bovine corneal endothelial cells. *Tissue and Cell*. **45**, 387-396.
- Li, H., Oehrlin, S.A., Wallerath, T., Ihrig-Biedert, I., Wohlfart, P., Ulshofer, T., Jessen, T., Herget, T., Forstermann, U., Kleinert, H., 1998. Activation of protein kinase C alpha and/or epsilon enhances transcription of the human endothelial nitric oxide synthase gene. *Molecular Pharmacology*. **53**, 630-637.
- Li, X., Yang, H.Y., Giachelli, C.M., 2006. Role of the sodium-dependent phosphate cotransporter, Pit-1, in vascular smooth muscle cell calcification. *Circulation Research*. **98**, 905-912.
- Liabeuf, S., Okazaki, H., Desjardins, L., Fliser, D., Goldsmith, D., Covic, A., Wiecek, A., Ortiz, A., Martinez-Castelao, A., Lindholm, B., Suleymanlar, G., Mallamaci, F., Zoccali, C., London, G., Massy, Z.A., 2014. Vascular calcification in chronic kidney disease: are biomarkers useful for probing the pathobiology and the health risks of this process in the clinical scenario? *Nephrology, Dialysis, Transplantation : Official Publication of the European Dialysis and Transplant Association - European Renal Association*. **29**, 1275-1284.
- Lincoln, T.M., Komalavilas, P., Cornwell, T.L., 1994. Pleiotropic regulation of vascular smooth muscle tone by cyclic GMP-dependent protein kinase. *Hypertension*. **23**, 1141-1147.
- Livak, K.J. & Schmittgen, T.D., 2001. Analysis of Relative Gene Expression Data Using Real-Time Quantitative PCR and the  $2^{-\Delta\Delta CT}$  Method. *Methods*. **25**, 402-408.
- Longstaff, C., Varju, I., Sotonyi, P., Szabo, L., Krumrey, M., Hoell, A., Bota, A., Varga, Z., Komorowicz, E., Kolev, K., 2013. Mechanical stability and fibrinolytic resistance of clots containing fibrin, DNA, and histones. *The Journal of Biological Chemistry*. **288**, 6946-6956.

Lorenzen, J.M., Kielstein, J.T., Hafer, C., Gupta, S.K., Kumpers, P., Faulhaber-Walter, R., Haller, H., Fliser, D., Thum, T., 2011. Circulating miR-210 predicts survival in critically ill patients with acute kidney injury. *Clinical Journal of the American Society of Nephrology*. **6**, 1540-1546.

Lote, C.J., 2000. *Principles of renal physiology*. 4th ed. Dordrecht ; London: Kluwer Academic Publishers.

Lotscher, M., Kaissling, B., Biber, J., Murer, H., Levi, M., 1997. Role of microtubules in the rapid regulation of renal phosphate transport in response to acute alterations in dietary phosphate content. *The Journal of Clinical Investigation*. **99**, 1302-1312.

Lowry, O.H., Rosebrough, N.J., Farr, A.L., Randall, R.J., 1951. Protein measurement with the Folin phenol reagent. *J Biol Chem*. **193**, 265-275.

MA, C., LU, X., LUO, Y., CAO, J., YANG, B., GAO, Y., LIU, X., FAN, L., 2012. Angiogenesis related gene expression profiles of EA. hy926 cells induced by irbesartan: a possible novel therapeutic approach. *Chinese Medical Journal*. **125**, 1369-1375.

Mackman, N., 2009. The role of tissue factor and factor VIIa in hemostasis. *Anesthesia and Analgesia*. **108**, 1447-1452.

Mallat, Z., Benamer, H., Hugel, B., Benessiano, J., Steg, P.G., Freyssinet, J.M., Tedgui, A., 2000. Elevated levels of shed membrane microparticles with procoagulant potential in the peripheral circulating blood of patients with acute coronary syndromes. *Circulation*. **101**, 841-843.

Mallat, Z., Hugel, B., Ohan, J., Leseche, G., Freyssinet, J.M., Tedgui, A., 1999. Shed membrane microparticles with procoagulant potential in human atherosclerotic plaques: a role for apoptosis in plaque thrombogenicity. *Circulation*. **99**, 348-353.

Malvern Ltd, M., 2012, 2012. *Zetasizer Nano Series User Manual*. [online]. Available at: [www.malvern.com/Manuals](http://www.malvern.com/Manuals) [accessed 12/04/2012].

Marieb, E.N. & Hoehn, K., 2007. *Human anatomy & physiology*. Seventh Edition ed. Pearson Education.

Marja J. VanWijk, E. VanBavel, A. Sturk, R.N., 2003. Microparticles in cardiovascular diseases. **59**, 277-287.

Martin, K.J. & Gonzalez, E.A., 2011. Prevention and control of phosphate retention/hyperphosphatemia in CKD-MBD: what is normal, when to start, and how to treat? *Clinical Journal of the American Society of Nephrology : CJASN*. **6**, 440-446.

Marulanda, J., Alqarni, S., Murshed, M., 2014. Mechanisms of Vascular Calcification and Associated Diseases. *Current Pharmaceutical Design*.

Matsubara, T. & Ziff, M., 1986. Increased superoxide anion release from human endothelial cells in response to cytokines. *Journal of Immunology (Baltimore, Md.: 1950)*. **137**, 3295-3298.

Mause, S.F. & Weber, C., 2010. Microparticles: protagonists of a novel communication network for intercellular information exchange. *Circulation Research*. **107**, 1047-1057.

- Mayes, P.A., 1993. Intermediary metabolism of fructose. *The American Journal of Clinical Nutrition*. **58**, 754S-765S.
- McGregor, L., Martin, J., McGregor, J.L., 2006. Platelet-leukocyte aggregates and derived microparticles in inflammation, vascular remodelling and thrombosis. *Frontiers in Bioscience : A Journal and Virtual Library*. **11**, 830-837.
- McVey, J.H., 1999. Tissue factor pathway. *Best Practice & Research Clinical Haematology*. **12**, 361-372.
- Mesri, M. & Altieri, D.C., 1999. Leukocyte microparticles stimulate endothelial cell cytokine release and tissue factor induction in a JNK1 signaling pathway. *The Journal of Biological Chemistry*. **274**, 23111-23118.
- Mesri, M. & Altieri, D.C., 1998. Endothelial cell activation by leukocyte microparticles. *Journal of Immunology (Baltimore, Md.: 1950)*. **161**, 4382-4387.
- Mezentsev, A., Merks, R.M., O'Riordan, E., Chen, J., Mendeleev, N., Goligorsky, M.S., Brodsky, S.V., 2005. Endothelial microparticles affect angiogenesis in vitro: role of oxidative stress. *American Journal of Physiology. Heart and Circulatory Physiology*. **289**, H1106-14.
- Michael J. Caplan, 2005. Functional Organization of the Cell. In Boron, W. F. & Boulpaep, E. L., eds, *Medical physiology*. Updated Edition ed. United States of America: Saunders Philadelphia, PA. 9-49.
- Miller, D.G., Edwards, R.H., Miller, A.D., 1994. Cloning of the cellular receptor for amphotropic murine retroviruses reveals homology to that for gibbon ape leukemia virus. *Proceedings of the National Academy of Sciences of the United States of America*. **91**, 78-82.
- Miller, D.G. & Miller, A.D., 1993. Inhibitors of retrovirus infection are secreted by several hamster cell lines and are also present in hamster sera. *Journal of Virology*. **67**, 5346-5352.
- Miller, D.G. & Miller, A.D., 1992. Tunicamycin treatment of CHO cells abrogates multiple blocks to retrovirus infection, one of which is due to a secreted inhibitor. *Journal of Virology*. **66**, 78-84.
- Miyamoto, K., Ito, M., Segawa, H., Kuwahata, M., 2000. Secondary hyperparathyroidism and phosphate sensing in parathyroid glands. *Renal Failure*. **1**, 3.
- Mizushima, N. & Yoshimori, T., 2007. How to interpret LC3 immunoblotting. *Autophagy*. **3**, 542.
- Mohamed, A., et al, 2005. Circulating endothelial cells in renal transplant recipients, *Transplantation proceedings*, 2005, Elsevier pp2387-2390.
- Molony, D.A. & Stephens, B.W., 2011. Derangements in phosphate metabolism in chronic kidney diseases/endstage renal disease: therapeutic considerations. *Advances in Chronic Kidney Disease*. **18**, 120-131.

Moncada, S., Higgs, E., Hodson, H., Knowles, R., López-Jaramillo, P., McCall, T., Palmer, R., Radomski, M., Rees, D., Schulz, R., 1991. The L-arginine: nitric oxide pathway. *Journal of Cardiovascular Pharmacology*. **17**, S1&hyphen.

Morel, O., Jesel, L., Freyssinet, J.M., Toti, F., 2011. Cellular mechanisms underlying the formation of circulating microparticles. *Arteriosclerosis, Thrombosis, and Vascular Biology*. **31**, 15-26.

Morel, O., Ohlmann, P., Morel, N., Jesel, L., Bareiss, P., Freyssinet, J.M., Toti, F., 2005. Microparticles and cardiovascular disease. *Archives Des Maladies Du Coeur Et Des Vaisseaux*. **98**, 226-235.

Mostefai, H.A., Agouni, A., Carusio, N., Mastronardi, M.L., Heymes, C., Henrion, D., Andriantsitohaina, R., Martinez, M.C., 2008. Phosphatidylinositol 3-kinase and xanthine oxidase regulate nitric oxide and reactive oxygen species productions by apoptotic lymphocyte microparticles in endothelial cells. *Journal of Immunology (Baltimore, Md.: 1950)*. **180**, 5028-5035.

Muhlbauer, R.C. & Fleisch, H., 1990. Inverse relation between plasma inorganic phosphate and phospholipids in mice: effect of dietary inorganic phosphate, fasting and glucagon. *Mineral and Electrolyte Metabolism*. **16**, 341-347.

Mullier, F., Bailly, N., Chatelain, C., Dogne, J., Chatelain, B., 2011. More on: calibration for the measurement of microparticles: needs, interests, and limitations of calibrated polystyrene beads for flow cytometry-based quantification of biological microparticles. *Journal of Thrombosis and Haemostasis*. **9**, 1679-1681.

Mune, S., Shibata, M., Hatamura, I., Saji, F., Okada, T., Maeda, Y., Sakaguchi, T., Negi, S., Shigematsu, T., 2009. Mechanism of phosphate-induced calcification in rat aortic tissue culture: possible involvement of Pit-1 and apoptosis. *Clinical and Experimental Nephrology*. **13**, 571-577.

Murer, H. & Biber, J., 1996. Molecular mechanisms of renal apical Na/phosphate cotransport. *Annual Review of Physiology*. **58**, 607-618.

Murer, H., Forster, I., Hernando, N., Lambert, G., Traebert, M., Biber, J., 1999. Posttranscriptional regulation of the proximal tubule NaPi-II transporter in response to PTH and dietary P(i). *The American Journal of Physiology*. **277**, F676-84.

Nadra, I., Mason, J.C., Philippidis, P., Florey, O., Smythe, C.D., McCarthy, G.M., Landis, R.C., Haskard, D.O., 2005. Proinflammatory activation of macrophages by basic calcium phosphate crystals via protein kinase C and MAP kinase pathways: a vicious cycle of inflammation and arterial calcification? *Circulation Research*. **96**, 1248-1256.

Näslund, B. & von der Decken, A., 1981. Chain length heterogeneity of nucleosomal DNA in mouse liver after dimethylnitrosamine administration. *Archives of Toxicology*. **47**, 169-177.

Navaneethan, S.D., Palmer, S.C., Craig, J.C., Elder, G.J., Strippoli, G.F., 2009. Benefits and harms of phosphate binders in CKD: a systematic review of randomized controlled trials. *American Journal of Kidney Diseases*. **54**, 619-637.

- Neal, C.S., Michael, M.Z., Pimlott, L.K., Yong, T.Y., Li, J.Y.Z., Gleadle, J.M., 2011. Circulating microRNA expression is reduced in chronic kidney disease. *Nephrology Dialysis Transplantation*. **26**, 3794-3802.
- Nima Abbasian, 2010. *The role of properdin and CD36 in chronic kidney disease (CKD)*. Ph. D. University of Leicester.
- Nishimura, M. & Naito, S., 2008. Tissue-specific mRNA expression profiles of human solute carrier transporter superfamilies. *Drug Metabolism and Pharmacokinetics*. **23**, 22-44.
- Noori, N., Kalantar-Zadeh, K., Kovesdy, C.P., Bross, R., Benner, D., Kopple, J.D., 2010. Association of dietary phosphorus intake and phosphorus to protein ratio with mortality in hemodialysis patients. *Clinical Journal of the American Society of Nephrology : CJASN*. **5**, 683-692.
- Nozaki, T., Sugiyama, S., Koga, H., Sugamura, K., Ohba, K., Matsuzawa, Y., Sumida, H., Matsui, K., Jinnouchi, H., Ogawa, H., 2009. Significance of a multiple biomarkers strategy including endothelial dysfunction to improve risk stratification for cardiovascular events in patients at high risk for coronary heart disease. *Journal of the American College of Cardiology*. **54**, 601-608.
- Nozaki, T., Sugiyama, S., Sugamura, K., Ohba, K., Matsuzawa, Y., Konishi, M., Matsubara, J., Akiyama, E., Sumida, H., Matsui, K., Jinnouchi, H., Ogawa, H., 2010. Prognostic value of endothelial microparticles in patients with heart failure. *European Journal of Heart Failure*. **12**, 1223-1228.
- O'Rourke, M.F. & Safar, M.E., 1999. Chronic kidney disease and cardiovascular risk. *Circulation*. **100**, 354-360.
- Obi, Y. & Hamano, T., 2012. Phosphate and the risk of mortality. *Clinical Calcium*. **22**, 1515-1523.
- Ogawa, H., Shinoda, T., Cornelius, F., Toyoshima, C., 2009. Crystal structure of the sodium-potassium pump (Na<sup>+</sup>,K<sup>+</sup>-ATPase) with bound potassium and ouabain. *Proceedings of the National Academy of Sciences of the United States of America*. **106**, 13742-13747.
- Oh, J., Wunsch, R., Turzer, M., Bahner, M., Raggi, P., Querfeld, U., Mehls, O., Schaefer, F., 2002. Advanced coronary and carotid arteriopathy in young adults with childhood-onset chronic renal failure. *Circulation*. **106**, 100-105.
- O'Hara, B., Johann, S.V., Klinger, H.P., Blair, D.G., Rubinson, H., Dunn, K.J., Sass, P., Vitek, S.M., Robins, T., 1990. Characterization of a human gene conferring sensitivity to infection by gibbon ape leukemia virus. *Cell Growth & Differentiation : The Molecular Biology Journal of the American Association for Cancer Research*. **1**, 119-127.
- Ohnishi, M. & Razzaque, M.S., 2010. Dietary and genetic evidence for phosphate toxicity accelerating mammalian aging. *FASEB Journal : Official Publication of the Federation of American Societies for Experimental Biology*. **24**, 3562-3571.

- Olah, Z., Lehel, C., Anderson, W.B., Eiden, M.V., Wilson, C.A., 1994. The cellular receptor for gibbon ape leukemia virus is a novel high affinity sodium-dependent phosphate transporter. *The Journal of Biological Chemistry*. **269**, 25426-25431.
- Onufrak, S.J., Bellasi, A., Shaw, L.J., Herzog, C.A., Cardarelli, F., Wilson, P.W., Vaccarino, V., Raggi, P., 2008. Phosphorus levels are associated with subclinical atherosclerosis in the general population. *Atherosclerosis*. **199**, 424-431.
- Ord, M.G. & Stocken, L., 1966. Metabolic properties of histones from rat liver and thymus gland. *Biochem.J.* **98**, 888-897.
- Orfanidou, T., Malizos, K.N., Varitimidis, S., Tsezou, A., 2012. 1,25-Dihydroxyvitamin D(3) and extracellular inorganic phosphate activate mitogen-activated protein kinase pathway through fibroblast growth factor 23 contributing to hypertrophy and mineralization in osteoarthritic chondrocytes. *Experimental Biology and Medicine (Maywood, N.J.)*. **237**, 241-253.
- Pallet, N., Sirois, I., Bell, C., Hanafi, L., Hamelin, K., Dieudé, M., Rondeau, C., Thibault, P., Desjardins, M., Hebert, M., 2013. A comprehensive characterization of membrane vesicles released by autophagic human endothelial cells. *Proteomics*. **13**, 1108-1120.
- Palmer, R.M., Ashton, D., Moncada, S., 1988. Vascular endothelial cells synthesize nitric oxide from L-arginine. *Nature*. **333**, 664-666.
- Pan, M.R., Chang, T.M., Chang, H.C., Su, J.L., Wang, H.W., Hung, W.C., 2009. Sumoylation of Prox1 controls its ability to induce VEGFR3 expression and lymphatic phenotypes in endothelial cells. *Journal of Cell Science*. **122**, 3358-3364.
- Peake, P.W., Pussell, B.A., Mackinnon, B., Charlesworth, J.A., 2002. The effect of pH and nucleophiles on complement activation by human proximal tubular epithelial cells. *Nephrology, Dialysis, Transplantation : Official Publication of the European Dialysis and Transplant Association - European Renal Association*. **17**, 745-752.
- Peerschke, E., Yin, W., Grigg, S., Ghebrehiwet, B., 2006. Blood platelets activate the classical pathway of human complement. *Journal of Thrombosis and Haemostasis*. **4**, 2035-2042.
- Peerschke, E.I., Yin, W., Ghebrehiwet, B., 2008. Platelet mediated complement activation. *Advances in Experimental Medicine and Biology*. **632**, 81-91.
- Pellegrin, S. & Mellor, H., 2007. Actin stress fibres. *Journal of Cell Science*. **120**, 3491-3499.
- Peng, A., Wu, T., Zeng, C., Rakheja, D., Zhu, J., Ye, T., Hutcheson, J., Vaziri, N.D., Liu, Z., Mohan, C., 2011. Adverse effects of simulated hyper- and hypo-phosphatemia on endothelial cell function and viability. *Plos One*. **6**, e23268.
- Peters, K., Unger, R.E., Brunner, J., Kirkpatrick, C.J., 2003. Molecular basis of endothelial dysfunction in sepsis. *Cardiovascular Research*. **60**, 49-57.
- Phillips, D., Aponte, A.M., French, S.A., Chess, D.J., Balaban, R.S., 2009. Succinyl-CoA synthetase is a phosphate target for the activation of mitochondrial metabolism. *Biochemistry*. **48**, 7140-7149.

- Portale, A.A., Halloran, B.P., Morris, R.C., Jr, 1989. Physiologic regulation of the serum concentration of 1,25-dihydroxyvitamin D by phosphorus in normal men. *The Journal of Clinical Investigation*. **83**, 1494-1499.
- Portela, M. & Richardson, H.E., 2013. Death takes a holiday--non-apoptotic role for caspases in cell migration and invasion. *EMBO Reports*. **14**, 107-108.
- Prater, C.A., Plotkin, J., Jaye, D., Frazier, W.A., 1991. The properdin-like type I repeats of human thrombospondin contain a cell attachment site. *The Journal of Cell Biology*. **112**, 1031-1040.
- Preston, R.A., Jy, W., Jimenez, J.J., Mauro, L.M., Horstman, L.L., Valle, M., Aime, G., Ahn, Y.S., 2003. Effects of severe hypertension on endothelial and platelet microparticles. *Hypertension*. **41**, 211-217.
- Puddu, P., Puddu, G.M., Cravero, E., Muscari, S., Muscari, A., 2010. The involvement of circulating microparticles in inflammation, coagulation and cardiovascular diseases. *Canadian Journal of Cardiology*. **26**, e140-e145.
- Quarles, L.D., 2008. Endocrine functions of bone in mineral metabolism regulation. *The Journal of Clinical Investigation*. **118**, 3820-3828.
- Rath, D.P., Bailey, M., Zhang, H., Jiang, Z., Abduljalil, A.M., Weisbrode, S., Hamlin, R.L., Robitaille, P.M., 1995. 31P-nuclear magnetic resonance studies of chronic myocardial ischemia in the Yucatan micropig. *The Journal of Clinical Investigation*. **95**, 151-157.
- Rautou, P.E., Vion, A.C., Amabile, N., Chironi, G., Simon, A., Tedgui, A., Boulanger, C.M., 2011. Microparticles, vascular function, and atherothrombosis. *Circulation Research*. **109**, 593-606.
- Ravera, S., Virkki, L.V., Murer, H., Forster, I.C., 2007. Deciphering PiT transport kinetics and substrate specificity using electrophysiology and flux measurements. *American Journal of Physiology-Cell Physiology*. **293**, C606-C620.
- Razzaque, M., 2011. Phosphate toxicity: new insights into an old problem. *Clinical Science*. **120**, 91-97.
- Reimer, R.J., 2013. SLC17: A functionally diverse family of organic anion transporters. *Molecular Aspects of Medicine*. **34**, 350-359.
- Reimer, R.J. & Edwards, R.H., 2004. Organic anion transport is the primary function of the SLC17/type I phosphate transporter family. *Pflügers Archiv*. **447**, 629-635.
- Robert, S., Poncelet, P., Lacroix, R., Arnaud, L., Giraudo, L., Hauchard, A., Sampol, J., DIGNAT-GEORGE, F., 2009. Standardization of platelet-derived microparticle counting using calibrated beads and a Cytomics FC500 routine flow cytometer: a first step towards multicenter studies? *Journal of Thrombosis and Haemostasis*. **7**, 190-197.
- Robert, S., Poncelet, P., Lacroix, R., Raoult, D., DIGNAT-GEORGE, F., 2011. More on: calibration for the measurement of microparticles: value of calibrated polystyrene beads for flow cytometry-based sizing of biological microparticles. *Journal of Thrombosis and Haemostasis*. **9**, 1676-1678.

- Robert, S., Lacroix, R., Poncelet, P., Harhour, K., Bouriche, T., Judicone, C., Wischhusen, J., Arnaud, L., Dignat-George, F., 2012. High-sensitivity flow cytometry provides access to standardized measurement of small-size microparticles--brief report. *Arteriosclerosis, Thrombosis, and Vascular Biology*. **32**, 1054-1058.
- Sabatier, F., Darmon, P., Hugel, B., Combes, V., Sanmarco, M., Velut, J.G., Arnoux, D., Charpiot, P., Freyssinet, J.M., Oliver, C., Sampol, J., Dignat-George, F., 2002. Type 1 and type 2 diabetic patients display different patterns of cellular microparticles. *Diabetes*. **51**, 2840-2845.
- Sage, A.P., Lu, J., Tintut, Y., Demer, L.L., 2011. Hyperphosphatemia-induced nanocrystals upregulate the expression of bone morphogenetic protein-2 and osteopontin genes in mouse smooth muscle cells in vitro. *Kidney International*. **79**, 414-422.
- Sakariassen, K.S., Nievelstein, P.F., Collier, B.S., Sixma, J.J., 1986. The role of platelet membrane glycoproteins Ib and IIb-IIIa in platelet adherence to human artery subendothelium. *British Journal of Haematology*. **63**, 681-691.
- Salaun, C., Leroy, C., Rousseau, A., Boitez, V., Beck, L., Friedlander, G., 2010. Identification of a novel transport-independent function of PiT1/SLC20A1 in the regulation of TNF-induced apoptosis. *The Journal of Biological Chemistry*. **285**, 34408-34418.
- Salaun, C., Rodrigues, P., Heard, J.M., 2001. Transmembrane topology of PiT-2, a phosphate transporter-retrovirus receptor. *Journal of Virology*. **75**, 5584-5592.
- santa cruz biotechnology, i., 2014. *PiT1/2 Antibody (SY-12): sc-101298*. [online]. Available at: <http://www.scbt.com/datasheet-101298-pit1-2-sy-12-antibody.html> [accessed 18/07/2014 2014].
- Schulz, E., Dopheide, J., Schuhmacher, S., Thomas, S.R., Chen, K., Daiber, A., Wenzel, P., Munzel, T., Keaney, J.F., Jr, 2008. Suppression of the JNK pathway by induction of a metabolic stress response prevents vascular injury and dysfunction. *Circulation*. **118**, 1347-1357.
- Schwaebler, W.J. & Reid, K.B., 1999. Does properdin crosslink the cellular and the humoral immune response? *Immunology Today*. **20**, 17-21.
- Schwarz, U., Buzello, M., Ritz, E., Stein, G., Raabe, G., Wiest, G., Mall, G., Amann, K., 2000. Morphology of coronary atherosclerotic lesions in patients with end-stage renal failure. *Nephrology, Dialysis, Transplantation : Official Publication of the European Dialysis and Transplant Association - European Renal Association*. **15**, 218-223.
- Scialla, J.J. & Wolf, M., 2014. Roles of phosphate and fibroblast growth factor 23 in cardiovascular disease. *Nature Reviews Nephrology*.
- Sebbagh, M., Renvoizé, C., Hamelin, J., Riché, N., Bertoglio, J., Bréard, J., 2001. Caspase-3-mediated cleavage of ROCK I induces MLC phosphorylation and apoptotic membrane blebbing. *Nature Cell Biology*. **3**, 346-352.
- Segawa, H., Kaneko, I., Takahashi, A., Kuwahata, M., Ito, M., Ohkido, I., Tatsumi, S., Miyamoto, K., 2002. Growth-related renal type II Na/Pi cotransporter. *The Journal of Biological Chemistry*. **277**, 19665-19672.

- Semenza, G.L., 2010. Vascular responses to hypoxia and ischemia. *Arteriosclerosis, Thrombosis, and Vascular Biology*. **30**, 648-652.
- Shah, M.D., Bergeron, A.L., Dong, J., López, J.A., 2008. Flow cytometric measurement of microparticles: pitfalls and protocol modifications. *Platelets*. **19**, 365-372.
- Shanahan, C.M., Crouthamel, M.H., Kapustin, A., Giachelli, C.M., 2011. Arterial calcification in chronic kidney disease: key roles for calcium and phosphate. *Circulation Research*. **109**, 697-711.
- Shantsila, E., Kamphuisen, P., Lip, G., 2010. Circulating microparticles in cardiovascular disease: implications for atherogenesis and atherothrombosis. *Journal of Thrombosis and Haemostasis*. **8**, 2358-2368.
- Sheerin, N.S., Risley, P., Abe, K., Tang, Z., Wong, W., Lin, T., Sacks, S.H., 2008. Synthesis of complement protein C3 in the kidney is an important mediator of local tissue injury. *The FASEB Journal : Official Publication of the Federation of American Societies for Experimental Biology*. **22**, 1065-1072.
- Shinaberger, C.S., Greenland, S., Kopple, J.D., Van Wyck, D., Mehrotra, R., Kovesdy, C.P., Kalantar-Zadeh, K., 2008. Is controlling phosphorus by decreasing dietary protein intake beneficial or harmful in persons with chronic kidney disease? *The American Journal of Clinical Nutrition*. **88**, 1511-1518.
- Shroff, R.C., Price, K.L., Kolatsi-Joannou, M., Todd, A.F., Wells, D., Deanfield, J., Johnson, R.J., Rees, L., Woolf, A.S., Long, D.A., 2013. Circulating angiopoietin-2 is a marker for early cardiovascular disease in children on chronic dialysis. *PLoS One*. **8**, e56273.
- Shuto, E., Taketani, Y., Tanaka, R., Harada, N., Isshiki, M., Sato, M., Nashiki, K., Amo, K., Yamamoto, H., Higashi, Y., 2009. Dietary phosphorus acutely impairs endothelial function. *Journal of the American Society of Nephrology*. **20**, 1504-1512.
- Simak, J., Gelderman, M., Yu, H., Wright, V., Baird, A., 2006. Circulating endothelial microparticles in acute ischemic stroke: a link to severity, lesion volume and outcome. *Journal of Thrombosis and Haemostasis*. **4**, 1296-1302.
- Simantov, R., Febbraio, M., Crombie, R., Asch, A.S., Nachman, R.L., Silverstein, R.L., 2001. Histidine-rich glycoprotein inhibits the antiangiogenic effect of thrombospondin-1. *Journal of Clinical Investigation*. **107**, 45-52.
- Sinauridze, E.I., Kireev, D.A., Popenko, N.Y., Pichugin, A.V., Panteleev, M.A., Krymskaya, O.V., Ataullakhanov, F.I., 2007. Platelet microparticle membranes have 50-to 100-fold higher specific procoagulant activity than activated platelets. *THROMBOSIS AND HAEMOSTASIS-STUTTGART*. **97**, 425.
- Sirois, I., Groleau, J., Pallet, N., Brassard, N., Hamelin, K., Londono, I., Pshezhetsky, A.V., Bendayan, M., Hebert, M.J., 2012. Caspase activation regulates the extracellular export of autophagic vacuoles. *Autophagy*. **8**, 927-937.

SLC TABLES, 2015. *SLC TABLES*. [online]. Available at: <http://slc.bioparadigms.org> [accessed 01/04/2015].

Smogorzewski, M., Zayed, M., Zhang, Y.B., Roe, J., Massry, S.G., 1993. Parathyroid hormone increases cytosolic calcium concentration in adult rat cardiac myocytes. *The American Journal of Physiology*. **264**, H1998-2006.

Stankevičius, E., Kėvelaitis, E., Vainorius, E., Simonsen, U., 2003. Role of nitric oxide and other endothelium-derived factors. *Medicina (Kaunas)*. **39**, 333-341.

Stenvinkel, P., Carrero, J.J., Axelsson, J., Lindholm, B., Heimbürger, O., Massy, Z., 2008. Emerging biomarkers for evaluating cardiovascular risk in the chronic kidney disease patient: how do new pieces fit into the uremic puzzle? *Clinical Journal of the American Society of Nephrology : CJASN*. **3**, 505-521.

Stevens, P., O'donoghue, D., De Lusignan, S., Van Vlymen, J., Klebe, B., Middleton, R., Hague, N., New, J., Farmer, C., 2007. Chronic kidney disease management in the United Kingdom: NEOERICA project results. *Kidney International*. **72**, 92-99.

Susztak, K., Ciccone, E., McCue, P., Sharma, K., Bottinger, E.P., 2005. Multiple metabolic hits converge on CD36 as novel mediator of tubular epithelial apoptosis in diabetic nephropathy. *PLoS Medicine*. **2**, e45.

Szajerka, G. & Kwiatkowska, J., 1984. The effect of cortisol on rabbit red cell acid phosphatase isoenzymes. *Molecular and Cellular Biochemistry*. **59**, 183-186.

Szczepanska-Konkel, M., Hoppe, A., Lin, J.T., Dousa, T.P., 1990. Irreversible inhibition of renal Na(+)-Pi cotransporter by alpha-bromophosphonoacetic acid. *The American Journal of Physiology*. **258**, C583-8.

Szczepanska-Konkel, M., Yusufi, A.N., VanScoy, M., Webster, S.K., Dousa, T.P., 1986. Phosphonocarboxylic acids as specific inhibitors of Na<sup>+</sup>-dependent transport of phosphate across renal brush border membrane. *The Journal of Biological Chemistry*. **261**, 6375-6383.

Takeshita, J., Mohler, E.R., Krishnamoorthy, P., Moore, J., Rogers, W.T., Zhang, L., Gelfand, J.M., Mehta, N.N., 2014. Endothelial cell-, platelet-, and monocyte/macrophage-derived microparticles are elevated in psoriasis beyond cardiometabolic risk factors. *Journal of the American Heart Association*. **3**, e000507.

Tang, K., Zhang, Y., Zhang, H., Xu, P., Liu, J., Ma, J., Lv, M., Li, D., Katirai, F., Shen, G., 2012. Delivery of chemotherapeutic drugs in tumour cell-derived microparticles. *Nature Communications*. **3**, 1282.

Tenenhouse, H.S., 2005. Regulation of phosphorus homeostasis by the type iia na/phosphate cotransporter. *Annu.Rev.Nutr.* **25**, 197-214.

Thambyrajah, J., Landray, M.J., McGlynn, F.J., Jones, H.J., Wheeler, D.C., Townend, J.N., 2000. Abnormalities of endothelial function in patients with predialysis renal failure. *Heart (British Cardiac Society)*. **83**, 205-209.

- Théry, C., Zitvogel, L., Amigorena, S., 2002. Exosomes: composition, biogenesis and function. *Nature Reviews Immunology*. **2**, 569-579.
- Tissot, J., Rubin, O., Canellini, G., 2010. Analysis and clinical relevance of microparticles from red blood cells. *Current Opinion in Hematology*. **17**, 571-577.
- Tonelli, M., Pannu, N., Manns, B., 2010. Oral phosphate binders in patients with kidney failure. *New England Journal of Medicine*. **362**, 1312-1324.
- Tonelli, M., Sacks, F., Pfeffer, M., Gao, Z., Curhan, G., Cholesterol And Recurrent Events Trial Investigators, 2005. Relation between serum phosphate level and cardiovascular event rate in people with coronary disease. *Circulation*. **112**, 2627-2633.
- Tramontano, A.F., Lyubarova, R., Tsiakos, J., Palaia, T., Deleon, J.R., Ragolia, L., 2010. Circulating endothelial microparticles in diabetes mellitus. *Mediators of Inflammation*. **2010**, 250476.
- Tual-Chalot, S., Guibert, C., Muller, B., Savineau, J.P., Andriantsitohaina, R., Martinez, M.C., 2010. Circulating microparticles from pulmonary hypertensive rats induce endothelial dysfunction. *American Journal of Respiratory and Critical Care Medicine*. **182**, 261-268.
- Tushuizen, M.E., Diamant, M., Sturk, A., Nieuwland, R., 2011. Cell-derived microparticles in the pathogenesis of cardiovascular disease: friend or foe? *Arteriosclerosis, Thrombosis, and Vascular Biology*. **31**, 4-9.
- Ueba, T., Haze, T., Sugiyama, M., Higuchi, M., Asayama, H., Karitani, Y., Nishikawa, T., Yamashita, K., Nagami, S., Nakayama, T., 2008. Level, distribution and correlates of platelet-derived microparticles in healthy individuals with special reference to the metabolic syndrome. *Thromb Haemost*. **100**, 280-285.
- van Beers, E.J., Schaap, M.C., Berckmans, R.J., Nieuwland, R., Sturk, A., van Doormaal, F.F., Meijers, J.C., Biemond, B.J., CURAMA study group, 2009. Circulating erythrocyte-derived microparticles are associated with coagulation activation in sickle cell disease. *Haematologica*. **94**, 1513-1519.
- van der Zee, P.M., Biro, E., Ko, Y., de Winter, R.J., Hack, C.E., Sturk, A., Nieuwland, R., 2006. P-selectin- and CD63-exposing platelet microparticles reflect platelet activation in peripheral arterial disease and myocardial infarction. *Clinical Chemistry*. **52**, 657-664.
- van Dommelen, S.M., Vader, P., Lakhali, S., Kooijmans, S., van Solinge, W.W., Wood, M.J., Schiffelers, R.M., 2012. Microvesicles and exosomes: opportunities for cell-derived membrane vesicles in drug delivery. *Journal of Controlled Release*. **161**, 635-644.
- van Hinsbergh, V.W., 2012. Endothelium—role in regulation of coagulation and inflammation, *Seminars in immunopathology*, 2012, Springer pp93-106.
- Vanholder, R., De Smet, R., Glorieux, G., Argilés, A., Baurmeister, U., Brunet, P., Clark, W., Cohen, G., De Deyn, P.P., Deppisch, R., 2003<sub>a</sub>. Review on uremic toxins: classification, concentration, and interindividual variability. *Kidney International*. **63**, 1934-1943.

- Vanholder, R., Glorieux, G., Lameire, N., European Uremic Toxin Work Group, 2003<sub>b</sub>. Uraemic toxins and cardiovascular disease. *Nephrology, Dialysis, Transplantation : Official Publication of the European Dialysis and Transplant Association - European Renal Association*. **18**, 463-466.
- VanWijk, M.J., VanBavel, E., Sturk, A., Nieuwland, R., 2003. Microparticles in cardiovascular diseases. *Cardiovascular Research*. **59**, 277-287.
- Vaziri, N.D., 2006. Dyslipidemia of chronic renal failure: the nature, mechanisms, and potential consequences. *American Journal of Physiology.Renal Physiology*. **290**, F262-72.
- Villa-Bellosta, R., Bogaert, Y.E., Levi, M., Sorribas, V., 2007. Characterization of Phosphate Transport in Rat Vascular Smooth Muscle Cells Implications for Vascular Calcification. *Arteriosclerosis, Thrombosis, and Vascular Biology*. **27**, 1030-1036.
- Villa-Bellosta, R. & Sorribas, V., 2009. Phosphonoformic acid prevents vascular smooth muscle cell calcification by inhibiting calcium-phosphate deposition. *Arteriosclerosis, Thrombosis, and Vascular Biology*. **29**, 761-766.
- Virkki, L.V., Biber, J., Murer, H., Forster, I.C., 2007. Phosphate transporters: a tale of two solute carrier families. *American Journal of Physiology-Renal Physiology*. **62**, F643.
- Wang, J., Yu, J., Tan, L., Tian, Y., Ma, J., Tan, C., Wang, H., Liu, Y., Tan, M., Jiang, T., 2015. Genome-wide circulating microRNA expression profiling indicates biomarkers for epilepsy. *Scientific Reports*. **5**, .
- Waterborg, J.H. & Matthews, H.R., 1984. The Burton assay for DNA. *Nucleic Acids*. Springer. 1-3.
- Weber, C. & Mause, S., 2011. Microparticles in Angiogenesis.
- Weisshaar, S., Gouya, G., Nguyen, D., Kapiotis, S., Wolzt, M., 2013. The LPS-induced increase in circulating microparticles is not affected by vitamin C in humans. *European Journal of Clinical Investigation*. **43**, 708-715.
- Werner, A., Dehmelt, L., Nalbant, P., 1998. Na<sup>-</sup>dependent phosphate cotransporters: the NaPi protein families. *J Exp Biol*. **201**, 3135-3142.
- Werner, N., Wassmann, S., Ahlers, P., Kosiol, S., Nickenig, G., 2006. Circulating CD31+/annexin V+ apoptotic microparticles correlate with coronary endothelial function in patients with coronary artery disease. *Arteriosclerosis, Thrombosis, and Vascular Biology*. **26**, 112-116.
- Wiedmer, T., Shattil, S.J., Cunningham, M., Sims, P.J., 1990. Role of calcium and calpain in complement-induced vesiculation of the platelet plasma membrane and in the exposure of the platelet factor Va receptor. *Biochemistry*. **29**, 623-632.
- Woods, H., Eggleston, L.V., Krebs, H., 1970. The cause of hepatic accumulation of fructose 1-phosphate on fructose loading. *Biochem.J*. **119**, 501-510.
- Yamada, S., Tokumoto, M., Tatsumoto, N., Taniguchi, M., Noguchi, H., Nakano, T., Masutani, K., Ooboshi, H., Tsuruya, K., Kitazono, T., 2014. Phosphate overload directly induces systemic

inflammation and malnutrition as well as vascular calcification in uremia. *American Journal of Physiology.Renal Physiology*.

Yamamoto, S. & Kon, V., 2009. Mechanisms for increased cardiovascular disease in chronic kidney dysfunction. *Current Opinion in Nephrology and Hypertension*. **18**, 181-188.

Yamazaki, M., Ozono, K., Okada, T., Tachikawa, K., Kondou, H., Ohata, Y., Michigami, T., 2010. Both FGF23 and extracellular phosphate activate Raf/MEK/ERK pathway via FGF receptors in HEK293 cells. *Journal of Cellular Biochemistry*. **111**, 1210-1221.

Yin, W., Ghebrehiwet, B., Peerschke, E.I., 2008. Expression of complement components and inhibitors on platelet microparticles. *Platelets*. **19**, 225-233.

Zeiger, F., Stephan, S., Hoheisel, G., Pfeiffer, D., Ruehlmann, C., Kokschi, M., 2000. P-Selectin expression, platelet aggregates, and platelet-derived microparticle formation are increased in peripheral arterial disease. *Blood Coagulation & Fibrinolysis*. **11**, 723-728.

Zhang, Q. & Rothenbacher, D., 2008. Prevalence of chronic kidney disease in population-based studies: systematic review. *BMC Public Health*. **8**, 117.

Zhang, Z.Y. & VanEtten, R.L., 1991. Pre-steady-state and steady-state kinetic analysis of the low molecular weight phosphotyrosyl protein phosphatase from bovine heart. *The Journal of Biological Chemistry*. **266**, 1516-1525.

Zhao, Y.Y., Cheng, X.L., Lin, R.C., 2014. Lipidomics applications for discovering biomarkers of diseases in clinical chemistry. *International Review of Cell and Molecular Biology*. **313**, 1-26.

Zhu, J., Xie, R., Piao, X., Hou, Y., Zhao, C., Qiao, G., Yang, B., Shi, J., Lu, Y., 2012. Homocysteine enhances clot-promoting activity of endothelial cells via phosphatidylserine externalization and microparticles formation. *Amino Acids*. **43**, 1243-1250.

Zwaal, R., Comfurius, P., Bevers, E., 2005. Surface exposure of phosphatidylserine in pathological cells. *Cellular and Molecular Life Sciences CMLS*. **62**, 971-988.